AD-A136 379 AN EVALUATION OF MARINE FOG FORECAST CONCEPTS AND A PRELIMINARY DESIGN FO..(U) ARVIN/CALSPAN ADVANCED TECHNOLOGY CENTER BUFFALO NY APPLIED T..

1/3

UNCLASSIFIED E J MACK ET AL. JUN 83 CALSPAN-6866-M-1 F/G 4/2 NL

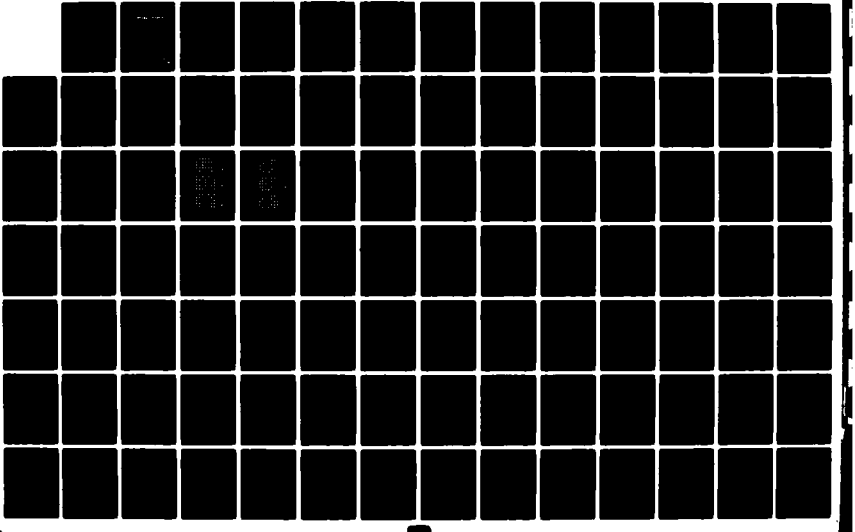

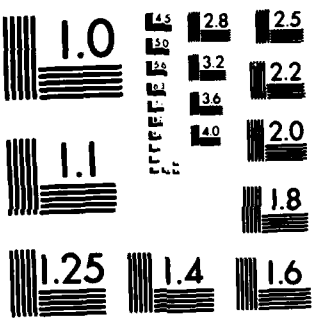

(12)

A136379

ARVIN/CALSPAN

AN EVALUATION OF MARINE FOG FORECAST CONCEPTS AND A PRELIMINARY DESIGN FOR A MARINE OBSCURATION FORECAST SYSTEM

By

E.J. Mack, C.W. Rogers and B.J. Wattle

Contract No. N00019-81-C-0102

June 1983

Project SEA FOG IX
FINAL REPORT

Calspan Report No. 6866-M-1

Prepared for:

Department of the Navy
Naval Air Systems Command
Room 472 Jefferson Plaza, No. 1
Washington, DC 20361

Attn: Dr. P.F. Twitchell, Code AIR-330 G

ADVANCED TECHNOLOGY CENTER
P.O. BOX 400, BUFFALO, NEW YORK 14225 TEL. (716) 632-7500

APPLIED TECHNOLOGY GROUP
ARVIN

SECURITY CLASSIFICATION OF THIS PAGE (When Data Entered)

REPORT DOCUMENTATION PAGE

READ INSTRUCTIONS BEFORE COMPLETING FORM

1. REPORT NUMBER	2. GOVT ACCESSION NO. AD-A136377 / 3. RECIPIENT'S CATALOG NUMBER
4. TITLE (and Subtitle) An Evaluation of Marine Fog Forecast Concepts and A Preliminary Design for a Marine Obscuration Forecast System	5. TYPE OF REPORT & PERIOD COVERED Final Report 5/15/81 - 5/15/83
	6. PERFORMING ORG. REPORT NUMBER 6866-M-1
7. AUTHOR(s) E.J.Mack, C.W. Rogers and B.J. Wattle	8. CONTRACT OR GRANT NUMBER(s) N00019-81-C-0102
9. PERFORMING ORGANIZATION NAME AND ADDRESS Calspan Corporation Box 400 Buffalo, N.Y. 14225	10. PROGRAM ELEMENT, PROJECT, TASK AREA & WORK UNIT NUMBERS
11. CONTROLLING OFFICE NAME AND ADDRESS Naval Air Systems Command (Air 330) Dept. of the Navy Washington, D.C. 20361	12. REPORT DATE June 1983
	13. NUMBER OF PAGES 250
14. MONITORING AGENCY NAME & ADDRESS(if different from Controlling Office)	15. SECURITY CLASS. (of this report) UNCLASSIFIED
	15a. DECLASSIFICATION/DOWNGRADING SCHEDULE

16. DISTRIBUTION STATEMENT (of this Report)

APPROVED FOR PUBLIC RELEASE;
DISTRIBUTION UNLIMITED

17. DISTRIBUTION STATEMENT (of the abstract entered in Block 20, if different from Report)

18. SUPPLEMENTARY NOTES

19. KEY WORDS (Continue on reverse side if necessary and identify by block number)

Marine Fog
Fog Forecasting
Numerical Models
Empirical Models
Phenomenologic Models
Model Evaluation
Test Cases
Marine Inversion

20. ABSTRACT (Continue on reverse side if necessary and identify by block number)

NASC (Air 370) instituted the Marine Fog Investigation (MFI), a basic research effort, in 1972 with the ultimate goal of an improved marine fog forecast capability. The overall MFI program comprised a series of cooperative but independent research efforts by Calspan and a number of Navy, industry and university laboratories and achieved progress through field study, intensive interpretive analyses and theoretical modeling. The field studies generated much new knowledge of the physics and meteorology of marine fog

DD FORM 1 JAN 73 1473

SECURITY CLASSIFICATION OF THIS PAGE (When Data Entered)

20. Abstract (Cont.)

occurrence and helped revise widely-held theories of marine fog formation. Calspan's studies produced phenomenological descriptions of at least five new fog types, provided realistic verification on which to base new numerical modeling techniques, and developed synoptic and statistical relationships which could be used in operational forecasting. Under the current contract, Calspan conducted an objective evaluation of these predictive approaches, along with a select group of numerical models, by testing against data sets derived from at-sea observational studies. The results of this evaluation demonstrated that, with high-quality data, certain models can provide operationally useful forecasts for marine obscuration. It is also concluded that new knowledge of the physics of marine fog occurrence can help optimize the application of various forecast techniques and also serve as a back-up forecast tool. As a chief objective of this investigation, we outlined a preliminary version of an obscuration forecast system which, when fully developed, would incorporate this new knowledge and delineate the application of specific numeric and/or synoptic and statistical approaches; i.e., the system would specify a forecast tool tailored to the attendant meteorological scenario and functional within operational constraints. This report summarizes the research effort and results which led to the conceptual design of this forecast system.

TABLE OF CONTENTS

TABLE OF CONTENTS (Cont.)

LIST OF ILLUSTRATIONS

LIST OF TABLES

ACKNOWLEDGEMENTS

The authors would like to thank all those scientists and forecasters who contributed time and effort to our site visits and interviews conducted during this study and who provided research work in parallel with the program. In particular, we wish to acknowledge the continued encouragement and suggestions of Dr. A. Weinstein, Director of Research at NEPRF during this study, without whose support a program of this magnitude and variety could not have been carried out.

Special thanks go to the participants in the numerical model testing: I. Sykes and S. Lewellen (ARAP), S. Burk, W. Thompson, and P. Tag (NEPRF), C. Fairall, K. Davidson, and P. Boyle (NPS), and M. Wurtele (UCLA). In addition we wish to acknowledge the valuable insight provided by W. Hoppel, J. Fitzgerald, and S. Gathman of NRL with respect to microphysics and boundary layer structure. Also, R. Dixon and J. Rosenthanl (PMTC) are recognized for their efforts in examining the visibility versus inversion height relation at PMTC. Special thanks go to R. Noonkester of NOSC and CDR at W. Hillyard and WO Haley of North Is. NAS for their illuminating discussions of fog occurrence and fog forecasting in the San Diego area. We would also like to acknowledge our debt to D. Leipper (NPS, Ret.) for providing the benefit of his extensive knowledge of West Coast marine fog. Finally, we would like to express our gratitude to our Calspan colleagues, R.J. Pilié, J. Hanley, and J. Kile, without whose criticisms, discussions, and endeavors this project could not have been brought to fruition.

Section 1
INTRODUCTION

In 1972, the Naval Air Systems Command (NASC, Air-370) instituted the Marine Fog Investigation (MFI) with the ultimate goal of improving the Navy's fog forecasting capability. The overall MFI effort, conducted as a cooperative, basic-research program, independently by a number of Navy laboratories and groups from both the academic and private sectors, achieved progress through field studies, intensive interpretive analyses and theoretical modeling. After nearly 10 years of research, our knowledge of the physics and meteorology of marine fog occurrence has increased to the extent that it is now feasible to incorporate this knowledge in operationally useful forecast concepts.

Calspan was actively involved in NASC's MFI from its inception and was responsible for a number of intensive field investigations which produced new information on the characteristics of marine fog and the processes which control fog formation and its lifecycle over the ocean. In recent years, this knowledge was summarized in phenomenological models which describe mechanisms of fog formation and persistence, was used to develop synoptic and statistical relationships pertaining to marine fog occurrence, and, to some extent, was utilized by other investigators in the development and tuning of numerical turbulence models designed for theoretical study of this marine boundary layer phenomenon. Specific results from Calspan's MFI studies are summarized in References 1-19.

Under the current contract, No. N00019-81-C-0102 with NASC (Air-330), Calspan assisted the Navy in a multi-task program designed to carefully examine the MFI achievements of the Seventies and to begin development of methods for utilizing this new understanding in the operational forecasting of marine fog. The principal objectives of this effort were to provide an impartial evaluation of the potential utility of a select group of existing numerical and synoptic models in the forecasting of marine fog and to initiate design of an operationally useful forecast scheme using the most appropriate combination of these models. Specific tasks in this effort included:

(1) Develop a thorough familiarity (through site visits, interviews and literature review) with the individual models in terms of modeling framework, required input, and output variables.

(2) Generate a number of data sets from actual meteorological situations with which cooperating investigators could exercise their models.

(3) Evaluate model performance both for previous tests and for the data sets provided by Calspan in terms of an individual model's potential utility in operational fog forecasting, considering the impact of input data availability in real time on model utility.

(4) Based on item (3), recommend a candidate list of models for consideration in designing an operationally useful fog forecast scheme and/or identify gaps in input data availability or in our knowledge of marine fog behavior.

(5) Initiate design of a fog forecast scheme, with particular attention to input data requirements, computer resources, and timeliness of forecast output.

(6) As a separate, related Task, analyze a 12-month record of acoustic sounder-inversion-height data in the context of marine fog occurrence and the attendant synoptic scenario to develop a better understanding of relationships between the marine inversion and marine fog.

As a chief objective of this contract, Calspan pursued design of a forecast scheme based on the potential utility of the candidate models in the operational forecasting of marine fog. An outline of a preliminary version of an obscuration forecast system, which could incorporate the new understanding of marine fog generated by the Navy's MFI and delineate the application of specific forecast approaches, is provided in Section 4. Characteristics of the candidate forecast approaches and models, evaluation protocol and test results are discussed in Section 3; additional details of the models, test cases and test results are provided in Appendices A, B & C. We continued study of relationships between the marine inversion and the occurrence of marine fog

and developed an Inversion Statistics Model for use in the forecasting of visibility; the model, which was evaluated on this program, is described in Section 5. A synopsis of marine fog occurrence—information resulting from Calspan's participation in the MFI--is presented in Section 4.1; additional detail pertinent to an overall understanding of marine fog is provided in Appendices D, E and F. The principal conclusions and specific recommendations derived from the program are discussed in Section 2, Summary and Conclusions.

Section 2
SUMMARY AND CONCLUSIONS

Under Contract No. N00019-81-C-0102 with the Naval Air Systems Command (NASC) and as a culmination of NASC's 10 year Marine Fog Investigation (MFI), Calspan has been assisting the Navy in a multi-task program designed to carefully examine the MFI achievements of the Seventies and to begin development of methods for utilizing this new understanding in the operational forecasting of marine fog. Recent study at Calspan has shown that the rational assembledge of knowledge and relationships derived from the observational studies, coupled with newly-developed numerical, synoptic and statistical models for marine fog and the marine boundary layer, can provide new, practical, and operationally useful forecast procedures for marine obscuration. Therefore, as a chief objective of this investigation, Calspan has pursued this goal and outlined a preliminary version of an obscuration forecast system which, when fully developed, would incorporate this new knowledge and delineate the application of specific numeric and/or synoptic and statistical approaches; i.e., the system would specify a forecast tool tailored to the attendant meteorological scenario and functional within operational constraints. This section summarizes the research effort and results which led to the conceptual design of this forecast system.

2.1 SUMMARY

The investigation supported under this Contract was designed to allow for objective evaluation of a limited number of 'research' numerical models and other forecast procedures and to thereby lead to recommendations as to the specific utility of any model or procedure in the operational forecasting of marine obscuration. From a select list of more than 20 candidate models, a group including five numeric and four empirical approaches was delineated for further evaluation. The numeric models ultimately tested were: ARAP's HOC (higher order closure), Burk's HOC, NPS' mixed-layer, Tag's K-theory and Wurtele's turbulence-based eddy-coefficients models. For the empirical approaches, Calspan's Decision Tree and Inversion Statistics and Leipper's Indices and Inversion Statistics models were tested. In addition in September 1981, Renard's Model Output Statistics (MOS) approach was recommended for immediate operational implementation and was not further considered in the evaluation phase of this investigation.

The predictive capabilities of the models were assessed by testing on a set of six 'blind' test cases (data sets) carefully selected and prepared from actual meteorological events encountered during Calspan's prior MFI at-sea studies, each with all required initialization data and each with downwind verification. The set of test cases covered a wide range of scenarios: nighttime and daytime, stable to near unstable, stratus and fog, warm and cold sea surface, Atlantic and Pacific locations, and both long and short-term forecast periods. In a sense, these were ideal data sets and not reflective of the data-sparse scenario typical of operational conditions; however, objective intercomparison of the models and forecast procedures required that the best possible data sets be made available.

Numerical simulations were performed 'blind' by individual cooperating investigators with their own models on their own computers. Model test results were then submitted to Calspan for evaluation based on overall cloud/fog predictions compared to observations and persistence forecasts. For the numerical models, their predictive capabilities for temperature profile and boundary layer depth were also assessed. In the initial test, no one model performed significantly better than the others; each of the models failed, in terms of their cloud/fog predictions, on at least two of the test cases. In particular, all but one of the models had difficulty with the daytime situations. However, the numerical models, on average, out-performed the persistence forecast and in some instances produced predictions which quantitatively matched observations.

For some of the situations in which numerical models failed, our analyses of early runs provided suggestions for minor modifications to certain weaknesses in these models. For other situations of failure, major problems with the modeling framework seemed to be indicated. Accordingly, at the option of the individual investigators, some of the test cases were run a second time. As anticipated, 'skill' was improved for most of the rerun simulations. However, the data sets were no longer 'blind', and the investigators were in possession of the verification data.

Based on subjective criteria, Burk's Higher Order Closure (HOC) model was judged superior to the other models, producing the greatest number of accurate simulations and providing operationally useful forecasts in 85% of the Fog/Cloud Representation and Boundary-Layer Profile evaluation categories. Tag's K-theory model was judged second-best, followed by Wurtele's Turbulence-based Eddy Coefficients model. ARAP's HOC model, although tied with the K-theory model in number of accurate

forecasts, was rated fourth-best because it also tied for the greatest number of 'missed' forecasts. Even the relatively simplistic NPS mixed-layer model, judged fifth best, outperformed persistence.

The leading candidate models (Burk's HOC and Tag's K-theory) did not do well in the two daytime situations which involved both short-wave solar radiation and superadiabatic lapse rates in the surface layer, conditions not present in the other test cases. Wurtele's model, on the other hand, which was designed for highly unstable situations and which incorporates a different radiation package, verified for both situations in both cloud and temperature structure categories. There is evidence that the models of Burk and Tag may not adequately describe surface fluxes under surface-layer superadiabatic conditions, and insufficient heat and moisture fluxes appear to be the cause of the problems that these models had with the two cases. This apparent weakness in Burk's and Tag's models should be remedied prior to operational testing.

For testing purposes, the empirical fog forecast procedures available to us were exercised 'objectively' by the Calspan principal investigators and staff meteorologists. By design these empirical forecast approaches emphasize specific prediction of fog or visibility and are not capable of the quantitative prediction of boundary layer variables expected of the numerical models; therefore, assessment based on simple fog or no-fog forecasts by synoptic models is more qualitative than that based on interpretation of humidity/LWC profiles required for numerical forecast methods. Further, it is recognized that proper evaluation of the synoptic procedures requires a statistical test much more rigorous than was provided by our six data sets. Even with these caveats, it is clear that the synoptic models as a group outperformed the persistence forecast but in general did not do any better than the numerical models.

Testing, and evaluation of the technical content of the empirical forecast approaches, disclosed that each has unique capability and merit for use in operational forecasting. Calspan's Decision Tree (Part 2, using the observed inversion height) and Leipper's Indices model verified on the greatest number of cases, while the Decision Tree (Part 2) and Calspan's Inversion Statistics model had the least number of 'missed' forecasts. Leipper's Indices method, used operationally at North Island NAS (San Diego), has limitations; however, the indices are objectively determined, and, in the absence of any other forecast approach, the technique can provide a forecast which can be better than persistence. The Decision Tree (which requires additional development)

provides useful phenomenological forecast and interpretation information not available from any other source. Finally, of the non-numeric methods tested, inversion statistics probably offers the most promise, providing objective, yet quantitative, forecast information on visibility.

In summary, the testing program provided a 'real world' baseline from which to make relative intercomparisons of model capabilities: the initial 'blind' test of the models served to delineate certain strengths and weaknesses of both the numeric and empirical models; the second test demonstrated improvements in the models which were achieved by minor modifications. Clearly, with the recent modifications, an HOC model outperformed all other models producing some near-quantitative predictions when complete input data requirements were satisfied (excluding the two superadiabatic situations). Both the K-theory and mixed-layer 'slab' models performed reasonably well, with operational utility, for the non-stable meteorological situations, indicating that the sophistication of HOC models is not always required. Likewise, Calspan's Decision Tree, Leipper's Indices and both Calspan's and Leipper's Inversion Statistics Models performed satisfactorily (with operational utility) in the non-stable situations for which they were intended. Nevertheless, if computer resources and sufficient initialization data were always available, and provided that the surface flux question can be resolved, the primary recommendation would be to utilize the HOC model for local (mesoscale) obscuration forecasting.

The models and forecast procedures performed well in this test, as summarized above, when used with 'ideal' input data. Further, the more sophisticated numerical models required a complete and accurate suite of initialization data; wind profiles, subsidence values and sea surface temperature patterns which actually occurred between the initialization and verification times--not forecast values--were provided. In the data sparse operational environment, it may not be possible to properly initialize HOC and K-theory models, and less sophisticated mixed-layer and empirical models may prove more utilitarian.

Recognizing that the operational environment is typified by a variety of constraints, meteorological situations, forecast requirements, data availability and computational resources, it was obvious from the results of the model evaluation that for the foreseeable future no single predictive tool would be universally applicable in the operational realm. However, the model evaluation demonstrated that quantitative

predictions are possible, that some models have strengths and unique capabilities, and that some numerical models are situation specific. Some synoptic models performed satisfactorily for the situations for which they were designed without the need for advanced computational capability. Further, the wealth of understanding of the phenomenology of marine fog formation (trigger mechanisms, life-cycle characteristics, physical features, etc.) and of the linkage of marine fog occurrence to synoptic scale features can provide operationally useful forecast information and interpretation which is not available as output from any numerical model. Hence, it is our belief that the rational assembledge of this knowledge, coupled with the ability to select the most appropriate forecast tool within operational constraints for the anticipated meteorological scenario, would provide a significant advance in marine obscuration forecast capability. We have outlined a preliminary version of a multi-faceted obscuration forecast system which would have the capability for this selection and forecast process.

The recommended obscuration forecast system can be developed exclusively from existing knowledge, procedures and numerical models for application with current, operationally-available data. A combined numeric and synoptic approach is suggested in which synoptics and phenomenology would be used to help initialize, to help select appropriate numerical forecast models, to help interpret numeric results and to serve as a back-up forecast tool. The system would make maximum usage of the new knowledge of the physics and meteorology of marine fog generated by the Navy's MFI, useful knowledge which has yet to find its way into the operational realm. As currently envisioned, the recommended tools for use in such a system include: Burk's HOC model, Tag's K-theory model, the NPS mixed-layer model, Renard's MOS model, Calspan's Decision Tree and Inversion Statistics models, Leipper's Indices, climatology and persistence. It is also recommended that provision be made for eventual use of aerosol generation and microphysics models and Calspan's LWC algorithm, constructed soundings and aerosol climatology models for use as data estimation techniques. It is estimated that such a system can be designed and configured into a computer-interactive system within an approximate two year time frame. Testing and advanced development would follow.

Finally, as an additional task of the current contract, we continued investigation of relationships between the marine inversion, synoptic meteorological events and the occurrence of marine fog. The study was made possible through the acquisition of a 12-month record of acoustic-sounder inversion-height data for Monterey,

California. Strip chart records for the period October 1975-September 1976 were reduced to provide hourly values of inversion height which were then correlated with surface observations at Monterey airport, with upper level data from Oakland and Vandenberg and with synoptic scale surface and 850 mb analyses. In addition to broadening our knowledge of the behavior of the marine inversion with respect to meso- and synoptic scale systems and the occurrence of marine fog, this investigation produced the Calspan Inversion Statistics Model which was evaluated on the model assessment phase of this program.

2.2 CONCLUSIONS AND RECOMMENDATIONS

The principal conclusions and recommendations resulting from this study include:

(1) It is recommended that the Navy develop an obscuration forecast system which is based on the physics and meteorology of marine fog occurrence and which can delineate the application of specific forecast tools according to a tool's capability for handling anticipated phenomena in the context of attendant operational constraints. The system should be functional for input data scenarios ranging from single station to battlegroup.

- The models recommended for inclusion in such a system are: Burk's HOC, Tag's K-theory (1-d), NPS mixed-layer, Inversion Statistics, Calspan's Decision Tree, Leipper's Indices and Renard's MOS.

- The forecast system should also incorporate the phenomenology of marine fog occurrence.

- Provision should be made for inclusion of data estimation techniques.

- The system should be designed as a computer-operator interactive procedure for eventual integration into the Tactical Environmental Support System (TESS).

- A hardcopy handbook version would provide improved forecast capability even at isolated single stations.

(2) For an immediate improvement in wide-area, objective, centrally prepared forecasts, it is recommended that Renard's MOS approach, designed for the summertime northern Pacific, be implemented operationally. If experience demonstrates its utility, MOS should then be tested for and/or expanded to include other oceans.

(3) Burk's HOC model was judged superior to all other models and forecast approaches tested on this program. Benefiting from ARAP's previously developed radiation package, the model demonstrated that quantitative forecasts of boundary layer structure are possible. It is recommended that Burk's model be implemented for use in operational mesoscale forecasting when sufficient computer resources and initialization data are available. The following areas requiring improvement are noted:

- the apparently inadequate accounting for surface fluxes under highly unstable conditions should be investigated;

- cloud droplet sedimentation should be included for better representation of the vertical transport of moisture to improve forecasts of cloud base;

- finer grid resolution at cloud top and in the surface layer is recommended.

(4) Tag's K-theory (2-d), NPS's mixed-layer and Wurtele's models tested reasonably well, providing operationally useful forecasts in well-mixed, neutral to unstable situations and demonstrating that the sophistication of HOC models is not always required. It is recommended that the K-theory (1-d) and mixed-layer models be available for operational use when available input data are not of sufficient quality to warrant use of an HOC model.

- If the surface-flux problem in the models of Burk and Tag cannot be corrected, Wurtele's model should be considered for use in forecasting for situations with surface-layer superadiabatic conditions.

(5) The evaluation of the empirical approaches disclosed that each has unique capability not found in numerical models. For the West Coast situations for which they were designed, the models provided operationally useful forecasts without the need for advanced computational capability. It is recommended that inversion statistics and the Decision Tree approaches be further developed and configured for operational use.

- Inversion statistics models, such as the one developed on this contract, offer the most promise for operational usage because they can provide objectively-determined, quantitative forecasts of visibility. However, the existing models are probably site specific, and study is required to generalize the technique for at-sea use. In addition, it is suggested that the models be formulated to provide resolution for light, moderate and dense fog and to define time periods which are more representative of fog occurrence. Such a model would offer visibility estimates based on numerically predicted inversion heights.

- Calspan's Decision Tree requires further study to delineate additional synoptic patterns, but the approach provides useful phenomenological forecast and interpretation information not available from any other source. Inversion statistics can be combined with the Decision Tree's prediction of inversion height to provide visibility estimates.

- Leipper's Indices have limitations; but they are <u>objectively</u> determined, and, in the absence of any other forecast approach, the technique can provide a forecast better than persistence.

(6) The wealth of new understanding of the physics and meteorology of marine fog occurrence generated by the Navy's MFI has yet to find its way into the operational realm. This new knowledge can provide operationally useful forecast information and interpretive capability which is not available from any numerical model.

- It is recommended that, as a minimum, this material be incorporated into forecast manuals.

- It should be recognized that most of the knowledge and concepts developed through MFI efforts focus on West Coast fog scenarios. While limited observations suggest that the same physics and trigger mechanisms are operative elsewhere, relationships to meteorology and oceanography may differ. Remote- and mid-ocean fog occurrence is relatively undocumented and remains a gap in our knowledge. It is recommended that some limited additional study of fog occurrence in these areas be performed.

(7) Microphysics and aerosol models which could not be tested within the scope of this program appear to show promise and should be considered for future operational application. The numerical models tested on this program, which generate liquid water content and relative humidity values for interpretation as cloud/fog, would benefit by the potential capability offered by microphysics.

- The addition of microphysics and/or aerosol models for operational forecasting would aid in the determination of visibility once LWC or RH profiles are specified.

- Further, incorporation of these models into the numerical modeling framework would produce LWC in high RH situations and provide feedback between LWC and radiative processes.

(8) The forecast approaches studied on this program were tested on a limited data set which employed a complete suite of initialization

data. It is recommended that the leading candidate models be further tested on a larger test set of situations more representative of the data-sparse operational environment and remote marine locales.

Section 3
EVALUATION OF FORECAST MODELS

A primary task of this contract was to provide an objective examination of the potential utility of newly-developed models and forecast concepts for improving the Navy's operational capability for marine fog forecasting. For the forecasting of marine fog two basic approaches were considered. On the one hand are numerical models which are based on physical equations and which are designed to simulate atmospheric behavior; they range from simple, well-mixed, single layer models to complex higher order closure (HOC) turbulence models. On the other hand are empirical techniques which are derived from observed fog behavior; they range from climatology and rules-of-thumb to synoptic and statistical models. This Section discusses the candidate techniques and predictive approaches, their assessment and our recommendations relative to their potential use in operational forecasting.

3.1 SUMMARY OF NUMERCIAL MODEL TESTING

3.1.1 Numerical Model Selection

For the numerical models, the recommendation was ultimately to be based on evaluation of model performance on a set of test cases. Obviously to conduct such a test, a manageable number of models had to be selected from those which, over the years, had been designed or could be adapted, to simulate fog. Most of the available models previously had been characterized in response to the Marine Fog Model Survey questionnaire carried out in 1980 under the auspices of the NASC Code 370 (now Code 330) Marine Fog Investigation. The list of responders served as the starting point for our model selections. The complete list of 'Navy' models delineated for consideration in this evaluation program is provided in Appendix A.

With operationally applicable models as the ultimate goal, we wanted to test a set of models which spanned the state of the art not only in terms of boundary layer turbulence but also in terms of required computer resources and input data. We recognized that HOC probably offered the best description of the physics of marine boundary layer behavior. However, under operational duress, it might be necessary to run a less sophisticated and less time consuming model than would otherwise be desired.

Another prime consideration was the availability of the model for testing on our data sets during the time frame of our contract. This constraint required that the researcher have both the time and resources to run his model, and ultimately lead, with one exception,[1] to investigators who were actively working on the problem of developing boundary-layer models geared to operational input data.

By name or organization, the five numerical models chosen[2] for evaluation were: the HOC of Aeronautical Research Associates of Princeton (S. Lewellen,I. Sykes, and D. Oliver) — Ref. 20, the HOC of S. Burk (NEPRF) — Ref. 21, the mixed-layer model of the Naval Postgraduate School (K. Davidson, C. Fairall, and P. Boyle) -Ref. 22, the K-theory of P. Tag (NEPRF) — Ref. 23, and the eddy coefficients model of M. Wurtele (UCLA) — Ref. 24. Salient features of these models are shown in Table 1. Each model contains a temperature variable, a water vapor variable, and a fog/cloud liquid water variable, all of which are predicted within the model domain as time is marched forward.

The HOC models of ARAP and Burk contain the most sophisticated turbulence formulism, with prognostic equations for the second order moments. Wurtele's model with a hybrid, turbulent-energy, K-theory system and Tag's with K's computed from local vertical gradients follow in order of turbulence sophistication. NPS' 'slab' model, with its predictions only of mean values for temperature and moisture in the well-mixed layer, has no internal turbulence structure.

The ARAP, Burk, and Tag models all use the ARAP radiation package (Oliver et al, Ref. 20), although in slightly different form, and the Wurtele model uses the Herman and Goody (Ref. 25) radiation model. Both of these radiation models include absorption and scattering for both long and short wave radiation, but the total wavelength intervals and computation of absorption and scattering effects differ. The

---

[1] While paring down the original list, it was obvious that the turbulence-based models used the same radiation scheme. Thus, Calspan engaged Prof. M. Wurtele of UCLA to run his turbulence-based, eddy coefficients model which contained a different radiation scheme and which also represented a middle-ground between HOC turbulence and K-theory turbulence frameworks.

[2] In addition, we recommended that Barker's (NEPRF) model (Ref. 29) be tested because it was one of the early K-theory models used in theoretical fog research and would serve as a baseline. Barker could not participate, but J. Weyman (AFGL), who was experimenting with a version of the Barker model, agreed to use our data sets; as of this writing, we have not received results of Barker-model runs.

TABLE 1

SALIENT FEATURES OF CANDIDATE NUMERICAL MODELS

MODEL	TURBULENCE	RADIATION	SURFACE FLUX	RADIATION FROM ABOVE BOUNDARY LAYER	SUBSIDENCE
ARAP	Higher Order Closure Prognostic Eqs. for 2nd Order Moments	ARAP Package; Cloud Droplet Scattering for Short Wave	Surface Similarity Approach	Yes	Yes
Burk	Higher Order Closure Prognostic Eqs. for 2nd Order Moments	ARAP Package; No Cloud Droplet Scattering for Short Wave	Surface Similarity Approach	Yes	Yes
NPS	Well-mixed Slab Model	Long wave emissivity from liquid water; Delta-Eddington Short Wave	Bulk Aerodynamic Approach	Yes	Yes
Tag	K-theory: Eddy Coefficient function of local wind shear and bouyancy	ARAP Package; Cloud Droplet Scattering for Short Wave	Surface Similarity Approach	Yes	Yes (only in 1-D mode)
Wurtele	Eddy Coefficient function of turbulent kinetic energy and scale length, local wind shear and bouyancy	Emissivity radiative transfer model	Bulk Transfer coefficients from surface similarity	Yes	Yes

NPS model (Ref. 22) uses longwave emissivity of the cloud based on liquid water content and a one-layer delta-Eddington method for solar heating in cloud.

Except for Tag's model, which ran in two-dimensions for some of the cases, the models ran in the one dimensional mode, which simulates the evolution of the vertical structure in an air column. All the models can handle external forcing by large-scale subsidence, although to do so Tag had to run in the 1-d mode. All models compute surface fluxes and longwave back radiation from the atmosphere above the top of the boundary layer. None of the models contain drop sedimentation or cloud microphysics. Detailed summaries of model characteristics and selection criteria can be found in Appendix A.

3.1.2 The Test Cases

The test data set consisted of six cases which covered a wide range of conditions (see Table 2): fog and stratus, both short and long term verification, nighttime and daytime, stable to near unstable, and warm and cold sea surface temperatures. The cases were selected through an exhaustive examination of situations encountered on 21 at-sea and coastal field studies conducted during the years 1971-1980. For numerical simulation and its subsequent verification, it was essential to select cases for which verification soundings could be linked to initial soundings by air trajectory over known sea surface temperatures. This data set satisfied those criteria. (Detailed documentation of case selection and conditions can be found in Appendix B.)

Cases 6, 4, 1 and 3 all involved initial stratus clouds, while cases 2 and 5 were clear-sky, stable situations in which advection fogs developed. In Case 6, a stratus cloud within a 200 m deep boundary layer lowered to form surface fog in the 3 hours after sunset. In Case 4, the initial 120 m deep stratus cloud was topped near 600 m; after sunset, 10 hours of net long wave cooling thickened the cloud to about 400 m in depth. In Case 1, stratus cloud initially 200 m thick near the top of a 800 m deep boundary layer grew to a depth of 300 m in 4 hours as the boundary layer deepened during the early morning hours and the air moved over a warmer sea surface. In Case 3, an early morning 100 m thick stratus in a 250 m thick boundary layer, thinned during the sunlight hours under strong, large scale subsidence and strong heating from the sea surface; after sunset, the stratus cloud re-formed and thickened in the 250 m boundary layer to form dense fog. In Case 2 an inverted, unsaturated profile at low levels,

Table 2

SUMMARY OF DATA SETS

Case	Type	Time Interval	Time of Day	Low Level Temp Structure	Initial Cloud	Winds	Synoptic Scale Vertical Motion	Sea Surface Temp	
								Relative to Air	Trend with Distance
Aug 29, 1972 Case 6	Stratus lowering to fog	3 hr	Evening	Neutral	Yes	lt.	zero	cold	---
July 14-15, 1973 Case 4	Stratus thickening	10	Night	Neutral	Yes	lt.	zero	warm	constant
May 22, 1978 Case 1	Stratus	4	Morning	Unstable to Neutral	Yes	mod.	zero	warm	warming
Aug 2, 1975 Case 2	Shallow cold water advection fog	3	Evening	Inverted	No	mod.	----	cold	cooling
Aug 5, 1975 Case 5	Shallow cold water fog deepening over warm water	3	Morning	Inverted to Isothermal	No	mod.	----	cold to warm	warming
Oct 7, 1976 Case 3	Thinning stratus re-developing to form fog	10, 20	Morning to Night	Neutral to Unstable	Yes	lt.	strong subsidence	warm	warming

which was observed in late afternoon, became more intense during a three hour travel over colder water and shallow fog formed in the low levels. In Case 5, an inverted, unsaturated profile at low levels, which was observed near sunrise, was transformed to isothermal over warmer water as deep fog formed.

3.1.3 Testing and Objective Evaluation of the Models

The numerical models were evaluated by comparing their computer simulations or predictions to the observed evolution in each of the six cases. Individual investigators were provided with initial and boundary conditions and were asked to run their models "blind", that is the modelers had no knowledge of the verification conditions or time. Our initial evaluation of the blind simulations lead to suggestions for improvements to some of the models. At a workshop conducted at NEPRF during May 1982, during which the modelers were given the verification times and data, the original simulations were evaluated, non-competitive simulations were discussed and our suggested modifications to the models were outlined. At the conclusion of the workshop, the modelers were invited to rerun any or all of the cases with their revised models.

ARAP and Tag reran all the cases, although for Tag's model, changes from the blind runs were minimal except for Case 3 which was rerun in a one-dimensional mode to permit inclusion of the strong subsidence. ARAP made two changes which materially affected their simulations. First they set the reflection of long wave radiation to zero at the ground, the original 10% value caused unwanted heating in the two stable cases (2 and 5). Secondly, they changed their finite differencing scheme from centered to one sided at cloud top in order to eliminate a large cooling in the dry air immediately above the cloud. Burk reran Cases 1,4, and 6, all of which were affected by his revised model which could now start with initial cloud liquid water and which eliminated spurious cooling in the warm air immediately above cloud top. NPS declined to rerun. Because of the unique circumstances under which Wurtele participated in the test program, reruns by his model were not practical. The set of simulations on which the ultimate evaluation was performed thus represented the best simulations that the models were then capable of producing. The actual fog/cloud predictions produced by the numerical models are summarized in Table 3. Detailed output from the model testing--i.e., tables and plots of initial, verification and simulation parameters-may be found in Appendix C.

TABLE 3

NUMERICAL MODEL PERFORMANCE ON CALSPAN DATA SETS

Fog/Cloud Forecast

	Case 1	2	3_{10}	3_{20}	4	5	6
Burk	270 m deep stratus	Inc. RH No Fog	100 m deep stratus	270 m deep Fog	420 m deep stratus	Inc. RH No Fog	190 m deep Fog
ARAP	500 m deep stratus	Inc. RH No Fog	No stratus cloud	No Cloud No Fog	320 m deep stratus	No Fog	No Cloud No Fog
NPS	400 m deep stratus	Inc. RH No Fog	50 m deep stratus	130 m deep stratus	650 m deep Fog	Inc. RH No Fog	220 m deep Fog
Tag	160 m deep stratus	Inc. RH No Fog	40 m deep stratus	260 m deep very low stratus	390 m deep stratus	No Fog	140 m deep stratus
Wurtele	440 m deep stratus	40 m deep Fog	<10 m deep stratus	230 m deep Fog	530 m deep stratus	10 m deep Fog	50 m deep Fog
Persistence	225 m deep stratus	No Fog	120 m deep stratus	120 m deep stratus	120 m deep stratus	No Fog	100 m deep stratus
Verification	330 m deep stratus	30 m deep Fog	Dissipated stratus	250 m deep Fog	360 m deep stratus	>50 m deep Fog	200 m deep Fog

Objective assessment of numerical model performance was based on comparison of simulations and verification in two categories: boundary layer parameters and fog/cloud parameters. The results of this comparison for each model and each case are summarized, through use of symbols for ease of reference, in Tables 4 and 5. The boundary layer parameters (Table 4) included mean differences between simulated and observed temperature and dewpoint through the boundary layer; boundary layer depth was defined as the distance between height of the inversion base and the earth's surface. The fog/cloud parameters (Table 5) were differences between simulated and observed fog/cloud base, top and thickness; for the simulations, cloud was defined as a liquid water content $\geq 0.03 g/m^3$. In the tables a full, dark circle represents a small difference, the half-dark circle represents a medium difference, and an open circle represents a large difference between simulation and verification. Dashes indicate where data were unavailable.

In each table, the models are arranged alphabetically according to person or organization. In the discussion which follows, reference to a model is usually made, for example, as "NPS's model". However, for variety and ease of reading, occasionally reference will be in the personified mode, e.g., "NPS was too cold". The test cases are ordered so that the first four represent stratus thickening situations where the simplest (Case 6, evening, short duration, air column stationary) is first and the most complex (Case 3, 20-hour simulation, including day and evening over a 250 km trajectory, 10- and 20-hour verification) is last. The last two cases are the stable, shallow fogs which initially have no cloud.

For Cases 6 and 4 (see Tables 4 and 5) the models did well overall, simulating verification conditions three times as often as they came close (and with only one "missed simulation".) The ARAP and Tag models predicted temperature and dewpoint profiles near quantitatively for Case 4; and for Case 6, Tag as well as Burk and NPS produced quantitative predictions of these parameters. The models should have simulated these two cases well since the cases represent simple, nighttime, stratus situations with small air-sea temperature differences. Under these conditions, cooling from long wave radiation at cloud top and turbulent transfer under neutral conditions are the primary driving forces; and overall the models simulated these processes well.

Cases 1 and 3 were daytime, initial stratus situations with the sea surface significantly warmer than the air. For these circumstances, the models missed the

Table 4 Objective Assessment of Model Performance: Boundary Layer Parameters
(Model Simulations vs. Verification Data)

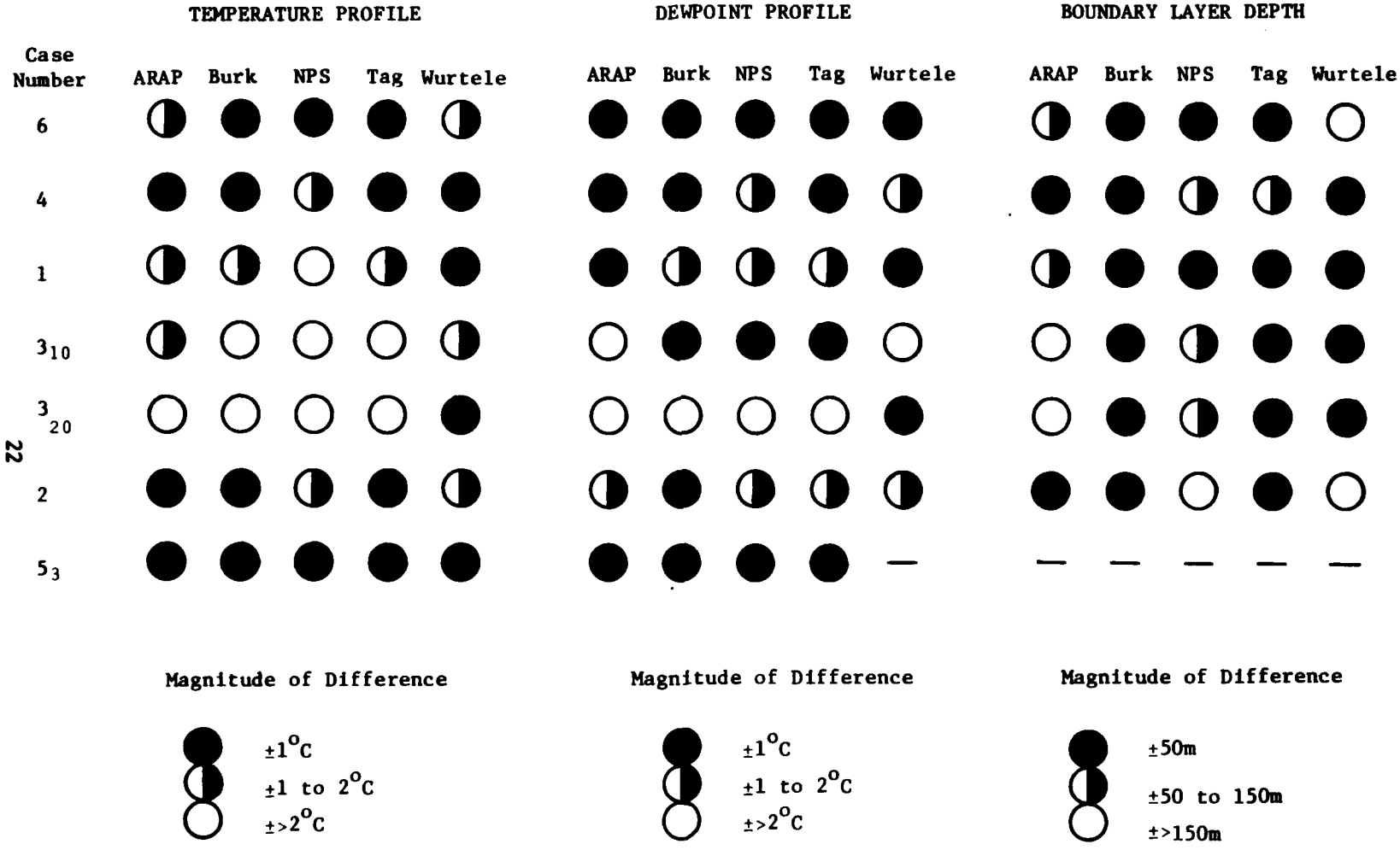

Table 5 Objective Assessment of Model Performance: Fog/Cloud Parameters
(Model Simulations vs. Verification Data)

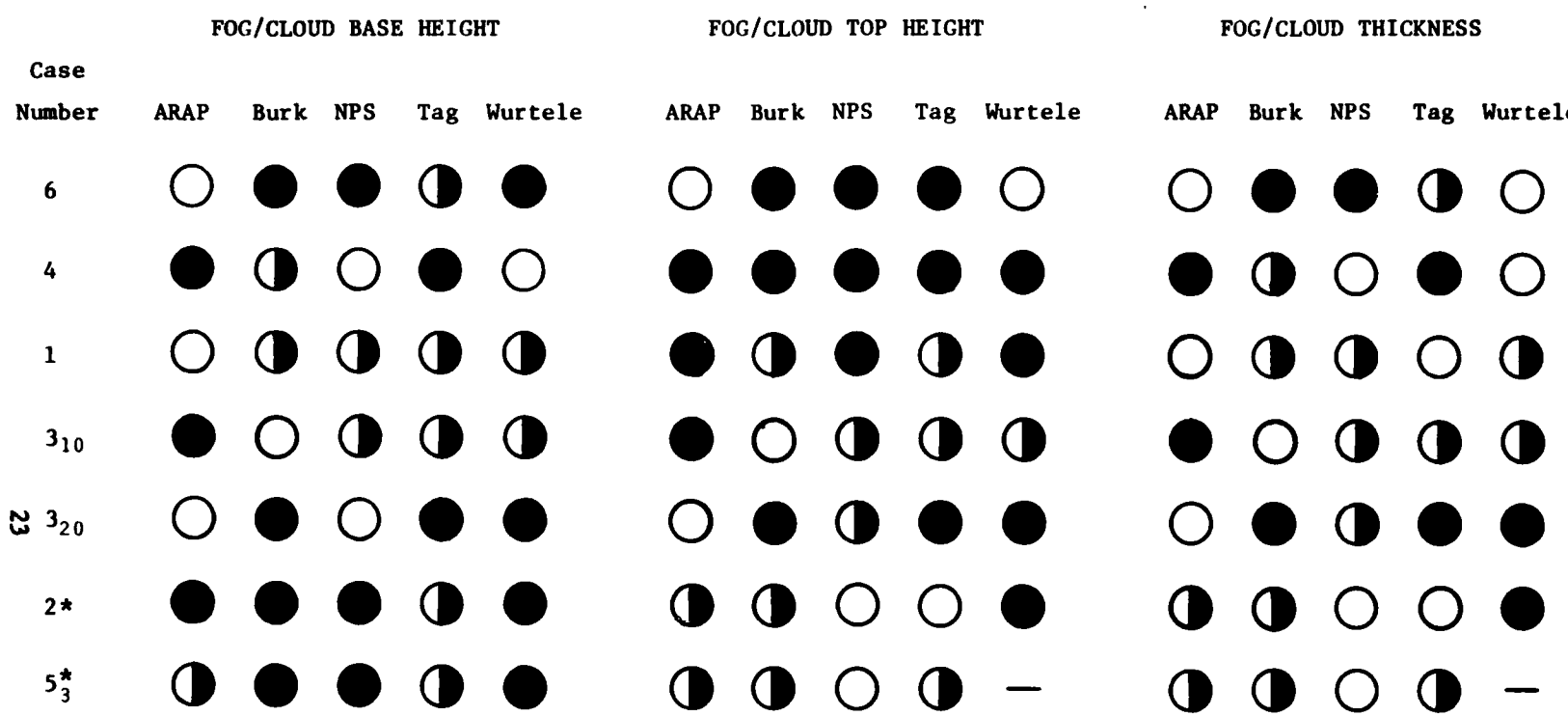

verification conditions nearly as often as they simulated them. Wurtele's model simulated the temperature and dewpoint much closer (almost quantitatively for Case 1 and for Case 3 at 20 hr) than did the other models, all of which produced temperatures that were too cold. Under these net warming conditions, heating from combined absorption of short wave radiation in cloud and positive surface heat flux and cooling from long wave radiation at cloud top were the major driving forces. Integration of the solar absorption computed by the ARAP radiation package (also used by Burk and Tag) and that by Wurtele's scheme showed that the two models produced essentially the same net heating by short-wave absorption. Additional evidence suggests that the simulated temperature profiles for Cases 1 and 3 were too cold in the ARAP, Burk & Tag simulations because the simulated heat fluxes were too small for these unstable meteorological situations. Burk and Tag computed surface fluxes through the Businger et al (Ref. 26) flux-profile relationships and there is some concern about these relationships for unstable conditions such as existed for Case 3. We have recommended that the modeling of heat flux for unstable conditions by these models be reexamined.

For both Cases 2 and 5, the initial temperature profile was inverted, with Case 2 becoming more strongly inverted after advection over colder water while Case 5 developed an isothermal profile over warmer water. The models simulated the verification temperature conditions three times more often than they come close and produced only two "missed" simulations. The common good performance for Case 5 indicates that the models can transform an inverted profile to an isothermal profile, suggesting that the surface flux processes are well modeled for stable to isothermal conditions such as these. For intensification of an existing inverted temperature profile as in Case 2, the HOC models and Tag's locally-computed-K model did the better job. The NPS model, which can only generate a lapse profile, was obviously inferior, and Wurtele's computation of a bulk transfer coefficient for the surface flux also did poorly.

Objective scoring of the specifics of these cloud/fog forecasts summarized in Table 3 is provided in Table 5. Note that for only two of the 21 data sets in Table 5 (Case 4-fog/cloud top and Case 2-fog/cloud base), did four or more models nearly simulate the verification conditions; of 35 possible simulations (7 case runs x 5 models), in only 9 runs did a model fully duplicate the verification cloud within the objectively-set limits. Conversely, in 17 of the 21 data sets at least one model produced a missed simulation. These results demonstrate the relatively poor simulation of cloud boundaries by the models. Considering that these models all lack cloud physics and cloud drop

sedimentation, and some lack fine vertical resolution at cloud boundaries, the relatively weak performance in simulating cloud base is not surprising.

For the fog/cloud top height category, the models did best for the first four (stratus) cases which included all but one of the near quantitative simulations. In stratus situations, the cloud top height is very closely associated with the height of the inversion, a feature which is primarily controlled by large scale subsidence and entrainment. In most of the test cases, the vertical temperature gradient in the inversion was large, so that turbulence and entrainment should be weak at cloud top. Further, the models were given good estimates of subsidence as a boundary condition and should, therefore, have modeled this effect well. Case 3 had strong subsidence and an intense inversion, and the models performed reasonably well except for the ARAP model (at 20 hours) which used too strong a subsidence value. In Cases 6, 4 and 1, where subsidence was nearly zero and entrainment was minimal (because of intense inversions), the models also did well in simulating the height of the fog/cloud top, except for ARAP and Wurtele on Case 6.

Since only one model formed fog in Cases 2 and 5, fog/cloud assessment for the other models was accomplished through use of their predicted relative humidity values in the fog layer. (Our subjective guideline was as follows: if microphysics models such as represented by Fitzgerald's (Ref. 27)[1], and aerosol generation models such as Gathman's (Ref 28) were supplied with the high relative humidity values which were predicted, obscuration would probably be formed within the corresponding fog layers.) The HOC and slab models produced very high RH in the boundary layer, while the K-theory model developed only moderately high RH. NPS shows relatively poor simulation overall for both cases, as the well-mixed model produces only shallow, neutral boundary layers. Wurtele's model produced fog in both cases although much too shallow for Case 5. The poor simulation of fog top heights for these two cases probably reflects the absence of liquid water in the simulations and the subsequent lack of feedback between fog liquid water and cooling from long wave radiation, a relation which is important to increasing fog depth and density in these situations.

The number of near simulations in the fog/cloud base category is only half of that in the fog/cloud top category, while the number of missed simulations is

---

[1] Fitzgerald successfully simulated Case 2, using his own data in 1978, and his results are published in this reference.

almost three times more. In the stratus situation, the turbulence regime is different at the cloud top from that at cloud base. The cloud top, which is located near the inversion at the top of the marine boundary layer where the turbulence is suppressed, is constrained to near the inversion. Contrastingly, cloud base which is located within the eddy structure of the turbulent marine boundary layer and more dependent on the absolute temperature-moisture profiles, is not so easily estimated by the models. In addition for proper simulation of the fog/cloud base, condensation and evaporation as well as vertical transport of cloud drops in a turbulent atmosphere must be modeled correctly; the current models contain neither cloud physics nor drop sedimentation to account for this moisture transport process. Thus the poorer simulation by the models for cloud base as compared to cloud top is not unexpected.

For Cases 2 and 5 in which the fog builds up from the sea surface, the temperature profile is inverted, and fog formation is driven by heat and moisture fluxes at the sea surface. For the model simulations, relative humidity was used to estimate fog height. Since these relative humidity values were chosen arbitrarily and subjectively, the scores should not be used in comparison with other cases; but rather to intercompare the performance of the models within the context of Cases 2 and 5.

In future development, we recommend merging of microphysics models with the boundary layer models. At a minimum, the predicted relative humidity at the forecast time could be used in the microphysics model to compute aerosol growth and visibility for situations such as Cases 2 and 5. A more sophisticated approach would be to use the microphysics model interactively, so that fog liquid water could be generated during the forecast interval and a feedback between LWC and radiation could be introduced during the simulation.

3.1.4 Subjective Assessment of Numerical Model Performance

Tables 4 and 5 provide an objective assessment of numerical model performance based on categorizing of numerical differences between simulated and verification conditions. However, such an assessment is overly restrictive as it does not take into account the "gray" situations in which, for example, a simulated cloud base height is 51 m different from the verification height or fog forms less than one hour after verification time. From an operational standpoint both of these example simulations would provide useful forecast information and could well be said to have

verified. With this consideration in mind, we carefully examined each simulation and assessed it subjectively, using our meteorological experience and judgment, as to whether it verified, was close, or was non-competitive, taking into account any "gray" conditions as well as factoring in the nuances of model framework and capability.

Verification obviously was scored when simulated conditions were very near verification conditions. Non-competitive (NC) occurred when a simulation was extremely far removed from the verification conditions, i.e., fog simulated when none occurred or the simulation was just not representative of verification. Close was scored when simulated conditions were not far removed from verification conditions or, by default, when a simulation either did not qualify as verify or was not really non-competitive. To add some discrimination to the close category we defined "close plus" (+) for simulations near verification, and "close minus" (-) for simulations which were near non-competitive, i.e., close by default. These guidelines then define "close" as being in between the two extremes.

Table 6 presents our subjective scoring or assessment of the numerical model performances using the categories defined above. (Details of how we arrived at the subjective assessments can be found in Appendix C.) On the basis of these six test cases, Burk's HOC model emerges as superior to the others as it scored the greatest number of verifies and least number of NC's. Following these criteria, Tag's K-theory is second and Wurtele's model, although it scored the same number of verifies as Burk, is ranked third because it tied for the greatest number of NC's. Although ARAP's model scored as many verifies as Tag's, it is ranked fourth since it is tied with Wurtele's model for the most NC's. NPS's model is ranked fifth as it had the fewest number of verifies and only one less NC than the models of Wurtele and ARAP. Adding (+) and (-) scores to the verify and NC totals, respectively, does not materially alter the rankings.

As a result of this testing and evaluation, it is recommended that Burk's HOC model be considered a primary model for future, operational fog forecasting. Burk's model is based on a good physics framework and will fit computer resources planned for TESS. However, we recommend that some modifications be carried out before the model is made operational.

TABLE 6 SUBJECTIVE EVALUATION OF NUMERICAL MODEL PERFORMANCE RELATIVE TO VERIFICATION

Fog/Cloud Representation: Position and Depth

	Case						
	1	2	3_{10}	3_{20}	4	5	6
ARAP	close(-)	close	verifies	NC	verifies	close(-)	NC
Burk	close(-)	close	NC	verifies	verifies	close(+)	verifies
NPS	verifies	close	close	NC	NC	close	verifies
Tag	NC	close(-)	close	close(+)	verifies	close(-)	close
Wurtele	verifies	verifies	close(+)	verifies	NC	close(-)	NC
Persistence	verifies	NC	NC	NC	NC	NC	NC

Boundary Layer Depth and Temperature/Moisture Profiles

ARAP	close	verifies	NC	NC	verifies	verifies	NC
Burk	close	verifies	close	close	verifies	verifies	verifies
NPS	close	NC	close	NC	close	verifies	verifies
Tag	close	verifies	close	close	verifies	verifies	verifies
Wurtele	verifies	NC	verifies	verifies	verifies	NC	NC

NC - not competitive

(1) An apparent problem with inadequate accounting for surface fluxes under unstable conditions should be remedied.

(2) Burk's model handles the stratus lowering situations well, for both long and short term simulations, although finer grid resolution at cloud top is recommended to prevent excessive cloud top increase under weak inversions.

(3) To improve simulation of moisture transport processes and the consequent fog/cloud-base forecast, droplet sedimentation should be included in the model.

(4) The model did a fair job in simulating temperature and dewpoint profiles for advection type fogs, in which unsaturated air with an inverted temperature profile moved over either colder or warmer water; however, in these situations, crosstalk with a microphysics model is recommended so that liquid water can be generated in the surface layer and feedback between the liquid water and long wave cooling can enter the simulation.

Although as shown in Table 6, ARAP's HOC model tied for the most NC's, the three of those from Case 3 would probably be upgraded if the large subsidence value which was used were corrected. The ARAP model which is basically similar to Burk's might then be tied with Burk's (in our scoring scheme). However, their model still has an unexplained problem in simulating Case 6, which was the simplest situation among the test cases. For these reasons, we cannot recommend ARAP's model in place of Burk's. However ARAP's model has finer resolution at cloud top which aids in more accurate descriptions of processes at that level. The ARAP model also has finer resolution in the surface layer, which apparently helped the model to better simulate the temperature profiles in the unstable cases. For this latter reason, we recommend that Burk consider some finer grid resolution in the surface layer.

Tag's model was primarily included in the test so that comparison could be made between K-theory and HOC models; the two-dimensional character of the model was secondary. Although Tag's model suffers from a lack of fine grid resolution (because of its two-dimensional resolution) and the surface heat flux problem, we

conclude from our analyses that the relatively good performance by Tag's model indicates that the K-theory approach may have some operational utility. If implementation of HOC-type models is going to strain computer resources, then it is recommended that Tag's K-theory approach be implemented in its one-dimensional mode; the one-dimensional mode is necessary in order to include subsidence in the model.

Wurtele's model, which was ranked third, does well on the neutral to unstable stratus-lowering cases, primarily because of its turbulence formulism. However, the model has a definite problem in simulating the boundary layer for stable situations, where water is colder than the air, despite the fact that it properly predicted fog; however even where fog is properly forecast, predicted liquid water contents are many times abnormally large. Since an operational model must be able to handle all types of conditions and LWC must eventually be used in the forecast interpretation, we do not at this time recommend use of Wurtele's model in lieu of HOC in operational forecasting unless the indicated problems with the HOC model cannot be solved.

The NPS model does reasonably well on short-term, neutral boundary layer stratus lowering cases, but its long wave radiation package generates too much cooling for an entire night. Further, this model can only produce well-mixed lapsed temperature conditions, which limits its performance in stable situations. However, it runs extremely quickly, and can be operated on current desk-top computers. For these reasons, we recommend that it be considered as a candidate operational method for obtaining a "quick-look" forecast, especially when a short term forecast is required and neutral to unstable conditions such as West Coast stratus are expected. Operational circumstances may at times dictate the use of some simplified numeric approach such as NPS' slab model.

3.2 SUMMARY OF SYNOPTIC/STATISTICAL MODEL TESTING

Assessment of the non-numerical techniques required a more qualitative approach than did assessment of the numerical models because predictions for only six cases were not judged sufficient to fully evaluate synoptic/statistical type forecast models. Since these procedures basically provide a yes-no forecast of fog occurrence, proper evaluation of the synoptic-type procedures requires a statistical test on an appropriately large data sample. Although such a test has been done previously on one of the synoptic models, such comprehensive tests on the other synoptic models were

outside the scope of the current contract. Therefore, evaluation of the synoptic models was based not only on skill with the six test cases but also on a critical examination of the technical, predictive capability of the model elements and the physical content of the models.

3.2.1 Synoptic Model Selection

From a potential list of approximately 10 non-numeric forecast approaches, four were ultimately selected for testing while several others were evaluated based on their conceptual design and physical content. The models which were selected for testing on the six data sets (previously described in Section 3.1.2 and Appendix B) included the following: Calspan's Decision Tree (Ref. 18) developed under an earlier NASC contract; Leipper's Indices (Ref. 30), an approach used operationally at North Island NAS (Ref. 31), Leipper's Inversion Statistics (Ref. 32) and Calspan's Inversion Statistics Model, developed under the current contract (see Section 5) and patterned after Leipper's. In this Section, emphasis is placed on the results of testing these four models on the six test cases. Additional discussion of these and other forecast procedures not tested can be found in Appendices A and C. Calspan's preliminary Decision Tree (the version tested on this program) is reproduced in Appendix D.

Salient features of the models which were selected for testing are shown in Table 7. Detailed information on the characteristics of all the synoptic/statistical models is provided in Appendix A. The key predictive element in the models listed in Table 7 is the height of the inversion. For the Leipper Indices model, an inversion below 400 m contributes a "yes" for fog occurrence. In the two inversion statistics models, the inversion height provides the predicted visibility (a probability value) through frequency-of-occurrence statistics, while in the Calspan Decision Tree both fog occurrence and phenomenology are functions of inversion height. With the exception of the Decision Tree's Part 1 which attempts to link synoptics to inversion height, a forecast of inversion height is crucial to the application of any of these models.

3.2.2 Evaluation of Synoptic Model Performance

Despite the belief that the six test cases are not sufficient for statistically meaningful evaluation of the synoptic approaches, for reference and comparison with the numerical models evaluation, this set of forecast procedures was exercised objectively

TABLE 7

SALIENT FEATURES OF CANDIDATE SYNOPTIC/STATISTICAL MODELS

MODEL	BASIC DESIGN	INPUT	OUTPUT
Calspan Decision Tree	Specifies inversion height from 850-mb pattern. Phenomenological fog occurrence determined from inversion height.	Predicted 850-mb flow pattern and middle or high cloud. Observed inversion intensity.	Qualitative fog occurrence and type.
Calspan Inversion Statistics	Probability of visibility categories vs. inversion height. Derived from coincident visibility values and inversion heights from acoustic sounder.	Predicted inversion height.	Probability of visibility by quarter of 24-hour day.
Leipper Inversion Statistics	Probability of early morning minimum visibility vs. inversion height, visibility values separated by 90 miles from inversion height determined from radiosonde data.	Predicted inversion height.	Probability of early morning, minimum visibility.
Leipper Indices	Fog occurrence vs. indices values. Indices are inversion height, air temperature and dewpoint vs. sea surface temperature, middle-level moisture content.	Indices values derived from previous day's measurements	Fog-no fog occurrence for period evening through next morning.

on the six data sets and assessed subjectively by the Calspan principal investigators and staff meteorologists. The results from these tests are presented in Tables 8 and 9.

Table 8 provides the actual forecasts produced by the models compared with verification and persistence forecasts. In the table, the Calspan Decision Tree results presented in the first row represent the consensus of all "forecasts" made using both Part 1 of the procedure which determines the inversion height from the synoptic patterns and Part 2 which provides the fog forecast from knowledge of inversion height. The second row of results for the Decision Tree was generated by using the verification inversion height as input to the fog forecast portion (Part 2) of the model. Verification inversion height was also used as input to both inversion statistics models. Since the Leipper Indices model is not designed to use forecast parameters as input, the observed initial conditions were used as input.

The NA's in Table 8 represent "not applicable" for the following reasons. The 10-hour verification time for Case 3 was at early afternoon, and the Calspan Inversion Statistics Model is the only one of these approaches designed for application at that time of day. This same model was NA in Case 2 which had a surface-based inversion, a condition for which no category is available.

Table 9 presents Calspan's subjective evaluation of the operational utility of the forecasts produced by synoptic/statistical models, comments on which can also be found in Appendix C. Examination of the table reveals that the synoptic models as a group outperformed the persistence forecast. The Calspan Decision Tree with use of the verification inversion and the Calspan Inversion Statistics model are the only two methods which scored only one non-competitive mark, both of which stem from the NA's discussed above. The full Decision Tree produced the greatest number of NC forecasts and still beat the persistence forecast. The Decision Tree with the verification inversion, along with Leipper's Indices, generated the greatest number of verifications.

Analysis of the Decision Tree scores suggests that use of this tool has merit for the West Coast synoptic patterns for which it was designed. Note that the Decision Tree tied for the most verifies when the verification inversion was used. However, it also had the most NC's when Part 1 was used to provide an inversion height as input to Part 2. In the latter format, the NC's for Cases 2 and 5 are not surprising

TABLE 8

SYNOPTIC MODEL PERFORMANCE ON CALSPAN DATA SETS

Fog/Visibility Forecast

	Case						
	1	2	3_{10}	3_{20}	4	5	6
Calspan Decision Tree	No Fog	No Fog	NA	Fog	No Fog	No Fog	Dense Fog
Calspan Decision Tree (using verification inversion)	No Fog	Shallow Patchy Fog	NA	Fog	No Fog	Shallow Patchy Fog	Dense Fog
Calspan Inversion Statistics (using verification inversion)	0/0/0*	NA	4/11/23	11/14/36	0/0/1	51/71/80	13/18/31
Leipper Indices (using initial conditions)	No Fog	Fog	NA	Fog	No Fog	Fog	No Fog
Leipper Inversion Statistics (using verification inversion)	6/-/40*	26/-/36	NA	34/-/71	6/-/40	59/-/94	59/-/94
Persistence	No Fog	No Fog	No Fog	No Fog	No Fog	No Fog	No Fog
Verification	No Fog	Shallow Fog	No Fog	Dense Fog	No Fog	Dense Fog	Dense Fog

* For the two inversion statistics models, forecasts are in probability (% frequency) of occurrence of visibilities ≤0.5/≤1.0/≤3.0 mi, respectively

NA = not applicable

TABLE 9

SUBJECTIVE EVALUATION OF SYNOPTIC MODEL PERFORMANCE RELATIVE TO VERIFICATION

Fog Forecast

	CASE 1	2	3_{10}	3_{20}	4	5	6
Calspan Decision Tree	verifies	NC	NC	verifies	verifies	NC	verifies
Calspan Decision Tree (using verification inversion)	verifies	verifies	NC	verifies	verifies	close	verifies
Calspan Inversion Statistics (using verification inversion)	verifies	NC	verifies	close(-)	verifies	verifies	close(-)
Leipper Indices (using initial conditions)	verifies	verifies	NC	verifies	verifies	verifies	NC
Leipper Inversion Statistics (using verification inversion)	close(+)	NC	NC	close	close(+)	close(+)	close(+)
Persistence	verifies	NC	verifies	NC	verifies	NC	NC

NC - not competitive

since these cases were stable atmosphere, advection-fog situations in the western Atlantic, circumstances for which the inversion height vs. synoptic pattern portion of the model was not designed. Both NC's are upgraded when the observed inversion height is used, thus substantiating that the problem with applying the Decision Tree occurred in the inversion height specification part. The only NC which occurs in both tests of the Decision Tree is the daylight portion of Case 3, a time of day which is not included in the model's present design but which is being investigated under further development of the Decision Tree Model. For the other cases involving a marine boundary layer of finite depth, the Decision Tree functioned as designed and verified; it also provided phenomenological information relative to the fog forecast.

The Leipper Indices approach produced the same number of verifies as the Decision Tree which used the observed inversion height, primarily because the Indices Model verified for the advection-fog type cases (numbers 2 and 5) but not necessarily for the proper physical reasons. Since these cases were characterized by a surface based inversion (with the lowest air temperature very near that of the sea surface), the indices for inversion height, upper air temperature and low level moisture (which were designed for the stratus lowering situation) were also satisfied for the advection fog situations. In addition, these advection fogs occurred under cloud free and dry conditions aloft, and the condition of low mixing ratio aloft was also satisfied. All the indices were, therefore, "yes" and the technique forecast fog for the advection fog cases.

Like the Decision Tree, the Indices model will nearly always forecast fog if skys are clear and an inversion exists below 400 m. However, as is the case for the Decision Tree, the Leipper Indices are not designed around the physics of advection type fog, and we cannot, therefore, recommend using either approach for this fog type until a proper statistical test demonstrates suitability. However, the Indices are objective and, in the absence of any other forecast approach, can provide a forecast which can be better than persistence, particularly for West Coast circumstances. In fact, results of a recent statistical study of the Indices' capability (Ref. 33) suggest that the technique does have merit, especially when its objectivity is considered.

Of the non-numeric techniques tested, the inversion statistics approach probably offers the most promise in providing objective, yet quantitative forecasts in the realm of marine fog. These relatively new models provide a probability of visibility

forecast, as a function of inversion height, based on frequency of occurrence data; hence, they are probably site and circumstance specific. For example, both of the models tested here were developed from slightly inland West Coast marine inversion situations: Leipper's from Monterey surface data and morning Oakland soundings, and Calspan's from Monterey surface data and 24-hour Monterey acoustic sounder records. Further, the capability of these models to produce operationally useful forecasts is also dependent on the size of the data set from which they were derived and the resolution afforded by the data classifications. Finally, these models require a forecast of inversion height for the verification period. Despite these caveats, the models produced quantitative forecasts and scored quite well on the six test cases, none of which occurred inland at Monterey.

The forecasts produced by the inversion statistics models for the six cases are provided in Table 8 in terms of percent probability for the visibility categories $\leq$0.5 mi, $\leq$ 1.0 mi and $\leq$ 3.0 mi; hence, the scoring shown in Table 9 was necessarily very subjective. Note that Leipper's model lacks the $\leq$ 1.0 mi category (resolution) and, largely for this reason, scored close (+) rather than verify for four cases. Calspan's model scored verify on four cases but rated close (-) on two others (cases 3 and 6 on which it should have done well) because the verification hour fell near the cut-off for the nighttime category and possibly because the model uses inland data in which late evening visibility can be effected by residual daytime heat. Leipper's model had an NA=NC in Case 3_{10} because it contains no daytime statistics and Calspan's model had an NA=NC in Case 2 because it contains no zero height (ground-based) inversion data.

Both inversion statistics models are based on data for Monterey, and studies are required for additional sites along the West Coast to determine the universality of the concept and/or the existing models. While a recent pilot study, carried out in parallel with this contract by Dixon (Ref. 34), indicated that the inversion statistics approach did not work well along the Santa Barbara Channel at Point Mugu, Beardsley's work (Ref. 35) suggests that the approach is applicable along the coast northward from Monterey to at least San Francisco. Earlier studies by Calspan suggest that it is applicable at least as far south as Point Conception (Ref. 36) and within several hundred kilometers offshore (Ref. 2,3,12). From our knowledge of the technical, predictive capability and the physical content of the synoptic/statistical models, we think that the approach can be operationally useful and recommend that inversion statistics be pursued on an individual basis for sites along the west coast of continents

and generalized for at-sea usage. In addition it is suggested that these models be formulated so as to provide resolution for light, moderate and dense fog and to define time periods which are more representative of fog occurrence and phenomenology than in current models.

Until a reliable, mesoscale forecast of inversion height becomes available in large scale numeric forecasts or from mesoscale numerical models such as described in Section 3.1, an inversion height derived through use of numerically predicted synoptic patterns and Part 1 of the Decision Tree Model may be the best approach to providing this information for the inversion statistics models. It should be recognized, however, that the current inversion statistics models were developed from West Coast data and should not in practice be applied to surface-based inversions associated with advection type fogs. Sites without numerical capability or visibility vs inversion statistics could use the entire Decision Tree with the phenomenological fog models in Part 2, the fog forecast portion. Sites with no forecast material available could default to the Leipper Indices approach for an objective forecast but should recognize its limitations and rely heavily on the subjective, phenomenological approach to help in interpretation of such fog forecasts. These ideas are elaborated in Section 4 which follows and which discusses a potential design for a fog forecast system which could aid the forecaster in the determination of the most appropriate forecast approach.

Section 4
A FORECAST SYSTEM FOR MARINE OBSCURATION

Since 1972 Calspan was actively involved in the Navy's Marine Fog Investigation (MFI) with the broad objective of improving Navy fog forecast capability. Early at-sea studies conducted by Calspan generated much new knowledge of the physics and meteorology of marine fog occurrence and helped revise widely-held theories of marine fog formation. These and later studies produced phenomenological descriptions of a number of fog types and developed synoptic and statistical relationships which can be used in operational forecasting of marine fog. More recently under the current contract, we conducted an impartial evaluation of the potential utility of a select group of existing numeric and synoptic models in the operational forecasting of marine fog (see Section 3).

As a chief objective of the current contract, we initiated design of an obscuration forecast system which, when fully developed, would incorporate this new understanding of marine fog occurrence and delineate the application of specific numeric and/or synoptic and statistical approaches; i.e., the system would specify a forecast tool(s) tailored to the attendant meteorological scenario and functional within operational constraints. The conceptual design of this system is discussed in Section 4.2. Detail on how the system could be configured and how the new knowledge of the physics and meteorology of marine fog occurrence could be employed in operational forecasting may be found in Section 4.3. A summary of state-of-the-art knowledge of marine fog occurrence, developed by Calspan under earlier NASC contracts, is provided in Section 4.1 and Appendix E.

4.1 A SYNOPSIS OF MARINE FOG OCCURRENCE

As a result of numerous at-sea observational programs, particularly those conducted by Calspan off the West Coast during the mid-Seventies, knowledge of the micro- and mesoscale physical and dynamic characteristics of marine fog has been substantially increased (e.g., Ref. 2,3,6,12). Physical models have been formulated to describe the formation and persistence of stratus-lowering fog and at least three other previously unidentified types of marine fog which occur off the West Coast: fog triggered by instability and mixing over warm water patches, fog associated with low-

level mesoscale convergence, and coastal radiation fog advected to sea with subsequent horizontal mixing.[1] Further, it has been found that the triggering of embryonic fogs and subsequent downwind growth can produce a synoptic-scale fog-stratus system and be responsible for redevelopment of the unstable marine boundary layer after Santa Ana events along the West Coast (Ref. 15).

Limited observations off the coast of Nova Scotia and in the northern Gulf of Mexico suggest that similar processes and fog formation mechanisms are also operative in those areas. However, the data also reveal some major differences in the relative contributions of the various factors involved in fog development and show that marine fog can be triggered or developed through mechanisms (such as by advection over cold water) not yet observed off the West Coast. Further, while fog was observed to form off Nova Scotia both through advection and mixing processes over warm water and through the radiation-driven stratus-lowering mechanism, the most dense fog (lowest visibility) was generally observed farther downwind where the fog subsequently advected over much colder water—i.e., lowest visibilities were clearly associated with the coldest sea surface, but most of the fogs were not triggered by the cold water patches. These results are not unexpected since, while the same physics should apply, the meteorology and oceanography of the three areas are substantially different (Ref. 8 and 18).

Detailed analyses of the observations have revealed that formation and persistence of the fog types described above is dependent on the dynamic interaction of a number of boundary layer processes along with meteorological and oceanographic features linked from the microscale to the synoptic scale. For example, Calspan data have conclusively shown that while heat transfer from air to ocean can be responsible in some instances for triggering fog formation, the direction of heat transfer is always the reverse after fog forms due to net radiative cooling of fog liquid water. Dynamic processes associated with radiative cooling at upper levels of embryonic fogs and warming from below are primarily responsible for continued development and persistence of all deep marine fogs. Further, our observations have verified the necessity for a capping inversion at a height of less than 400 m for dense fog occurrence at the surface and demonstrated the relationship (at sea) between the relative heights of the inversion and the lifting condensation level and its influence on the formation of stratus and subsequent obscuration at near-surface levels. Similarly, the development of synoptic

---

[1] These fog types are discussed in greater detail in Appendix E.

scale fog-stratus systems evolving from microscale boundary-layer exchange processes which trigger embryonic fog also demonstrates the existence of links between the micro-, meso- and synoptic scales (Ref. 15).

In terms of fog microphysics and density, direct relationships between the ambient aerosol population and the microphysical characteristics of marine fog have been demonstrated. Calspan data show that the marine aerosol population, which becomes increasingly less continental and drops markedly in number concentration with increasing distance offshore, varies considerably, both spatially and temporally, in both concentration and chemical composition and does not necessarily comprise primarily sea salt aerosols (Ref. 8,11,12,13,14,19). On the other hand, the liquid water generated by processes which produce dense fog is relatively conservative compared to variations in aerosol content. Hence, higher concentrations of condensation nuclei generally give rise to fog droplet populations with greater numbers of smaller drops, resulting in fogs of lower visibility. As a result, for a given liquid water content, fogs formed immediately along a coastline or downwind of land masses tend to exhibit lower visibilities than those occurring farther to sea or upwind of aerosol sources (Ref. 8,12 19).

Key factors in the occurrence of marine fog, particularly along the west coast of the United States, include the open-ocean marine layer which is modified by cold water in upwelling areas, adjacent patches of warm and cold water in the upwelling zone, low-level subsidence such as found in the semi-permanent subtropical high, and coastal mountain ranges. In order for marine fog to develop, these elements must combine to produce a relatively shallow marine layer, capped by an inversion whose strength and height are controlled by a balance between dynamic vertical motions aloft in the layer up to 1500 m and thermodynamic processes within the surface marine layer. Superimposed on this general situation are the influences of migrating mesoscale systems and their dynamic vertical motions, downslope motion, the land/sea breeze cycle, low-level convergence patterns, the height of the lifting condensation level, airmass aerosol characteristics, and radiation from condensed liquid water and coastal land surfaces. Marine fog rarely develops if high clouds prevent net radiative cooling within the marine boundary layer or if the marine boundary layer is greater than 400 m in depth.

Dense fog seldom exceeds 400 m in total thickness; therefore, dense fog will not exist at a point which is more than 400 m below the base of the marine

inversion unless a secondary surface-based inversion is first established. When the inversion is at heights higher than 400 m, 400 m thick stratus can develop, and reduced visibilities (dense haze) can occur in the high relative humidity zone beneath cloud base. The situation is described by the model of a stratus cloud at the top of a well-mixed layer: wet adiabatic lapse rate and consequent LWC profile (Ref. 37) within cloud and dry adiabatic temperature structure and RH profile below cloud base. Visibilities are dependent on the aerosol burden and the relative humidity structure, but in the mean can be related to distance from cloud top—i.e., the inversion height (see Section 5).

As suggested, sea fog occurs in the surface marine layer, and, given a variety of trigger mechanisms, its occurrence is primarily dependent on the height, fluctuations and strength of the inversion which caps the marine layer. Study of synoptic sequences and associated fog episodes has shown that fluctuations in the height of the marine inversion over periods of days are generally caused by evolution and movement of both large and small scale synoptic disturbances. It is the vertical motion in these disturbances and flow patterns in the layer up to 1500 m which control the height of the inversion. (Superimposed on these vertical motions are downslope motions along the coast, the land/sea breeze cycle and the influences of convergence-induced vertical motions such as have been documented in the vicinity of prominent points along the coast and over warm water patches.) These flow patterns are manifestations of (1) slowly-moving long-wave systems, (2) large-scale synoptic systems whose driving forces operate at mid-atmospheric levels, and (3) small-scale synoptic systems concentrated in the 500-1500 m layer. Our studies suggest that inversion height along the West Coast can be related to these types of flow regimes (Ref. 18 and Appendix D).

Thus, forecasting the occurrence of marine fog requires information on the structure of the marine inversion, the sea surface temperature pattern, surface to 850 mb synoptic and sub-synoptic systems (and by implication, the wind field in the layer up to 1500 m) and knowledge of their impact on height and strength of the inversion, the height of the lifting condensation level or surface-level temperature and dewpoint, the potential for influence of downslope motion, subsidence, the land/sea-breeze cycle and convergence patterns on inversion height, and the potential for long-wave radiation from either condensed liquid water or coastal land surfaces. An improved fog forecast capability based on physics and meteorology requires knowledge of the physical characteristics and dynamic processes attendant to various fog types

and an understanding of the links in these processes from the microscale to the synoptic scale. Operationally, this understanding must be factored into attendant meteorological and oceanographic circumstances to produce a fog forecast.

It should be recognized that the understanding and information required for development of the ultimate fog forecast capability also has direct applicability to the Navy's electro-optic obscuration and propagation problems. The same physics, dynamic processes and aerosols which lead to visibility restrictions due to development of a supersaturation (fog/stratus), first, and probably more frequently, lead to obscuration through increases in relative humidity (below saturation) and growth of hygroscopic aerosols to form "clear air" visibility restrictions (haze). In the haze situation, the aerosol population (size spectra and composition) and relative humidity structure are variables which must be estimated in order to produce useful visibility forecasts.

In summary, Calspan's efforts have produced a substantial portion of the basic knowledge and current understanding of marine fog occurrence. Certainly, the elucidation of four mesoscale fog types, the concept of a synoptic scale fog-stratus system, the demonstration of the important influences of the marine inversion, the lifting condensation level, radiative flux divergence, warm water patches, low-level convergence and the ambient aerosol population, the linkage of dynamic vertical motion at low altitudes in meso- to synoptic scale systems to the height and strength of the inversion (Ref. 18), and the demonstration that certain fog features are recognizable from current meteorological satellites (Ref. 6) is knowledge which can lead to some immediate improvement in fog forecast capability particularly along the West Coast.

In recent years we have begun development of experimental tools such as the Decision Tree (Ref. 18) and the Inversion Statistics model (see Section 5) in an attempt to link the physics of fog formation to the meteorological scenarios which typically give rise to marine fog. Under this current contract, we have been carefully examining these and other MFI achievements of the Seventies in a search for methods for utilizing this new understanding in the operational forecasting of marine fog. All questions have not yet been answered, and gaps in our knowledge remain. However, the recommended rational assembly of this new knowledge, coupled with the best of newly-developed numeric, synoptic, statistical and phenomenological models for marine fog and the marine boundary layer (see Section 3) is expected to lead to improved, operationally-useful forecast schemes. A preliminary version of a forecast system for

marine obscuration, which attempts to incorporate the fruits of the MFI, is outlined in the next Section.

4.2 SUMMARY OF THE BASIC CONCEPTS OF CALSPAN'S PRELIMINARY DESIGN FOR AN OBSCURATION FORECAST SYSTEM

The following summarizes Calspan's preliminary design and basic concepts for an obscuration forecast system. The system is designed to guide the forecaster to the appropriate forecast procedure within the context of available data, available computational capabilities, operational constraints and the most likely meteorological phenomena. Determination of the latter is based on much of the new knowledge of the physics and meteorology of marine fog occurrence developed from the Navy's Marine Fog Investigation. Determination of the former is based on the ability of specific forecast tools to handle the anticipated meteorological scenario in the context of available initialization data. It is recommended that the system incorporate approximately three different numerical models and approximately five synoptic/ statistical approaches from which a selection(s) can be made.

The system described here is intended for use in operational scenarios ranging from the battlegroup to single stations. For eventual integration into the Tactical Environmental Support System (TESS), it should utilize anticipated TESS observational, computational and graphics capabilities. The most sophisticated of the numerical models available for use in this forecast system require computational capabilities which should be locally available when TESS becomes operational. With appropriate provision for look-up tables, data estimation and manual decision-making, the envisioned forecast system (in hard copy) would provide a significantly enhanced obscuration forecast capability even for data- and computer-poor, isolated single stations. In a 'tactical applications guide' format, the knowledge derived from the MFI could also serve in the training of new forecasters.

As envisioned, the forecast system would comprise a set of procedures each of which would be keyed to forecasting a specific type (or set) of obscuration phenomena. Conceptually, a guide would be designed to aid in the preliminary determination of the obscuration type(s) most likely to occur in the existing meteorological scenario and to then determine which forecast procedure or tool(s) should be applied. However, data availability may range from single station observation to

battlegroup observations to synoptic scale analyses, and forecast requirements will range from very short to long-term; forecast procedure utilization would be affected accordingly. Therefore each procedure would also have different levels of application designed on input data availability: i.e., in some instances a certain numerical model might be called for; in other situations, sufficient data may not be available to properly initialize a more sophisticated numerical technique, and less sophisticated numerical, statistical or synoptic approaches may be required; in still other situations, computer facilities might be incapacitated or not available, and the determination would default to the best synoptic and/or statistical approach for the anticipated obscuration phenomena.

Practical applications of such a forecast system will occur with sets of situations, data availability and computer capabilities which lie somewhere between the extremes suggested above. A procedure, such as outlined schematically in Figure 1, can be designed so that if the input data for the numerical models were not directly available from observations, appropriate approximation for the data could be provided: e.g., estimation of vertical soundings from surface temperature and dewpoint observations and estimates of boundary layer depth. The system, whose conceptual design is discussed here, could be organized in a decision tree format. It could consist of a series of questions and answers to determine from the meteorological scenario the most likely phenomena to be encountered (a preliminary forecast) and the forecast approach which could be best utilized given the available data.

In summary a combined numeric and synoptic approach is recommended in which synoptics and phenomenology could be used to help initialize, to help select appropriate numerical forecast models, to help interpret numeric results and to serve as a back-up forecast tool. The obscuration forecast system described herein could be developed exclusively from existing knowledge, procedures and numerical models for application with current, operationally-available data. The system could make maximum usage of the new knowledge of physics and meteorology of marine fog generated by the Navy's MFI, useful knowledge which has yet to find its way into the operational realm. The system could also take advantage of recent evaluations of numerical models and other forecast tools. As currently envisioned the recommended tools for use in such a system include: Burk's HOC model, Tag's K-theory model, the NPS' mixed-layer model, Renard's MOS model, improved versions of Calspan's Decision Tree and Inversion Statistics models, Leipper's Indices, climatology and persistence. It is also recommended

Figure 1

SCHEMATIC OF CALSPAN'S PRELIMINARY DESIGN OF AN OBSCURATION FORECAST SYSTEM FOR USE IN THE MARINE BOUNDARY LAYER

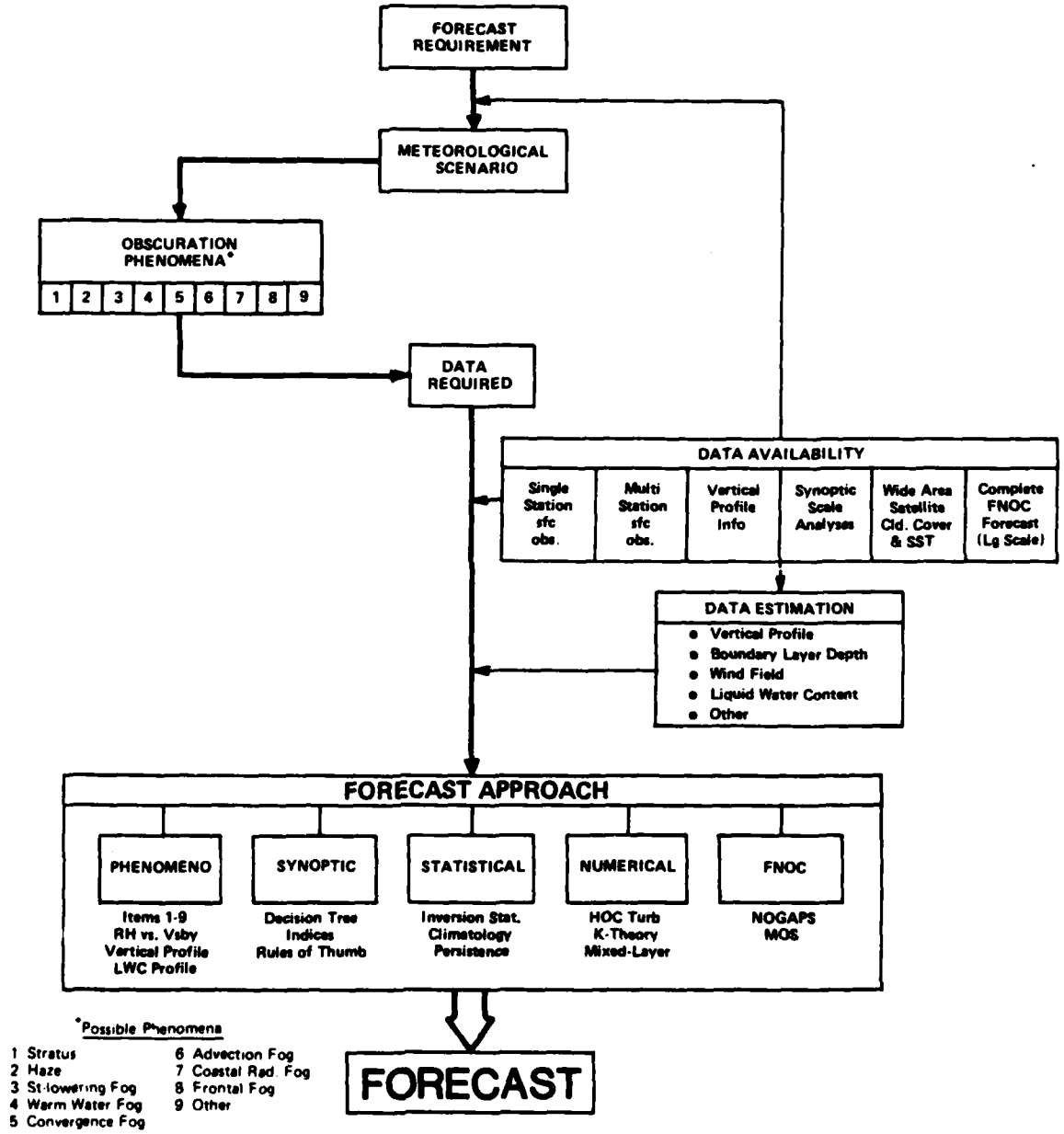

that provision be made for eventual use of Gathman's aerosol generation model, Fitzgerald's microphysics model, and Calspan's LWC algorithm (Ref. 37), constructed soundings and aerosol climatology models. It is estimated that such a system could be designed with an approximate one-man-year effort. Preliminary testing and development of the concept into a computer-interactive system could require an additional one-man-year effort. Operational testing and advanced development would require additional effort.

However, some gaps remain in our knowledge of marine fog behavior in remote ocean regions and areas other than west coasts. It should be recognized that most of the knowledge and concepts developed through MFI efforts focus on West Coast fog scenarios. The limited studies of marine fog at other locales suggest that the physics and trigger mechanisms observed off the West Coast are operative elsewhere while the meteorology and oceanography which give rise to these conditions are different. Mid-ocean fog development is undocumented and remains a major gap in our knowledge. Synoptic techniques and numerical models, which were 'tuned' by West Coast fog conditions, may not be as functional in the meteorological scenarios of other locales. Further, many of these models, including synoptic/statistical approaches, are untested in the data-sparse operational environment. We therefore recommend that some limited additional research into these aspects be undertaken. Results of such applied studies should significantly add to our confidence in the knowledge of marine fog behavior and, consequently, in the validity of numerical models, in the utility of the forecast system and in the accuracy of forecasts.

4.3 DISCUSSION OF A POTENTIAL CONFIGURATION FOR AN OBSCURATION FORECAST SYSTEM

In the preceding discussion, the conceptual design of Calspan's recommended forecast system was discussed and presented schematically in Figure 1. In summary, we envision a combined numeric and synoptic approach in which synoptics and phenomenology (such as discussed in Section 4.1) are used to help select and initialize the most appropriate forecast tool available (for the anticipated meteorological scenario and in the context of operational constraints), to help interpret numeric results, and to serve as a back-up forecast tool. The following discussion provides detail on how the system could be configured and describes how new knowledge of the

physics and meteorology of marine fog occurrence could be employed in operational forecasting.

4.3.1 The Framework

The envisioned system comprises three basic components: (1) phenomenological description of obscuration phenomena and determination of anticipated phenomena in the context of the anticipated synoptic/mesoscale meteorologic scenario; (2) determination of available initialization data and the anticipated meteorologic scenario and provision for estimation of required initialization data not locally available; and (3) selection and exercise of the most appropriate forecast tool for the anticipated meteorologic phenomena (in the context of data availability and operational constraints) and interpretation of numeric output as required. The heart or basic framework of the system is the logic for the required decision processes: "What are the criteria? What are the questions? What are the decisions? Which predictive tools should be used and under what circumstances?" Generation of the logic and determination of the decisions to be made within and interactively between these components is required as the next step in development of the system outlined below.

The major parts or operating steps of the forecast system diagrammed in Figure 1 are shown schematically in Figure 2. The starting point is a user-supplied requirement for a forecast of obscuration at some density level and time in the future. The user's need-to-know requirement may range from conditions of mild to severe visibility restriction, (i.e., $\geq$ 10 km to $\leq$ 500 m, light haze to dense fog); and time frames of the forecast may range from the very near-term (1-2 hours) to 12 to 24 hours. Distances from the current ship location and size of the forecast area will also vary, largely in tune with the time scale of the forecast. Thus, the forecast system must be able to handle conditions covering a wide spectrum of visibility restrictions and time and space scales to be operationally useful.

Given that no single forecast tool can suffice for the variety of operational circumstances and constraints and meteorological scenarios likely to be encountered, between the request and the forecast there can be a process or series of decisions to assist the forecaster in the selection of the most appropriate forecast tool. For example, in the context of the attendant meteorological situation, an initial estimate of most likely obscuration phenomena could be developed from phenomenology (see

Figure 2

OVERVIEW OF OBSCURATION FORECASTING SYSTEM

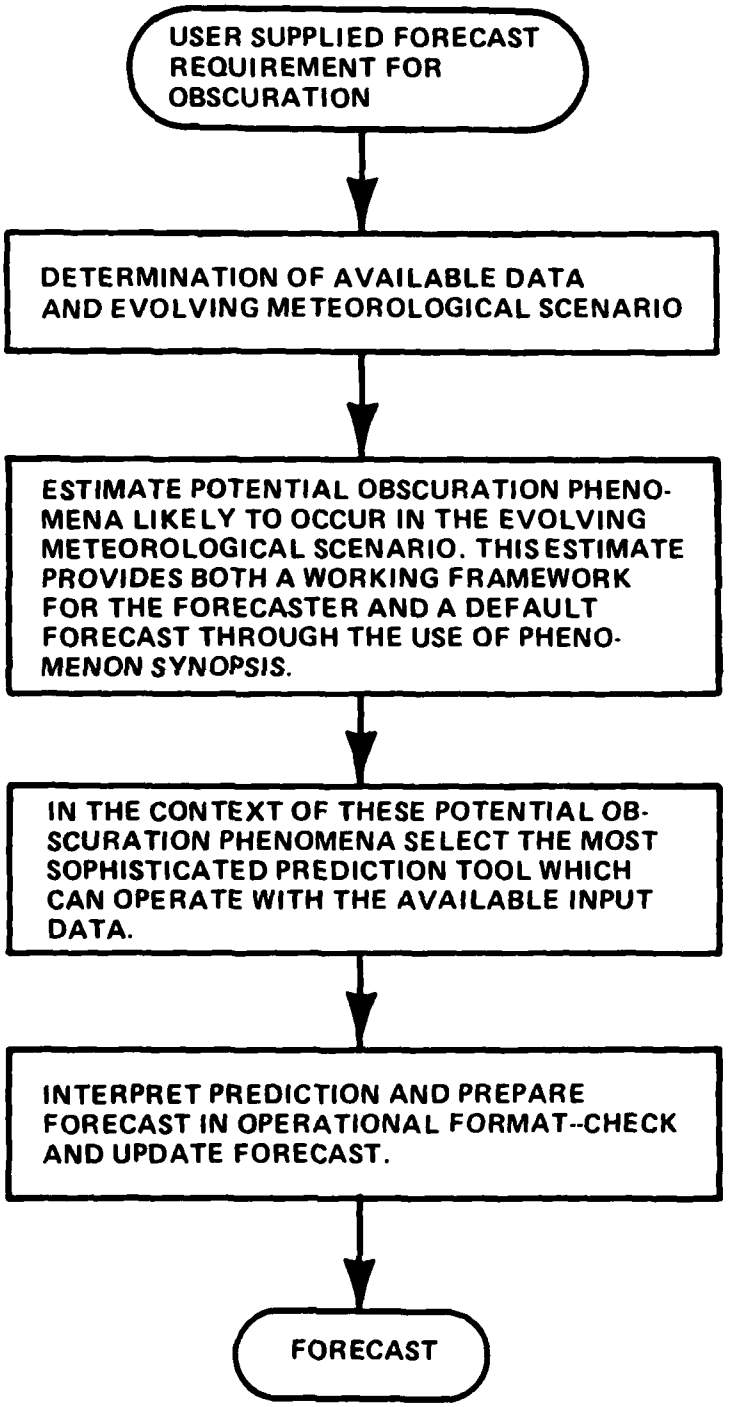

Section 4.1 and Ref. 8, 15) and would materially aid in determining the ultimate forecast. In the case of sufficient data, the estimated obscuration phenomenon could play a large role in the selection of the optimum forecast approach by the forecast system. When sufficient data are not available to initialize a numerical model or other forecast technique, a synopsis of the obscuration's phenomenological behavior, by itself, could provide forecast information not otherwise available. In the event that the forecast system elects a numerical model to make the forecast, knowledge of phenomenological behavior could be used to help interpret numeric output.

The selection of the most likely obscuration phenomenon requires knowledge of the evolving meteorological scenario which implies a certain level of data availability. The synoptic scale meteorological scenario is ascertained routinely in operational weather offices; but selection of mesoscale obscuration phenomena requires that attention be given to the mesoscale space and time scenario, and, thus, more detailed local data are required. In addition, for a given obscuration phenomenon, a set of forecasting approaches exists which can be ranked according to the amount of input data they require. For example, higher order closure models require more detailed information in the vertical than do mixed-layer models. In the contemplated forecast system, these data requirements would be compared to available data until a match is found and the forecast approach is determined. In the event that some or all mesoscale data are missing, provision could be made for estimation of some variables so that a 'library' forecast tool could be used.

4.3.2 Data Availability and Estimation

The design of the scheme presented in Figure 2 must be carried out in the context of the operational world of a ship at sea in which available data may vary from one extreme of having all possible data on hand to the other extreme of having only those data which can be observed from that ship alone. As previously discussed, determination of both the meteorological scenario and the forecast approach is directly influenced by data availability. Figure 3 shows a schematic of a simple process for determining what data are available. The sample list of potential data is ordered from large to small meteorological scale as well as ordered by scale of communication distance involved. The schematic also indicates that if a piece of data is not directly available, then the question, "Can it be estimated?" is asked. If so, a library of

Figure 3

DETERMINATION OF AVAILABLE DATA TO BE USED IN FORECAST PREPARATION

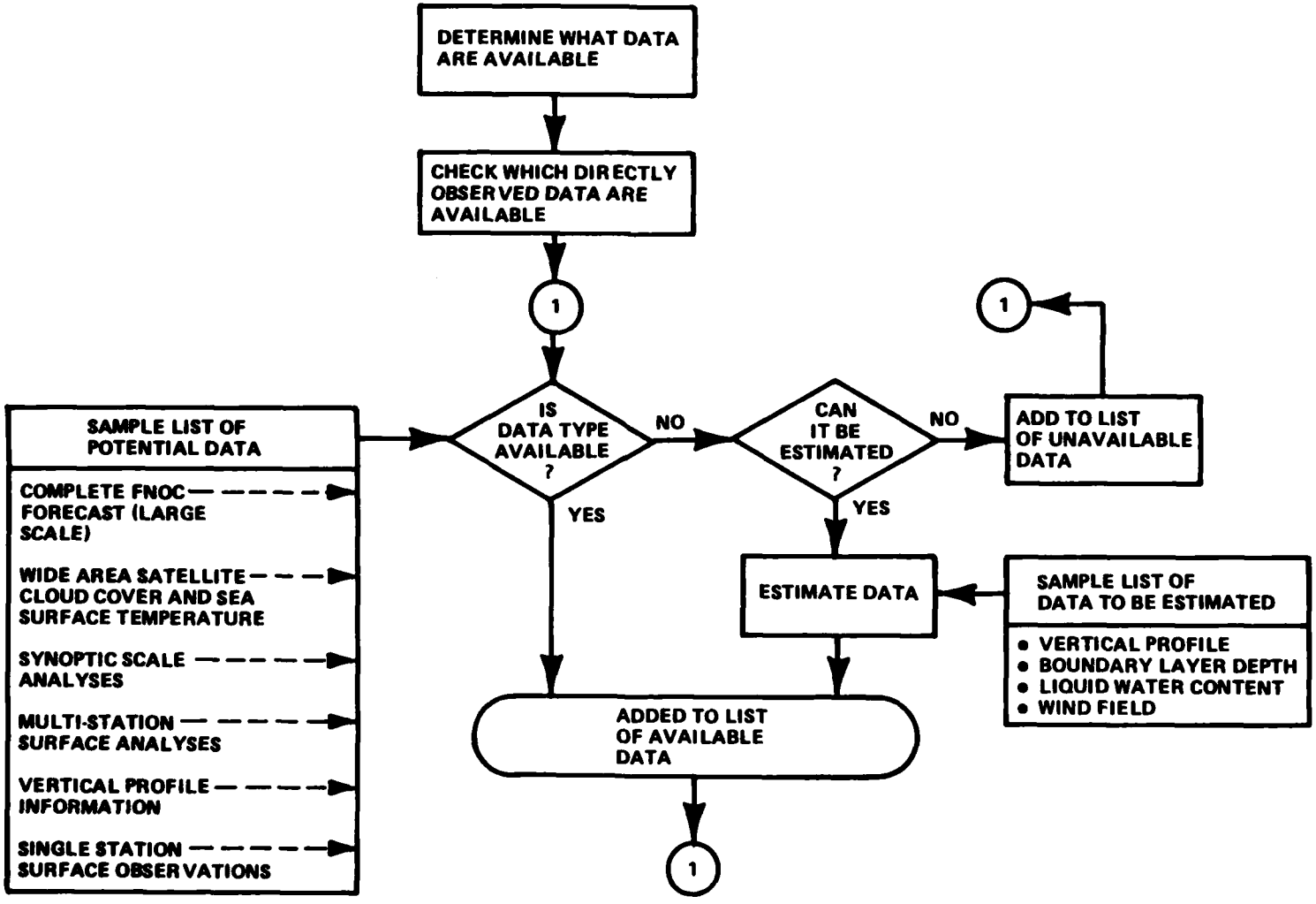

estimation procedures can be called upon to provide the required initialization parameters.

In a new forecast scheme which anticipates use of 'research' models for operational forecasting, provision must be made for estimation of missing data. From our numerous at-sea fog studies and our recent experience in generating data sets and testing of fog forecast tools, we have developed considerable background knowledge in data availability and quality and the input data requirements of the numerical models. It is our belief that, in the absence of specific data, certain parameters may be estimated with sufficient accuracy from currently available knowledge and techniques. Such estimated data may include vertical profiles of temperature and humidity, mean laver-temperature, boundary layer depth, sea surface temperature patterns, stratus thickness (top and base heights), liquid water content profiles, aerosol loading and/or visibility. Some variables will be easy to estimate; others, more difficult. Estimates could be generated through simple algorithms or libraries of climatological information with use of single station observations such as surface temperature and relative humidity, sea state, cloud height, etc. Satellite derived information about cloud top and sea surface temperatures could be of considerable value in this process.

The sample list of data-to-be-estimated focuses on mesoscale parameters. Techniques to estimate these parameters from information provided on the battlegroup scale down to that provided by a single ship need to be developed and programmed for the system. Similar lists of data-to-be-estimated can be prepared for other scales for the variables shown in the potential data list, such as hemispheric analyses and forecasts from FNOC.

4.3.3 Selection of Potential Obscuration Phenomena

A principal process in the forecast system shown in Figure 2 is the selection of the obscuration phenomenon most likely to occur in the context of the evolving meteorological scenario. The meteorological scenario is ascertained first before the most likely obscuration phenomenon is selected. Obviously, the ability to determine both the meteorological scenario and most likely obscuration phenomena implies a certain level of data availability, whether actual measurements or estimated values. Thus, an interaction and feedback between data determination and phenomenological

estimation is required. These interlinked selection processes are shown schematically in Figure 4.

Selecting the most likely obscuration phenomena from the meteorological scenario presents special requirements in terms of mesoscale space and time meteorological parameters. Determining the large-scale meteorological scenario from synoptic scale weather information is a routine task at every weather office. However, specialized procedures, such as Calspan's Decision Tree (see Appendix D), which will characterize this meteorological scenario in terms of both the large-scale synoptic situation and the mesoscale components, can be designed. For example, in fog forecasting in general, the location of the forecast area relative to areas of vertical motion associated with synoptic scale highs and lows must be determined, inversion height must be estimated and the surface wind flow relative to the mesoscale pattern in sea surface isotherms must also be defined.

Research has shown that a number of basic types of sea fog occur — e.g., stratus lowering, low-level convergence, cold water advection, low-level mixing over warm water, and coastal radiation — and, although primarily driven by micro- to mesoscale physical processes, the fogs form and evolve within the context of synoptic and mesoscale meteorological circumstances. For example, warm water mixing fogs and cold water advection fogs do not form unless a surface-based (perhaps secondary) inversion is first developed. As another example, stratus lowering (thickening) fog does not occur unless the subsidence inversion is below 400 m, a situation which occurs when the synoptic scale downward motion in the warm air above the inversion pushes it below 400 m. Further, if the inversion is pushed below the LCL, stratus lowering fogs cannot form, and the situation can be conducive to coastal radiation and shallow advection/mixing fogs. Such downward vertical motion aloft can be found at the eastern end of the semi-permanent subtropical highs (west coast of continents), the west side of an oceanic high undergoing anticyclogenesis, in sub-synoptic scale anticyclonic patterns, or in downslope flow off coastal mountain ranges.

Descriptions of linkages between fog types and characteristics and synoptic and mesoscale patterns, which are discussed in Section 4.1, Appendices D and E, and Ref. 1-19, need to be condensed and organized in logical sequence for use in the selection of most likely obscuration phenomena by the forecast system. Such a Synopsis of our current understanding of the phenomenology of marine fog occurrence would

Figure 4

DETERMINATION OF MOST LIKELY OBSCURATION PHENOMENON

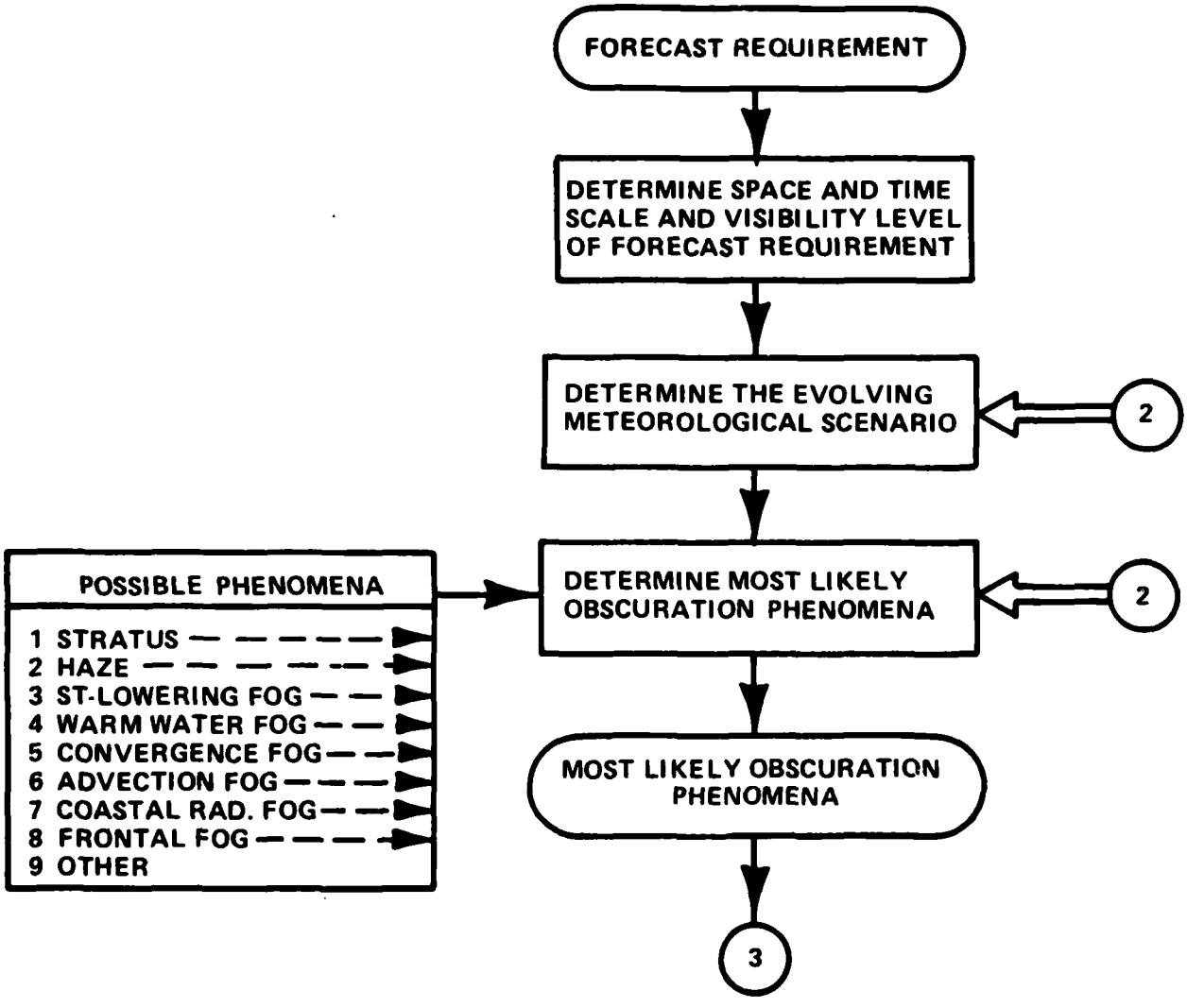

materially aid the forecaster and the forecast recipient in their understanding of the forecast phenomenon, even if a numerical model were used to provide the base forecast. The logic, content and computerization of this selection process should be designed around information which could be either computer accessible or readily available in hard-copy format to the user. In a 'tactical applications guide' or other hard-copy format and with appropriate provision for look-up tables and manual decision-making, such a guide would be a useful forecast tool for computer-poor, isolated single stations and could even serve in the training of new forecasters.

The information now available for generating such a synopsis was developed chiefly from studies of West Coast fog. Some very limited data from other locales and our knowledge of fog physics suggest that, while the oceanography and meteorology may differ, the basic phenomenology and physics of fog occurrence should remain universal. Verification of the universality of the physics of fog occurrence and its correlation with attendant meteorological regimes elsewhere, would increase confidence in the Synopsis and broaden the applicability of all forecast approaches for marine fog. It is, therefore, suggested that some limited, combined climatologic-synoptic review of fog occurrence elsewhere (perhaps in the North Atlantic) be performed as part of the development of a *synopsis of fog phenomenology*.

4.3.4 Selection of a Forecast Method

Figure 5 outlines schematically a procedure for selection of a forecast method for previously determined obscuration phenomena. Basically, for each obscuration phenomenon, there is a set of appropriate forecast approaches which covers a spectrum of input data requirements. In terms of amount of data required, these approaches can be ranked from numerical methods, such as higher order closure turbulence models, at the top through mixed-layer, phenomenological and statistical models and down to persistence. The selection process would involve matching each approach's data requirements against the available data for the level of forecast required. Further, if only minimal data were available (e.g., that which can be observed from a single ship), then the selected forecast approach would default to that one which requires the least amount of data, yet is still best for the anticipated obscuration phenomena. Again, note that the selection of a forecast tool would be a multiple-interactive procedure linked to data availability, computer availability and a model's capability to handle a given meteorological situation.

Figure 5

DETERMINATION OF FORECAST APPROACH

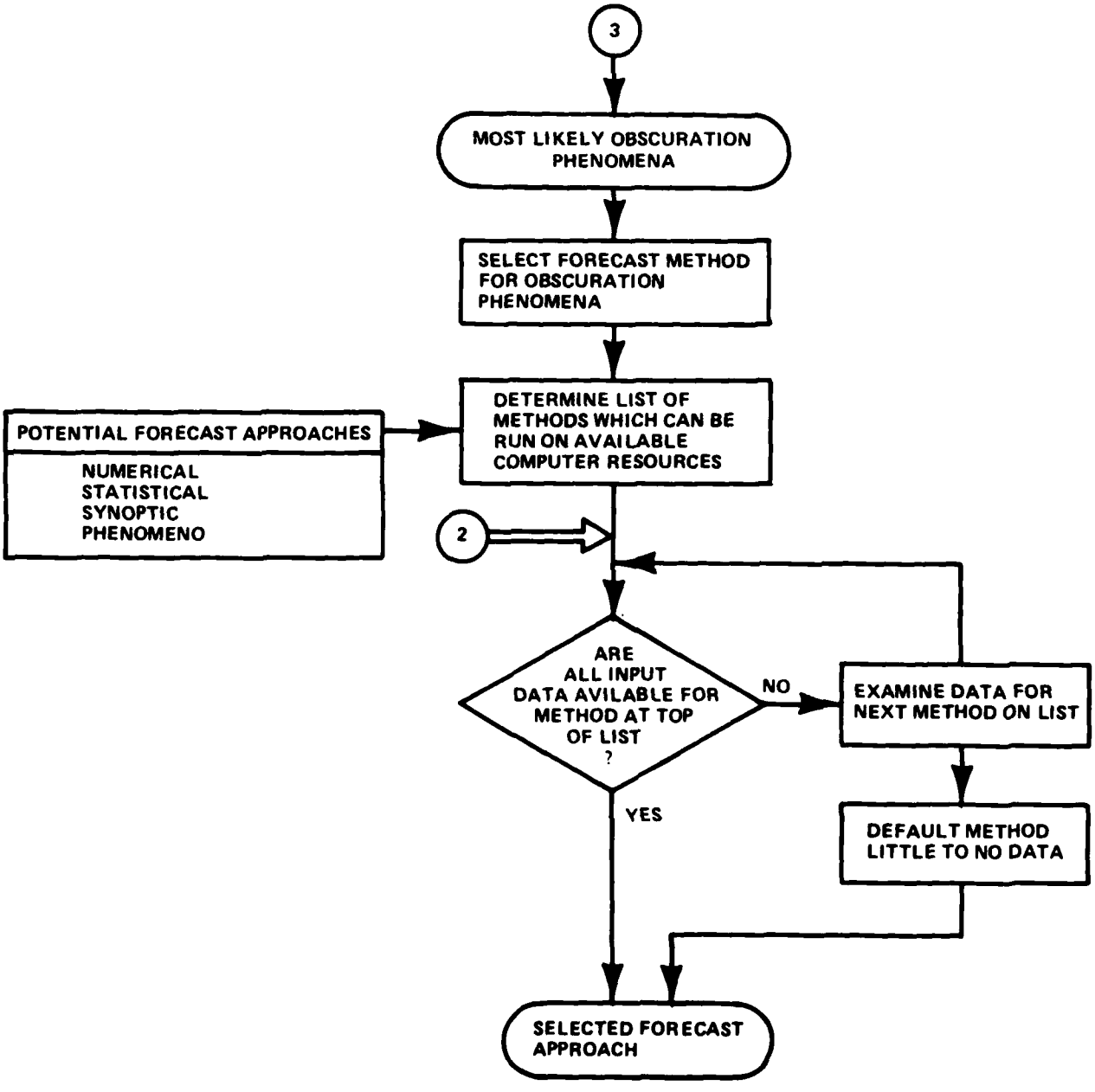

The major development effort required for this portion of the system revolves around the design of logic and content for the processes involved in selection of a forecast approach. For operational purposes, different phenomena can be forecast with specially tailored synoptic and statistical forecast approaches which have individual input data requirements -- e.g., use of the Decision Tree or Inversion Statistics models for stratus-lowering requires inversion height information. These same phenomena also require different input data if they are to be forecast from within the spectrum of the more sophisticated numerical models. For example, simulation of a stratus cloud thickening and lowering to form surface fog by HOC models requires a liquid water content profile as well as fine resolution on the atmospheric structure near the inversion; simulation of advection fog on the other hand does not need this information but requires data on the particular sea surface temperature pattern.

For the numerical models, certain restrictions will occasionally limit their overall utility in the operational realm. If sufficient data and computational resources were always available, there is no question that an HOC model should always be used, and there would be no need for this forecast system. In the real world, data will be missing or the main computer will occasionally be down or otherwise unavailable, and the unguided forecaster might elect to use a less sophisticated mixed-layer model which could be run on a desk-top computer. However, if a stable boundary layer situation were indicated, the mixed-layer model would not be suitable. With a properly designed forecast system, the forecaster would be lead to the appropriate tool.

For each phenomenon and each operational scenario, certain data are crucial to making a detailed specific forecast. Without these data, the forecast will be more general. Further, a numerical model will provide a specific mesoscale forecast over a specified trajectory, while a synoptic/statistical approach will produce a more general wide-area forecast. The data necessitated by a given phenomenon or forecast requirement need to be ranked according to their impact on the forecast. By testing for the existence of data which are ranked according to their importance relative to the forecast requirement, the selection of a forecast approach can be made efficient and expeditious.

Finally, once a forecast tool has been selected and operated, its numeric output must be interpreted. Current numerical models produce LWC or RH profiles, and use of microphysics and aerosol generation models (or some algorithm) might provide

a means for estimating visibility. Or, in addition to the prescribed prime forecast approach, other forecast tools could be run to provide increased confidence or additional information. For example, an inversion statistics model could provide the forecast of visibility given a numerically-predicted boundary layer depth and/or cloud top for use as the inversion height value. Perhaps most importantly, the wealth of understanding of the phenomenology of marine fog (trigger mechanisms, life-cycle characteristics, physical features, etc.) and of the linkage of marine fog occurrence to synoptic scale features can provide operationally useful forecast information and interpretation (of numeric results) which is not available as output from any numerical model.

Section 5

SUMMARY OF MARINE INVERSION STUDIES

5.1 INTRODUCTION AND BACKGROUND

The presence of a marine inversion at or below 400 m has long been known to be a necessary condition for the occurrence of marine fog along the West Coast of the United States (e.g., Ref. 3,15,30,38, and Section 4.1). Further, a recent pilot study (Ref. 32) suggested a relationship between inversion height and visibility values in fog, as well as between time of fog onset and duration of fog episodes; but exploitation of this information for forecasting fog requires knowledge of processes which control the height of the inversion. More recently, study at Calspan (Ref. 18) demonstrated a qualitative relation between synoptic scale flow patterns and the height of the inversion, the link between the two being the vertical motion in the warm air above the marine boundary layer. However, while considerable qualitative information about inversion height fluctuations has been collected via case studies, very little is known quantitatively about the scales of fluctuation of inversion height or the relationships between these fluctuations and meso- and synoptic scale phenomena. As a task under this contract, Calspan analyzed inversion height data obtained from acoustic sounder records to study various aspects of marine inversion height behavior.

Since about 1975, the Naval Postgraduate School (NPS) operated an acoustic sounder for measurement of inversion height at sea and on shore at Monterey, California. For a near-continuous period from October 1975 to September 1976, the device was operated approximately 24 hours per day at the NPS. Strip chart records[1] for this period were reduced and digitized under this contract to provide data for investigation of inversion statistics. Approximately 1500 hourly observations of inversion height were obtained from the acoustic sounder record. The corresponding inversion height measurements were mated with the appropriate hourly surface observations from Monterey Airport to form a computer-based data set, which could be further processed. These data were analyzed to provide information: (1) on the statistics of surface visibility in fog versus inversion height, (2) on the scales of temporal fluctuations of the inversion, and (3) on the relationship of inversion height to synoptic flow patterns.

---

[1] The acoustic sounder records were graciously loaned to Calspan by Drs. K. Davidson

The primary result of this investigation is the Calspan Inversion Statistics model which is discussed in Section 5.2. The model was tested on the model evaluation phase of this program, and results are included in Section 3.2. Summary discussions of the results of other analyses of the inversion height data are presented in Sections 5.3 and 5.4. Detailed discussions of the acoustic sounder data set, its interpretation and analyses, and case studies can be found in Appendix F.

5.2 THE CALSPAN INVERSION STATISTICS MODEL

The computer-based data set was analyzed for the distribution of inversion height by visibility category, and the cumulative percentages are shown in Table 10. When the visibility is less than or equal to 0.5 mile, 92% of the inversion heights are below 400 m. This result substantiates the well known 400 m inversion height threshold for fog, i.e., an inversion below 400 m is a necessary but not sufficient condition for fog occurrence.

For the three visibility categories in the 1 to 10 mile range (columns 3,4, and 5), the inversion height at which a given cumulative percentage value occurs increases as visibility range increases, e.g., 80% at 400, 500 and 600 m for 1-3, 3-5, and 5-10 mile visibilities, respectively. This result is consistent with the earth's surface being located progressively farther below the top of a stratus cloud which is only 400 m thick. With the inversion height below 400 m, the earth's surface is in the cloud and visibility $<$ 1 mile occurs. In the 400-450 m inversion height range, the surface is located just below cloud base in the region of high relative humidity and dense haze (visibility in the 1 to 3 mile range). In the 450-500 m range, the surface is in a region of still lower relative humidity farther below cloud base, and the visibility increases to 3-5 miles.

Exploiting the relationship between inversion height and visibility in the forecast of fog requires the frequency of occurrence of visibility versus inversion height. Figure 6 presents these frequencies in cumulative form stratified into arbitrary 6-hour time periods, starting with the climatologically most favorable period (0100-0600 LST) for West Coast fog. Note that the highest percentages for visibility $<$1 mile occur in the morning hours, almost no fog occurs during the afternoon, and fog frequencies then

---

(cont.)
and G. Schacher of the Naval Postgraduate School, Monterey, California.

TABLE 10

DISTRIBUTION OF INVERSION HEIGHT ABOVE AIRPORT ELEVATION FOR MONTEREY AIRPORT VISIBILITIES

Inversion Height Above Airport Elevation (m)	Monterey Airport Visibility (Statute Miles)					
	V≤0.5	0.5<V≤1	1<V≤3	3<V≤5	5<V≤10	10<V
	Cumulative Percent of Observations					
0-50	1 %	0 %	0 %	0 %	0 %	0 %
51-100	6	5	1	0	0	0
101-150	20	14	3	1	1	0
151-200	46	30	10	4	4	4
201-250	61	50	21	9	7	8
251-300	87	84	51	26	14	13
301-350	91	89	66	32	22	19
351-400	92	100	79	53	35	31
401-450	96	0	89	64	45	39
451-500	97	0	96	78	58	52
501-550	97	0	98	86	66	58
551-650	98	0	100	94	84	73
651-750	100	0	0	98	93	89
751-850	0	0	0	99	99	97
851-1000	0	0	0	100	100	100
TOTAL # of OBS.	80	44	128	189	818	220

CALSPAN INVERSION STATISTICS MODEL

Probability of Visibility in Fog/Haze as a Function of Inversion Height

VISIBILITY (miles)

Inversion Height IH (m)	<.25	<=.5	<=1	<=3	<=5	<=10	<50	
0-100	30	50	67	87	93	100	100	
100-200	40	51	71	80	83	94	100	Time Period
200-300	19	25	40	65	75	99	100	
300-400	4	9	13	36	72	96	100	0100-0600 L
400-500	3	3	3	16	33	96	100	
500-600	0	0	0	1	15	91	100	
600-700	0	4	4	6	15	89	100	
700-800	0	0	0	4	18	86	100	
>800	0	0	0	3	17	75	100	

VISIBILITY (miles)

Inversion Height IH (m)	<.25	<=.5	<=1	<=3	<=5	<=10	<50	
0-100	50	50	50	50	50	100	100	
100-200	38	43	52	71	76	95	100	Time Period
200-300	10	13	30	55	60	90	100	
300-400	0	0	7	23	39	89	100	0700-1200 L
400-500	0	2	2	14	31	87	100	
500-600	0	0	0	5	24	82	100	
600-700	0	0	0	0	15	90	100	
700-800	0	0	0	0	5	74	100	
>800	0	0	0	0	0	50	100	

VISIBILITY (miles)

Inversion Height IH (m)	<.25	<=.5	<=1	<=3	<=5	<=10	<50	
0-100	0	0	0	0	0	100	100	
100-200	0	0	0	0	0	67	100	
200-300	4	4	11	23	32	96	100	Time Period
300-400	0	0	0	1	6	75	100	1300-1800 L
400-500	0	0	0	0	9	78	100	
500-600	0	0	0	0	6	70	100	
600-700	0	0	0	0	0	25	100	
700-800	0	0	0	0	0	38	100	
>800	0	0	0	0	0	70	100	

VISIBILITY (miles)

Inversion Height IH (m)	<.25	<=.5	<=1	<=3	<=5	<=10	<50	
0-100	33	33	67	67	67	100	100	
100-200	13	13	18	31	41	90	100	
200-300	10	11	14	36	69	93	100	Time Period
300-400	0	0	0	14	33	96	100	1900-0000 L
400-500	0	0	0	1	21	79	100	
500-600	0	0	0	0	2	86	100	
600-700	0	0	0	0	5	86	100	
700-800	0	0	0	0	0	78	100	
>800	0	0	0	0	0	100	100	

Figure 6 Calspan Inversion Statistics Model. Cumulative Probability of Visibility as a Function of Inversion Height.

increase in the evening period. The presentation provided in Figure 6 is the Calspan Inversion Statistics Model.

For the early morning hours—i.e., the prime fog period--the fog visibility versus inversion height relationship shows dense fog (visibility $\leq$ 0.5 mile) occurs most often at low inversion heights, and higher visibilities with higher inversion heights. In particular:

(1) With the inversion at or below 200 m, the chance of dense fog is 50% and the chance of visibility $\leq$ 1mi. is 70%. In the 200-300 m height range, the percentages decrease with the chance of visibility $\leq$1mi at 40%, but the chance of dense fog is only 25%.

(2) In the 300-400 m range there is only a 13% chance of visibility less than 1 mi., but a 72% chance of visibility $\leq$5 mi.

(3) For inversions above 400 m, visibility occurs predominantly at values above 3 mi.

In summary, visibility versus inversion height is dominated by a process in which stratus cloud or fog in the marine boundary layer thickens during nocturnal hours when there is cooling from net divergence of long wave radiation at cloud top. The visibility values are related to inversion height such that dense fog occurs with low inversion height and the predominant visibility value increases with increasing inversion height, primarily as suggested by the model of a 400 m thick stratus at the top of a well-mixed layer cloud and the reduced-visibility in the high relative humidity haze region immediately below cloud base.

It should be recognized that the Model formulated here is preliminary and for a specific, slightly inland site. For operational forecasting, the data presented in Figure 6 should be stratified by time periods which are better defined according to known phenomenological behavior of stratus thickening fog. For example, this type of fog is known to begin in the late evening hours before midnight. Thus the visibility versus inversion height data for these hours should be included in a time period designed to encompass the most likely time of fog occurrence, say 2200-0800LST, as opposed to the 0100-0600 period used in our preliminary Model. Further, the data shown in Figure

6 are from an onshore site at which heat from the ground (warmed during the day) probably retards the thickening of the stratus cloud and surface level visibility deterioration in the early evening. Observations over the ocean show that thickening stratus typically reaches the surface a few hours earlier and persists a few hours longer than over land, probably because sea surface (water) temperature is little affected by insolation. Thus, the data derived from an inland site, for 2200-0800LST for example, might be best applied over the ocean to the period 2000-1000LST.[1] Additional study is required to establish the appropriate time shifts between fog behavior over the ocean and at near coastal sites and to determine the universality of the concept.

5.3 TEMPORAL VARIATIONS OF INVERSION HEIGHT

An analysis was performed on the inversion height data to determine if lag statistics might be used to forecast the inversion height. Processing of the computer-based data set consisted simply of advancing forward the prescribed number of hours and recording the change in inversion height between its initial and lagged value. Table 11 shows the percentage of occurrence of both increase, decrease and zero change in inversion height for lag periods out to 24 hours. For this table, zero change was defined as $\pm$20 m because that appears to be the accuracy of specification of the inversion height from the acoustic sounder record.

Examination of the table shows that the probability of zero change at 6 hours decreases to one-third of its 1-hour value, and that this change is accompanied by the decrease percentage nearly doubling. Thus the zero changes are frequent at one hour lag, but they then decrease to a relatively rare event at six hours and greater, primarily as the occurrence of a reduction in inversion height increases. By 6 hours, the probabilities for decrease or increase in inversion height are about equal.

For the 12-24 hour periods, the percentages are uniform, with small probability of zero change and nearly equal probability for increase and decrease of the inversion height. This result indicates that for the 12-24 hour period (and perhaps including the 6-hour period), the lag in inversion height provides essentially no descrimination between increase or decrease.

---

[1] Had these suggested modifications been incorporated in Calspan's Model, it would have scored an additional "verifies" in the model testing (for Case 6) phase of this program (see Section 3 2).

TABLE 11

PERCENTAGE OF INVERSION HEIGHT CHANGE FOR VARIOUS LAG TIMES

Inversion Height Change	Lag Time (hr) 1	3	6	12	18	24
Increase	40%	46	49	48	49	48
Zero	38%	20	13	10	10	10
Decrease	22%	34	38	42	41	42

TABLE 12

PERCENTAGE OF INVERSION HEIGHT CHANGES BY 100m CATEGORIES VS LAG PERIODS

	DECREASE					INCREASE			
Lag Period (Hr)	<-300m	-200 to -300	-100 to -200	0 to -100	-100 to +100	0 to 100m	100 to 200m	200 to 300m	>+300m
1	.07	0.3	2	36	(92)	56	4	0.8	0.2
3	.07	0.8	9	32	(76)	44	11	2	0.2
6	0.4	3	13	28	(63)	35	15	5	0.8
12	2	5	15	25	(52)	27	17	8	3
18	4	6	13	24	(51)	27	17	6	4
24	4	7	11	23	(48)	25	16	8	4

Although the lag statistics appear to have little value in forecasting the direction of change in inversion height, when presented by magnitude of change, the data offer information about inversion height behavior which impacts on fog forecast techniques which require inversion height information.

The percent of occurrence of inversion height change by 100 m intervals for lags out to 24-hours are shown in Table 12. At first glance the distribution looks similar to that in Table 11 especially when the -100 to +100 m category is compared to the zero category in Table 11. The percentage steadily decreases from 1 to 12 hours and then is constant at nearly 50% out to 24 hours. As the percentage in this category decreases, the percentages increase almost identically for both inversion increases and decreases beyond 100 m.

From these analyses we can enumerate a few characteristics of the inversion height behavior with time:

(1) At the short tine intervals (one to six hours), inversion height changes are primarily within the $\pm$100 m range, with a signficant fraction of those at shorter periods being within the $\pm$20 m range. Inspection of individual daily time series of inversion height shows that these small changes are primarily associated with diurnal fluctuations of the sea breeze, with inversion heights increasing in the morning and decreasing in the evening.

(2) For the longer lags (12-24 hrs), the percentages of the larger height changes increase, but about 50% of the time the changes are still within $\pm$100 m and nearly all are $\geq \pm$20 m. Large height changes occurring only over long time periods and indications of quasi-steady state conditions over long time periods are both consistent with synoptic scale processes as the major driving mechanism for inversion height changes.

In summary, although the frequency of occurrence of zero change in inversion height is low, the lag approach appears to have little value as a forecast of inversion height since the frequency of occurrence shows little discrimination in the direction of change in inversion height. However, the data do show that the inversion

is very likely to remain within ±100 m of its observed value for 1 to 6 hours (92-63% probability, respectively); and for 12 to 24 hours, the probability of the inversion remaining within ±100 m is still 50%. The lag analysis indicates that for short time intervals, fluctuations in inversion at this near coastal site are driven by the sea breeze and that over long time intervals the fluctuations are driven by synoptic scale processes.

5.4 INVERSION HEIGHT VS. SYNOPTIC FLOW PATTERNS

Fog off the west coast of continents occurs in the surface marine layer, and, given a variety of trigger mechanisms, its occurrence and intensity are primarily dependent on the height of the inversion which caps the marine layer. Study of synoptic sequences and associated fog episodes has shown that changes in the height of the marine inversion over periods of a day or so are generally caused by the vertical motion associated with both large and small scale synoptic disturbances, with a modulation by orographic vertical motion.

The controlling flow patterns are (1) slowly-moving long-wave systems, (2) large-scale synoptic systems, and (3) small-scale synoptic systems whose dynamics and flow patterns are concentrated in the 500-1500 m layer. In a previous study of a limited number of cases, Rogers et al (Ref. 18) identified inversion height behavior as related to generic types of flow patterns, specific patterns within these generic types, and transitions between the various generic types.

In the realm of large scale disturbances, for example, when a long wave trough is located near the coast, dynamic upward vertical motion can raise the inversion to heights of 1000 m or greater. After the trough moves out, the subtropical high usually ridges in with downward motion and the inversion lowers to around 500 m. At times the subtropical high builds eastward to produce a separate center over the continent and causes northeasterly flow (in its SE quadrant)in the layer between 500-1500 m. Since the orientation of the mountain ranges along the coast is approximately north to south this northeasterly flow produces downslope motion which can help drive the inversion downward to lower levels. Occasionally, when the high pressure cell and the downward motion are intense, the inversion and warm air are driven all the way down to the surface at the coastline and for some distance out to sea. Although the marine layer may not be too far from the coast, a stratus-free area may extend some

distance out to sea since the inversion is forced below the lifting condensation level of the marine layer.

In addition to the patterns of long wave trough and synoptic scale ridge, smaller-scale systems also occur in the layer around 1000 m. Between occurrences of the large scale regimes, this layer may be meteorologically active, as small-scale cyclonic and anticyclonic patterns form in, dissipate or move through the coastal region. These small-scale systems can also produce easterly (and downslope) flow, for which fog occurrence and intensity vary more widely than in the large scale systems.

It was recognized in the previous study that the descriptions outlined above were but a framework built from the limited sample available, and that further study might uncover other unique flow patterns which might be used to improve the relationship between inversion height and flow patterns. Under the current contract, additional investigation was carried out to utilize the continuous nature of the inversion height record derived from the acoustic sounder. This limited effort is summarized below; additional detail may be found in Appendix F.

From the previous data set, closed flow patterns and large scale troughs and ridges made up the majority of the patterns (see Ref. 18). From the current study, we have found that two other synoptic patterns, inverted trough and col, also influence inversion behavior. The inverted trough can occur south of the subtropical ridge or as the southern member of the trough pair associated with a col pattern.

Different inversion height levels appear to be associated with these separate occurrences. If a col is involved and the inverted trough is narrow in the east-west direction, the inversion is in the 250-300 m range. On the other hand, when the inverted trough is located on the south side of an east-west oriented high pressure ridge, the inversion resides at or near the ground. In this case, our analysis indicates that the vertical motion produced by orographic downslope aids greatly in lowering the inversion to the surface.

To specify the synoptic flow patterns in our analyses we used the 850-mb surface because it is an operationally available chart. However, our study indicates that a lower level well within the warm air above the inversion, such as 900 mb, may be more appropriate. Use of a lower level appears to be particularly important in

situations of weak large scale pressure gradients, like those found with col patterns. In this situation, the wind direction in the warm air is crucial to specification of the inversion height. With easterly winds (downslope) the inversion is found around 300 m, while with westerly winds (upslope) the inversion is located higher.

In summary, the current study has added the synoptic patterns of inverted trough and col to the set of patterns used to obtain inversion height from synoptic charts for the forecast of marine fog. However, the character of both these patterns reinforces the need to investigate the use of a level below 850 mb for the specification of the synoptic patterns. Further research is recommended to examine what is the most appropriate level to use to specify the synoptic flow patterns.

REFERENCES

1. Mack, E. J., W. C. Kocmond, R. J. Pilié, W. Katz, and O. H. Vaughan, 1972: "Some Microphysical Features of Coastal and Inland Fogs" presented at the First International Conference on Aerospace and Aeronautical Meteorology Washington, D. C. May 22-26, 1972

2. Mack, E. J., R. J. Pilié, and W. C. Kocmond, 1973: "An Investigation of the Microphysical and Micrometeorological Properties of Sea Fog" Project SEA FOG, First Annual Summary Report, Calspan No. CJ-5237-M-1, 39 pp.

3. Mack, E. J., U. Katz, C. W. Rogers, and R. J. Pilié, 1974: "The Microstructure of California Coastal Stratus and Fog at Sea" Project SEA FOG: Second Annual Summary Report, Calspan No. CJ-5404-M-1, 67 pp.

4. Pilié, R. J., E. J. Mack, W. C. Kocmond, C. W. C. Rogers, and W. J. Eadie, 1975: "The Life Cycle of Valley Fog: Part I, Micrometeorological Characteristics" J. Appl. Met., 14, 3, pp 347-363

5. Pilié, R. J., E. J. Mack, W. C. Kocmond, W. J. Eadie, and C. W. C. Rogers, 1975: "The Life Cycle of Valley Fog: Part II, Fog Microphysics" J. Appl. Met., 14, 3, pp 364-374

6. Mack, E. J., R. J. Pilié, and U. Katz, 1975: "Marine Fog Studies Off the California Coast" Project SEA FOG: Third Annual Summary Report, Calspan No. CJ-5608-M-1, 75 pp.

7. Pilié, R. J. and E. J. Mack, 1975: "Fog Water Collector" United States Patent No. 3,889,532

8. Mack, E. J. and U. Katz, 1976: "The Characteristics of Marine Fog Occurring Off the Coast of Nova Scotia" Project SEA FOG: Fourth Annual Summary Report, Part 1, Calspan Report No. CJ-5756-M-1, 180 pp.

9. Mack, E. J., U. Katz, and R. J. Pilié, 1976: "The Influence of Continental Aerosols on the Microphysics of Marine Fogs Occurring in Coastal Areas" Proceedings of the Conference on Coastal Meteorology, Virginia Beach, Virginia

10. Pilié, R. J., E. J. Mack, U. Katz, and D. F. Leipper, 1976: "The Importance of Organized Vertical Motions in Coastal Fog" Proceedings of the Conference on Coastal Meteorology, Virginia Beach, Virginia

11. Katz, U. and E. J. Mack, 1977: "Direct Measurements of Sea Spray Size Spectra at the NCSL Offshore Platform" presented at the Fifth Annual Marine Fog Investigation Program Review Conference, Buffalo, N.Y., Calspan Report No. CH-6067-M-1, 95 pp.

12. Mack, E. J., U. Katz, C. W. Rogers, D. W. Gaucher, K. R. Piech, C. K. Akers, and R. J. Pilié, 1977: "An Investigation of the Meteorology, Physics, and Chemistry of Marine Boundary Layer Processes" Project SEA FOG: Fifth Annual Summary Report, Calspan Report No. CJ-6017-M-1, 122 pp.

13. Mack, E. J., Anderson, R. J., Akers, C. K., and Niziol, T. A. "Aerosol Characteristics of the Marine Boundary Layer of the North Atlantic and Mediterranean during May-June 1977" Project SEA FOG: Sixth Annual Summary Report, Calspan Report No. 6232-M-1, October 1978, 215 pp.

14. Mack, E. J., Niziol, T. A., Rogers, C. W., Akers, C. K., 1979: "The Meteorological and Aerosol Characteristics of the Marine Boundary Layer in the Vicinity of San Nicolas Island During CEWCOM-78," Calspan Report No. 6437-M-1, December, 127 pp.

15. Pilié, R. J., E. J. Mack, C. W. Rogers, U. Katz and W. C. Kocmond, 1979: "The Formation of Marine Fog and the Development of Fog-Stratus Systems Along the California Coast" J. Appl. Met., 36, 10, October 1979.

16. Rogers, C. W., J. T. Hanley, R. J. Pilié and E. J. Mack, 1980: "Deformation of the Marine Inversion and the Development of Marine Fog and Stratus Resulting from Warm Water Patches: Numerical Modeling and Verification with Satellite Imagery," Proceedings of the Second Conference on Coastal Meteorology, 30 January - 1 February, 1980, Los Angeles.

17. Fitzgerald, J. W., S. G. Gathman, E. J. Mack and U. Katz, "Comparison of Laboratory and Numerical Model Studies of the Initial Phase of Cloud Droplet Growth by Condensation" VIII International Conference on Cloud Physics, 15-19 July 1980 Clermont-Ferrand, France.

18. Rogers, C. W., E. J. Mack, R. J. Pilié and B. J. Wattle: "An Investigation of Marine Fog Forecast Concepts," Eighth Ann. Summary Report, Calspan Report No. 6673-M-1, January 1981, 97 pp.

19. Mack, E. J., J. T. Hanley, R. J. Pilié, C. K. Akers and B. J. Wattle: "Aerosol Composition in the Marine and Coastal Boundary Layer," Proceedings 25th Annual SPIE Symposium, Vol. 305, San Diego, 27-28 Aug. 81.

20. Oliver, D. A., W. S. Lewellen and G. G. Williamson, 1978: "The Interaction between Turbulent and Radiative Transport in the Development of Fog and Low-Level Stratus" J. Atmos. Sci., 33, 301-316.

21. Burk, S. D., 1978: "Use of a Second Moment Turbulence Closure Model for Computation of Refractive Index Structure Coefficients" December 1978, NAVENPREDRSCHFAL Technical Report TR 78-04, NEPRF, Monterey, CA 93940

22. Davidson, K. L., C. W. Fairall, P. J. Boyle and G. E. Schacher, 1982: "Verification of an Atmospheric Mixed-Layer Model for a Coastal Region." Submitted for Publication. Naval Postgraduate School, Monterey, CA 93940

23. Tag, P. M., 1983: "Marine Fog/Stratus Forecasting with a 3-D Boundary Layer Model" presented at Sixth Conference on Numerical Weather Prediction, 6-9 June 1983, Omaha, Neb.

24. Moeng, F. J. and M. G. Wurtele, 1981: "Model Simulation of California Stratus, Diurnal Formation and Dissipation." Submitted for Publication, UCLA, Dept. of Atmos. Sci., Los Angeles, CA 90024.

25. Herman, G. and R. Goody, 1976: "Formation and Persistence of Summertime Arctic Stratus Clouds" J. Atmos. Sci., 33, 1537-1553.

26. Businger, J. A., J. C. Wyngaard, Y., Izumi and E. F. Bradley, 1971: "Flux-Profile Relationships in the Atmospheric Surface Layer," JAS, 28, 2, pp 181-189.

27. Fitzgerald, J. W., 1978: "A Numerical Model of the Formation of Droplet Spectra in Advection Fogs at Sea and Its Applicability to Fogs off Nova Scotia", J. Atmos. Sci., 35, 1522-1535.

28. Gathman, S. G., 1982: "A Time-Dependent Oceanic Aerosol Profile Model" NRL Report 8536 Naval Research Laboratory, Washington, D.C. 20375.

29. Barker, E. M., 1977: "A Maritime Boundary-Layer Model for the Prediction of Fog", Boundary-Layer Meteor., 11, 267-294.

30. Leipper, D. F., 1948: Fog Development at San Diego, California, Journal of Marine Research, VII, 3, 337-346.

31. Naval Oceanography Command Facility, 1980: Forecasters Handbook, NAS North Island, San Diego, CA. Prepared for Commander, Naval Oceanography Command, NSTL Station, Bay St. Louis, MS 39529

32. Leipper, Dale F., 1980: "Coastal Fog Forecasting at Monterey, California, An Open-Ended, Objective, 3 to 6 Day Approach. Preprint Volume: Eighth Conference on Weather Forecasting and Analysis, June 10-13, 1980, Denver, Colo. American Meteorological Society, Boston, MA 02108.

33. Noonkester,V. R. and L. E. Logue, 1976: Fog Related to Stratus Clouds in Southern California. NELC/TR 1989 Naval Electronics Laboratory Center, San Diego, CA 92152.

34. Dixon, R., 1983: Results of Inversion/Visibility Study 1982. Geophysical Sciences Technical Note No. 67. Geophysics Division, Range Operations Department, Pacific Missile Test Center, Point Mugu, CA 93042.

35. Beardsley, J. W., 1976: "Fog on the Central California Coast for 1973; Analysis of Trends" Masters Thesis, NPS-58LR76031, Naval Postgraduate School, Monterey, CA 93940.

36. Rogers, C. W., E. J. Mack, U. Katz, C. C. Easterbrook, and R. J. Pilié, 1974: The Life Cycle of California Coastal Fog Onshore". AFCRL-TR-74-0419. CJ-5076-M-3 Calspan Corp., P. O. Box 400, Buffalo, N.Y. 14225.

37. Rogers, C. W. and J. T. Hanley, 1980: "An Algorithm for the Increase of Liquid Water Content with Height in Fog and Water Hazes." Calspan Report No. 6711-M-1. Calspan Corp., P. O. Box 400, Buffalo, N.Y. 14225.

38. Anderson, J. B., 1931: "Observations from Airplanes of Cloud and Fog Conditions Along the Southern California Coast," Mon. Weather Review, July, 1931, pp. 264-270.

APPENDIX A

I. Synopsis of Rejection or Retention of Model for Test With Calspan Data Set

II. Details of Models

Tables

I. SYNOPSIS OF REJECTION OR RETENTION OF MODEL FOR TEST WITH CALSPAN DATA SET

1.0 MODELS INCLUDED FOR FURTHER TESTING

1.1 NUMERICAL MODELS

ARAP -- Highly sophisticated turbulence formulism (Higher Order Closure) and being tested for theoretical improvements.

Burk -- Sophisticated turbulence formalism (HOC) and being developed toward operational application.

NPS -- Simplest model with no turbulence which could be applied to fog forecasting problem; the then current version was running operationally on desk top computer.

Tag -- K-theory turbulence formulism which lay between HOC and no turbulence approaches.

Wurtele -- Different radiation package than ARAP's (which was also used by Tag and Burk). Also hybrid K-theory, turbulent energy turbulence modeling.

Barker -- Had both K-theory turbulence and drop sedimentation capability, but investigator had previous commitments and could not participate in test case simulations. Model was run by investigator with another agency; results in press but unavailable for current analysis.

1.2 EMPIRICAL MODELS

Calspan -- Decision Tree -- Included because only technique which contains operational method for predicting inversion height which is crucial to application of other empirical approaches. Only method which contains fog phenomenology knowledge.

Inversion statistics -- Developed on the current program and, therefore, tested because of its availability.

Leipper -- Inversion Statistics -- promising approach derived from observed fog behaviour at Monterey and Oakland CA.

Indices -- Default objective method when any and all other approaches cannot be used.

Rosenthal -- To prepare inversion statistics for location other than Monterey (Point Mugu) in parallel with our study.

2.0 NOT FURTHER TESTED BUT SHOULD BE EXAMINED IN THE FUTURE

Fitzgerald --microphysics model which needed input of relative humidity time history. Model was previously applied to situation which became our Test Case 2, but not on the data we used to define Case 2. Model also requires initial and verification aerosol which were not available for test cases.

Gathman -- Aerosol model needed verification aerosol data which were not available for test cases.

Meteorological profile model -- was not in fog predictive category. However model should be considered as possible means of providing input data to forecast models in operational scenario.

3.0 NOT FURTHER TESTED BUT RECOMMENDED FOR OPERATIONAL USE

Renard -- Model Output Statistics based on summer conditions in North Pacific.

4.0 CURRENT OPERATIONAL MODEL

Clarke-Fter--FNOC's current operational fog forecast model.

5.0 EXCLUDED FROM FURTHER TESTING

5.1 NUMERICAL

Eadie et at — Turbulence formulation weak, no solar radiation and currently inactive

Rogers -- No turbulence, crude long wave radiation, no solar radiation, and currently inactive.

Telford -- Model is focused on theoretical applications.

5.2 EMPIRICAL

Jung -- Slight variation of Leipper Indices which was already included for testing.

Noonkester -- Research analysis but no forecast model which could be tested.

Himinez -- Site specific technique for Los Angeles International Airport requiring multi-day time history of temperature and moisture variables not available in our data sets or operationally at sea and thus was judged not generally applicable.

Driggers -- Site specific rule-of-thumb for NAS Pensacola, FL and thus not generally applicable.

Leipper -- Sequences -- Needed further research.

Table A-1

Models and Forecast Procedures Identified for Potential Use
In an Improved Marine Fog Forecast Scheme

Individual	Organization	Date Visited	Description of Model	Reference
S. Burk	NEPRF	27 May 1981	Higher Order Closure-Turbulence	"Use of a Second Moment Turbulence Closure Model for Computation of Refractive Index Structure Coefficients"-S.D.Burk - December 1978, NAVENPRFINRSCHFAL Technical Report TR 78-04, NEPRF, Monterey, CA 93940
S. Lewellen	ARAP	6 May 1981	Higher Order Closure-Turbulence	Oliver, D.A., W.S. Lewellen and G.G Williamson, 1978. "The Interaction Between Turbulent and Radiative Transport in the Development of Fog and Low-Level Stratus", J. Atmos. Sci., 35, 301-316.
M. Wurtele	UCLA	8 July 1981	Eddy coefficients based on turbulent kinetic energy and turbulent length scale.	Moeng, F.J. and M.G. Wurtele, 1980 "Model Simulation of Stratus Formation and Dissipation", Proc. of Second Conference on Coastal Meteorology, Jan 1980, Los Angeles, CA. American Meteorological Society, 45 Beacon Street, Boston, MA 02108
P. Tag	NEPRF	29 May 1981	Three-dimensional model with eddy coefficients tied to wind shear and stability.	Tag, P.M. and T.E. Rosmond, 1980 "Accuracy and Energy Conservation in a Three Dimensional Anelastic Model, J. Atmos. Sci., 37, 2150-2168.
E. Barker	NEPRF	27 May 1981	Eddy coefficients based on atmospheric stability through Monin-Obukhov similarity theory.	Barker, E.M., 1977: "A Maritime Boundary-Layer Model for the Prediction of Fog", Boundary-Layer Meteor., 11, 267-294.
W. Eadie & W. Rogers	Calspan	-	Eddy coefficients based on turbulent length scale	Rogers, C.W., W.J. Eadie, D. Katz, and W.C. Kocmond, 1975: Project Fog Drops V. NASA Contractor Report, NASA CR-2633. NASA Wash. D.C. 20546. Mack, E.J. and C.W. Rogers, 1976: Simulation of Marine Advection Fog with the Calspan Advection Fog Model using Prognostic Equations for Turbulent Energy. Project Sea Fog Fourth Annual Summary Report, Part 2. Contract No. N00019-75-C-0508, Calspan Report No. CJ-5756-M-2. Calspan Corporation, PO Box 400, Buffalo, NY 14225
K. Davidson (et al)	NPS	27 May 1981	Entrainment model for well-mixed layer capped by inversion.	Davidson, K.L., G.E. Schacher, C.W. Fairall and T.M. Houlihan, 1980: "Observations of Atmospheric Mixed-Layer Changes off the California Coast (CEWCOM-76)", Proc. of Second Conference on Coastal Meteorology, January 1980, Los Angeles, CA. AMS, 45 Beacon Street, Boston, MA 02108.

Table A-1 (Cont.)

Individual	Organization	Date Visited	Description of Model	Reference
W. Rogers	Calspan	-	Horizontal two-dimensional model for well-mixed layer.	Rogers, C.W. and J.T. Hanley, 1981. "A Feasibility Study of Numerical Simulation of Inversion-Rising Marine Stratus and Fog", Final Report, Co. N00014-79-C-0459, Calspan Report No. 6512-M-2. Calspan Corp., PO Box 400, Buffalo, NY 14225.
J. Fitzgerald	NRL	30 April 1981	Computes evolution of fog droplet size distribution	Fitzgerald, J.W., 1978: "A Numerical Model of the Formation of Droplet Spectra in Advection Fogs at Sea and Its Applicability to Fogs off Nova Scotia", J. Atmos. Sci, 35, 1522-1535.
J. Telford	DRI	-	Simulates a field of identical convective plumes	Telford, J.W., 1980: Response to Marine Fog Model Survey.
R. Renard	NPS	1 June 1981	Model output statistics approach applied to FNOC analyses and predictions	Naval Postgraduate Theses: G.P. Willms: 1975; MC. Koziara: December 1980; H.Dew.Selsor: December 1980; T.N. Tabot: June 1981 Naval Postgraduate School, Monterey, CA 93940
L. Clarke	FNOC	29 May 1981	FNOC's operational fog forecast model based on advection fog formed over colder water	Personal Communication, May 1981.
S. Gathman	NRL	30 April 1981	Estimates meteorological profiles from shipboard observations. Currently using this model to provide relative humidity profiles to an aerosol model which is based on sea-state and stability criteria.	Gathman, S.G., 1978: "Model for Estimating Meteorological Profiles from Shipboard Observations", NRL Report 8279. Naval Research Laboratory, Wash. DC. **Gathman, S. G., 1982: "A Time-Dependent Oceanic Aerosol Profile Model" NRL Report 8536 Naval Research Laboratory, Washington, D.C. 20375**
			EMPIRICAL MODELS	
D. Leipper	NPS	27 May 1981	Uses post Santa-Ana rise in the inversion height and visibility frequency vs. inversion height climatology to forecast fog; also developed indices model for San Diego	Leipper, D.F., 1948: "Fog Development at San Diego, CA" J. of Marine Res., VII, 3, 337-346; Leipper, D.F. 1980: "Coastal Fog Forecasting at Monterey, CA, An Open-Ended, Objective, 3 to 6 Day Approach." Proc. Eighth Conference on Weather Forecasting and Analysis, June 1980, AMS, 45 Beacon St., Boston, Mass 02108.
G. Jung	NPS	2 June 1981	Uses a variation of Leipper's Indices plus observed wind velocity over the ocean	Leipper, D. F., 1948 (as above); R. J. Clark, 1981: "An Open Ocean Marine Fog Development and Forecast Model for Ocean Weather Station PAPA, NPS Thesis.

Table A-1 (Cont.)

Individual	Organization	Date Visited	Description of Model	Reference
W. Rogers & E. Mack	Calspan	-	The inversion height is forecast from the 850-mb synoptic pattern and then probability of fog is specified from a decision tree based on phenomenological models and involving long-wave radiation and transfer across the inversion	Pilié, R.J., E.J. Mack, C.W. Rogers, U. Katz and W.C. Kocmond, 1979: "The Formation of Marine Fog and the Development of Fog-Stratus Systems Along the California Coast," J. Appl. Met., 36, 1275-1286; Rogers, C.W., E.J. Mack, R.J. Pilié, and B.J. Wattle, 1981: "An Investigation of Marine Fog Forecast Concepts," Eighth Annual Summary Report Contract No. N00019-80-C-0248. Calspan Report No. 6673-M-1. Calspan Corp., PO Box 400, Buffalo, NY 14225
R. Noonkester	NOSC	6 July 1981	Synoptic type model stressing importance of mesoscale trajectory for fog formation, in particular for Santa-Ana type fog in southern Calif.	Noonkester, V.R., 1979: "Coastal Marine Fog in Southern California", Monthly Wx Rev., 107, 830-851
J. Rosenthal	PMTC	7 July 1981	Preparing climatology of visibility frequency vs inversion height for Pt. Mugu; Engaged in operational fog forecasting	Rosenthal, J., 1972: Point Mugu Forecasting Handbook, Pacific Missile Range, Point Mugu, CA 93042
E. Mack & W. Rogers	Calspan	-	Visibility forecast (by quarter of day) as function of inver. height.	Mack, E., W. Rogers and B. Wattle, 1983: An Evaluation of Marine Fog Forecast Concepts and A Preliminary Design for a Marine Obscuration Forecast System, Calspan Rept 6866-M-1, Final Report, Project SEA FOG.
			OPERATIONAL FORECAST OFFICES	
CDR W. Hillyard (WO Haley)	NOCF (North Is.)	6 July 1981	Operational fog forecasting using Leipper's Indices	Leipper, D.F., 1948: "Fog Development at San Diego, CA", J. of Marine Res., VII, 3, 337-346; Naval Oceanography Command Facility, Naval Air Station, North Is, 1980: Forecasters Handbook, NAS North Island, San Diego, CA
R. Jimenez (D. Sankey)	Co Airlines Los Angeles International Airport	7 July 1981	Operational fog forecasting for up to 24 hrs using current semi-objective method. Attempting development of a 24-48 hr fog forecast technique using extreme values of temperature and dew point.	Gales, D.M., 1962: "A Semi-Objective Method for Forecasting Fog and Stratus Clouds at los Angeles International Airport", Trans-World Airlines, Inc. Meteorology Dept. Technical Bulletin No. 62-2, Kansas City
D. Driggers (J. Fannin)	NAS Pensacola, FL	17 June 1981	Operational fog forecasting primarily based on wind velocity and temperature difference between near shore water and open Gulf water	Personal Communication: Local Area Forecaster's Handbook for NAVOCEANCOMDET PENSACOLA/WHITING FIELD, NAVOCEANCOMDET INST 3140.2, Nov 1980.

Table A-2

Model Characteristics and Capabilities

Model	Model Description	Currently Active	Model Usage	Does Model Predict From Initial State Only?	Does Model Consider Radiative Effects? Longwave, Water Vapor	Liquid	Solar	Most Notable Features	Verification
Burk	H.O. Closure	YES	Research with operational testing	YES	YES	YES	YES	Predicts detailed behaviour in marine boundary layer, including cloud & fog.	O'Neill Data Operationally against ocean ship stations in Pacific and Atlantic
ARAP	H.O. Closure	YES	Research	YES	YES	YES	YES	Predicts detailed turb. dynamics and coupling with radiation and condensation	Laboratory turbulence studies; simulated West Coast fog types
Nurtele	Turb. Based Eddy Coeff.	YES	Research	YES	YES	YES	YES	Uses surface heat balance equation	El Monte, CA observational series
Tag	3-Dimension K-Theory	YES	Research	YES	YES	YES	YES	Fully 3-D	O'Neill Data
Barker	2-Dimension K-Theory	NO	Research	YES	YES	YES	NO	Uses theory on entrainment	Simulated fog formation from idealized data
Eadie and Rogers	2-Dimension K-Theory	NO	Research	YES	NO	YES	NO	Reproduces shallow cold water fog	Nova Scotia 1975 Data
NPS	Entrainment Slab (1-D)	YES	Research for fog applications	Needs prediction of near sfc conditions as functions of time	NO	YES	YES	Uses routinely available surface layer data	CEWCOM 1976 Data
Rogers	Slab (2-D, Horizontal)	NO	Research	YES	NO	Specified not calc.	NO	2-D Horizontal response of atmos.	July 1977 Case Study
Fitzgerald	Microphysics	NO	Research	Needs prediction of RH vs time	NO	NO	NO	Cloud microphysics	Nova Scotia 1975 Data
Telford	Plume	YES	Research	YES	NO	YES	NO	Entrainment at inversion	-

Table A-2 (Cont.)

Model	Model Description	Currently Active	Model Usage	Does Model Predict From Initial State Only?	Does Model Consider Radiative Effects?			Most Notable Features	Verification
					Longwave, Water Vapor	Liquid	Solar		
Renard	M O S	YES	Operational (but not yet used)	YES	NO	NO	NO	Ready for operational implementation	Independent data set
Clark	F-ter	YES	Operational	YES	NO	NO	NO	Currently operational	Synoptic ship reports
Gathman	Empirical; Aerosol Profile	YES	Research	YES	NO	NO	NO	Vertical profile of aerosols	North Sea data
Leipper	Fog Freq. vs. Inv. Ht.	YES	Testing with operational data	Needs prediction of inv. height	NO	NO	NO	Relates fog occur. to observed feature	-
Jung	Indices	YES	Research	YES	NO	NO	NO	Applies Leipper indices to open ocean	Ship Papa Summer 1975
Rogers and Mack	Decision Tree	YES	Testing with operational data	Needs prediction of 850 mb pattern	NO	From mid & high clouds	NO	Relates fog to synoptic patterns	-
Noonkester	Mesoscale Trajectories	NO	Research	--	NO	NO	NO	Relates fog to trajectory history	-
Rosenthal	Synoptic Forecast	YES	Operational	YES	NO	NO	NO	Produces daily operational forecasts	Daily
North I (NOCF)	Leipper's Indices	YES	Operational	YES	NO	NO	NO	Produces daily objective operational forecasts	Daily
Co Airlines	Sfc. Pressure Gradients	YES	Operational	YES	NO	NO	NO	Produces daily objective operational forecasts	Daily
NAS Pensacola	Synoptic Forecast	YES	Operational	YES	NO	NO	NO	Uses sfc water temp gradient	Daily
Mack & Rogers	Inversion Statistics	YES	Research	Needs prediction of inv. height	NO	NO	NO	Predicts visibility	-

Table A-3

Computing Characteristics and Modeling Framework
for the Numerical Models

Model	Model Description	Computer	Core	Running Time		Coordinates		Resolution		
				Iteration (sec)	24-hr Forecast (min)	Vert	Horiz	Vert	Horiz	Near Sfc High Res
Burk	H.O. Closure	CDC 6500	75 KB	0.40	10	1-D 2-D	- 2-D	25-50m	0.5m	YES
ARAP	H.O. Closure	PDP-11/70	28 KB	1.20	24	X	-	Var	-	YES
Wurtele	Turb-based eddy coeff	?	?	?	?	X	-	25m	-	NO
Tag	3-Dim, K-Theory	CYBER175	35K Words	0.43	-	X	X	20-100m	10km	YES
Barker	2-Dim, K-Theory	CDC 6500	32K Words	1.00	13	X	X	Var	20-200km	YES
Eadie	2-Dim, K-Theory	370/168	192 KB	0.17	2	X	X	Var	Var	YES
NPS	Entrainment/Slab (1-D)	HP 9845	150KB	?	10	-	-	Slab	-	-
Rogers	Slab, 2-D Horiz.	PE 7/32 CII	58 KB	4.00	24	-	X	Slab	20-40km	-
Fitzgerald	Microphysics	TI (ASC)	30K Words	?	24	-	-	-	-	-
Telford	Plume	CDC 6400	60K Words	-	-	X	-	?	-	?

Table A-4

Summary of Models' Input Data Requirements

Model	Model Description	Profile (P) and Well-Mixed (WM) Variables						Non-Profile Variables							Individualized Inputs
				Temperature		Moisture		Earth's Surface		Atmospheric					
		$\vec{V}$	$\vec{V}_g$	Below Inv.	Above Inv.	Below Inv.	Above Inv.	Temp	Moisture	Temp	Moisture	Subsidence	$\vec{V}$	$\vec{V}_g$	
Burk	H.O. Closure-Turb	P	P	P	P	P	P	X	X			X			Can utilize advective changes above mixed layer
ARAP	H.O. Closure-Turb	P		P	P	P	P	X	X			X			Cloud amount above mixed layer
Wurtele	Turb-based eddy coefficient	P		P	P	P	P	X				X		X	Soil Temperature at 50 cm
Tag	3-Dimension K-Theory	P		P	P	P	P	X	X						Three-dimensional inputs
Barker	2-Dimension K-Theory		P	P	P	P	P	X	X			X			
Eadie	2-Dimension K-Theory	P		P	P	P	P	X	X						
NPS	Entrainment/Slab (1-Dimen)			WM	P	WM	P	X	X	X	X	X	X		Inversion jump in θ and specific humidity; near surface wind, temp, humidity and surface temps as functions of time
Rogers	Slab (2-D, horizontal)	WM		WM	WM	WM		X	X					X	Height of inversion
Fitzgerald	Microphysics										X				CCN activation spectrum; Aerosol size spectrum; time rate of change of RH
Telford	Plume									X	X				*At top boundary of model*, temp total pressure, water vapor & LWC
Renard	M-O-S	——— (uses variables contained in FNOC products) ———													FNOC operational observations & predictions
Clark	F-ter	——— (uses variables contained in FNOC products) ———													FNOC operational observations & predictions
Gathman	Empirical: Aerosol Profile							X		X	X		X		Air-sea temp difference & obs. of cloud cover. Surf wind & sea state
Leipper	(1) Indices(Op. at North Is.,NOCF)							Sea Sfc Temp		X	X				Inv. ht. and max. temp. above inversion; moisture at 10,000 ft.
	(2) Fog Freq. vs Inv. Ht.														Prediction of inversion height
Jung	Indices							Sea Sfc Temp		Y	X				Inv. ht. and max. temp. above inversion and wind velocity
Calspan	Decision Tree	——— (required variables implied in large scale [illegible]eric forecast) ———													Prediction of 850-mb pattern obs of cloud and vertical sounding
Rosenthal	Synoptic Forecast	——— (uses standard met. observations) ———													Also requires special local winds
Co. Air.	Sfc Press Gradients	——— (uses standard met. observations) ———													
NAS Pens.	Synoptic Forecast	——— (uses standard met. observations) ———													Also requires local sfc water temp
Calspan	Inversion Statistics														Prediction of inversion height

Table A-5

Summary of Models' Output Capability

Model	Model Description	Profile (P) and Well-Mixed (WM) Mean Variables			Various Turbulence Quantities	Meteorological Visibility	Probability or Likelihood of Fog
		Temperature	Moisture	Fog/Liquid Water Content			
Burk	H.O. Closure	P	P	P	YES	-	-
ARAP	H.O. Closure	P	P	P	YES	-	-
Wurtele	Turb-based eddy coefficient	P	P	P	-	-	-
Tag	3-Dimension K-Theory	P	P	P	-	-	-
Barker	2-Dimension K-Theory	P	P	P	-	-	-
Eadie	2-Dimension K-Theory	P	P	P	-	-	-
NPS	Entrainment/Slab (1-Dimen)	WM	WM	WM	-	-	-
Rogers	Slab (2-D, horizontal)	WM	WM	WM	-	-	-
Fitzgerald	Microphysics	-	-	(single height)	-	YES	-
Telford	Plume	P	P	P	YES	-	-
Renard	M-O-S	-	-	-	-	YES	YES
Clark	F-ter	-	-	-	-	-	YES
Gathman	Empirical: Aerosol Profile	P	P	P	-	-	-
Leipper (1)	Indices(Op. at North Is.,NOCF)	-	-	-	-	-	YES
(2)	Fog Freq. vs Inv. Ht.	-	-	-	-	YES	YES
Jung	Indices	-	-	-	-	-	YES
Calspan	Decision Tree	-	-	-	-	(fog density)	YES
Rosenthal	Synoptic Forecast	-	-	-	-	-	YES
Co. Air.	Sfc. Press Gradients	-	-	-	-	-	YES
NAS Pens.	Synoptic Forecast	-	-	-	-	-	YES
Calspan	Inversion Statistics	-	-	-	-	YES	YES

Table A-6

COMPLETE LISTING OF INDIVIDUALS INTERVIEWED RELATIVE TO THIS PROGRAM

INDIVIDUAL	AFFILIATION	LOCATION
E. Barker	NEPRF	Monterey, CA
S. Burk	NEPRF	Monterey, CA
L. Clarke	FNOC	Monterey, CA
K. Davidson	NPS	Monterey, CA
R. Dixon	PMTC	Pt. Mugu, CA
D. Driggers	NAS Pensacola	Pensacola, FL
C. Fairall	BDM/NPS	Monterey, CA
J. Fannin	NAS Pensacola	Pensacola, FL
R. Fett	NEPRF	Monterey, CA
J. Fitzgerald	NRL	Washington, DC
A. Fox	PMTC	Pt. Mugu, CA
S. Gathman	NRL	Washington, DC
A. Goroch	NEPRF	Monterey, CA
WO Haley	NOCF	San Diego (North Is.)
R. Helvey	PMTC	Pt.Mugu, CA
CDR Hillyard	NOCF	San Diego (North Is.)
W. Hopple	NRL	Washington, DC
H. Hughes	NOSC	San Diego, CA
R. Jimenez	Co. Airlines	Los Angeles, CA
B. Kunkel	AFGL	Bedford, MA
D. Leipper	NPS	Monterey, CA
S. Lewellen	ARAP	Princeton, NJ
E. Mack	Calspan	Buffalo, NY
J. Mueller	NPS	Monterey, CA
R. Nagle	NEPRF	Monterey, CA
C. Nelson	Navy/NOAA	Monterey, CA
R. Noonkester	NOSC	San Diego, CA
S. Payne	NEPRF	Monterey, CA
R. Pilié	Calspan	Buffalo, NY
R. Renard	NPS	Monterey, CA
W. Rogers	Calspan	Buffalo, NY
J. Rosenthal	PMTC	Pt.Mugu, CA
T. Rosmond	NEPRF	Monterey, CA
L. Ruhnke	NRL	Washington, DC
D. Sankey	Co. Airlines	Los Angeles, CA
G. Schacher	NPS	Monterey, CA
I. Sykes	ARAP	Princeton, NJ
P. Tag	NEPRF	Monterey, CA
J. Telford	DRI	Reno, NV
CPO Webster	NOCF	San Diego (North Is.)
A. Weinstein	NEPRF	Monterey, CA
M. Wurtele	UCLA	Los Angeles, CA
G. Yung	NPS	Monterey, CA

APPENDIX B

CALSPAN TEST DATA SETS

Appendix B contains documentation and the blind data sets for all six test cases. The data for each case contains the following information:

1) A plot of verification and initial temperature and dewpoint profiles and location of initial and verification cloud base and top. In these plots, dewpoint temperatures less than the minimum temperature on the abcissa were plotted at their correct height, but at the minimum dewpoint value.

2) Documentation package containing
   a) Locator Map
   b) Synoptic Charts
   c) Sea surface temperature distribution
   d) List of data sources

3) The blind data set as transmitted to the individual investigators. This section contains
   a) Initial sounding
   b) Initial cloud liquid water content
   c) An estimate of subsidence
   d) Sea surface temperature distribution
   e) Surface actual and geostrophic wind
   f) Sunrise and/or sunset time, sun's declination and latitude of case
   g) Low-level vertical profile of wind
   h) Upper level temperature and dewpoint sounding
   i) Instructions for running the model on the case study.

Subsidence values were obtained by comparing initial and verification temperature profiles in the warm air above the marine boundary layer and attributing any changes to adiabatic warming or cooling as the air sank or rose. To minimize effects of entrainment at the top of the boundary layer on temperature changes, the lowest point used on the profile was that defined by the first measured point in that portion of the profile in which the temperature increased with height. With this definition, the lowest part of the temperature profile in the warm air, which is partially defined by the minimum temperature at the top of the marine boundary layer (and entrainment), was not used to specify subsidence.

AD-A136 379 AN EVALUATION OF MARINE FOG FORECAST CONCEPTS AND A PRELIMINARY DESIGN FO..(U) ARVIN/CALSPAN ADVANCED TECHNOLOGY CENTER BUFFALO NY APPLIED T..

2/3

UNCLASSIFIED E J MACK ET AL. JUN 83 CALSPAN-6866-M-1 F/G 4/2 NL

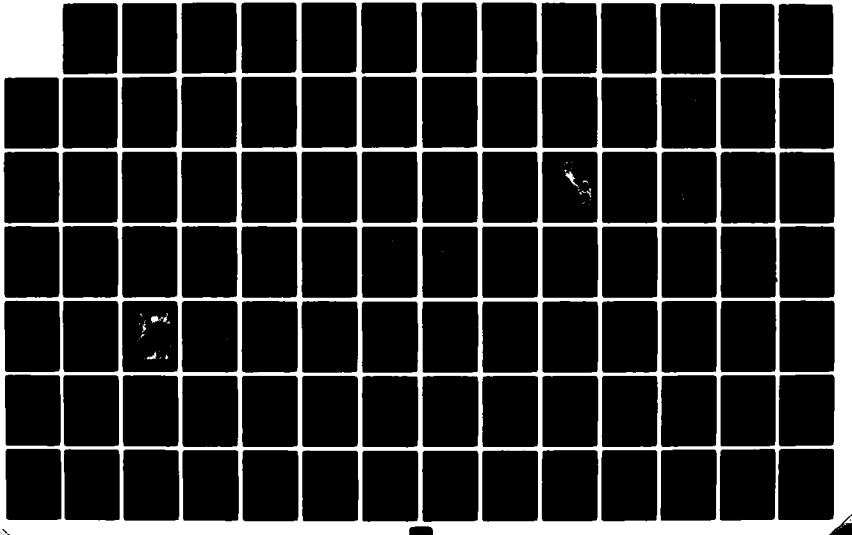

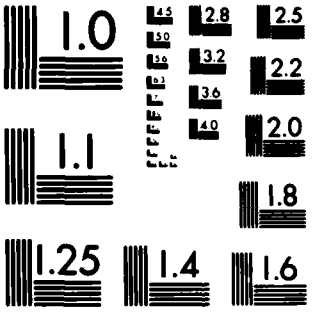

MICROCOPY RESOLUTION TEST CHART
NATIONAL BUREAU OF STANDARDS-1963-A

Geostrophic wind was computed by assuming a balance of forces at the surface between pressure, coriolis and friction. Because of the mesoscale areas generally involved in these case studies and because of the mostly weak and/or spatially variable large scale pressure fields involved, it was decided that the locally observed wind would provide a better measure of the local pressure gradient than pressure gradients measured from synoptic charts. The value of the coefficient of drag which was used was 1.5×10^{-3}, typical of that used for ocean surfaces. In the cases, the thermal wind in the boundary layer was essentially zero, so we assumed the geostrophic wind was constant with height; it was also assumed to be constant during the simulation.

Definition of Wind Direction for All Cases

With + (plus) (X) in the direction of increasing distance for the sea surface temperature distribution, a wind velocity with 0° points along the positive X-axis, and wind direction is positive in a clockwise direction from this 0° orientation.

Table B-1

SUMMARY OF DATA SETS

Case	Type	Time Interval	Time of Day	Low Level Temp Structure	Initial Cloud	Winds	Synoptic Scale Vertical Motion	Sea Surface Temp	
								Relative to Air	Trend with Distance
Aug 29, 1972 Case 6	Stratus lowering to fog	3 hr	Evening	Neutral	Yes	lt.	zero	cold	---
July 14-15, 1973 Case 4	Stratus thickening	10	Night	Neutral	Yes	lt.	zero	warm	constant
May 22, 1978 Case 1	Stratus	4	Morning	Unstable to Neutral	Yes	mod.	zero	warm	warming
Aug 2, 1975 Case 2	Shallow cold water advection fog	3	Evening	Inverted	No	mod.	----	cold	cooling
Aug 5, 1975 Case 5	Shallow cold water fog deepening over warm water	3	Morning	Inverted to Isothermal	No	mod.	----	cold to warm	warming
Oct 7, 1976 Case 3	Thinning stratus re-developing to form fog	10, 20	Morning to Night	Neutral to Unstable	Yes	lt.	strong subsidence	warm	warming

CASE 1

22 May 1978

Northwest of San Nicolas Island
(to 85 km)
(CEWCOM-78)

Time Zero: 0500 PDT

Verification Time: 0900 PDT

Sunrise: 0600 PDT

Scenario: No fog; thickening high stratus cloud as inversion base rises ∿100 m. Air colder than sea.

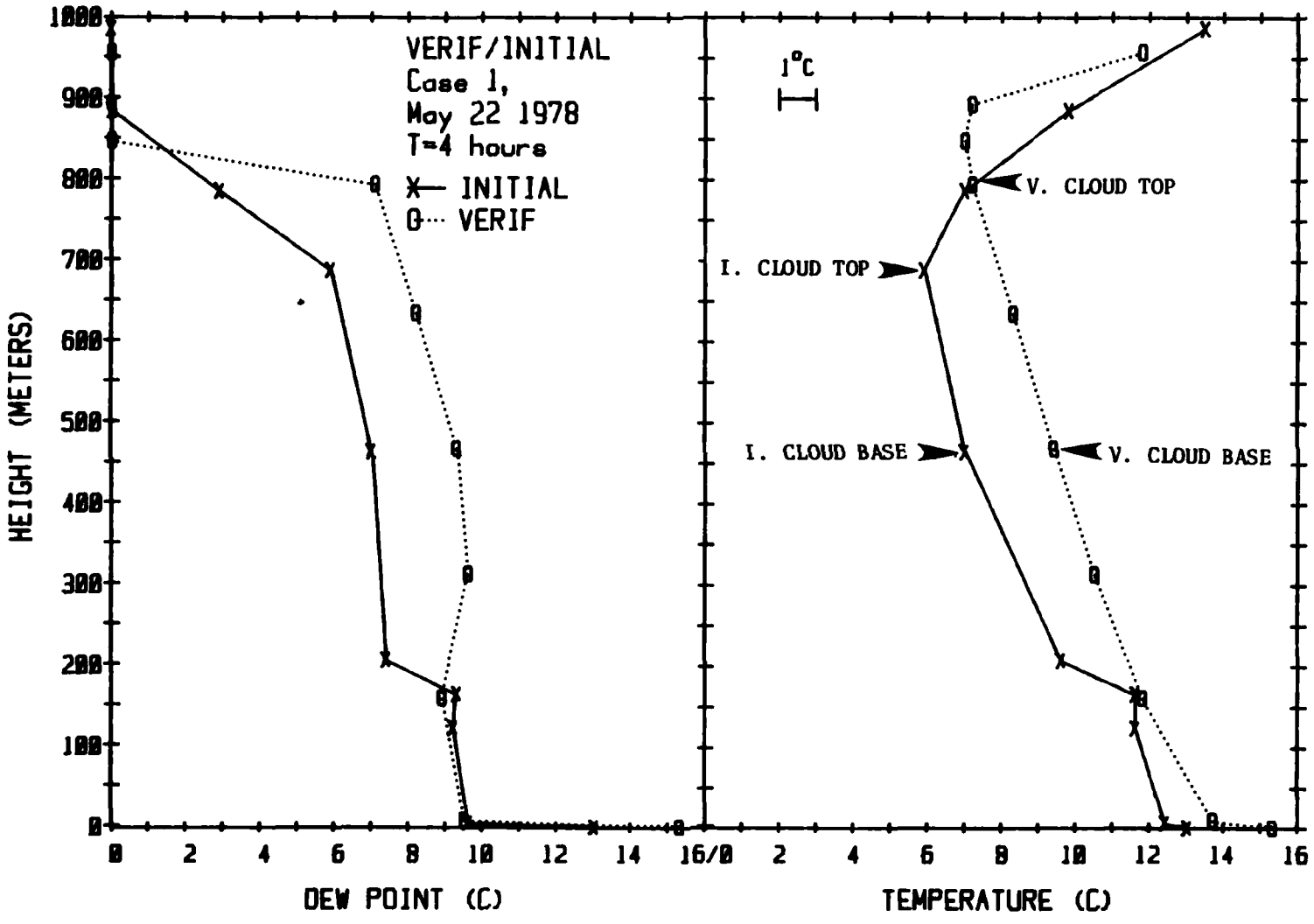
VERIF/INITIAL
Case 1,
May 22 1978
T=4 hours
INITIAL
VERIF
1°C
V. CLOUD TOP
I. CLOUD TOP
I. CLOUD BASE
V. CLOUD BASE
HEIGHT (METERS)
DEW POINT (C)
TEMPERATURE (C)
1000
900
800
700
600
500
400
300
200
100
0
0 2 4 6 8 10 12 14 16/0 2 4 6 8 10 12 14 16

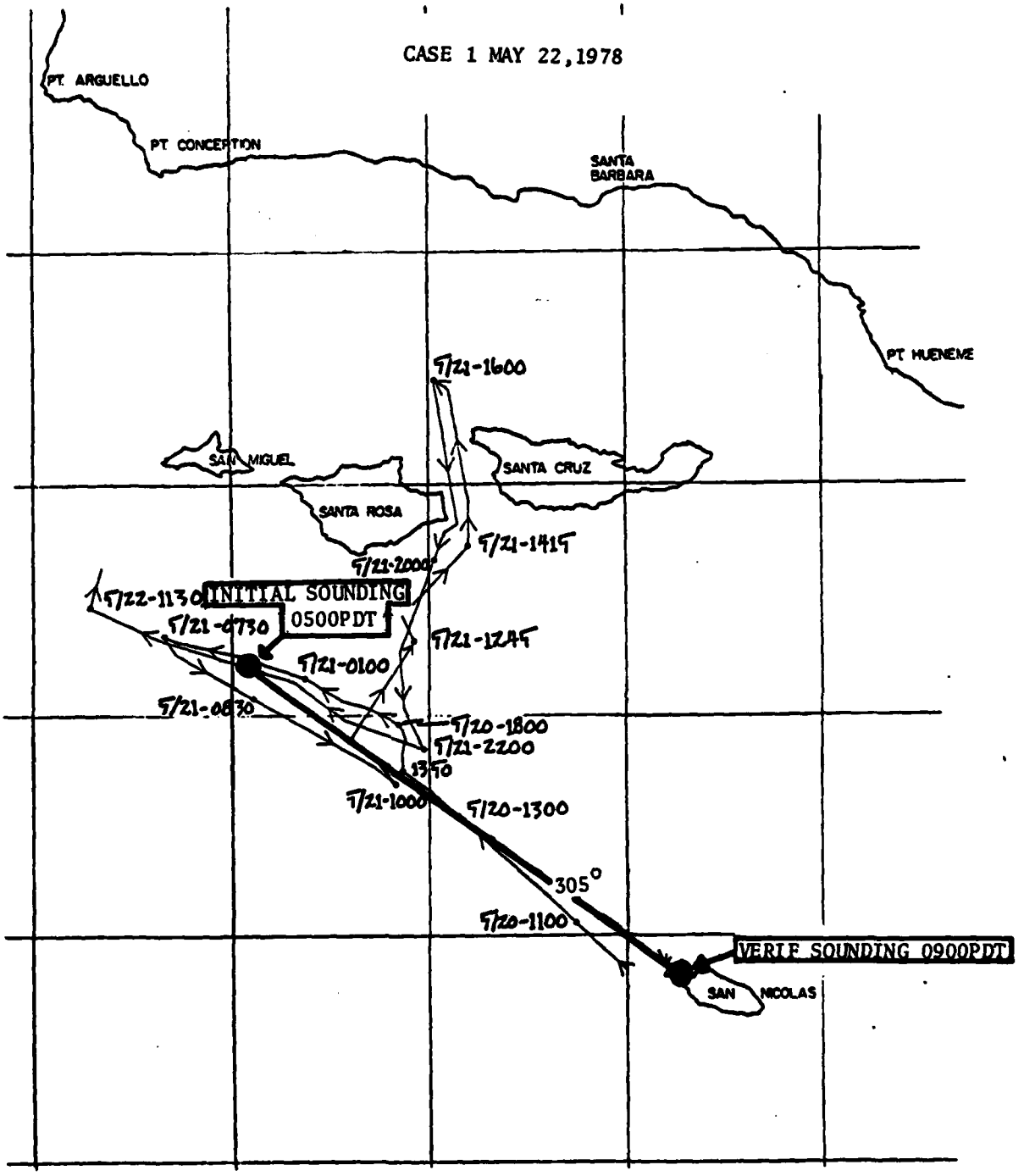

Positions of R/V Acania from 5/18/78 to 5/25/78

After Fairall et al 1978

Surface Analysis 15Z 22 May 1978

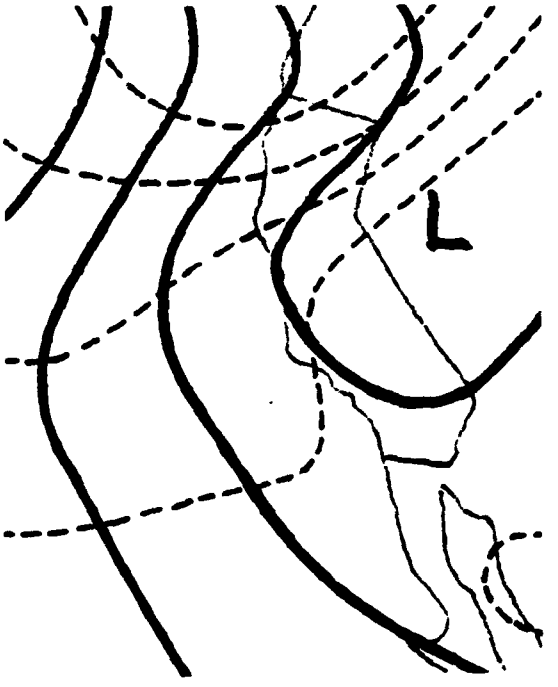

850 mb Analysis 12Z 22 May 1978

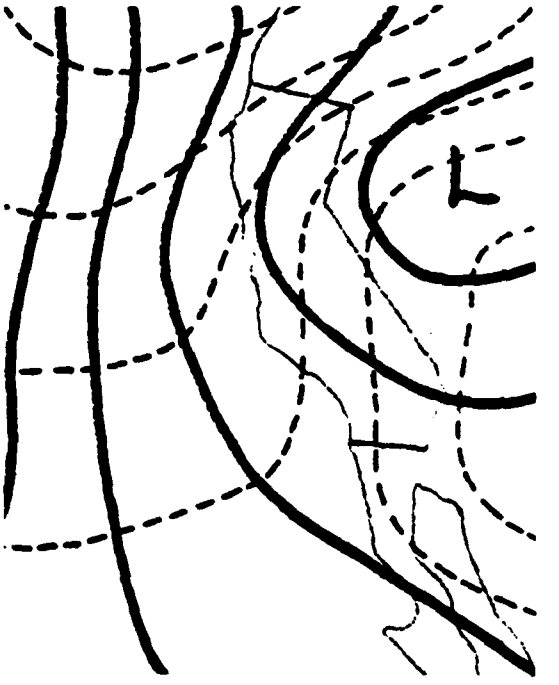

850 mb Analysis 00Z 23 May 1978

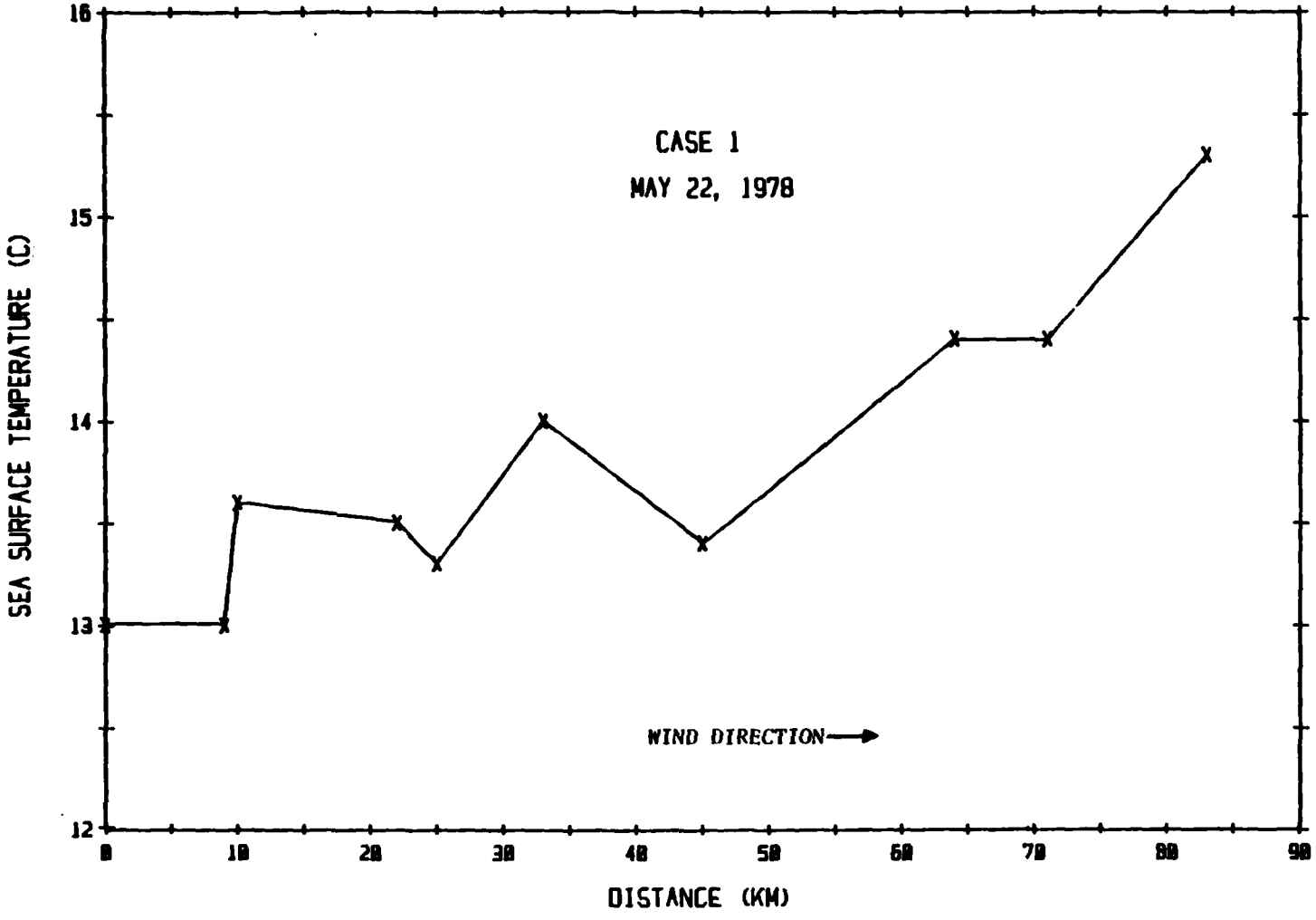
CASE 1
MAY 22, 1978
SEA SURFACE TEMPERATURE (C)
16
15
14
13
12
WIND DIRECTION
0
10
20
30
40
50
60
70
80
90
DISTANCE (KM)

DATA SOURCES

CASE 1
May 22, 1978

1.) Locator Map, Pg. 12, Fig. 2

Fairall, C.W., Schacher, G.E., Davidson, K.L., and Holihan, T.M., 1978: Atmospheric Marine Boundary Layer Measurements in the Vicinity of San Nicolas Island During CEWCOM-78. NPS61-78-007, September 1978. Naval Postgraduate School, Monterey, CA 93940.

2.) Initial Sounding - Acania - Calspan Data Set

Verification - San Nicolas Is. after

Rosenthal, J., Battaline, T. et al and Noonkester, V.R., 1979: Marine/ Continental History of Aerosols at San Nicolas Island During CEWCOM-78 and OSP III. Technical Publication TP-79-33. April 1979 Pacific Missile Test Center, Point Mugu, CA 93042.

3.) a) Sea Surface Temperature Data -

Mack, E.J. and T.A. Niziol, 1978: Reduced Data from Calspan's Participation in the CEWCOM-78 Field Experiment off the Coast of Southern California During May 1978. October 1978. Co. No. N00019-78-C-0179. Calspan Report No. 6232-M-2. Calspan Corp. PO Box 400 Buffalo, N.Y. 14225.

b) Fairall et al 1978. Ibid.

4.) Surface Winds

Acania - Mack and Niziol, 1978 Ibid.

SNI - Blanc, T.V., 1978: Micrometeorological Data for the 1978 Cooperative Experiment for West Coast Oceanography and Meteorology (CEWCOM-78) at San Nicolas Island, California. Vol. II, May 16-22 Data. NRL Memorandum Report 3871. August 1978. Naval Research Laboratory, Washington, DC 20375.

5.) Synoptic Charts - National Meteorological Center, 850 mb and Surface.

CASE 1:'BLIND' DATA SETS

1.0 Initial Sounding (at time zero)

Height (m)	Pressure (mb)	Temperature (°C)	Dewpoint (°C)	RH (%)
6	1014	12.4	9.6	83
123	1000	11.6	9.2	85
165	995	11.6	9.3	86
207	990	9.6	7.4	86
688	934	6.4	6.4	100
786	923	7.0	2.9	75
885	912	9.8	-11.5	21
986	901	13.5	-9.7	19
1090	890	15.1	-8.4	19
1478	850	12.9	-10.2	19

1.1 Initial sky condition was observed as seven-tenths (7/10's) coverage by strato-cumulus. The above sounding appears flawed and shows cloud at only 688 m. We have attempted to reconstruct that portion of the sounding by computing the lifting condensation level from the 207 m level data. Cloud base is, therefore, at 464 m (960 mb) with the following profile data between 207 and 786 m:

464	960	7.0	7.0	100
688	934	5.9	5.9	100

The sounding is unchanged between 6 m and 207 m and between 786 m and 1478 m.

1.2 Cloud Liquid Water Content

Height (m)	LWC (g/m^3)
464	.000
632	.360
688	.000

Liquid water content, calculated according to adiabatic method of Rogers and Hanley (1980)*, varies linearly between these levels.

*Rogers, C.W. and J.T. Hanley, 1980: "An Algorithm for the Increase of Liquid Water Content with Height in Fog and Water Hazes," Calspan Rpt. 6711-M-1, 14 pp.

2.0 Inversion Base

Our estimate of height of base of inversion is 688 m.

3.0 Subsidence

Vertical motion is zero at 904 mb, and a positive maximum of +0.41 cm/sec at 915 mb.

4.0 No cloud present above the marine mixed layer.

5.0 Sea Surface Temperature

The following is the sea surface temperature variation along the air column's straight line trajectory.

Distance (km)	Temperature (°C)
0	13.0
9	13.0
10	13.6
22	13.5
25	13.3
33	14.0
45	13.4
64	14.4
71	14.4
83	15.3
102	14.8
109	14.0
120	15.0
134	15.0
160	15.7

6.0 Wind

Surface wind direction is parallel to the column trajectory with a constant speed of 7.3 m/sec. Geostrophic wind is uniform with height and constant with time.

7.0 Sun Information

	Declination (degrees)	Latitude (degrees)
Elevation Angle: 76° (at 12 noon)		
Sunrise occurs one (1) hour after time zero.	+20	33

8.0 Instructions

A) Please run model twice:

(1) Once with initial sounding with no cloud LWC at time zero, even though 688 m level shows 100% RH. Use information of 7/10's cloud coverage as necessary.

(2) Once with the second sounding with cloud layer, 464 to 688 m.

B) Output model results at one-hour intervals until model column traverses entire length of sea surface temperature distribution.

C) Please document all, if any, supplementary processing which you have to make to this data set in order to run your model.

ADDENDA

Surface Wind is 000° @ 7.3 m/sec.

Low Level Geostrophic Wind is + (plus) 25° @ 9.2 m/sec.

A representative wind sounding is:

Height (m-msl)	Direction (degrees)	Speed (m/sec)
Surface	0	8.2
313	+12	7.7
635	+23	6.2
957	+23	6.2
1262	-12	2.1
1579 (840 mb)	-25	2.6

	Time (1) Soundings			Time (1) + 6 Hours		
Level (mb)	Height (m)	Temp. (°C)	Dewpoint (°C)	Height (m)	Temp. (°C)	Dewpoint (°C)
850	1429	15.3	-40.5	1447	15.3	-40.3
700	2985	8.1	-26.4	3073	6.6	-22.3
500	5708	-10.7	-32.8	5671	-11.3	-36.0
400	7334	-22.6	-40.1	7338	-24.3	-37.4
300	9517	-41.2	-47.0	9517	-42.6	-48.4
200	11953	-58.5	-80.3	11765	-58.8	-65.9

Neither the initial nor verification soundings went above 850 mb so the above soundings are from a station in the vicinity of the test area. Time (1) is at time zero plus 5 hours.

CASE 2

2 August 1975

Near Southeast Coast of Nova Scotia
(∿50 km offshore)
(USNS HAYES Marine Fog Cruise)

Time Zero: 1700 EDT

Verification Time: 2000 EDT

Sunset: 1940 EDT

Scenario: Shallow advection fog formed over cold sea surface.

ISOPLETHS OF SEA SURFACE TEMPERATURE (°C) AND REGIONS OF REDUCED VISIBILITY (< 1000 M DUE TO FOG) ALONG SHIP'S TRACK

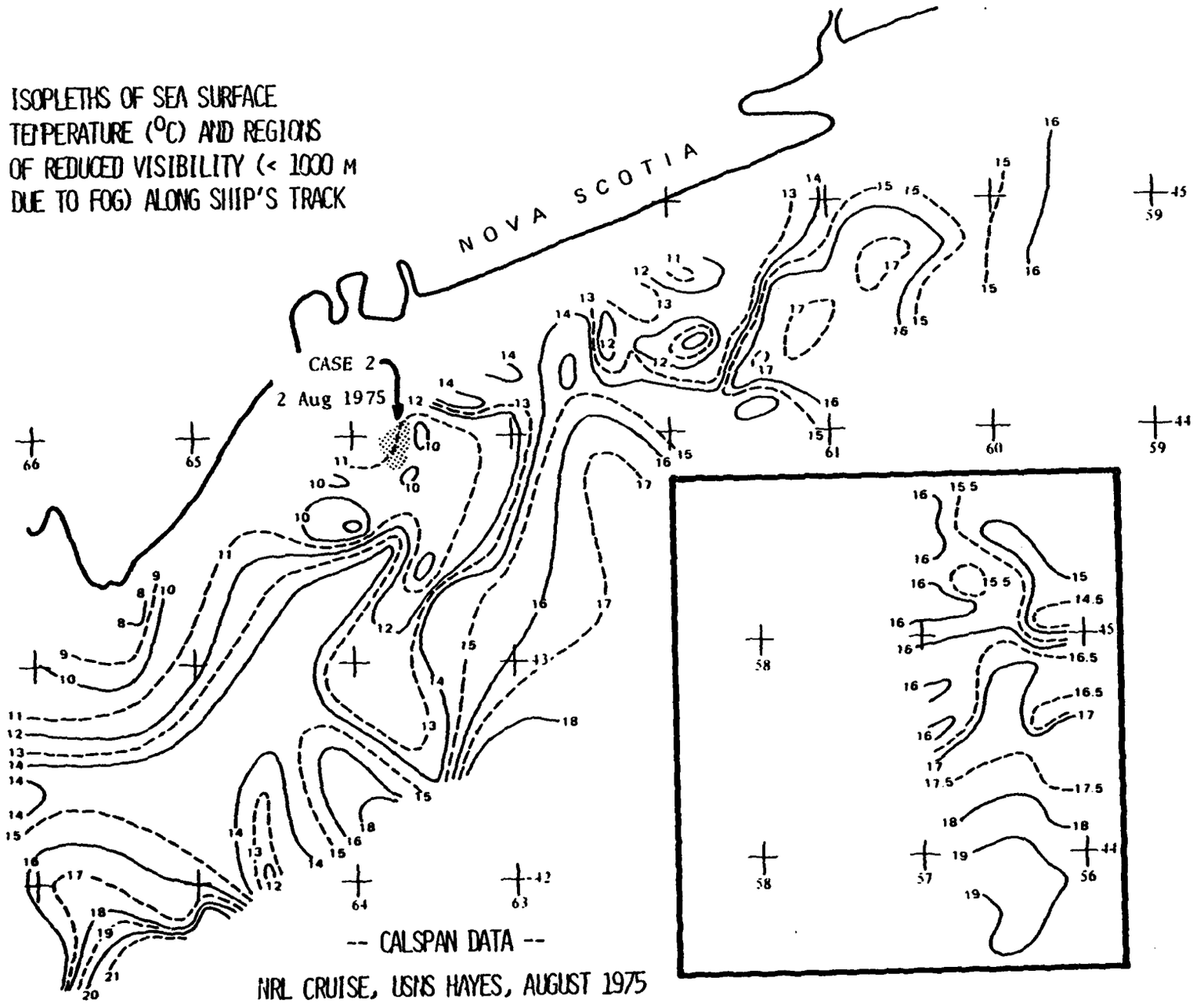

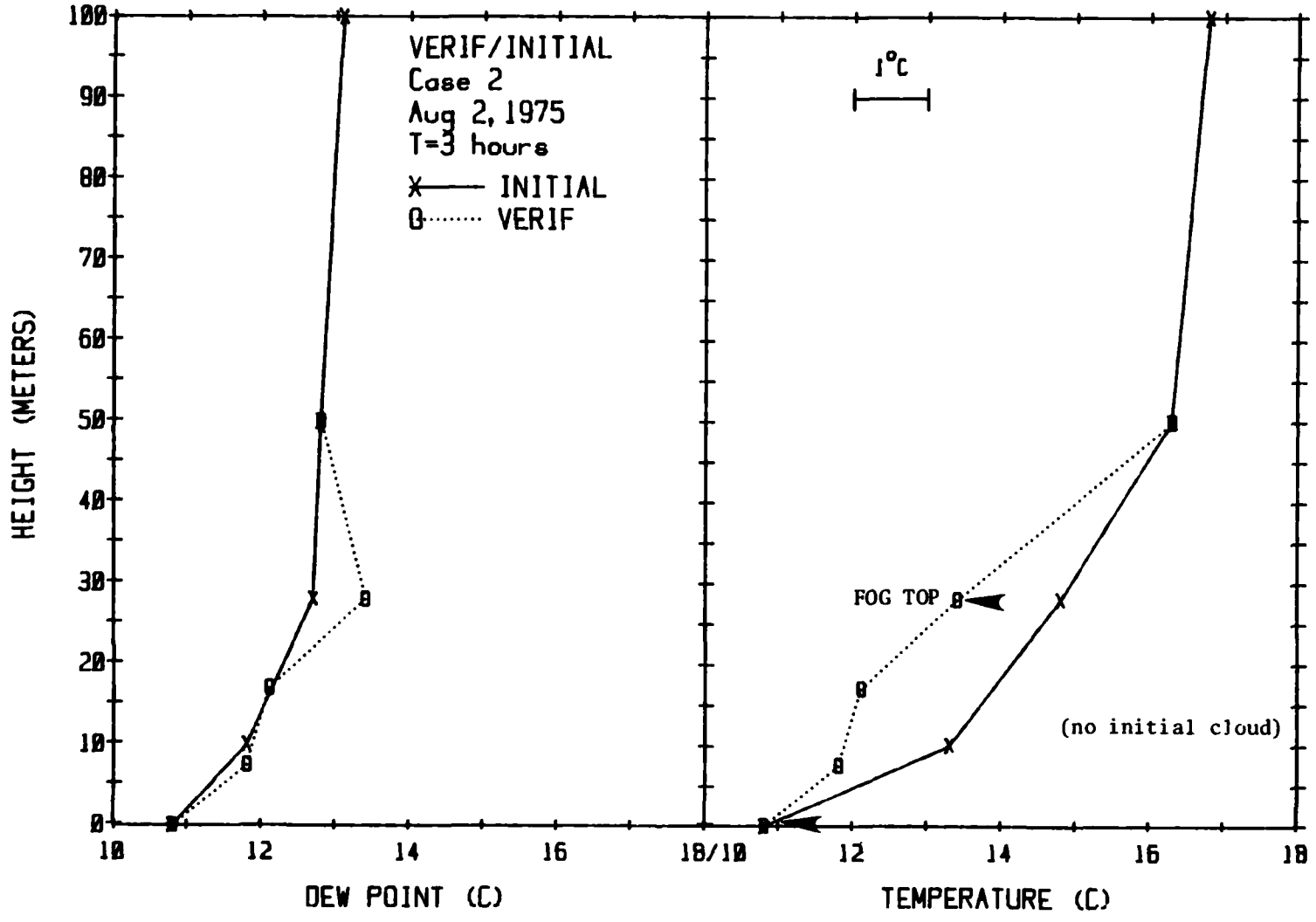
VERIF/INITIAL
Case 2
Aug 2, 1975
T=3 hours
INITIAL
VERIF
1°C
FOG TOP
(no initial cloud)
HEIGHT (METERS)
DEW POINT (C)
TEMPERATURE (C)
100
90
80
70
60
50
40
30
20
10
0
10
12
14
16
18/10
18

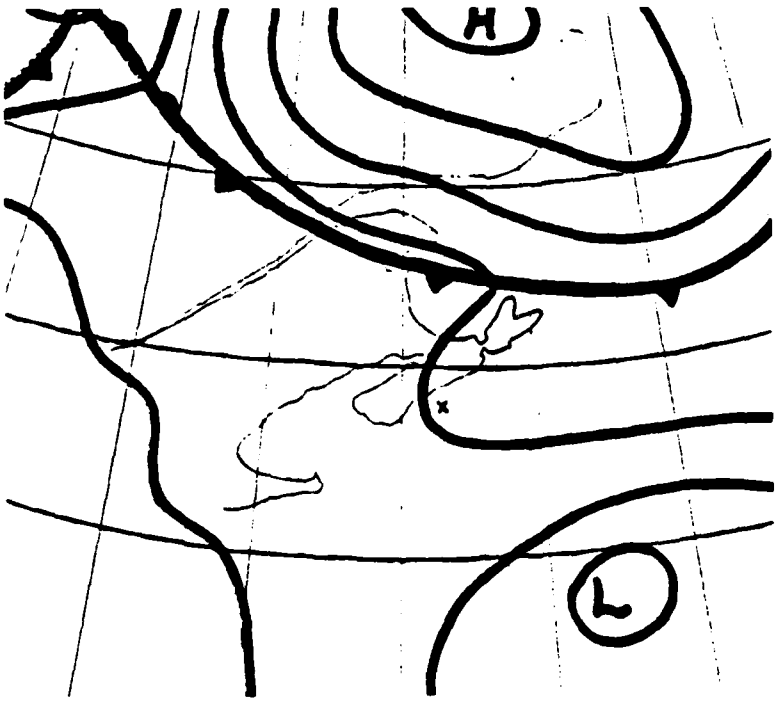

Surface Analysis 00Z 3 Aug 1975

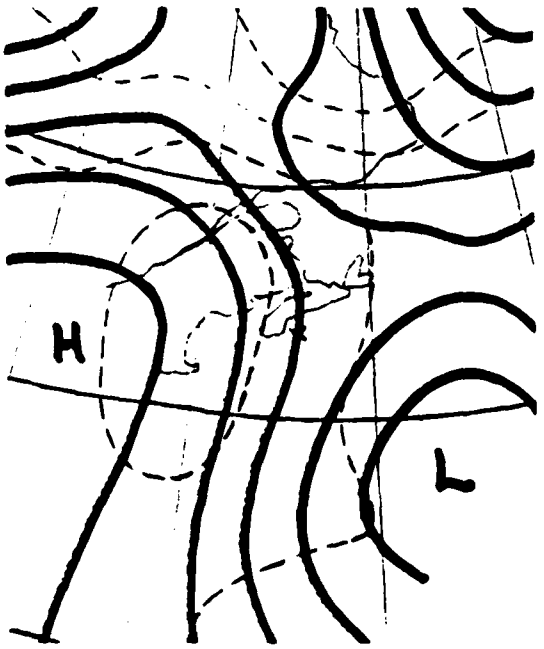

850 mb Analysis 12Z 2 Aug 1975

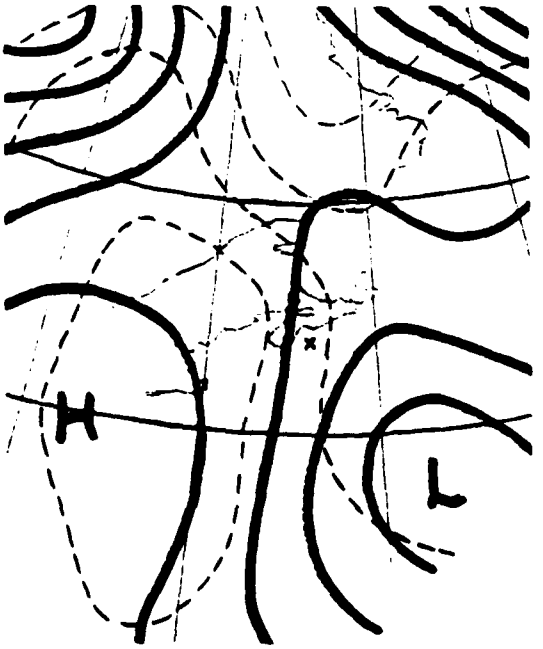

850 mb Analysis 00Z 3 Aug 1975

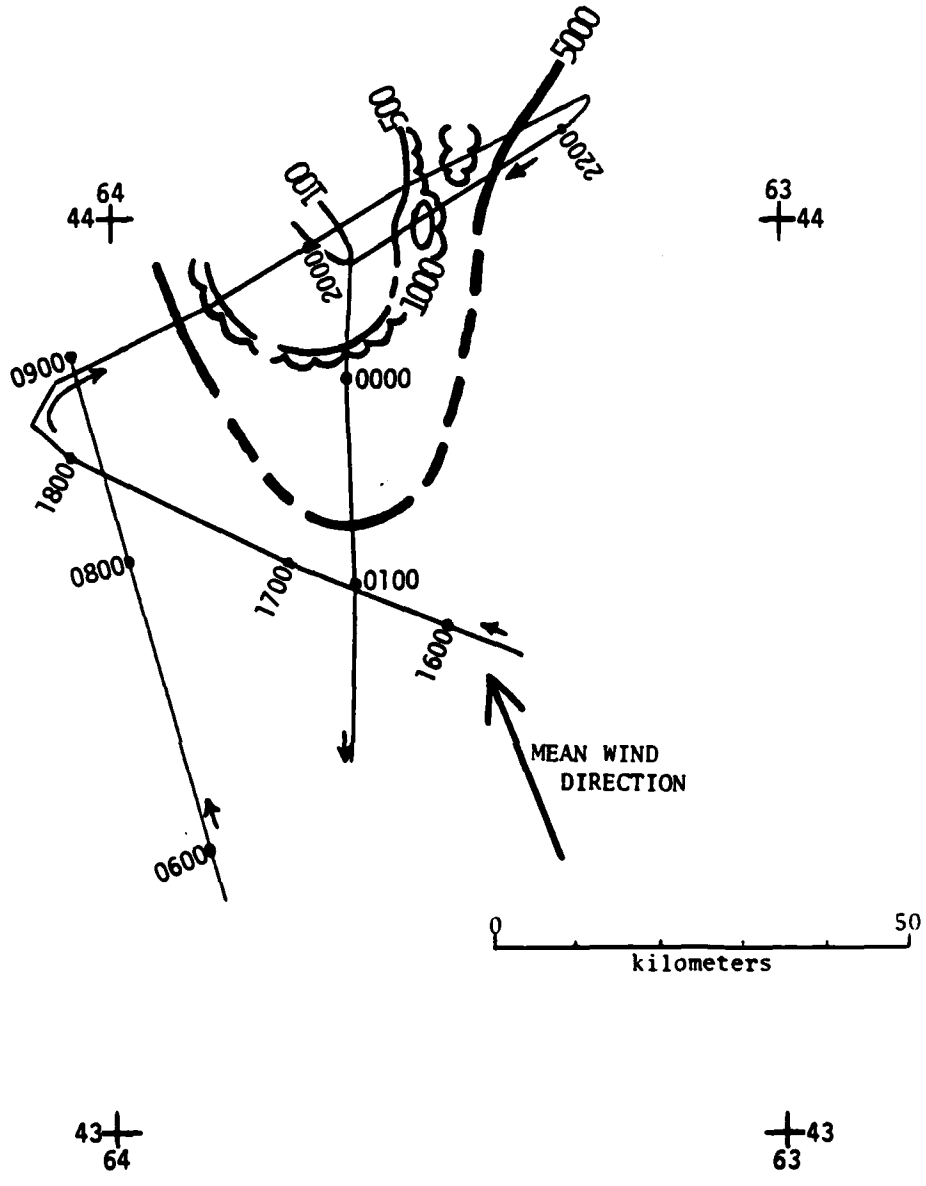

FIGURE CONTOURS OF VISIBILITY (M) FOR THE FOG OF 1915-0040 EDT, 2-3 AUGUST 1975.

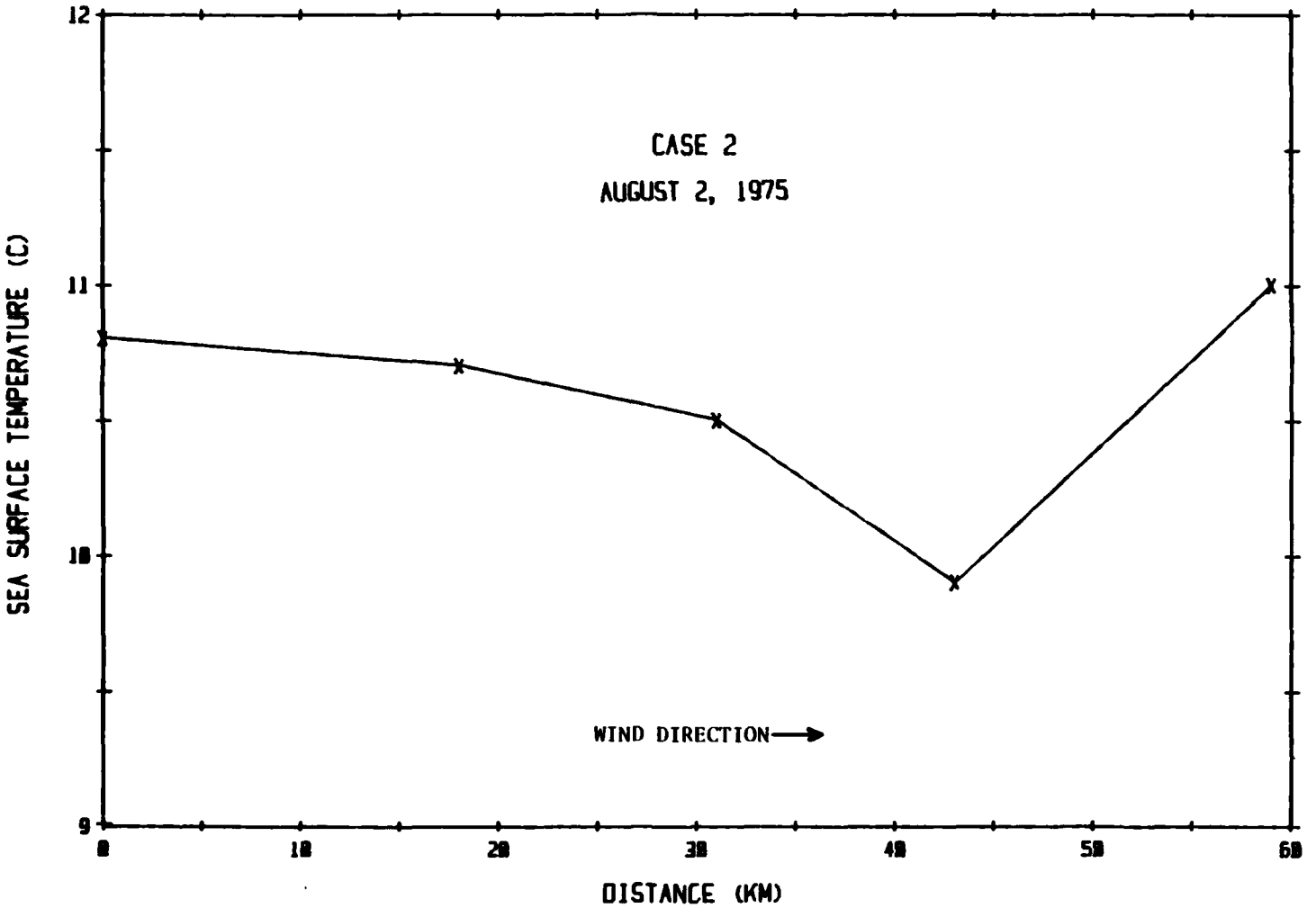
CASE 2
AUGUST 2, 1975
SEA SURFACE TEMPERATURE (C)
12
11
10
9
0
10
20
30
40
50
60
WIND DIRECTION
DISTANCE (KM)

DATA SOURCES

CASES 2 and 5
August 2 and August 5, 1975

1.) Locator Map -

Mack, E.J. and U. Katz, 1976: The Characteristics of Marine Fog Occurring off the Coast of Nova Scotia. Fourth Annual Summary Report Co. No. N00019-75-C-0508 June 1976. Calspan Report No. CJ-5756-M-1. Calspan Corp. PO Box 400 Buffalo, NY 14225.

2.) a.) Initial Sounding

Mack, E.J. and U. Katz, 1976: Ibid. Naval Research Laboratory, Naval Air Systems Command, and Office of Naval Research: Marine Fog Cruise, USNS Hayes 29 July-28 August, 1975.

Shelburne, N.S. Radiosonde $43^{o}43^{1}$N, $65^{o}15^{1}$W

b.) Verification

Mack, E.J. and U. Katz, 1976: Ibid.

3.) Sea Surface Temperature Data

Marine Fog Cruise, USNS Hayes, Ibid.
Mack, E.J. and U. Katz, 1976: Ibid.

4.) Surface Winds

Marine Fog Cruise, USNS Hayes, Ibid
Shearwater, AFB, Halifax, N.S.

5.) Synoptic Charts - National Meteorological Center 850 mb and Surface.

CASE 2: 'BLIND' DATA SETS

1.0 Initial Sounding (at time zero)

Height (m)	Pressure (mb)	Temperature (°C)	Dewpoint (°C)	RH (%)
10	1011.0	13.3	11.8	91
28	1009.4	14.8	12.7	87
50	1007.4	16.3	12.8	80
100	1002.9	16.8	13.1	79
150	998.4	17.2	13.5	79
200	993.9	17.5	13.9	79
250	989.4	17.7	13.9	78
300	984.9	17.5	13.7	78

1.1 Initial Sky Clear

1.2 Cloud Liquid Water Content

None

2.0 Inversion

Temperature profile is inverted all the way to the ocean surface.

3.0 Subsidence

Subsidence is zero.

4.0 No cloud present above the marine mixed layer.

5.0 Sea Surface Temperature

Distance (km)	Temperature (°C)
0	10.8
18	10.7
31	10.5
43	9.9
59	11.0
78	11.5

6.0 Wind

Surface wind direction is parallel to the column trajectory with a constant speed of 5.5 m/sec. Geostrophic wind is uniform with height and constant with time.

7.0 Sun Information

	Declination (degrees)	Latitude (degrees)
Elevation Angle: 62.5° (at 12 noon)	+18	44

Sunset occurs 2 hr. 40 min after time zero.

8.0 Instructions

A) Output model results at one-hour intervals until model column traverses entire length of sea surface temperature distribution.

B) Please document all, if any, supplementary processing which you have to make to this data set in order to run your model.

ADDENDA

Surface Wind is 000° @ 5.5 m/sec.

Low-level Geostrophic Wind is +(plus) 38° @ 7 m/sec.

A representative wind sounding is

Height (m-msl)	Direction (degrees)	Speed (m/sec)
Surface	000	5.5
90	-006	5.5
530	-067	1.0
1000	-139	5.0
1496 (850 mb)	-140	7.0

Soundings

Time (1)				Time (1) + 12 hours		
Level (mb)	Height (m)	Temp. (°C)	Mixing Ratio (g/Kg)	Height (m)	Temp. (°C)	Mixing Ratio (g/Kg)
950	546	20.2	12.0	530	20.1	15.7
900	1014	20.5	10.2	1000	21.9	14.7
850	1508	19.7	8.4	1496	19.1	9.9
700	3143	7.3	6.1	3134	8.7	1.4
500	5829	-9.4	0.8	5810	-5.3	0.4
400	7525	-19.5	0.2	7498	-20.3	0.2
300	9595	-35.5	0.1	9565	-35.6	0.3
200	12301	-53.9	-	12264	-55.4	-
100	16601	-59.2	-	16571	-62.5	-

T (1) is at time zero minus (-) 9 hours.

CASE 3

7 October 1976

Between San Nicolas Island and San Diego
(CEWCOM-76)

Time Zero: 0400 PDT

Verification Time: 1400 PDT
2400 PDT

Sunrise: 0720 PDT

Sunset: 1840 PDT

Scenario: 100 m thick stratus cloud, beneath a 250 m inversion, which dissipates during daytime and redevelops during early evening to produce fog under strong subsidence above the inversion.

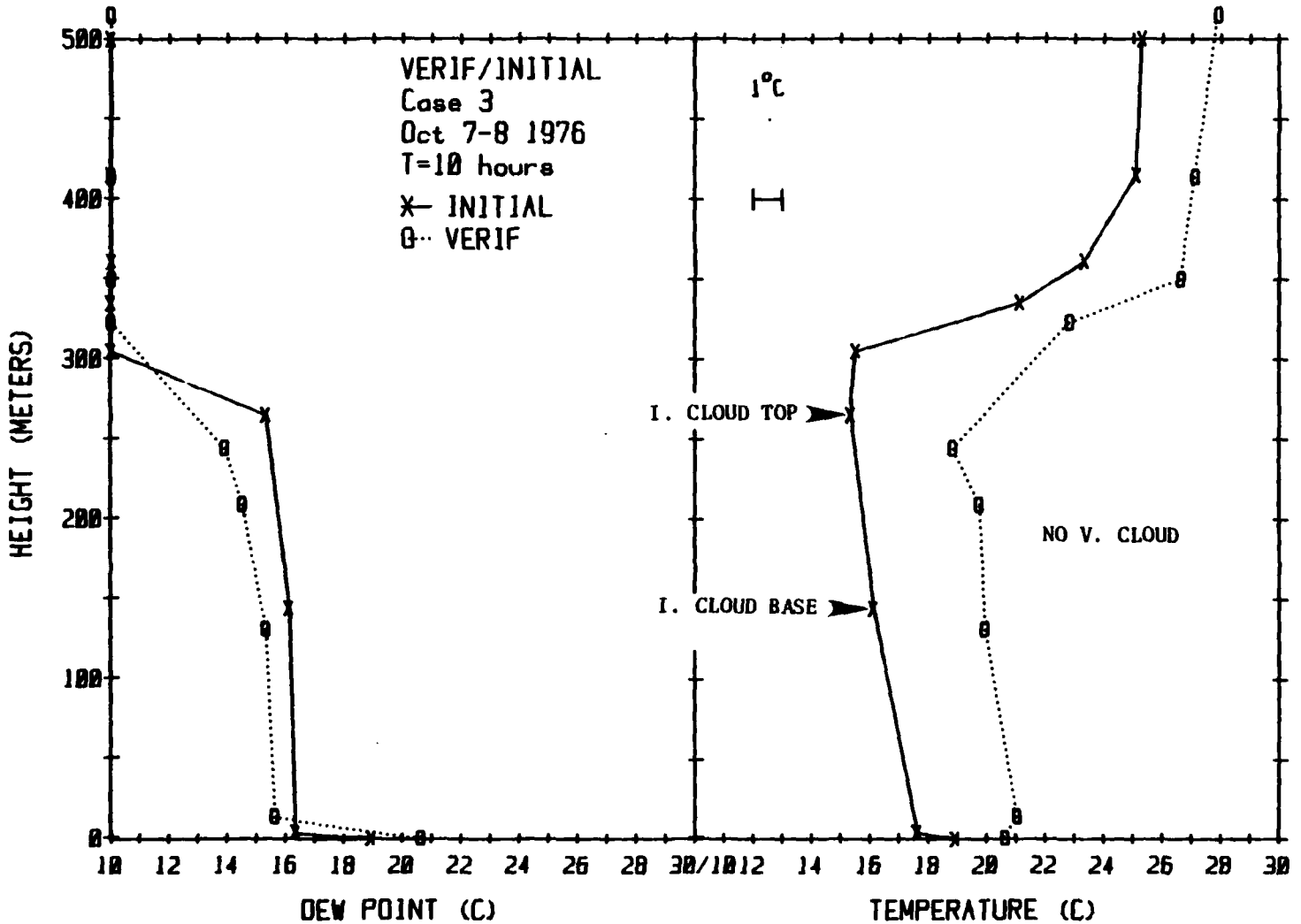
VERIF/INITIAL
Case 3
Oct 7-8 1976
T=10 hours
X— INITIAL
0··· VERIF
1°C
I. CLOUD TOP
I. CLOUD BASE
NO V. CLOUD
HEIGHT (METERS)
500
400
300
200
100
0
10 12 14 16 18 20 22 24 26 28 30/10 12 14 16 18 20 22 24 26 28 30
DEW POINT (C)
TEMPERATURE (C)

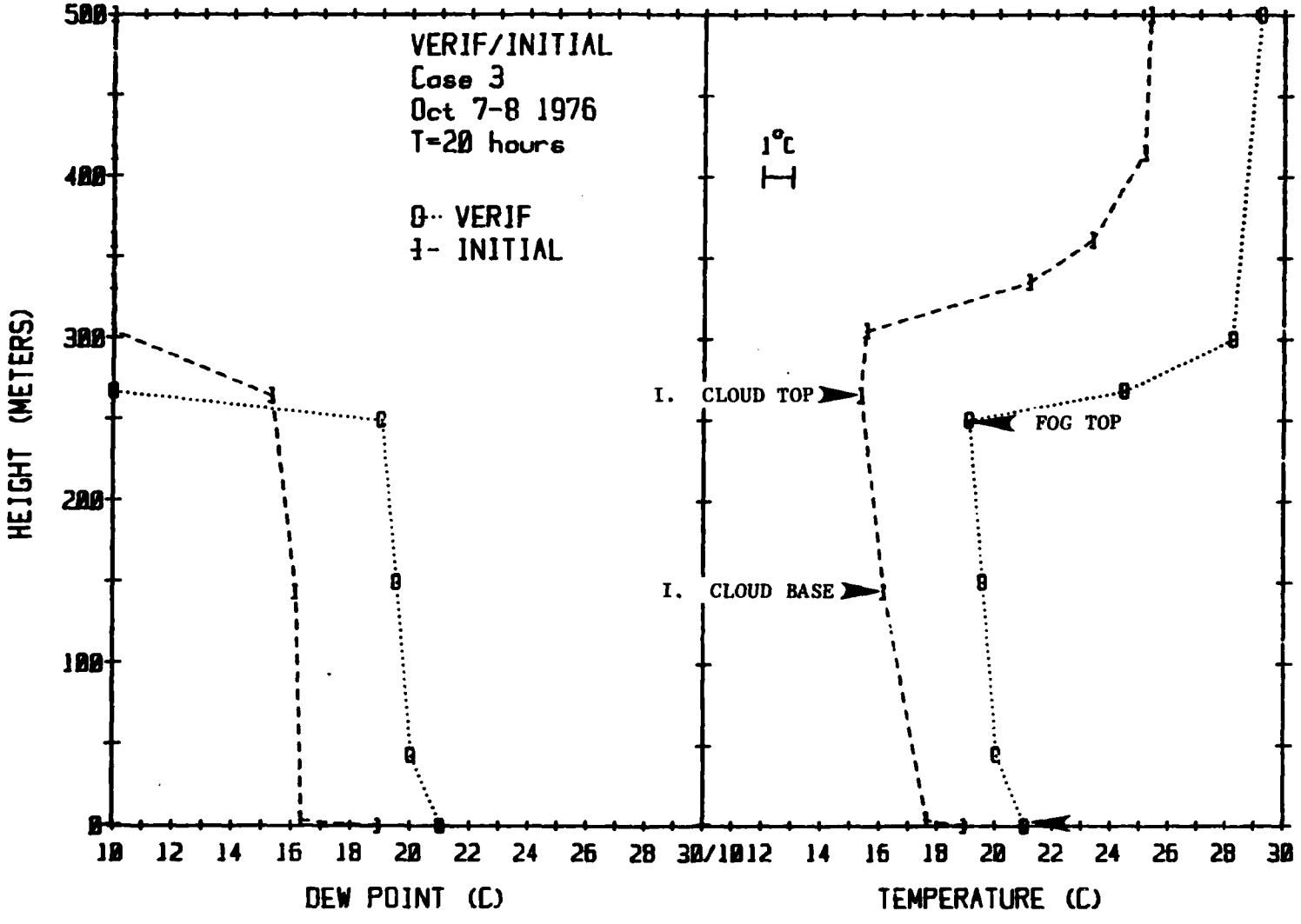
VERIF/INITIAL
Case 3
Oct 7-8 1976
T=20 hours
0 VERIF
I INITIAL
1°C
I. CLOUD TOP
FOG TOP
I. CLOUD BASE
HEIGHT (METERS)
500
400
300
200
100
0
10 12 14 16 18 20 22 24 26 28 30/10 12 14 16 18 20 22 24 26 28 30
DEW POINT (C)
TEMPERATURE (C)

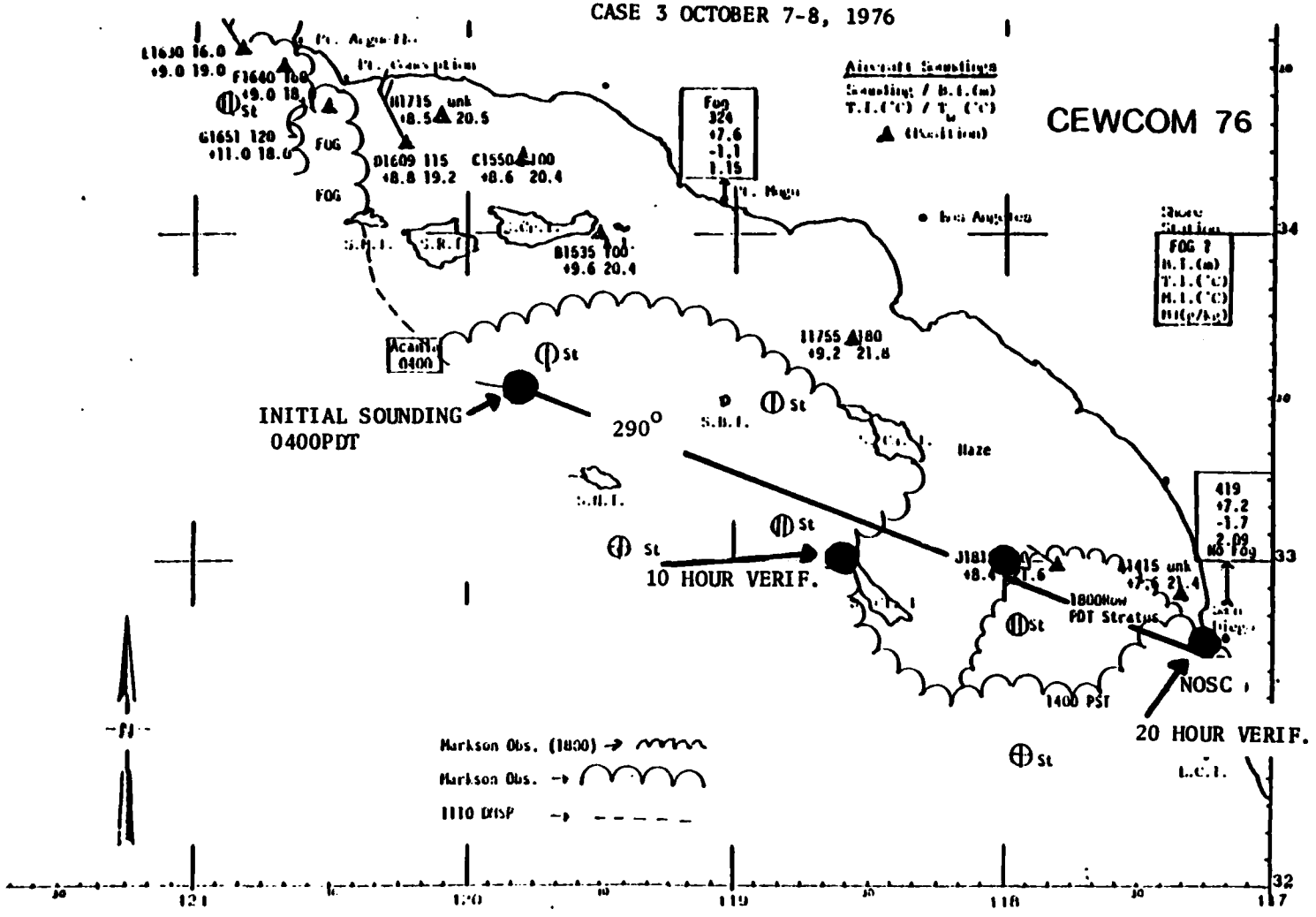

Indices and Weather Depiction 7 Oct

After Backes 1977

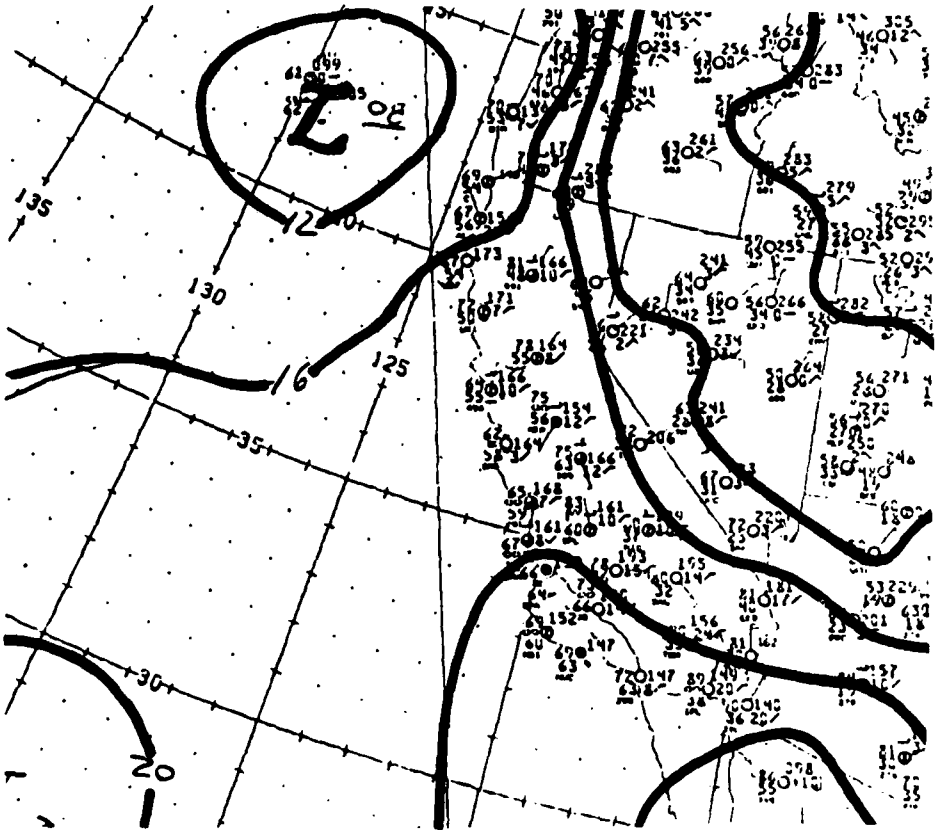

Surface Analysis 18Z 7 Oct 1976

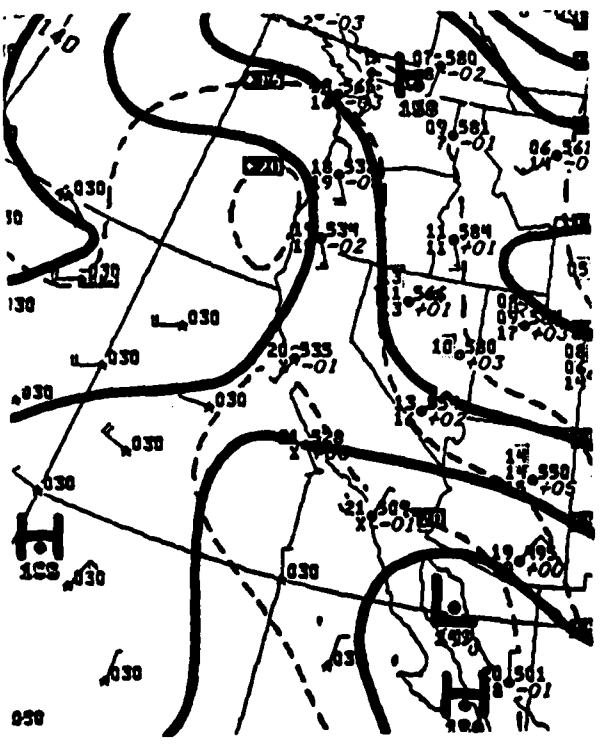

850 mb Analysis 12Z 7 Oct 1976

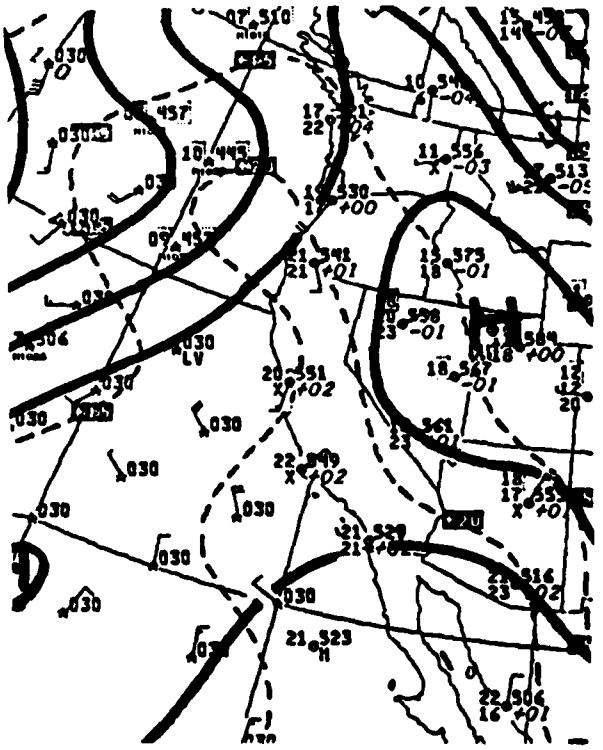

850 mb Analysis 00Z 8 Oct 1976

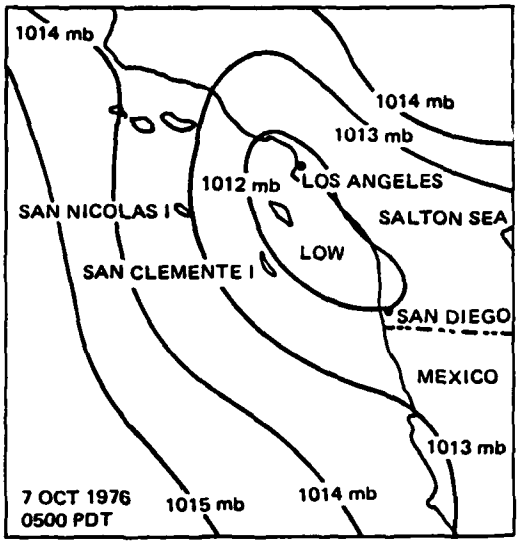

Figure 16. Surface, synoptic pressure pattern, 7 October 1976.

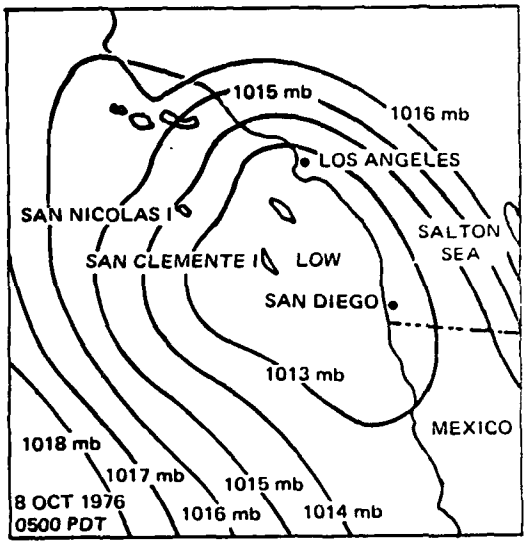

Figure 17. Surface, synoptic pressure pattern, 8 October 1976.

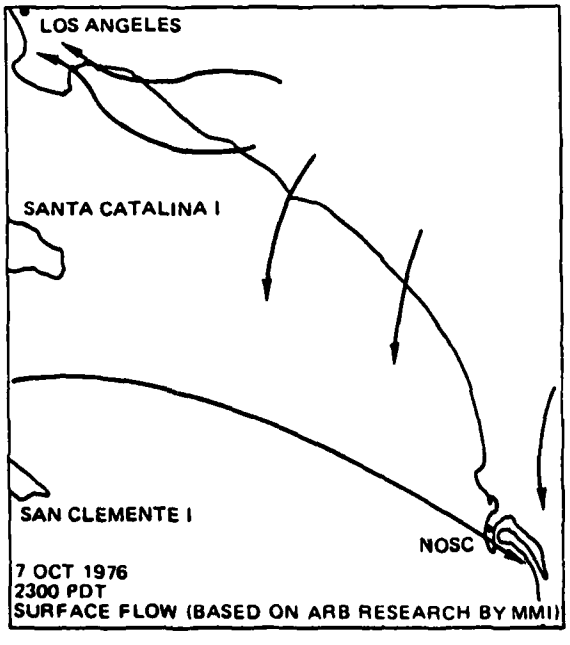

Figure 18. Estimated streamlines, 7 October 1976.

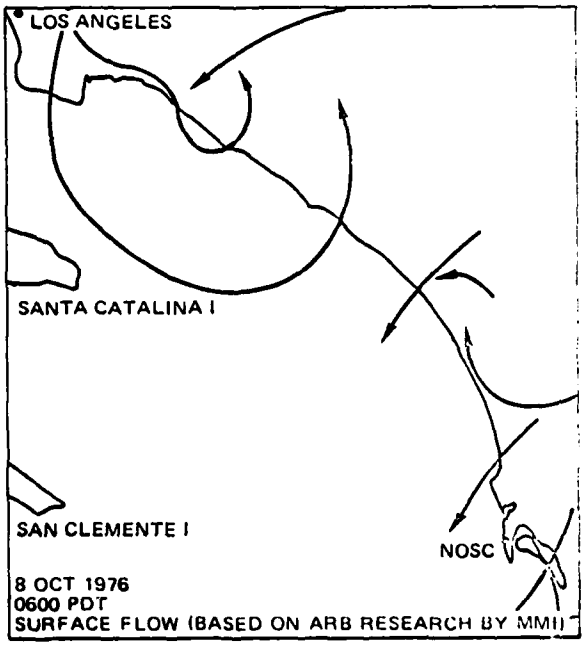

Figure 19. Estimated streamlines, 8 October 1976.

After Noonkester 1977

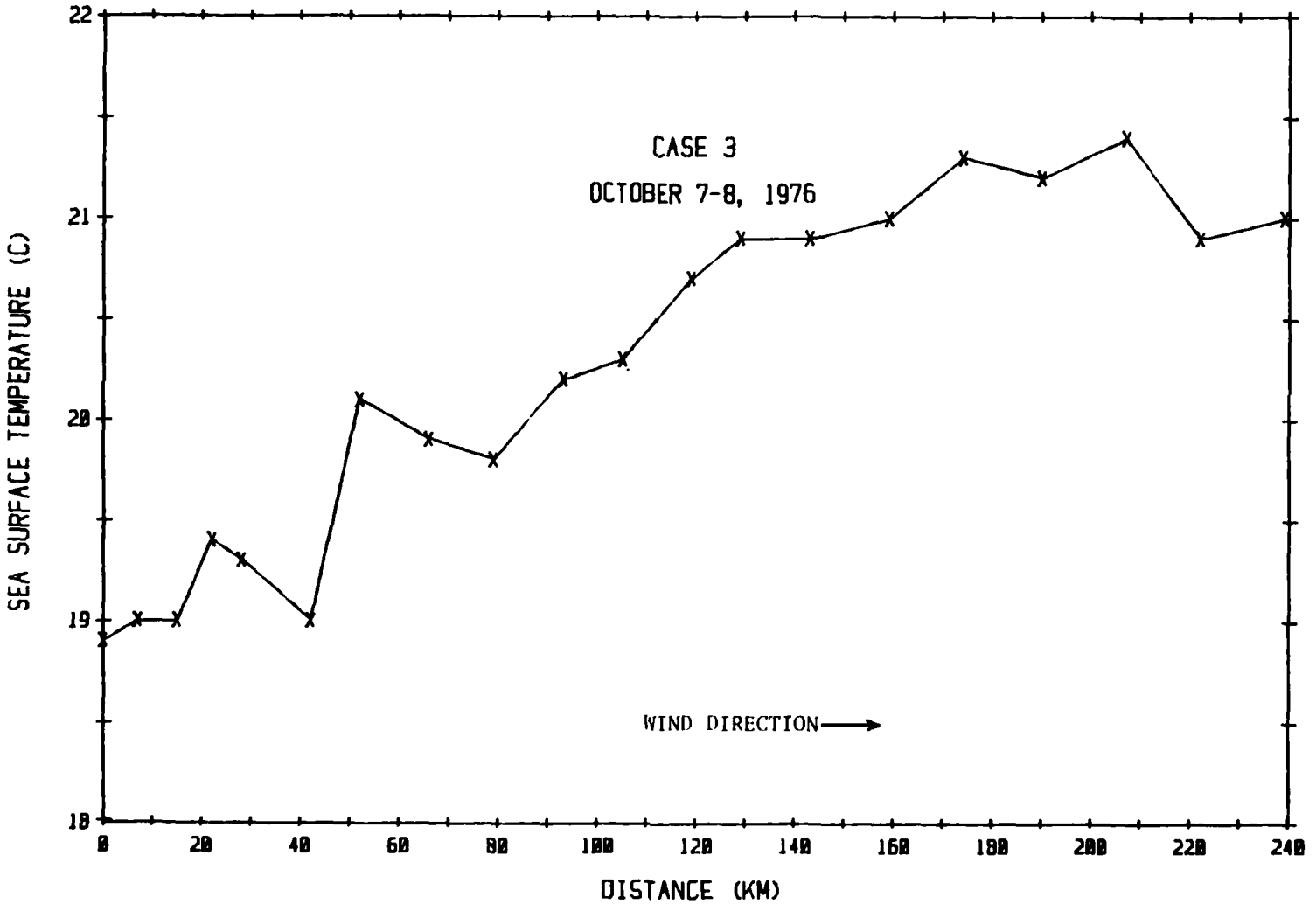
CASE 3
OCTOBER 7-8, 1976
SEA SURFACE TEMPERATURE (C)
22
21
20
19
18
WIND DIRECTION
0
20
40
60
80
100
120
140
160
180
200
220
240
DISTANCE (KM)

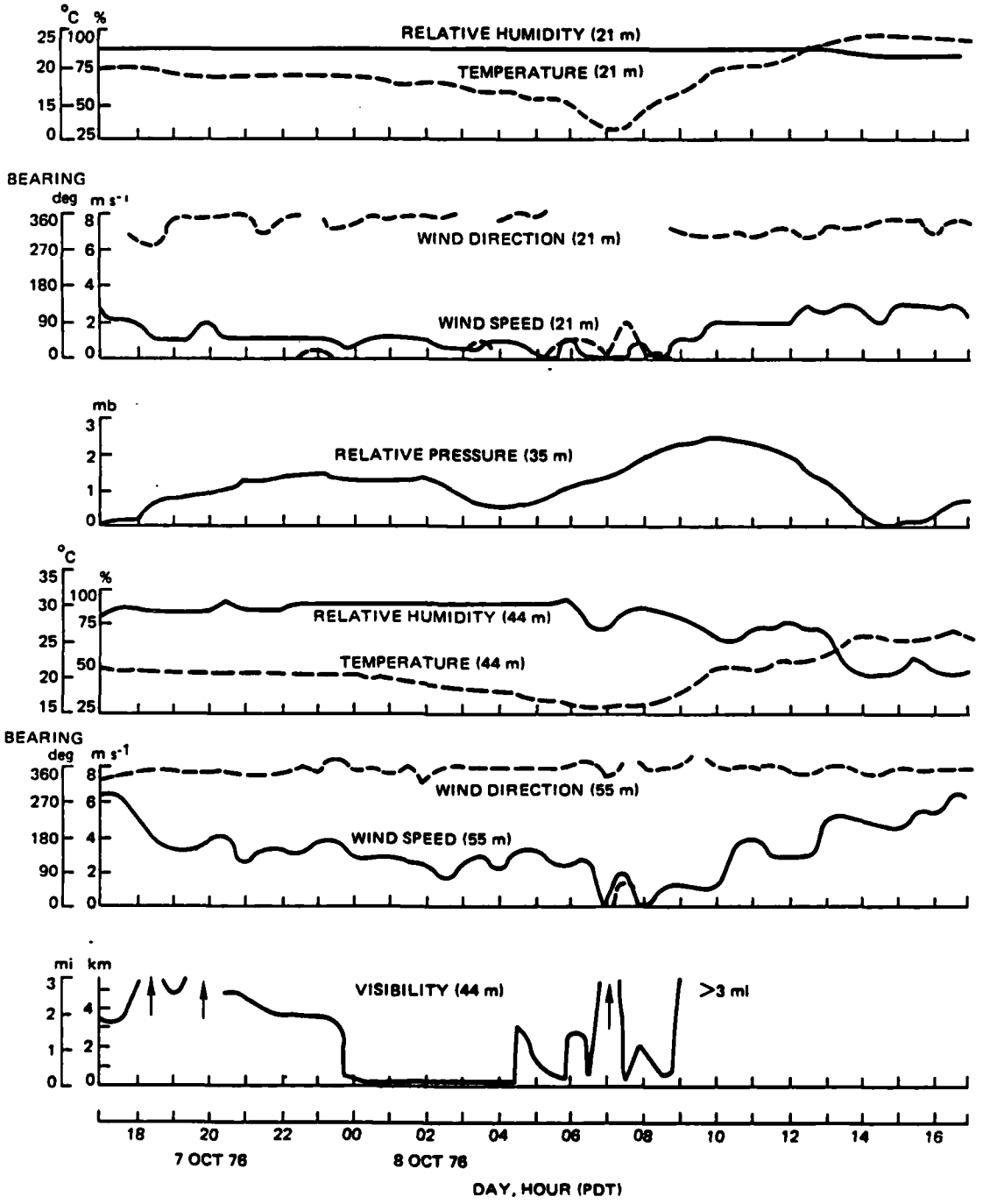

Figure 7. Surface observations at NOSC, 7-8 October 1976.

DATA SOURCES

CASE 3

October 7-8, 1976

1.) Locator Map, Page 93, Fig. A-4-e

Backes, D.A., 1977: Santa Ana Associated Offshore Fog: Forecasting with a Sequential Model. Thesis. Naval Postgraduate School, Monterey, CA.

2.) a.) Initial Sounding - Acania 0400 PDT - CEWCOM 1976 Data Sets.

10hr b.) Verification Sounding - San Clemente Is. 1400 PDT.

14hr c.) Verification Sounding - Ralph Markson in Backes ibid pg. 72, 1800 PDT.

20hr d.) Verification - NOSC surface data and remote sensing observations. 0000 PDT/8th. Noonkester, V.R., 1977: Marine Fog Investigation at San Diego During CEWCOM - 1976. Technical Report 172 13 October 1977 Naval Ocean Systems Center, San Diego, CA 95152.

3.) Sea Surface Temperature Data - *Measurements* by Calspan.
Sea Surface Temperature Probe on the Acania.

4.) Surface Winds - Calspan Observations from Acania, 24 hr Surface.
Observations from San Clemente Is and San Diego Airport.

5.) Synoptic Charts - National Meteorological Center 850 mb and surface.

CASE 3: 'BLIND' DATA SETS

1.0 Initial Sounding (at time zero)

Height (m)	Pressure (mb)	Temperature (°C)	Dewpoint (°C)	RH (%)
4	1012	17.6	16.3	92
144	996	16.1	16.1	100
265	982	15.3	15.3	100
305	977	15.5	7.4	58
335	974	21.1	-2.0	21
361	971	23.3	-1.5	19
415	965	25.1	-0.0	19
664	938	25.7	0.4	19
768	927	25.1	-0.0	19
1075	895	23.3	-1.5	19
1311	871	21.7	-2.9	19
1411	861	21.2	-3.3	19
1522	850	20.4	-3.9	19

1.1 Low level cloud cover is overcast.

1.2 Cloud Liquid Water Content (after Rogers & Hanley, as noted for Case 1)

Height (m)	LWC (g/m^3)
144	.000
234	.200
265	.000

2.0 Inversion Base

Our estimate of height of base of inversion is 265 m.

3.0 Subsidence

Vertical motion aloft is negative as follows:

910 mb	-0.712 cm/sec
940 mb	-0.588 cm/sec
970 mb	-0.375 cm/sec
975 mb	-0.150 cm/sec

4.0 Cloud Above Marine Mixed Layer

Time zero +8 hours to +11 hours: base 25000 feet, thin scattered cirrus

Time zero +12 hours to end: base 25000 feet, thin broken cirrus

5.0 Sea Surface Temperature (SST)

The following is the sea surface temperature variation along the air column's straight line trajectory.

Distance Along a Straight Line (km)	Temperature (°C)
0	18.9
7	19.0
15	19.0
22	19.4
28	19.3
42	19.0
52	20.1
66	19.9
79	19.8
93	20.2
105	20.3
119	20.7
129	20.9
143	20.9
159	21.0
174	21.3
190	21.2
207	21.4
222	20.9
239	21.0
270	20.8
287	20.7
302	20.9

6.0 Wind

Actual wind direction is parallel to the column trajectory with changing speed as shown in table below.

Time (hours) (Relative to Time Zero	Wind Speed (meters/sec)
0.5	6.7
1	6
2	6
3	5
4	4
5	3.5
6	3
7	3
8	3
9	3
10.5	2.5
11	3
12	4
13	5
14	4
15	3.5
16	3
17	2.5
18	2.5
19	2.5

Geostrophic wind is uniform with height and changes in time in proportion to above wind speed.

7.0 Sun Information

	Declination (degrees)	Latitude (degrees)
Sun Elevation Angle: 52° (at 12 noon)		
Sunrise: Time Zero +3 hour 20 min	-5	33
Sunset: Time Zero +13 hour 40 min		

8.0 Instructions

A) Please run model twice:

(1) Output model results at two-hour intervals until model column traverses entire length of sea surface temperature distribution.

(2) Run model a second time using an average wind speed of 3 m/sec; output model results at two-hr. intervals until column traverses SST distribution.

Case 3

ADDENDA

We have broken this time period into two parts.

1) Hours 0 to 4 - Geostrophic wind is + (plus) 32° @ 6.9 m/sec.

2) The remaining hours geostrophic wind is + (plus) 19° @ 3.2 m/sec.

A representative wind sounding is

Height (m)	Direction (degrees)	Speed (m/sec)
Surface	000	3.0
512	+112	3.0
733	+130	3.0
987	+150	3.0
1253	+138	5.8
1519	+125	8.5

Soundings

Time (1)				Time (1) + 12 hours		
Level (mb)	Height (m)	Temp. (°C)	Dewpoint (°C)	Height (m)	Temp. (°C)	Dewpoint (°C)
850	1509	20.4	-3.9	1529	20.6	-3.8
700	3151	9.6	-12.8	3179	10.5	-9.7
500	5875	-5.6	-35.6	5921	-4.1	-34.1
		24-hour changes at 400 mb and above				
400	7580	-20.1	-50.1	7596	-19.9	-49.9
300	9641	-36.9	-66.9	9655	-37.8	-44.7
200	12319	-56.8	*	12329	-56.2	*
100	16494	-73.4	*	16551	-72.3	*

*Motorboating

Time (1) is at time zero in simulation

CASE 4

14-15 July 1973

Northwest of Pt. Conception
(80 km to coastline)
(Calspan/ACANIA Marine Fog Cruise)

Time Zero: 2000 PDT, 14 July

Verification Time: 0530 PDT, 15 July

Sunset: 2020 PDT

Sunrise: 0620 PDT

Scenario: Coastal stratus thickening during entire night from ∿100 m to ∿350 m depth under inversion at 500 m.

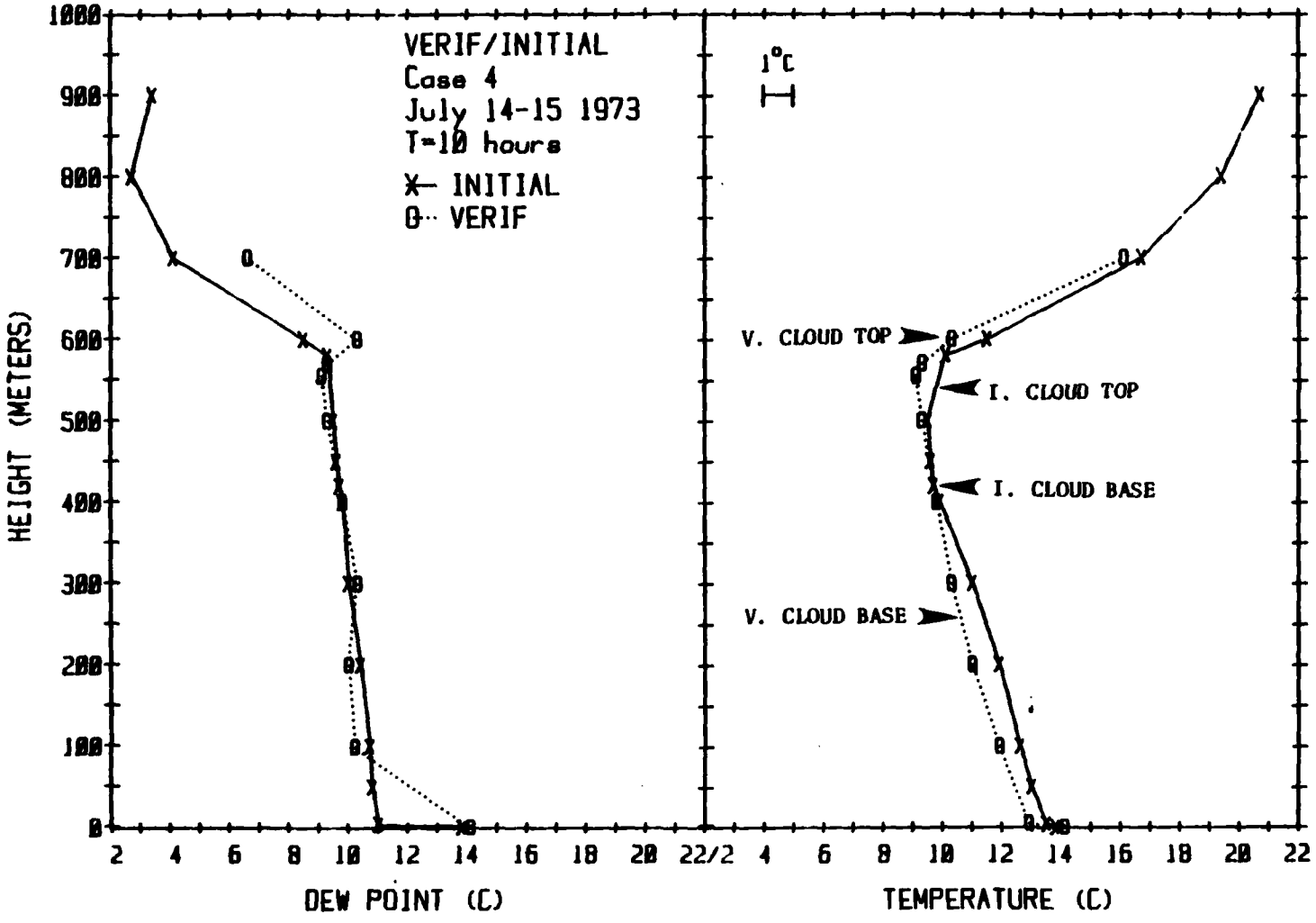
VERIF/INITIAL
Case 4
July 14-15 1973
T=10 hours
X— INITIAL
0·· VERIF
1°C
V. CLOUD TOP
I. CLOUD TOP
I. CLOUD BASE
V. CLOUD BASE
HEIGHT (METERS)
DEW POINT (C)
TEMPERATURE (C)
1000
900
800
700
600
500
400
300
200
100
0
2 4 6 8 10 12 14 16 18 20 22/2 4 6 8 10 12 14 16 18 20 22

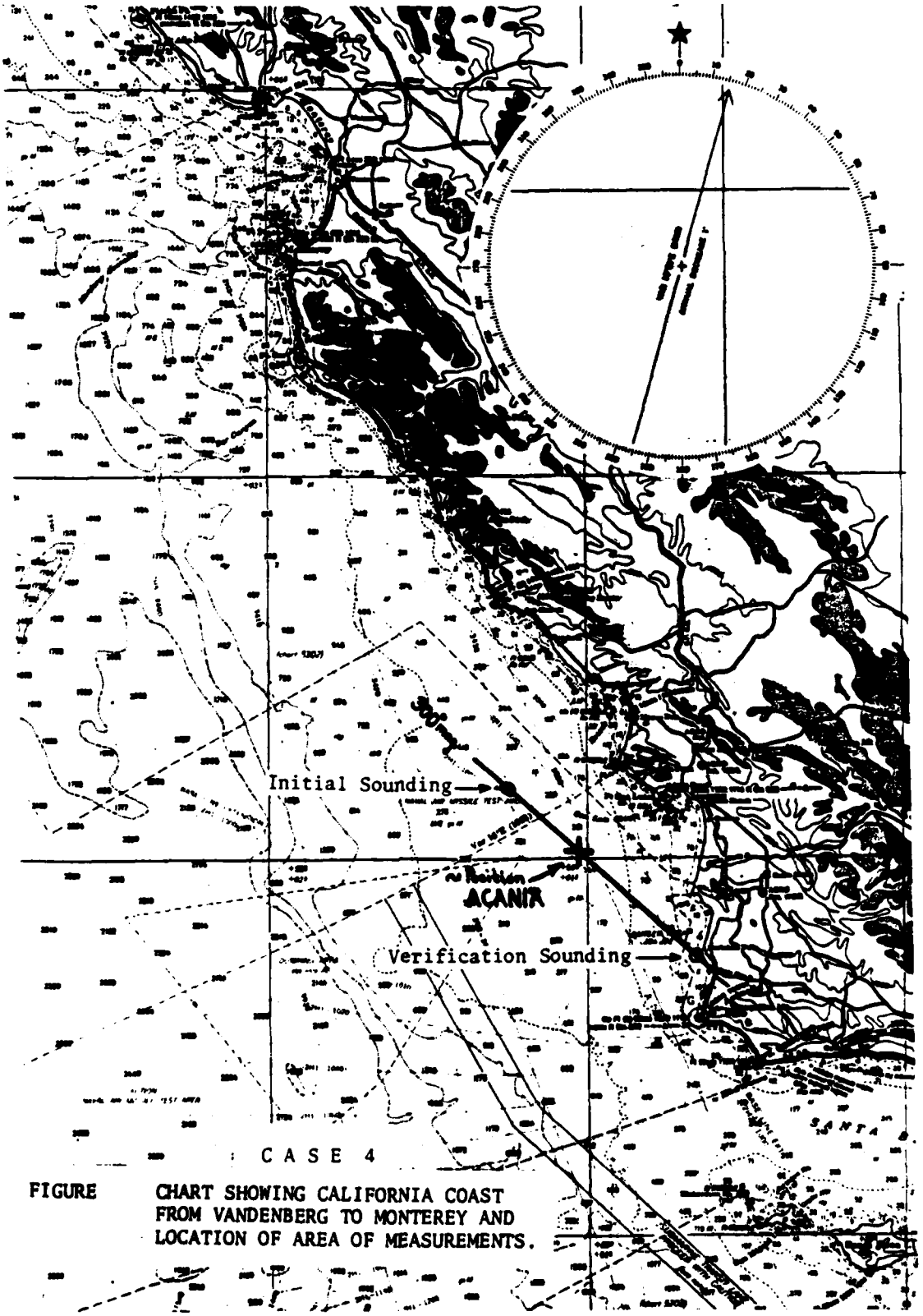

FIGURE CHART SHOWING CALIFORNIA COAST FROM VANDENBERG TO MONTEREY AND LOCATION OF AREA OF MEASUREMENTS.

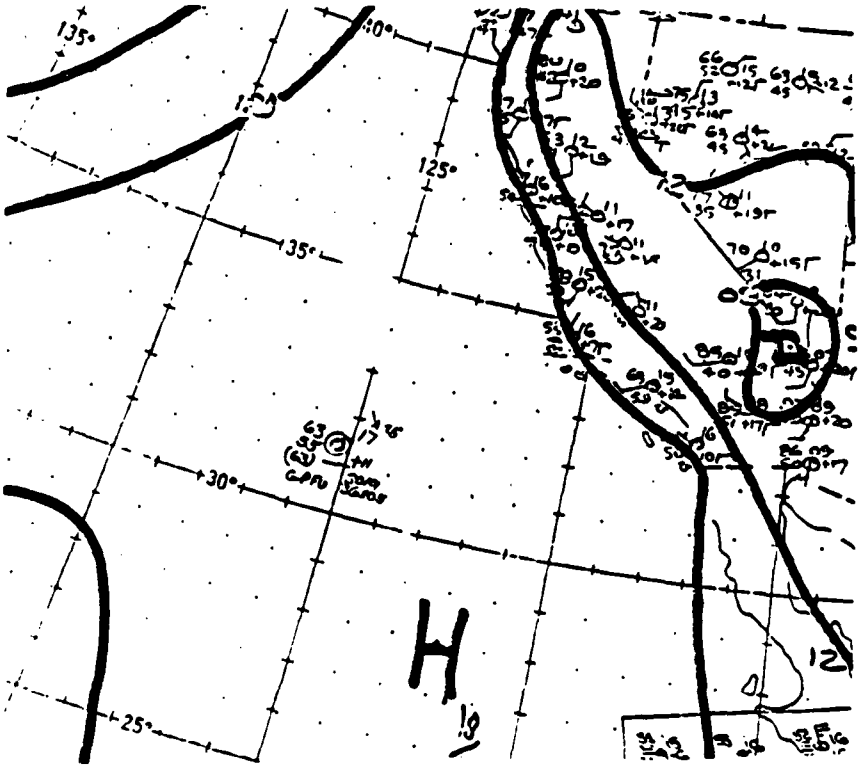

Surface Analysis 06Z 15 Jul 1973

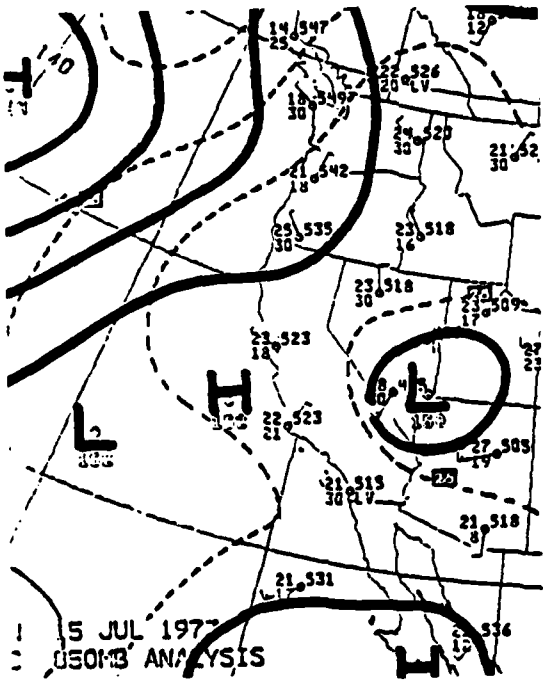

850 mb Analysis 00Z 15 Jul 1973

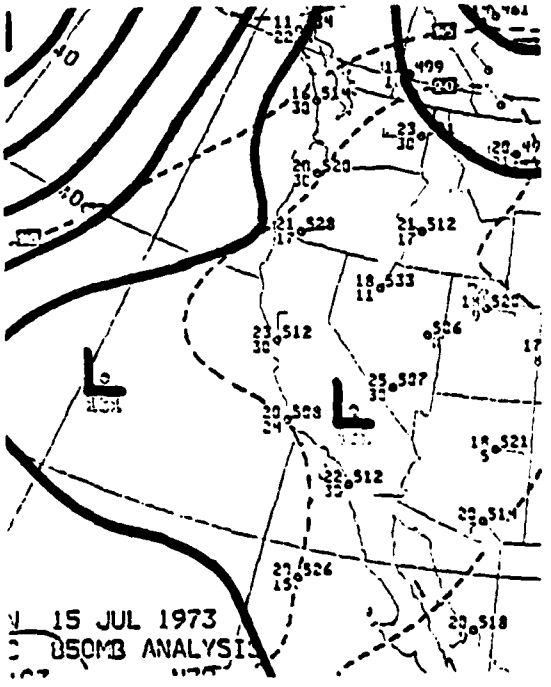

850 mb Analysis 12Z 15 Jul 1973

FIGURE VERTICAL CROSS-SECTION DEPICTING TEMPERATURE DISTRIBUTION AND LOCATION OF STRATUS CLOUD UPWIND OF THE VANDENBERG COASTLINE AT APPROXIMATELY 0600 PDT ON 15 JULY 1973.

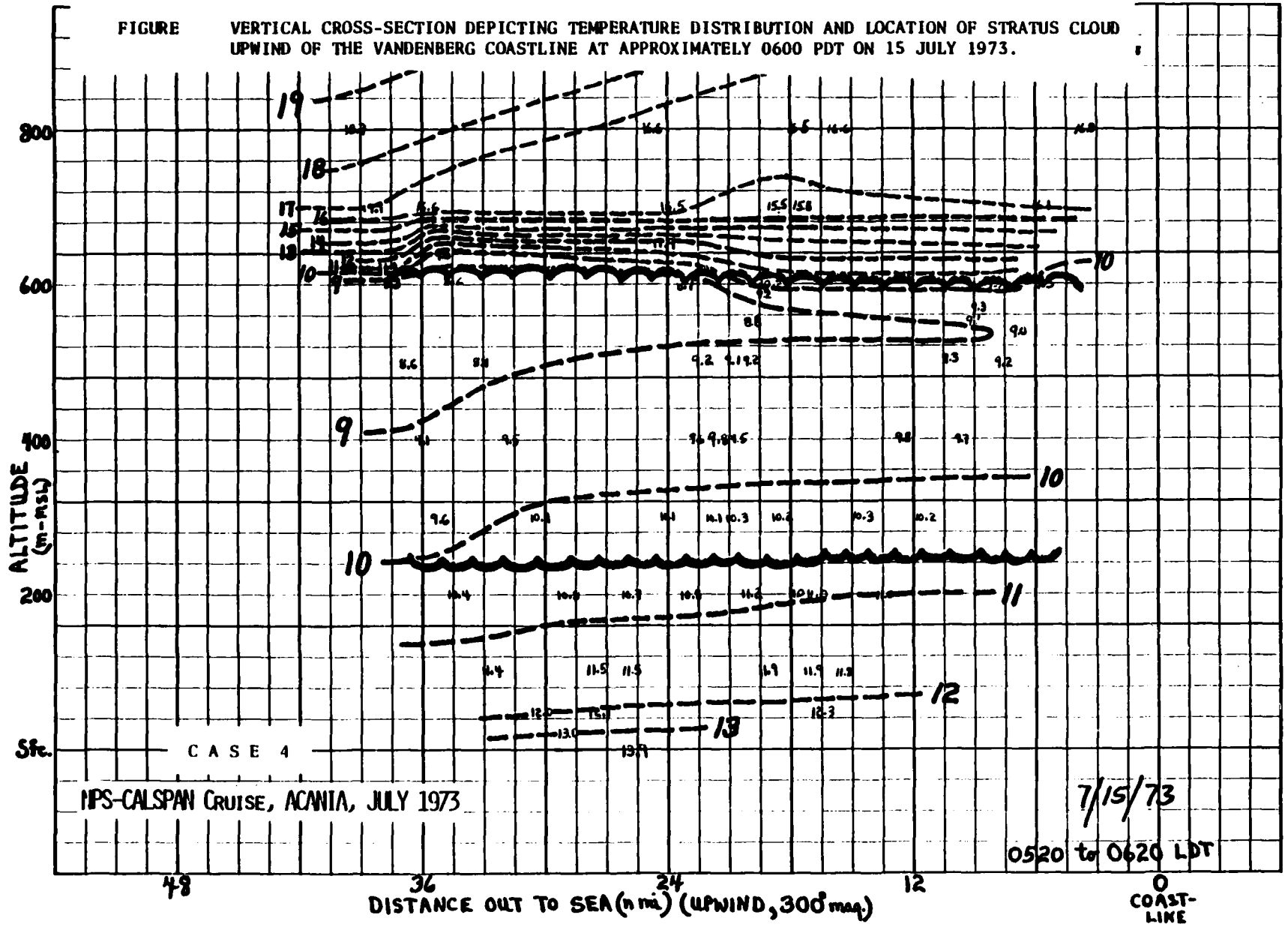

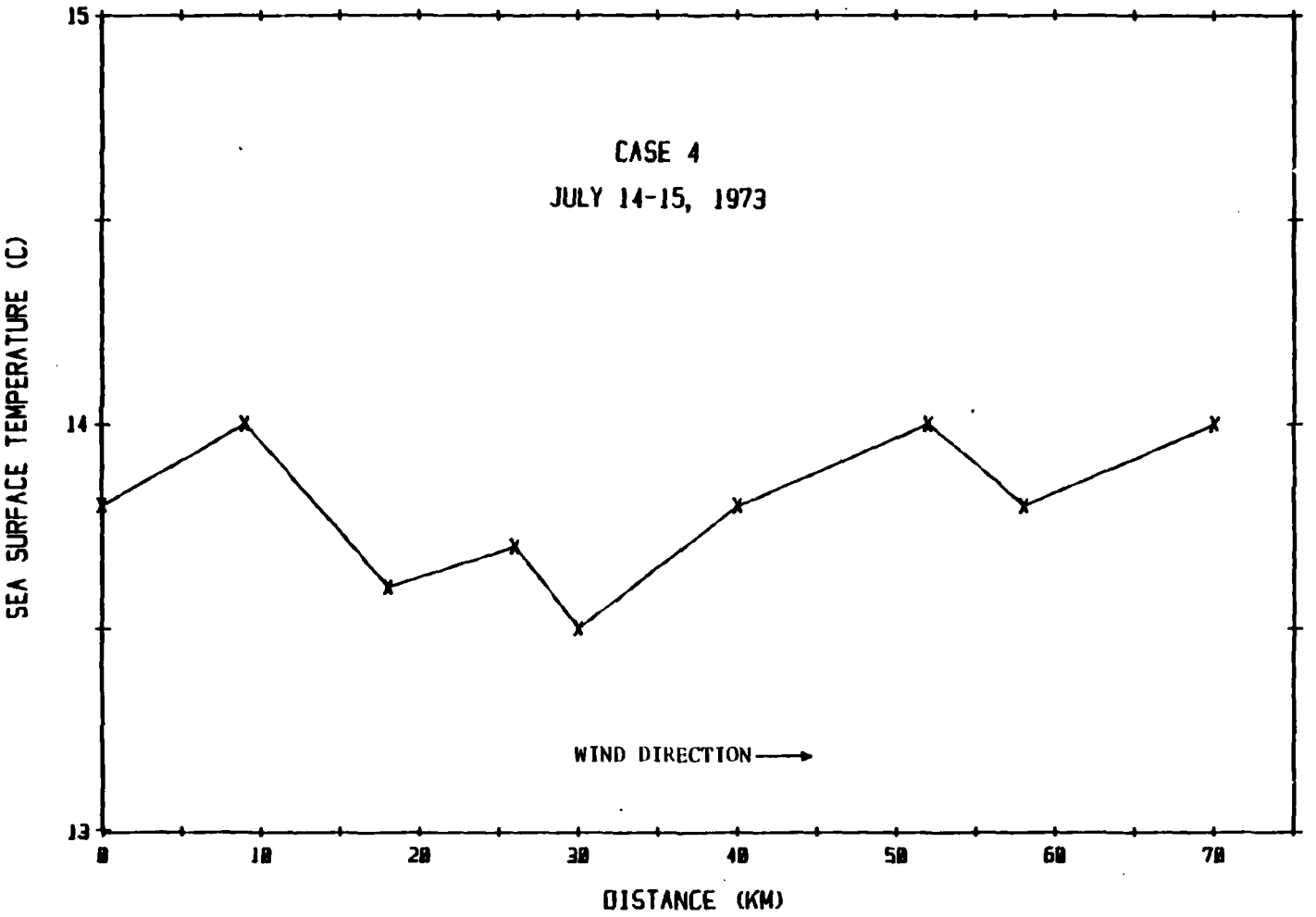
CASE 4
JULY 14-15, 1973
SEA SURFACE TEMPERATURE (C)
15
14
13
WIND DIRECTION
0
10
20
30
40
50
60
70
DISTANCE (KM)

DATA SOURCES

CASE 4
July 14-15, 1973

1.) Locator Map -

Mack, E.J., Katz, U., Rogers, C.W., and Pilie, R.J., 1974: The Microstructure of California Coastal Status and Fog at Sea. Second Annual Summary Report. Co. No. N00019-74-C-0045. July 1974. Calspan Report No. CJ-5404-M-1. Calspan Corp. PO Box 400, Buffalo, NY 14225.

2.) a.) Initial Sounding, Mack et al, 1974: Ibid.

b.) Verification Sounding

Same as a.)

3.) Sea Surface Temperature

Calspan Probe and Data Log for above Cruise.

4.) Surface Winds - Acania Ship Log and Vandenberg AFB Surface Observations.

5.) Synoptic Charts - National Meteorological Center 850 mb and Surface.

CASE 4: 'BLIND' DATA SETS

1.0 Initial Sounding (at time zero)

Height (m)	Pressure (mb)	Temperature (°C)	Dewpoint (°C)	RH (%)
4	1017	13.5	11.0	85
50	1010	13.0	10.8	86
100	1004	12.6	10.7	88
200	992	11.9	10.4	91
300	980	11.0	10.0	94
400	969	9.9	9.8	99
420	967	9.7	9.7	100
450	963	9.6	9.6	100
500	958	9.5	9.5	100
580	949	10.1	9.3	95
600	946	11.5	8.5	88
700	934	16.7	4.1	43
800	923	19.4	2.7	33
900	913	20.7	3.4	32
1220	880	22.6	3.5	29
1530	850	21.7	0.4	24

1.2 Cloud Liquid Water Content (after Rogers and Hanley, as in Case 1)

Height (m)	LWC (g/m^3)
420	.000
540	.260
580	.000

2.0 Inversion Base

Our estimate of height of base of inversion is 500 m.

3.0 Subsidence

Vertical motion is positive, +.05 cm/sec at 935 mb and maximum +0.075 cm/sec at 945 mb.

4.0 No cloud present above the marine mixed layer.

5.0 Sea Surface Temperature

The following is the sea surface temperature variation along the air column's straight line trajectory.

Distance (km)	Temperature (°C)
0	13.8
9	14.0
18	13.6
26	13.7
30	13.5
40	13.8
52	14.0
58	13.8
70	14.0
89	14.1
102	13.9

6.0 Wind

Actual surface wind direction is parallel to the column trajectory with a constant speed of 2 m/sec.

Geostrophic wind is uniform with height and constant with time.

7.0 Sun Information

Elevation Angle: 75° (at 12 noon)
Sunrise: Time zero plus 10 hr. 20 min.
Sunset: Time zero plus 00 hr. 20 min.

Declination (degrees)	Latitude (degrees)
+22	35

8.0 Instructions

A) Output model results at one-hour intervals until model column traverses entire length of sea surface temperature distribution.

B) Please document all, if any, supplementary processing which you have to make to this data set in order to run your model.

ADDENDA

Wind - Change wind speed to 3 m/sec at 000°.

Low Level Geostrophic wind is + (plus) 10° @ 3.1 m/sec.

A representative wind sounding is:

Height (m-msl)	Direction (degrees)	Speed (m/sec)
Surface	000	3
100	000	2
305	-18	2
610	-47	1
915	+110	1
1220	+63	2.5
1535 (850 mb)	+75	2.5

Soundings

Time (1)				Time (1) + 12 Hours	
Level	Height	Temp.	Dewpoint	Temp.	Dewpoint
850	1535	21.7	0.4	19.6	-4.0
700	3049	11.8	-12.1	11.0	-16.6
500	5793	-5.5	-28.2	-6.5	-32.6
400	7622	-19.0	-39.1	-20.5	-37.3
300	9756	-34.4	-49.6	-36.6	-50.1
200	12500	-55.5	*	-56.5	*
100	16768	-63.9	*	-64.7	*

*Motorboating

Time (1) is 3 hours before time zero of simulation.

CASE 5

5 August 1975

Off Southeast Coast of Nova Scotia
(~80 km offshore)
(USNS HAYES Marine Fog Cruise)

Time Zero: 0600 EDT

Simulation Times: 3 hours

Sunrise: 0500 EDT

Scenario: Shallow advection fog formed over cold water, dramatically increased in depth farther downwind over substantially warmer water.

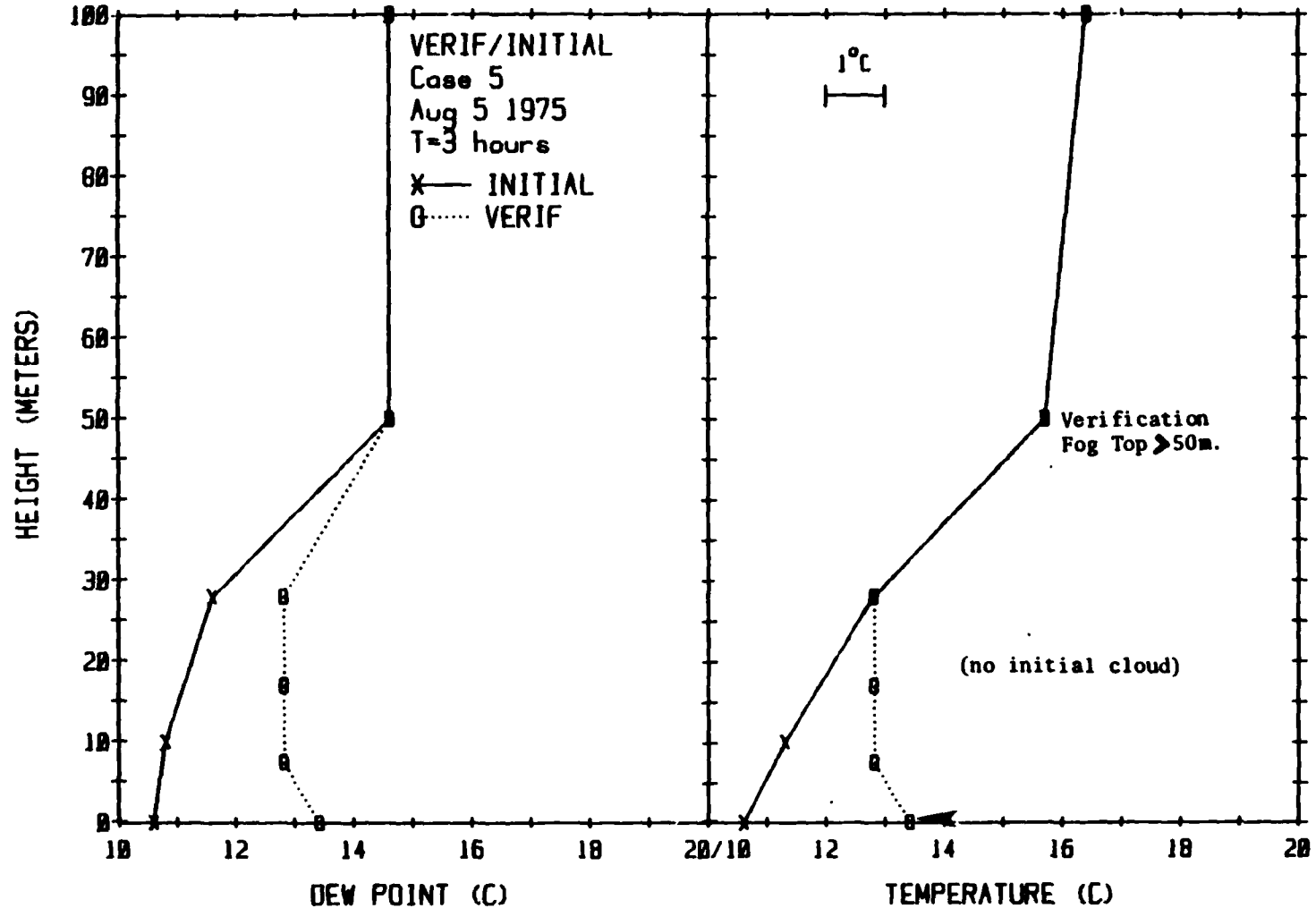
VERIF/INITIAL
Case 5
Aug 5 1975
T=3 hours
X—— INITIAL
0····· VERIF
1°C
Verification
Fog Top >50m.
(no initial cloud)
HEIGHT (METERS)
100
90
80
70
60
50
40
30
20
10
0
10
12
14
16
18
20/10
12
14
16
18
20
DEW POINT (C)
TEMPERATURE (C)

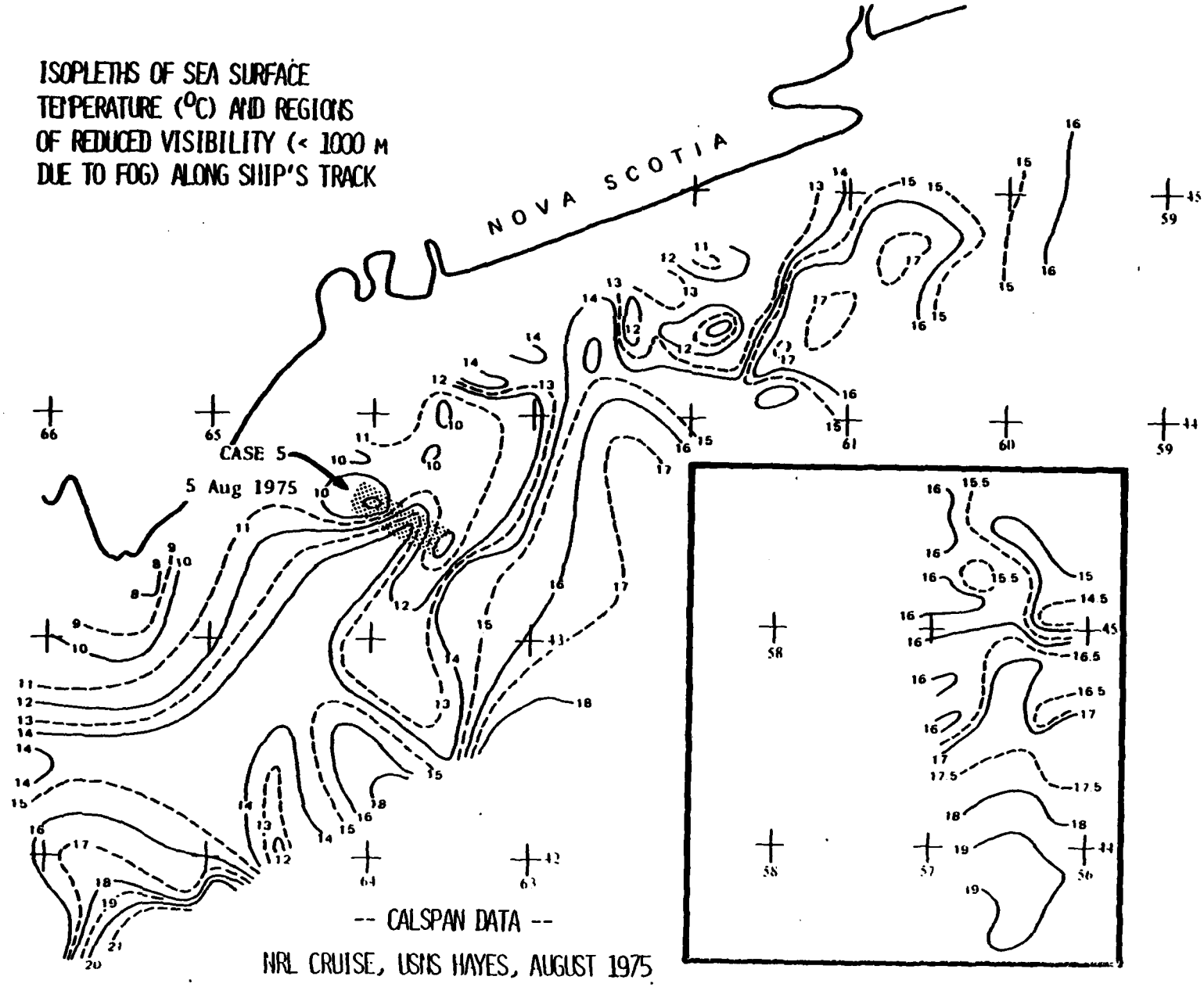
ISOPLETHS OF SEA SURFACE TEMPERATURE (°C) AND REGIONS OF REDUCED VISIBILITY (< 1000 M DUE TO FOG) ALONG SHIP'S TRACK
NOVA SCOTIA
CASE 5
5 Aug 1975
-- CALSPAN DATA --
NRL CRUISE, USNS HAYES, AUGUST 1975

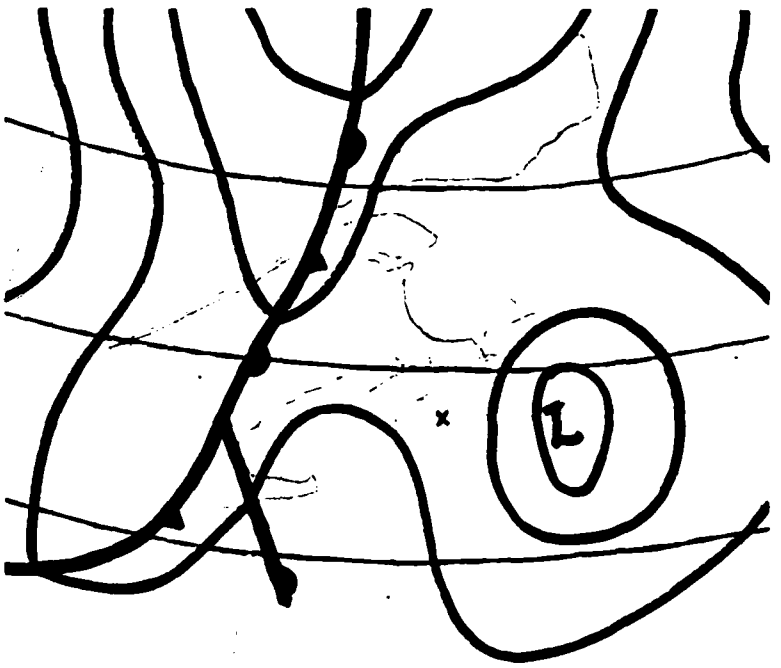

Surface Analysis 12Z 5 Aug 1975

850 mb Analysis 00Z 5 Aug 1975

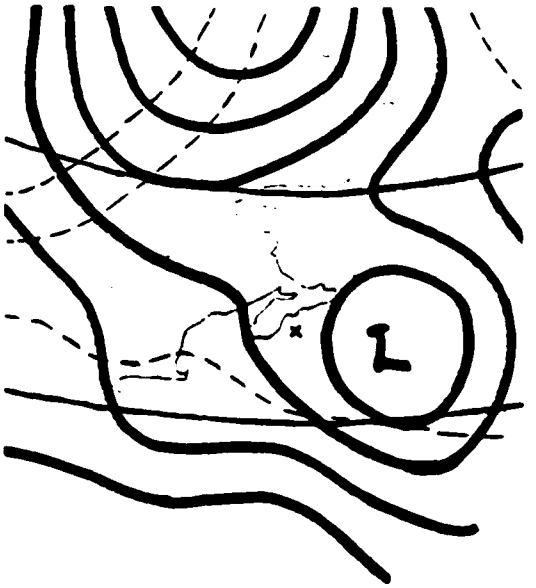

850 mb Analysis 12Z 5 Aug 1975

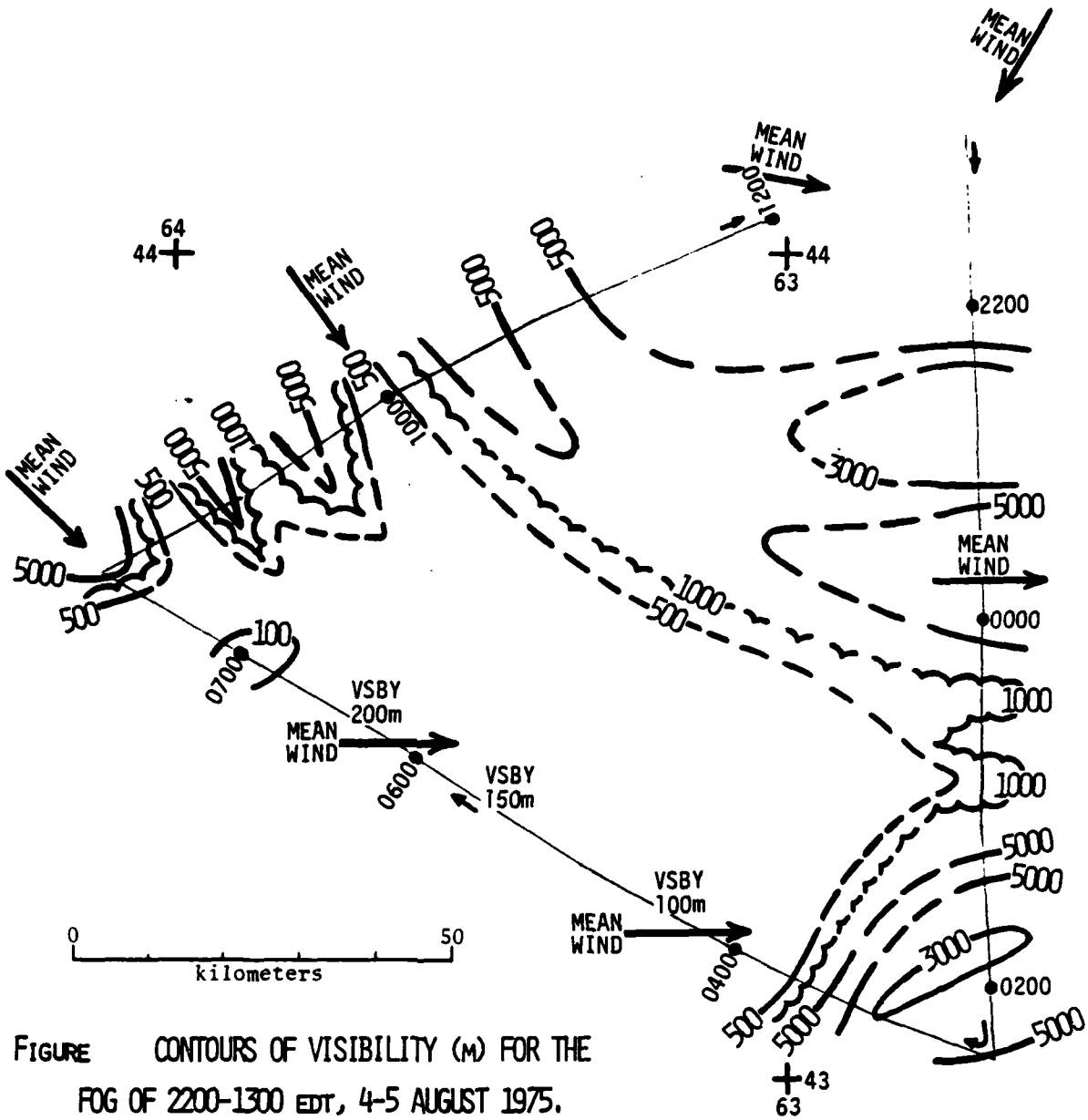

FIGURE CONTOURS OF VISIBILITY (M) FOR THE FOG OF 2200-1300 EDT, 4-5 AUGUST 1975.

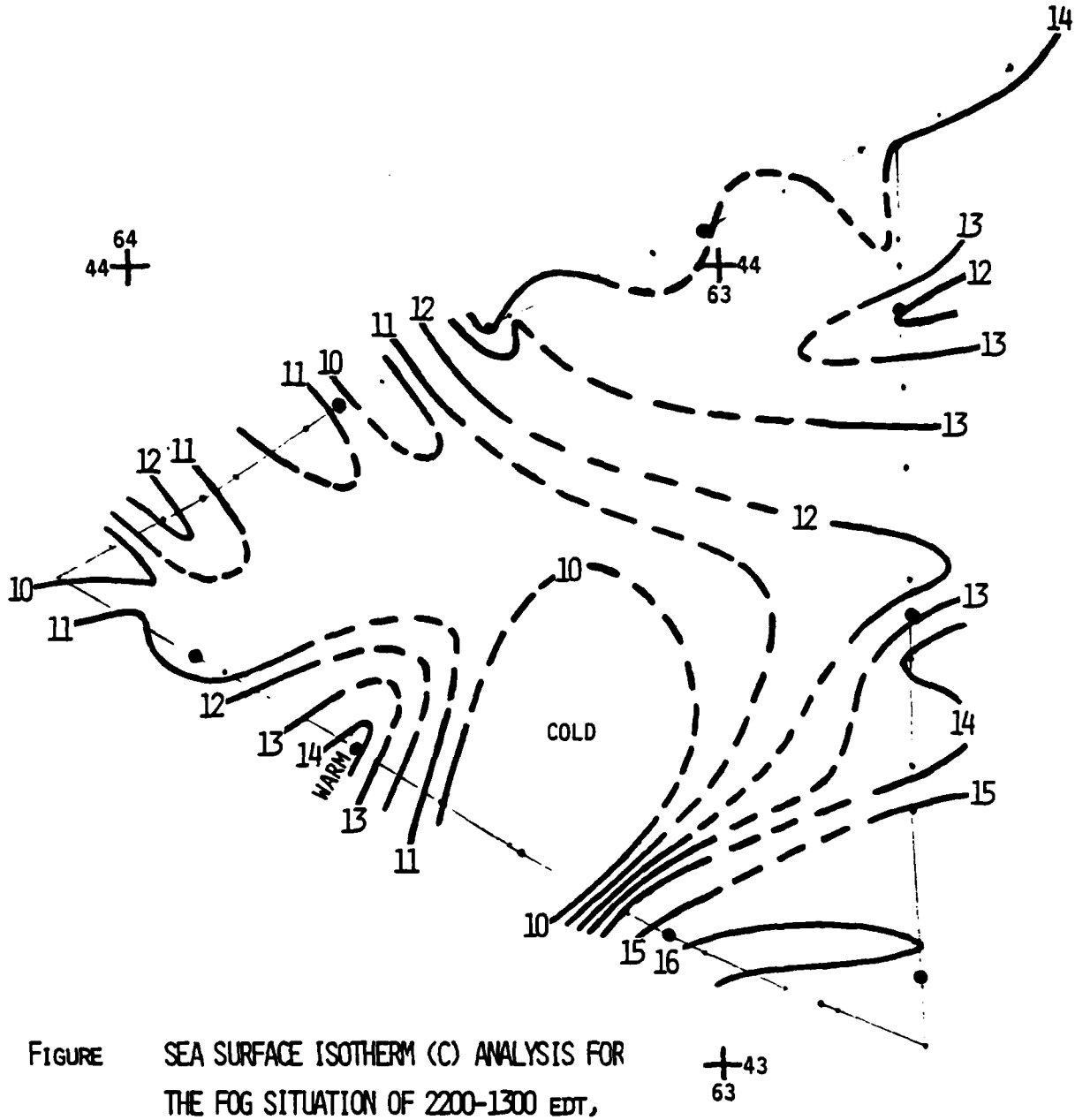

FIGURE SEA SURFACE ISOTHERM (C) ANALYSIS FOR THE FOG SITUATION OF 2200-1300 EDT, 4-5 AUGUST 1975.

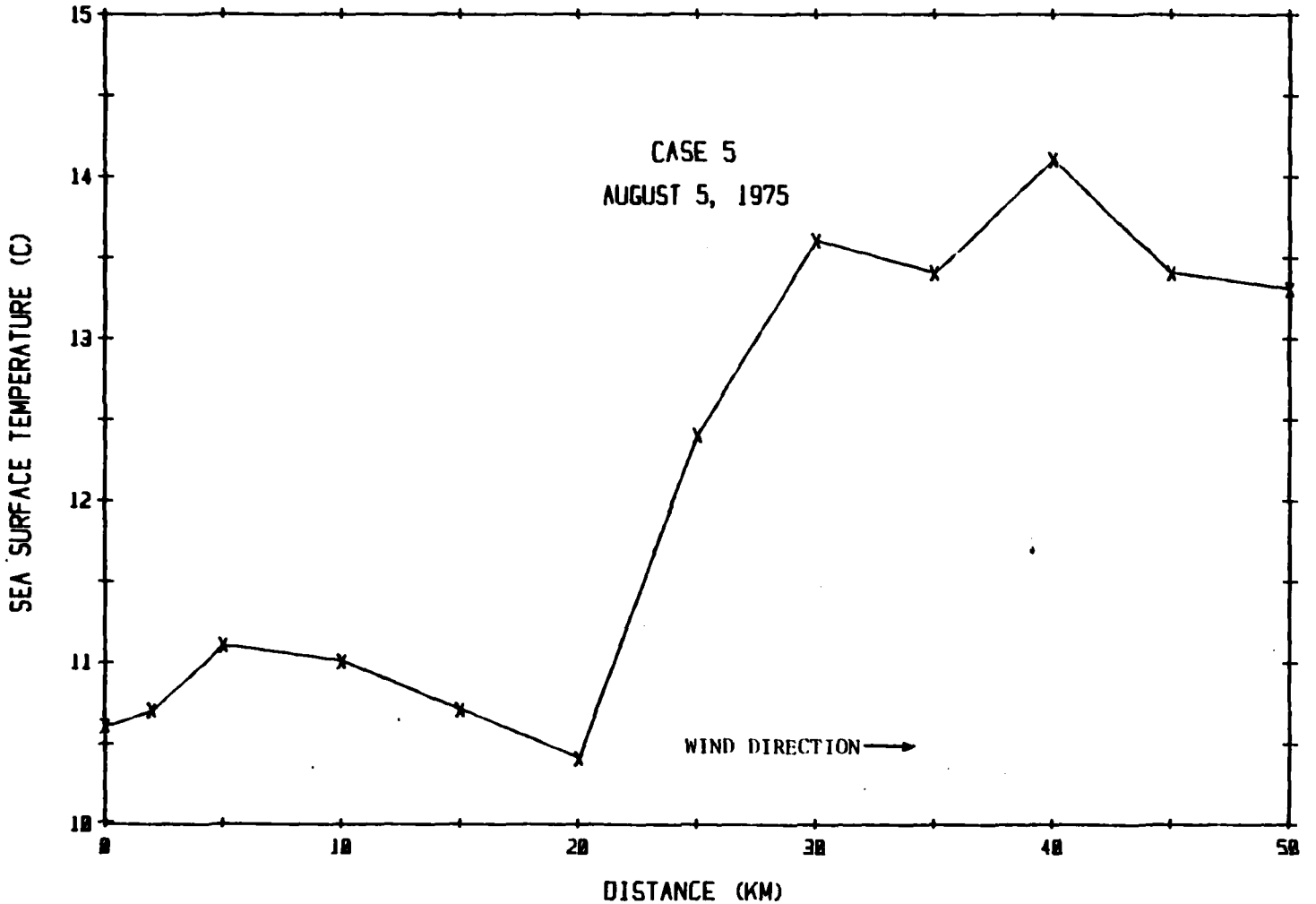
CASE 5
AUGUST 5, 1975
SEA SURFACE TEMPERATURE (C)
15
14
13
12
11
10
0
10
20
30
40
50
DISTANCE (KM)
WIND DIRECTION

DATA SOURCES

CASES 2 and 5

August 2 and August 5, 1975

1.) Locator Map -

Mack, E.J. and U. Katz, 1976: The Characteristics of Marine Fog Occurring off the Coast of Nova Scotia. Fourth Annual Summary Report Co. No. N00019-75-C-0508 June 1976. Calspan Report No. CJ-5756-M-1. Calspan Corp. PO Box 400 Buffalo, NY 14225.

2.) a.) Initial Sounding

Mack, E.J. and U. Katz, 1976: Ibid. Naval Research Laboratory, Naval Air Systems Command, and Office of Naval Research: Marine Fog Cruise, USNS Hayes 29 July-28 August, 1975.

Shelburne, N.S. Radiosonde $43^{o}43^{1}N$, $65^{o}15^{1}W$

b.) Verification

Mack, E.J. and U. Katz, 1976: Ibid.

3.) Sea Surface Temperature Data

Marine Fog Cruise, USNS Hayes, Ibid.
Mack, E.J. and U. Katz, 1976: Ibid.

4.) Surface Winds

Marine Fog Cruise, USNS Hayes, Ibid
Shearwater, AFB, Halifax, N.S.

5.) Synoptic Charts - National Meteorological Center 850 mb and Surface.

CASE 5: 'BLIND' DATA SETS

1.0 Initial sounding (at time zero)

Height (m)	Pressure (mb)	Temperature (°C)	Dewpoint (°C)	RH (%)
10	1011.0	11.3	10.8	97
28	1009.0	12.8	11.6	92
50	1007.0	15.7	14.6	93
100	1002.5	16.4	14.6	89
150	998.0	17.1	14.4	84
200	993.5	17.5	14.5	83
250	989.0	17.0	14.8	87

1.1 Marine layer cloud-free at time zero

1.2 Cloud Liquid Water Content:

None

2.0 Inversion Base

Temperature profile is inverted all the way to the surface.

3.0 Subsidence

Subsidence is zero.

4.0 Cloud cover is ∿30% with cirro stratus.

5.0 Sea Surface Temperature

The following is the sea surface temperature variation along the air column's trajectory:

CASE 5

Distance (km)	Sea Surface Temperature (°C)
0	10.6
2	10.7
5	11.1
10	11.0
15	10.7
20	10.4
25	12.4
30	13.6
35	13.4
40	14.1
45	13.4
50	13.3
60	13.4

6.0 Wind

Surface winds are 4.5 m/sec along the direction of the sea surface temperature distribution. Geostrophic wind is uniform with height and constant with time.

7.0 Sun Information

Elevation angle: 62° (at 12 noon)
Sunrise is one (1) hour before time zero.

Declination (degrees)	Latitude (degrees)
+17	44

8.0 Instructions

A) Output model results at one-hour intervals until model column traverses entire length of sea surface temperature distribution.

B) Please document all, if any, supplementary processing which you have to make to this set in order to run your model.

Case 5

ADDENDA

Surface wind is 000° @ 4.5 m/sec.

Low-level Geostrohpic Wind is +(plus) 34° @ 5.5 m/sec.

A representative wind sounding is

Height (m-msl)	Direction (degrees)	Speed (m/sec)
Surface	000	4.5
96	+009	4.0
533	+005	3.0
992	000	3.0
1472 (850 mb)	+021	5.0

Soundings

Time (1)				Time (1) + 12 hours		
Level (mb)	Height (m)	Temp (°C)	Mixing Ratio (g/Kg)	Height (m)	Temp (°C)	Mixing Ratio (g/Kg)
950	556	15.1	10.5	533	16.5	10.5
900	1013	13.8	9.9	992	14.2	9.7
850	1498	12.5	8.4	1472	11.8	8.9
700	3111	6.5	3.0	3083	5.7	3.8
500	5791	-9.5	0.9	5762	-9.0	0.5
400	7476	-21.1	0.7	7450	-20.7	0.9
300	9536	-37.0	0.1	9519	-35.0	0.1
200	12217	-54.8	-	12216	-55.3	-
100	16596	-56.9	-	16548	-58.3	-

Time (1) is time zero (-) minus 10 hours.

CASE 6

29 August 1972

At Farallon Islands
(Calspan/ACANIA Marine Fog Cruise)

Time Zero: 1700 PDT

Verification Time: 2000 PDT

Sunset: 1930 PDT

Scenario: Stratus thickening to produce fog at surface; marine layer capped at height of 200 m.

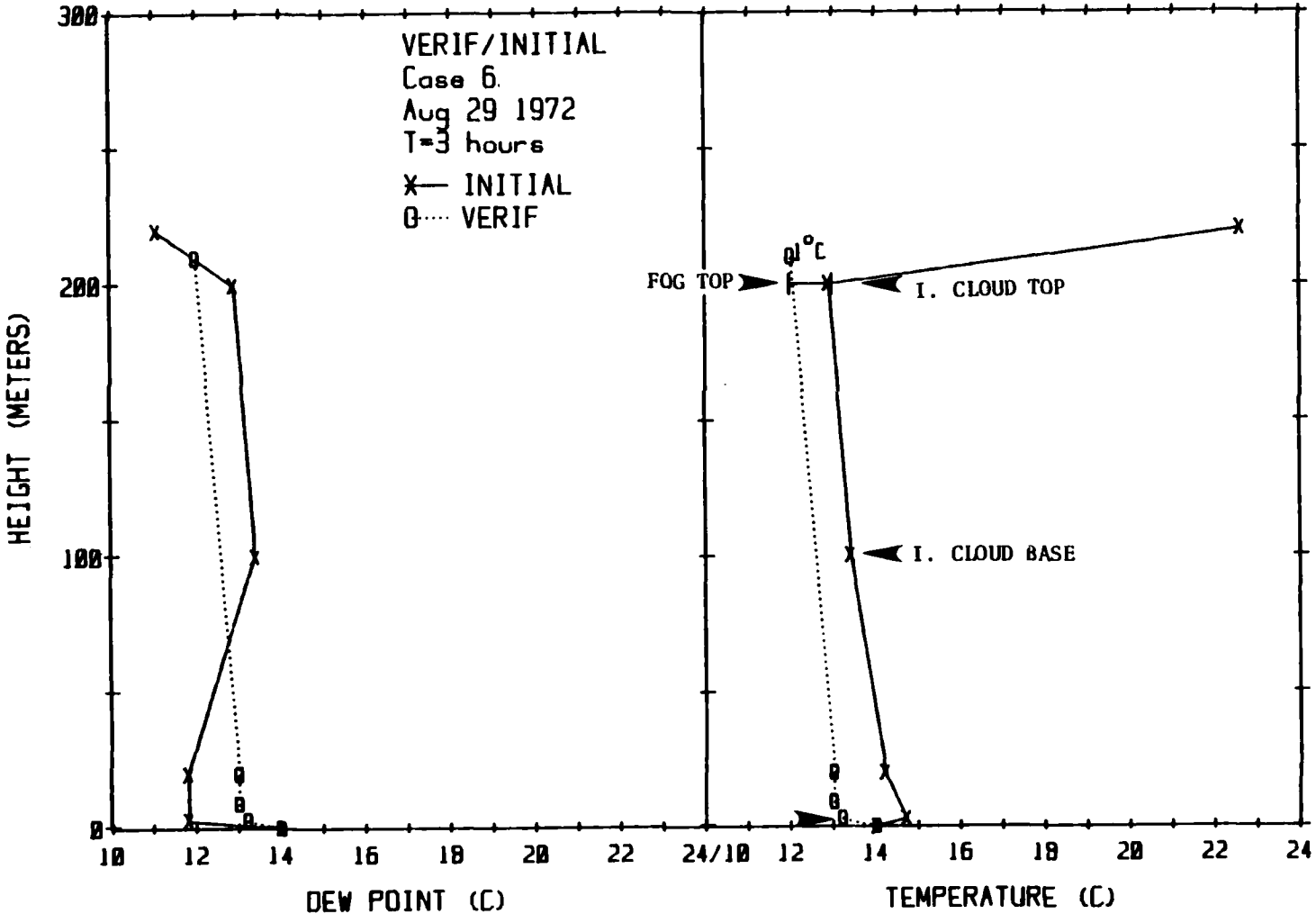
VERIF/INITIAL
Case 6.
Aug 29 1972
T=3 hours
X— INITIAL
0···· VERIF
300
200
100
0
HEIGHT (METERS)
10
12
14
16
18
20
22
24/10
12
14
16
18
20
22
24
DEW POINT (C)
TEMPERATURE (C)
0°C
FOG TOP
I. CLOUD TOP
I. CLOUD BASE

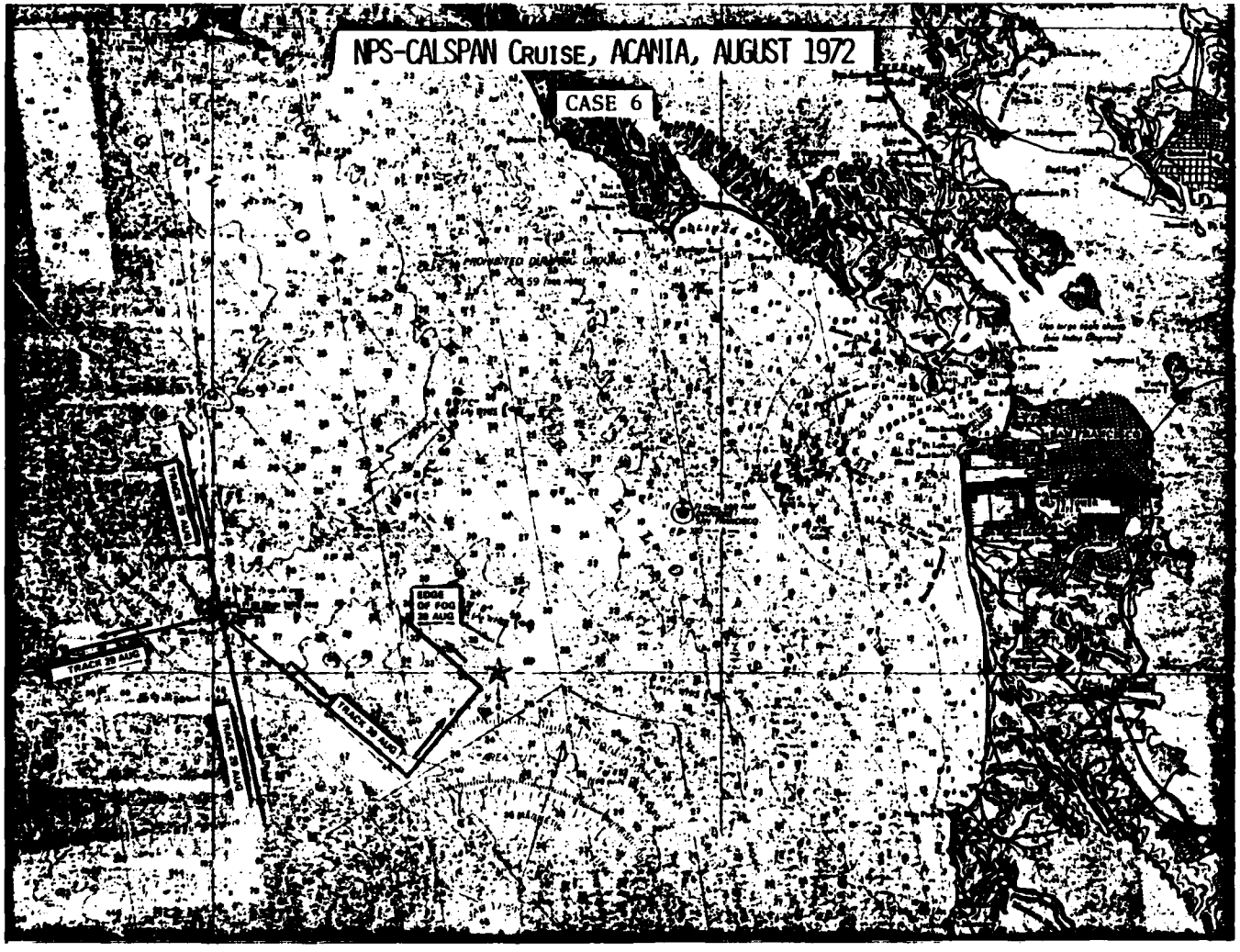

FIGURE NAVIGATION CHART SHOWING POSITIONS OF FARALLON ISLANDS, SAN FRANCISCO AND THE MEASUREMENT TRACKS FOR FOGS OF 29-30 AUGUST AND 30 AUGUST 1972

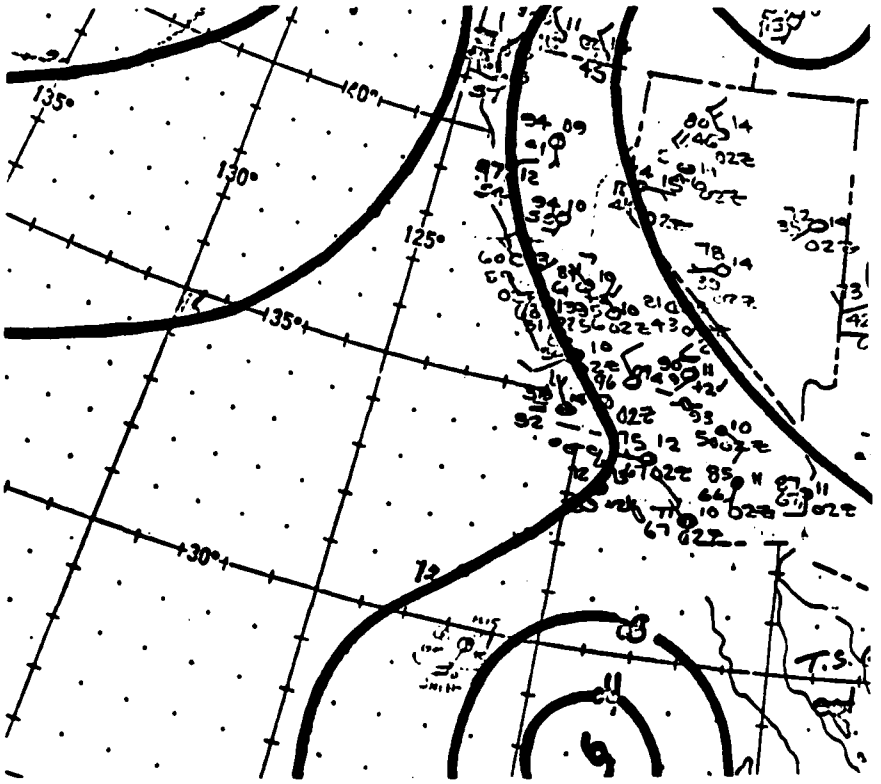

Surface Analysis 03Z 30 Aug 1972

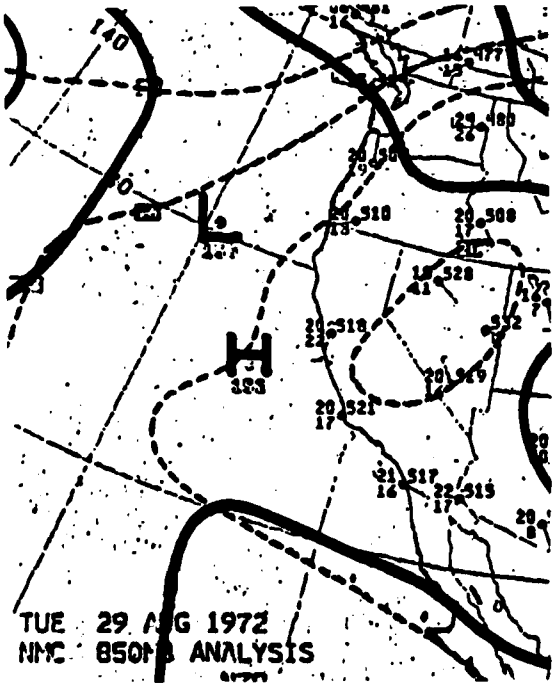

850 mb Analysis 12Z 29 Aug 1972

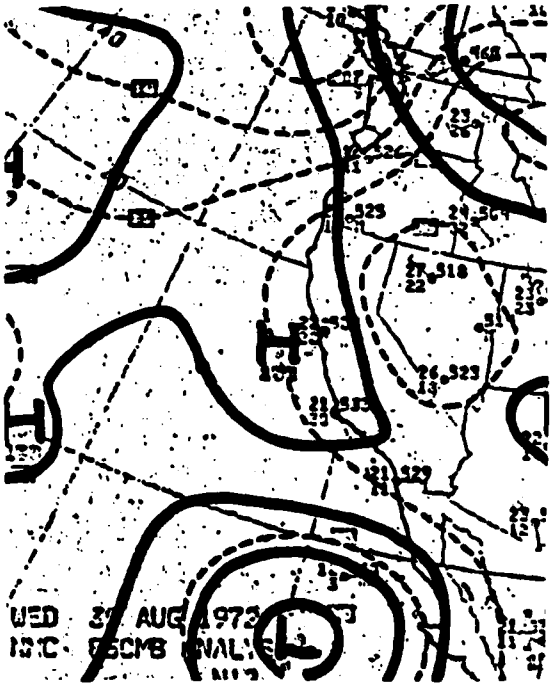

850 mb Analysis 00Z 30 Aug 1972

CASE 6

NPS-CALSPAN CRUISE, ACANIA, AUGUST 1972

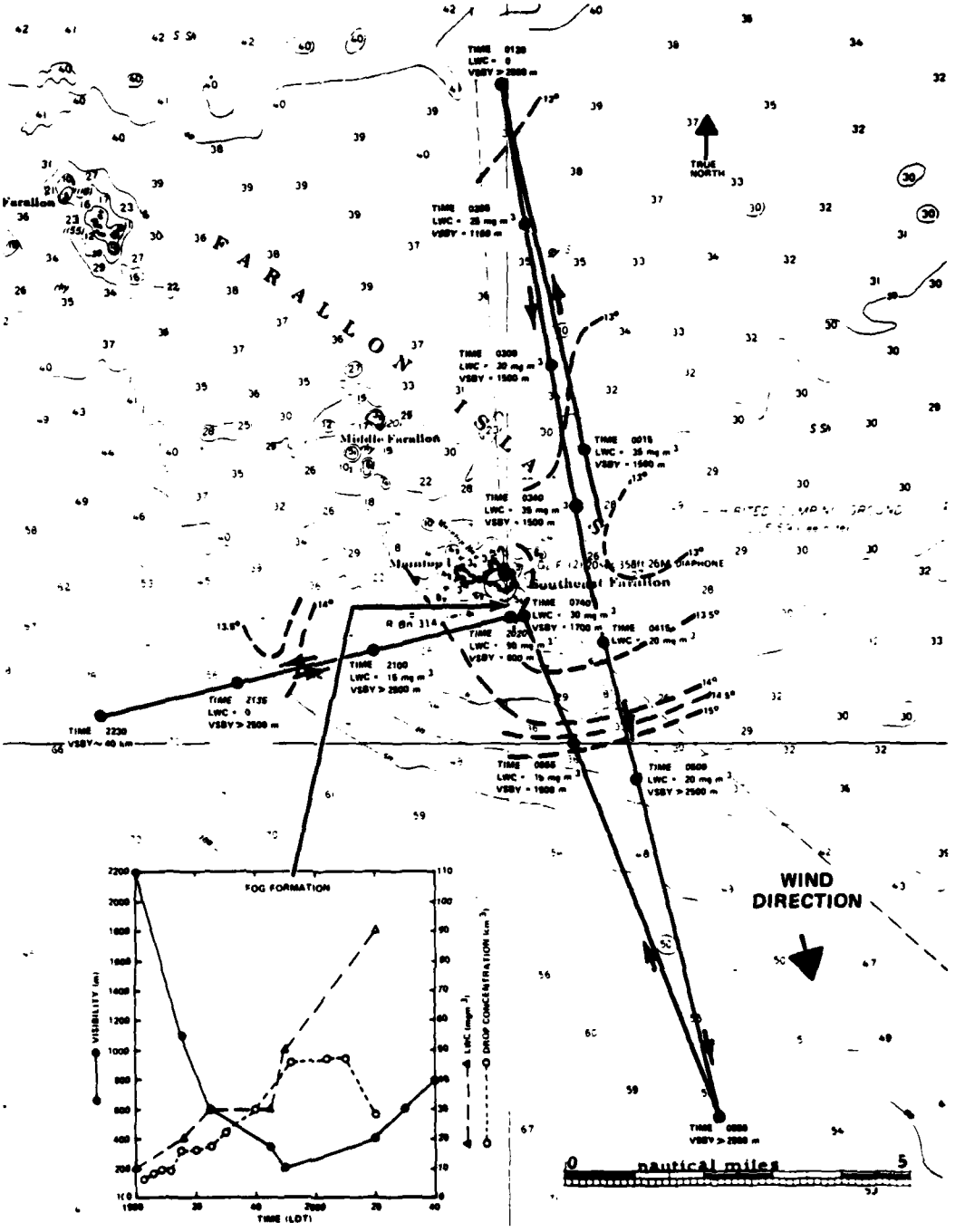

Figure OBSERVATIONS OBTAINED IN THE FOG OF 29-30 AUGUST 1972. ISOPLETHS OF SURFACE WATER TEMPERATURE (°C) ARE PLOTTED AND TIME, LWC AND VISIBILITY ARE SHOWN FOR EACH MEASUREMENT POSITION

DATA SOURCES

CASE 6

August 29, 1972

1.) Locator Map -

Mack, E.J., Pilie, R.J., and Kocmond, W.C., 1973: An Investigation of the Microphysical and Micro-meteorological Properties of Sea Fog. First Annual Summary Report Contract No. N00019-73-C-0094 May 1973. Calspan No. CJ-5237-M-1. Calspan Corp., PO BOX 400, Buffalo, NY 14225.

2.) a.) Initial Sounding
Mack et al, 1973: Ibid
Oakland Radiosonde.

b.) Verification Sounding
Same as a.)

3.) Sea Surface Temperature
Calspan Probe and Data Log for above cruise.

4.) Surface Winds
Calspan instrumentation.

5.) Synoptic Charts - National Meteorological Center 850 mb and Surface.

CASE 6: 'BLIND' DATA SETS

1.0 Initial Sounding at time zero at the location of forecast area.

Height (m)	Press (mb)	Temp (°C)	Dewpoint (°C)
3	1013	14.7	11.8
20	1010.7	14.2	11.8
100	1001.5	13.4	13.4
200	990.2	12.9	12.9
220	990	22.6	11.1
347	974	26.9	+2.8
1316	872	23.3	-3.1
1538	850	22.2	+0.5

1.1 Sky is overcast with stratus for past hour.

1.2 Cloud Liquid Water Content (after Rogers & Hanley, as noted for Case 1)

Height (m)	LWC (g/m^3)
90	.000
175	.150
210	.000

2.0 Inversion Base

Our estimate of height of the base of the inversion is 200 m.

3.0 Subsidence

Vertical motion is zero over the forecast period.

4.0 No cloud present above the marine mixed layer.

5.0 Sea Surface Temperature

Sea surface temperature exhibits values in the range 13.5-15.5°C over the forecast area.

6.0 Wind

Surface wind is constant in direction and speed at ∿3.5 m/sec. Geostrophic wind is uniform with height and also constant with time.

7.0 Sun Information	Declination (degrees)	Latitude (degrees)
Elevation angle at zenith: 65° (at 12 noon)	+10	38
Sunset: Time zero plus 2.5 hours		

8.0 Instructions

A) This is a horizontally homogeneous situation, please run model twice:

(1) with sea surface temperature of 15.3°C

(2) with sea surface temperature of 14.0°C

B) Output model results at 1, 2, 4, 8 and 12 hours after time zero.

C) Please document any supplementary processing which you have to make to this data set in order to run your model.

ADDENDA

If direction to which surface wind points is 000°, then geostrophic wind is plus (clockwise) + 15° @ 3.5 m/sec.

A representative wind sounding is

Height (m-msl)	Direction (degrees) (clockwise is positive as for geostrophic wind)	Speed (m/sec)
Surface	000	3.0
326	-44	2.5
655	-60	3.6
960	-47	4.4
1258	-60	4.1
1557	-95	3.9

850 mb is at 1538 m.

Soundings

Time (1)				Time (1) + 12 Hours		
Level (mb)	Height (m)	Temp. (°C)	Dewpoint (°C)	Height (m)	Temp. (°C)	Dewpoint (°C)
850	1538	22.2	+0.5	1532	21.3	-2.7
700	3186	9.5	-3.1	3177	9.3	-9.5
500	5873	-9.3	-25.8	5860	-9.4	-33.7
400	7561	-20.9	-38.1	7547	-20.8	-45.2
300	9621	-36.5	-53.5	9605	-37.2	-56.2
250	10859	-40.1	-56.1	10845	-44.4	*

*Motorboating

Time (1) is the same as time zero for the simulation.

APPENDIX C

DETAILED RESULTS FROM
MODEL TESTING AND EVALUATION

Results from the model simulations and subsequent evaluation are provided, as follows, in this Appendix:

(1) brief comments documenting the subjective evaluation of model performance (summarized in Tables 6 and 9, Section 3) for each model and each test case;

(2) summary Tables (C-1 to C-4) of numerical simulation results; and

(3) a complete set of individual plots which compare both initial and observed temperature and dewpoint profiles and cloud base and top heights to model predictions.

A few comments regarding the simulation profile plots are in order. These plots are arranged by test case so that all simulations for a given test case are grouped together. As for the initial and verification plots presented in Appendix B, dewpoint temperatures less than the minimum temperature on the abcissa were plotted at their correct height, but at the minimum dewpoint value. Cloud base and top are indicated by arrows on the plots. The arrows are located next to the profile to which they apply; in addition, the arrows for the simulated conditions are larger than those for initial and verification conditions. For Cases 2 and 5, in which only one model formed fog in the low levels, the height and value of the simulated maximum relative humidity in the low levels is plotted on the figure.

Appendix C
SUBJECTIVE EVALUATION OF MODEL PERFORMANCE: COMMENTS

I. Fog/Cloud Representation--Numerical Models

Case 1: verification--330 m deep stratus with top at 800 m
ARAP: close(-)--cloud too thick and base too low
Burk: close(-)--cloud too thin; top and base too high
NPS: verifies--cloud base and top each within 50 m of verification
Tag: NC--cloud much too thin
Wurtele: verifies--cloud base and top each within 50 m of verification

Case 2: verification--shallow fog (30 m depth)
ARAP: close--no fog predicted but moderate to high RH generated in lowest 30 m
Burk: close--no fog predicted but moderate to high RH generated in lowest 30 m
NPS: close--no fog predicted; very high RH generated but only up to 10 m
Tag: close(-)--no fog predicted; only moderately high RH below 30 m
Wurtele: verifies--predicted 40 m deep fog

Case 3, 10 hr: verification--cloud dissipating and hole developing near verification site; no cloud evident in sounding
ARAP: verifies--completely dissipated initial cloud
Burk: NC--did not dissipate cloud or reduce LWC significantly
NPS: close--partially dissipated cloud (50 m thick)
Tag: close--partially dissipated cloud (40 m thick)
Wurtele: close(+)--almost completely dissipated cloud (10 m thick)

Case 3, 20 hr: verification-250 m deep, dense fog
ARAP: NC--neither fog nor cloud predicted
Burk: verifies--270 m deep fog; LWC of 0.03 g/m^3 at 20 m ht.
NPS: NC--Fog not predicted; cloud base at 225 m
Tag: close(+)--thick, low cloud; base at $\sim$40 m (interpolated)
Wurtele: verifies--230 m deep fog

Case 4: verification—360 m deep stratus with top at 610 m
ARAP: verifies—stratus depth 320 m with top at ~580 m
Burk: verifies—stratus base a little too low, top at correct height
NPS: NC--predicted fog
Tag: verifies—stratus depth 390 m with top at 630 m
Wurtele: NC—predicted thick, low stratus

Case 5: verification—shallow cold water advection fog deepening to ~50 m over warm water
ARAP; close(-)—no fog predicted; only moderately high RH generated to heights ~50 m; slight reduction in RH at lowest level
Burk: close(+)—no fog predicted; very high RH generated to heights ~50 m
NPS: close—no fog predicted; very high RH but only to 26 m
Tag: close(-)—no fog predicted; only moderately high RH generated to heights ~50 m; slight reduction in RH at lowest level
Wurtele: close(-)—generated fog, but only in lowest 10 m; not representative

Case 6: verification—200 m deep, dense fog
ARAP: NC—neither fog nor cloud predicted
Burk: verifies—190 m deep fog
NPS: verifies—220 m deep fog
Tag: close—thick low cloud, base not close enough to surface
Wurtele: NC—predicted 50 m deep fog (much too shallow)

II. Boundary-Layer and Profiles—Numerical Models

Case 1: verification—lapsed profile with 850 m boundary-layer
ARAP: close—temperature and dewpoint too cold
Burk: close—temperature and dewpoint much too cold
NPS: close—temperature and dewpoint much too cold
Tag: close—temperature and dewpoint too cold
Wurtele: verifies—temperature and dewpoint within 0.5°C of observed

Case 2: verification—low-level inverted profile
ARAP: verifies—quantitatively matched temperature profile in lowest 30 m; dewpoint too cold

Burk: verifies—good match for temperature and dewpoint profiles in lowest 30 m
NPS: NC—predicted adiabatic profile
Tag: verifies—quantitatively matched temperature profile; dewpoint too cold
Wurtele: NC—profiles not representative of lowest 30 m

Case 3, 10 hr: verification—shallow boundary layer with near-adibatic profile
ARAP: NC—boundary layer too shallow; dewpoint too warm and temperature too cold
Burk: close—boundary layer depth and dewpoint are good; temperature much too cold
NPS: close—boundary layer depth and dewpoint are good; temperature much too cold
Tag: close—boundary layer depth and dewpoint are good; temperature much too cold
Wurtele: close—good boundary layer depth; dewpoint too warm, temperature too cold

Case 3, 20 hr: verification—250 m deep boundary layer, moist adiabatic profile
ARAP: NC— predicted much too shallow boundary layer
Burk: close—boundary layer depth good; temperature and dewpoint much too cold
NPS: NC—temperature and dewpoint much too cold; boundary layer too deep
Tag: close—boundary layer depth good; temperature and dewpoint much too cold
Wurtele: verifies—quantitatively predicted boundary layer, temperature and dewpoint

Case 4: verification—lapsed profile with 560 m boundary layer
ARAP: verifies—quantitatively predicted boundary layer, temperature and dewpoint
Burk: verifies—boundary layer depth good; temperature and dewpoint a little too cold in upper levels
NPS: close—boundary layer too high; temperature and dewpoint too cold
Tag: verifies—quantitatively predicted temperature and dewpoint; boundary layer a little too deep
Wurtele: verifies—good approximation of boundary layer and profiles

Case 5: verification—inverted profile evolved to near-isothermal below 30 m in deep fog
ARAP: verifies—modified inverted profile to isothermal below 30 m
Burk: verifies—modified inverted profile to isothermal below 30 m
NPS: verifies—modified inverted profile to isothermal below 30 m
Tag: verifies—modified inverted profile to isothermal below 30 m
Wurtele: NC—failed to modify profile to isothermal

Case 6: verification—200 m deep boundary layer, moist adiabatic profile
ARAP: NC—predicted boundary layer and profiles not representative
Burk: verifies—quantitatively predicted boundary layer and profiles
NPS: verifies—quantitatively predicted boundary layer and profiles
Tag: verifies—quantitatively predicted boundary layer and profiles
Wurtele: NC—predicted boundary layer and profiles not representative

III. Fog/Visibility Forecast - Synoptic Models

Case 1: verification—No fog; 330 m deep stratus with base at 470 m
Calspan D.T.: verifies—forecast no fog
Calspan D.T. (Inv).: verifies—forecast no fog
Calspan Inv. Stat: verifies—zero probability of low visibility
Leipper Indices: verifies—forecast no fog
Leipper Inv. Stat.: close(+)—low probability of dense fog, but moderate probability of light fog

Case 2: verification—shallow fog (30 m depth), sfc-based inversion
Calspan D.T.: NC—predicted no fog
Calspan D.T. (Inv).: verifies—predicted shallow fog patches over SST gradients
Calspan Inv. Stat: NC—model NA due to lack of sfc-based inversion category
Leipper Indices: verifies—predicted fog
Leipper Inv. Stat.: NC—fog probability forecast too low

Case 3, 10 hr: verification—daytime, dissipating stratus cloud
Calspan D.T.: NC—not currently applicable to daytime situations
Calspan D.T. (Inv).: NC—not currently applicable to daytime situations
Calspan Inv. Stat: verifies—forecast of low probability for fog and low vsby
Leipper Indices: NC—not designed for daytime situations
Leipper Inv. Stat.: NC—not designed for daytime situations

Case 3, 20 hr: verification—dense fog, 250 m deep
Calspan D.T.: verifies—model forecast dense fog probable
Calspan D.T.(Inv).: verifies—model forecast dense fog probable
Calspan Inv. Stat: close(-)—probability of fog not high enough

Leipper Indices: verifies--model forecast fog
Leipper Inv. Stat.: close--probability of dense fog not high enough

Case 4: verification: 360 m deep stratus with base at 250 m
Calspan D.T.: verifies--model forecast no fog
Calspan D.T.(Inv).: verifies--model forecast no fog
Calspan Inv. Stat: verifies--very low probability of low visibility
Leipper Indices: verifies--model forecast no fog
Leipper Inv. Stat.: close(+)--low probability of dense fog but moderate probability of light fog

Case 5: verification--shallow advection fog deepening to ~50 m; large scale inversion at 100 m
Calspan D.T.: NC--predicted no fog
Calspan D.T.(Inv.): close--predicted shallow fog patches
Calspan Inv. Stat: verifies--high probabilities for fog
Leipper Indices: verifies--predicted fog
Leipper Inv. Stat.: close(+)--high probabilities for light fog

Case 6: verification--200 m deep, dense fog
Calspan D.T.: verifies--predicted dense fog
Calspan D.T. (Inv.): verifies--predicted dense fog
Calspan Inv. Stat: close(-)--low probabilities for fog; but recommended use of next time period category provides forecast of high probability for fog
Leipper Indices: NC--no fog forecast because of unfavorable moisture index
Leipper Inv. Stat.: close(+)--high probabilities for light fog

TABLE C-1

SUMMARY OF SIMULATIONS--TEMPERATURE DIFFERENTIAL RELATIVE TO VERIFICATION

Case	Height Range	Burk (°C)	ARAP (°C)	NPS (°C)	Tag (°C)	Wurtele (°C)
1	0-800 m	-1.0 to -2.0	-1.0 to -1.5	-2.0	-1.0 to -2.0	-0.5
2	0-28 m	0 to +0.5	-0.5 to +0.5	-0.5 to -2	0 to +0.5	-1 to -2
3_{10}	0-250 m	-4.0	-2.0	-4.0	-3.5	-1.5
3_{20}	0-250 m	-4.0	0.0 to +7.0	-4.0	-3.5 to -3.0	-0.5
4	0-560 m	-0.5	0.0	-1 to -2	0 to -0.5	+1.0
5_3	0-30 m	-0.5	+0.5	-0.5	+1.0	0 to +1
6	0-200 m	+0.5 to -0.5	+1.0 to +2.0	0	+0.5	+1 to +1.5

TABLE C-2

SUMMARY: DEPTH OF BOUNDARY LAYER

Case	Initial (m)	Verification (m)	Burk (m)	ARAP (m)	NPS (m)	Tag (m)	Wurtele (m)
1	790	850	870	767	800	838	830
2	inverted	inverted	inverted	inverted	10	inverted	inverted
3_{10}	270	250	270	124	320	298	250
3_{20}	270	250	270	50	340	298	230
4	500	560	570	580	650	628	600
5_3	inverted	>30	20	27	26	inverted	inverted
6	200	200	200	125	220	194	50

TABLE C-3

SUMMARY OF SIMULATIONS--HEIGHT OF FOG/CLOUD* BASE AND TOP

CASE	Initial		Verification		Burk		ARAP		NPS		Tag		Wurtele	
	Cloud Base (m)	Cloud Top (m)	Cloud Base (m)	Cloud Top (m)	Cloud Base (m)	Cloud Top (m)	Cloud Base (m)	Cloud Top (m)	Cloud Base (m)	Cloud Top (m)	Cloud Base (m)	Cloud Top (m)	Cloud Base (m)	Cloud Top (m)
1	464	688	468	800	600	870	250	755	400	800	570	728	395	835
2*	@10m 91	@28m 87	0	28	96	90	97	92	99	(@10m) 99		(@20m) 90	0	40
3_{10}	144	265	None		170	270	None		270	320	258	298	175	175
3_{20}	144	265	0	250	20	270	None		210	340	40	298	0	230
4	420	540	250	610	150	570	260	580	0	650	240	628	70	600
5_3*	@10m 97	@28m 92	0	>50	98	(@28m) 96	(@2m) 94	(@28m) 93	97	(@26m) 98	(@10m) 94	(@28m) 93	0	10
6	100	200	0	200	< 10	200	None		0	220	53	194	0	50

* Where cloud was not formed in the simulation, relative humidities (underlined) are shown for the appropriate verification heights, unless otherwise indicated. Cloud boundaries defined by 0.03 g/m^3 LWC.

TABLE C-4

SUMMARY CLOUD THICKNESS* AND MAXIMUM LIQUID WATER CONTENT

Case	Initial		Verification		Burk		ARAP		NPS		Tag		Wurtele	
	Thick (m)	Max LWC (g/m^3)	Thick (m)	Max LWC (g/m^3)	Thick (m)	Max LWC (g/m^3)	Thick (m)	Max LWC (g/m^3)	Thick (m)	Max LWC (g/m^3)	Thick (m)	Max LWC (g/m^3)	Thick (m)	Max LWC (g/m^3)
1	224	.36	330		270	.27	500	.45	400	.97	100	.21	440	.87
2	0	0	30		None		None		None		None		40	.48
3_{10}	121	.20	None		120	.19	None		50	.20	40	.09	<10	.05
3_{20}	121	.20	250		250	.41	None		130	.28	260	.59	230	1.20
4	120	.26	360		420	.59	320	.55	650	1.54	390	.80	530	1.08
5_3	0	0	>50		None		None		None		None		10	.48
6	100	.15	200		190	.41	None		220	.34	140	.42	50	1.02

*Cloud boundaries defined by 0.03 g/m^3 LWC.

TABLE C-5

NUMERICAL MODEL PERFORMANCE ON CALSPAN DATA SETS

SUBJECTIVE CLOUD/FOG FORECAST

	Case 1	2	3_{10}	3_{20}	4	5	6
Burk	270 m deep stratus	Inc. RH No Fog	100 m deep stratus	270 m deep Fog	420 m deep stratus	Inc. RH No Fog	190 m deep Fog
ARAP	500 m deep stratus	Inc. RH No Fog	No stratus cloud	No Cloud No Fog	320 m deep stratus	No Fog	No Cloud No Fog
NPS	400 m deep stratus	Inc. RH No Fog	50 m deep stratus	130 m deep stratus	650 m deep Fog	Inc. RH No Fog	220 m deep Fog
Tag	160 m deep stratus	Inc. RH No Fog	40 m deep stratus	260 m deep very low stratus	390 m deep stratus	No Fog	140 m deep stratus
Wurtele	440 m deep stratus	40 m deep Fog	<10 m deep stratus	230 m deep Fog	530 m deep stratus	10 m deep Fog	50 m deep Fog
Persistence	225 m deep stratus	No Fog	120 m deep stratus	120 m deep stratus	120 m deep stratus	No Fog	100 m deep stratus
Verification	330 m deep stratus	30 m deep Fog	Dissipated stratus	250 m deep Fog	360 m deep stratus	>50 m deep Fog	200 m deep Fog

TABLE C-6

SYNOPTIC MODEL PERFORMANCE ON CALSPAN DATA SETS

Fog/Visibility Forecast

	Case						
	1	2	3_{10}	3_{20}	4	5	6
Calspan Decision Tree	No Fog	No Fog	NA	Fog	No Fog	No Fog	Dense Fog
Calspan Decision Tree (using verification inversion)	No Fog	Shallow Patchy Fog	NA	Fog	No Fog	Shallow Patchy Fog	Dense Fog
Calspan Inversion Statistics (using verification inversion)	0/0/0*	NA	4/11/23	11/14/36	0/0/1	51/71/80	13/18/31
Leipper Indices (using initial conditions)	No Fog	Fog	NA	Fog	No Fog	Fog	No Fog
Leipper Inversion Statistics (using verification inversion)	6/-/40*	26/-/36	NA	34/-/71	6/-/40	59/-/94	59/-/94
Persistence	No Fog	No Fog	No Fog	No Fog	No Fog	No Fog	No Fog
Verification	No Fog	Shallow Fog	No Fog	Dense Fog	No Fog	Dense Fog	Dense Fog

* For the two inversion statistics models, forecasts are in probability (% frequency) of occurrence of visibilities ≤0.5/≤1.0/≤3.0 mi, respectively

NA = not applicable

CASE 1

May 22, 1978

ARAP, Burk, and NPS ran starting with an initial cloud layer; Tag and Wurtele could not run with this initial condition so they started with no cloud. Consequently, Tag and Wurtele have different initial temperature and dewpoint profiles from those of the other three modelers..

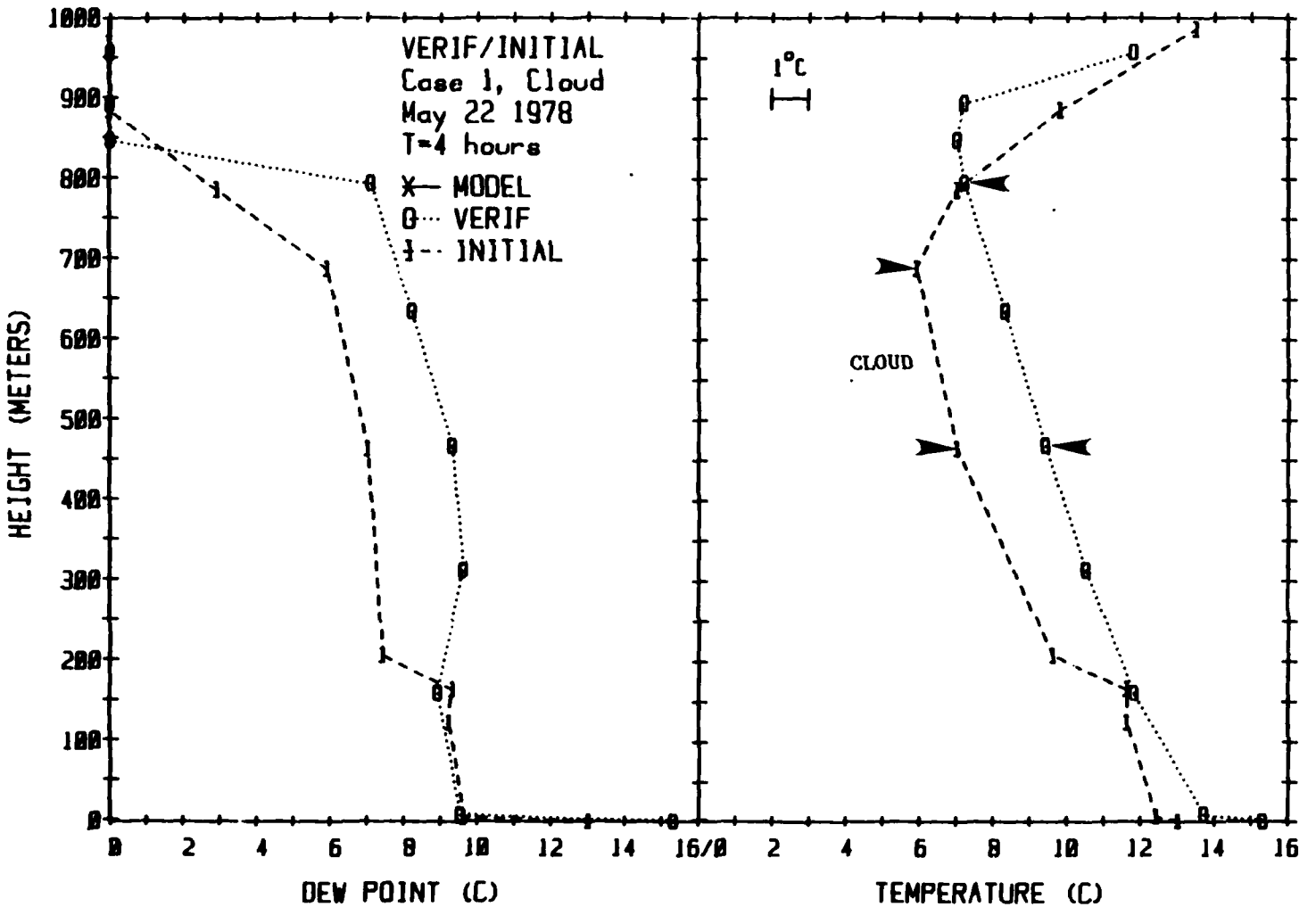
VERIF/INITIAL
Case 1, Cloud
May 22 1978
T=4 hours
MODEL
VERIF
INITIAL
1°C
CLOUD
HEIGHT (METERS)
DEW POINT (C)
TEMPERATURE (C)
1000
900
800
700
600
500
400
300
200
100
0
0 2 4 6 8 10 12 14 16/0
2 4 6 8 10 12 14 16

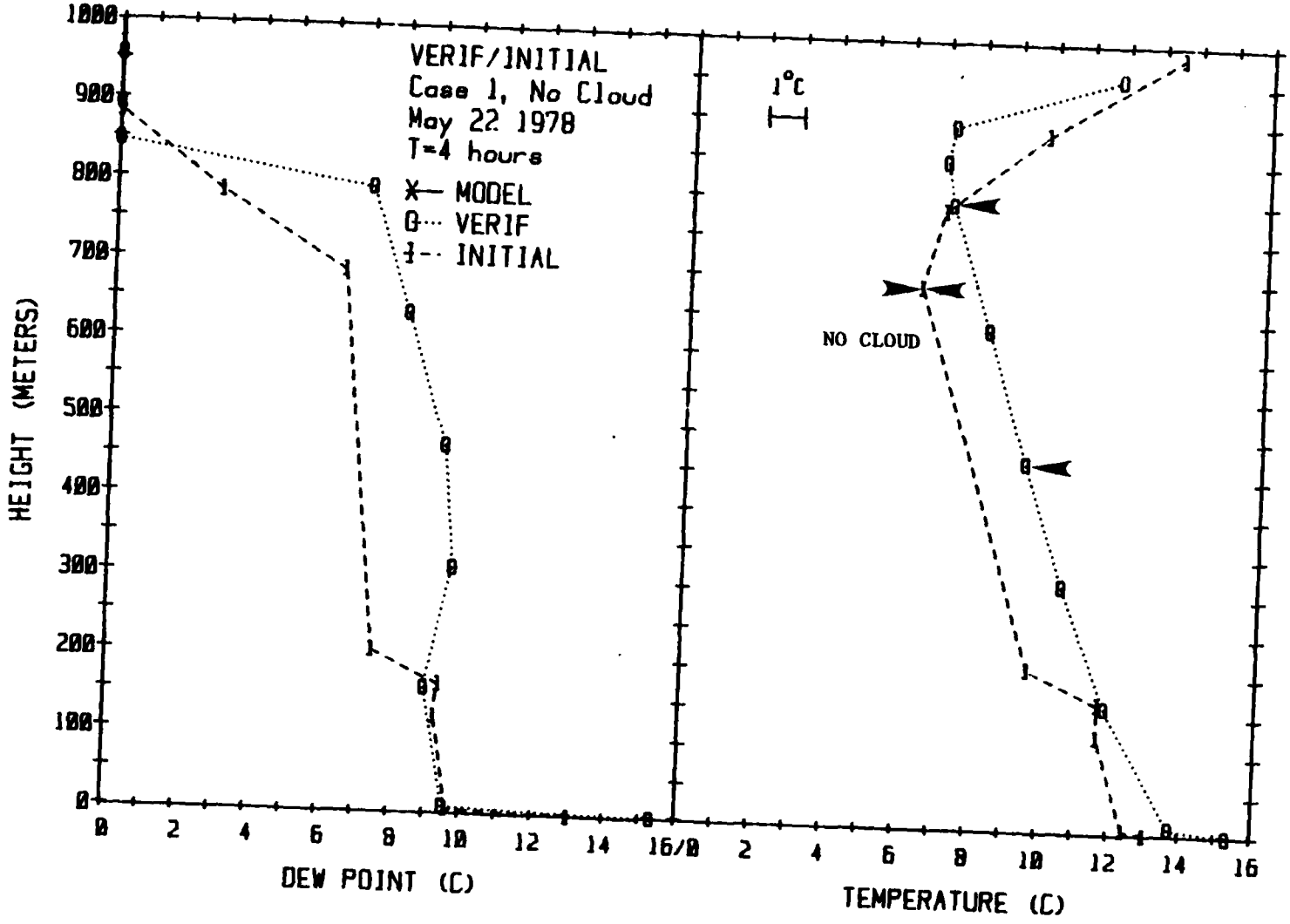
VERIF/INITIAL
Case 1, No Cloud
May 22 1978
T=4 hours
MODEL
VERIF
INITIAL
1°C
NO CLOUD
HEIGHT (METERS)
DEW POINT (C)
TEMPERATURE (C)
1000
900
800
700
600
500
400
300
200
100
0
0 2 4 6 8 10 12 14 16/0 2 4 6 8 10 12 14 16

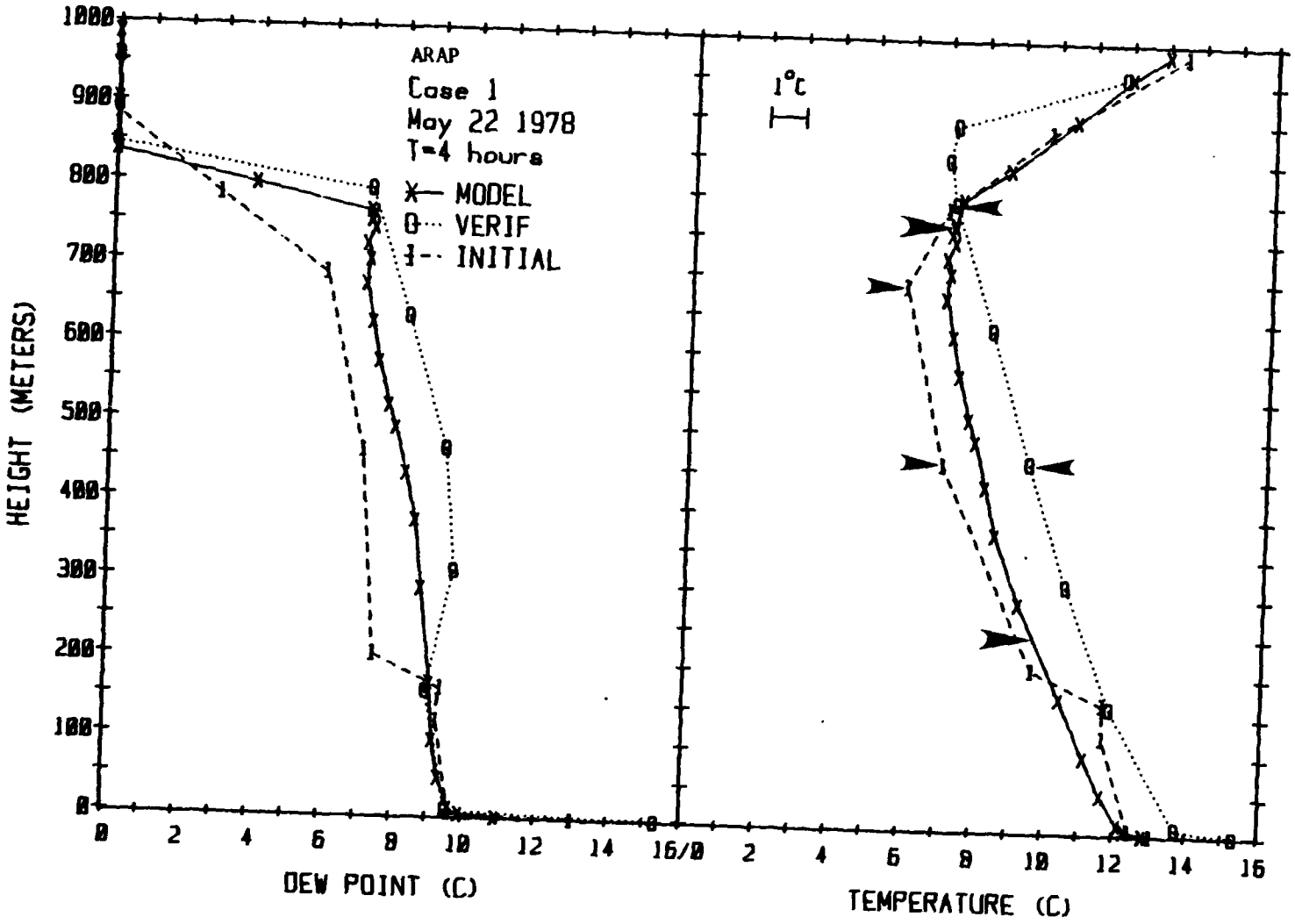
ARAP
Case 1
May 22 1978
T=4 hours
MODEL
VERIF
INITIAL
1°C
HEIGHT (METERS)
1000
900
800
700
600
500
400
300
200
100
0
0 2 4 6 8 10 12 14 16/0
DEW POINT (C)
2 4 6 8 10 12 14 16
TEMPERATURE (C)

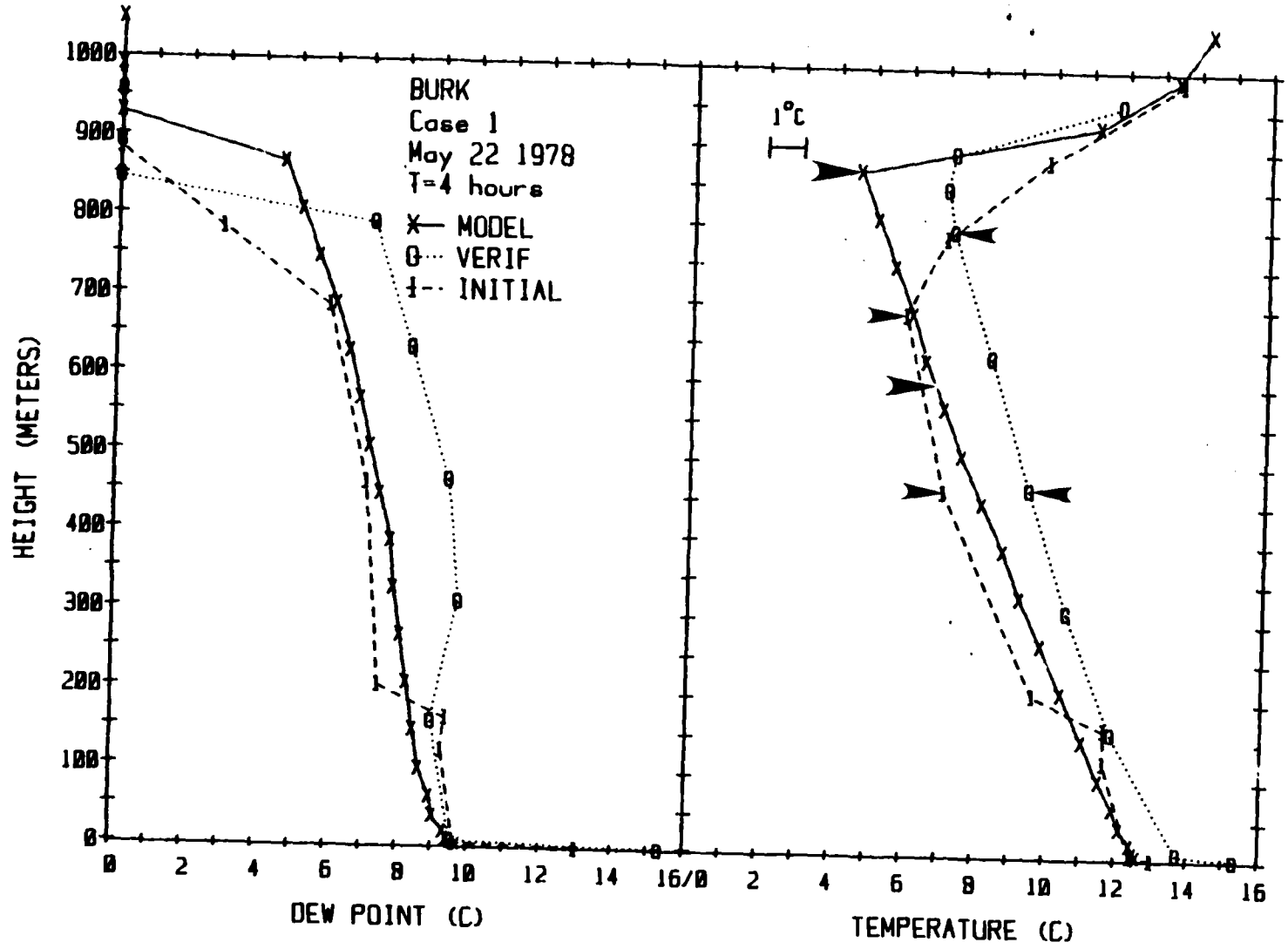
BURK
Case 1
May 22 1978
T=4 hours
X— MODEL
0··· VERIF
I·· INITIAL
HEIGHT (METERS)
1000
900
800
700
600
500
400
300
200
100
0
0 2 4 6 8 10 12 14 16/0
DEW POINT (C)
1°C
2 4 6 8 10 12 14 16
TEMPERATURE (C)

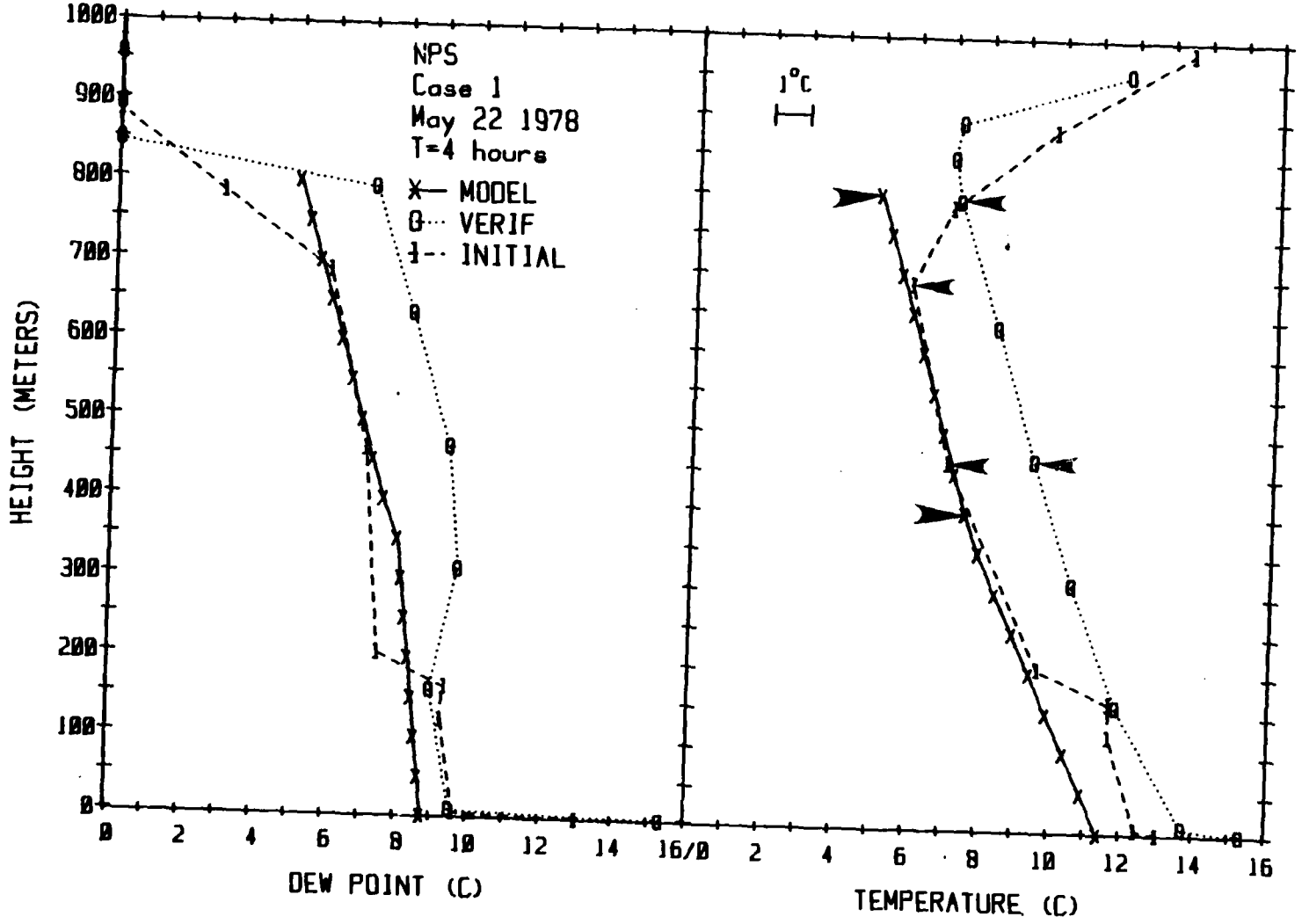
NPS
Case 1
May 22 1978
T=4 hours
X— MODEL
0··· VERIF
1-- INITIAL
1°C
HEIGHT (METERS)
1000
900
800
700
600
500
400
300
200
100
0
0 2 4 6 8 10 12 14 16/0
DEW POINT (C)
2 4 6 8 10 12 14 16
TEMPERATURE (C)

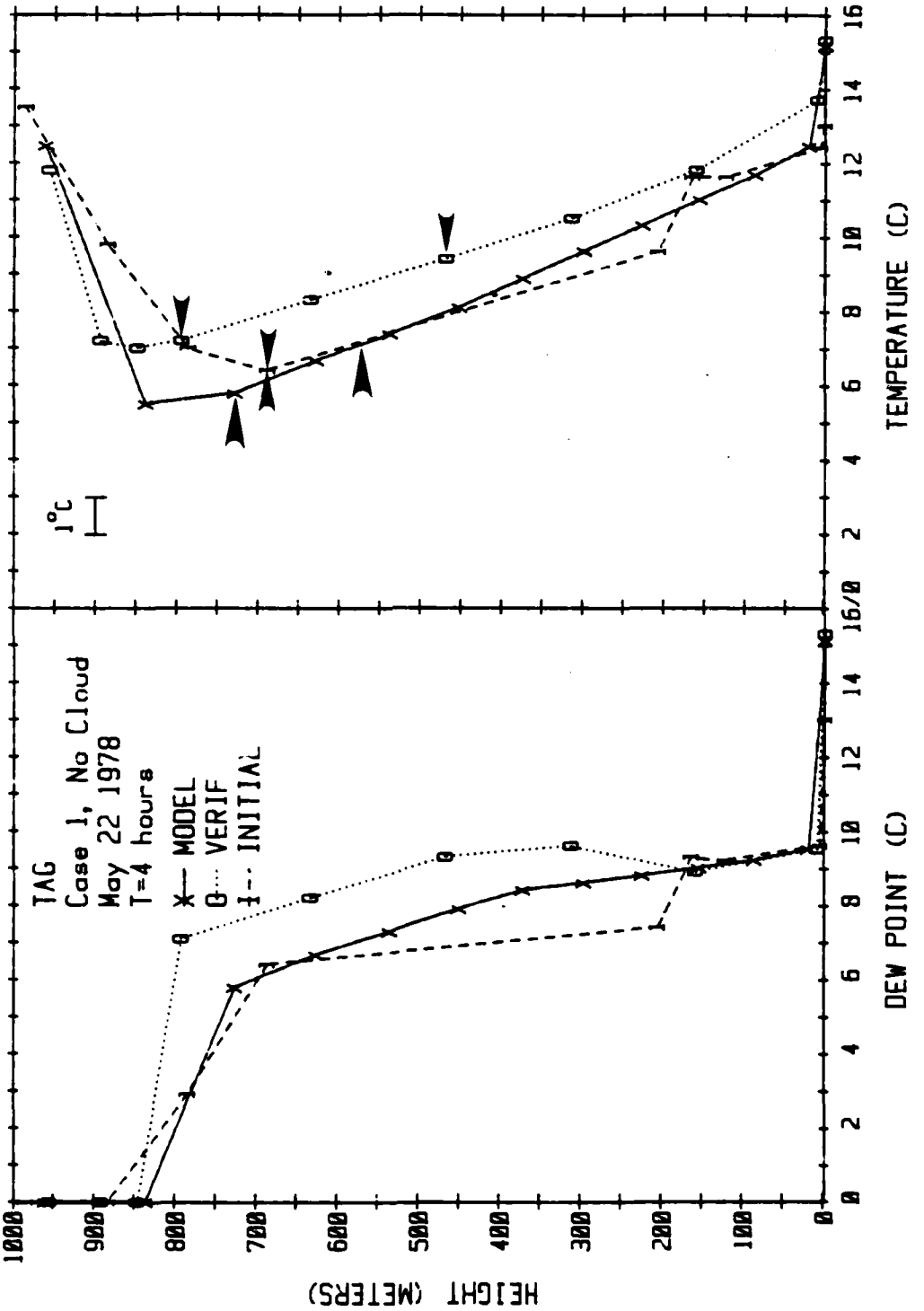
TAG
Case 1, No Cloud
May 22 1978
T=4 hours
MODEL
VERIF
INITIAL
1°C
HEIGHT (METERS)
TEMPERATURE (C)
DEW POINT (C)

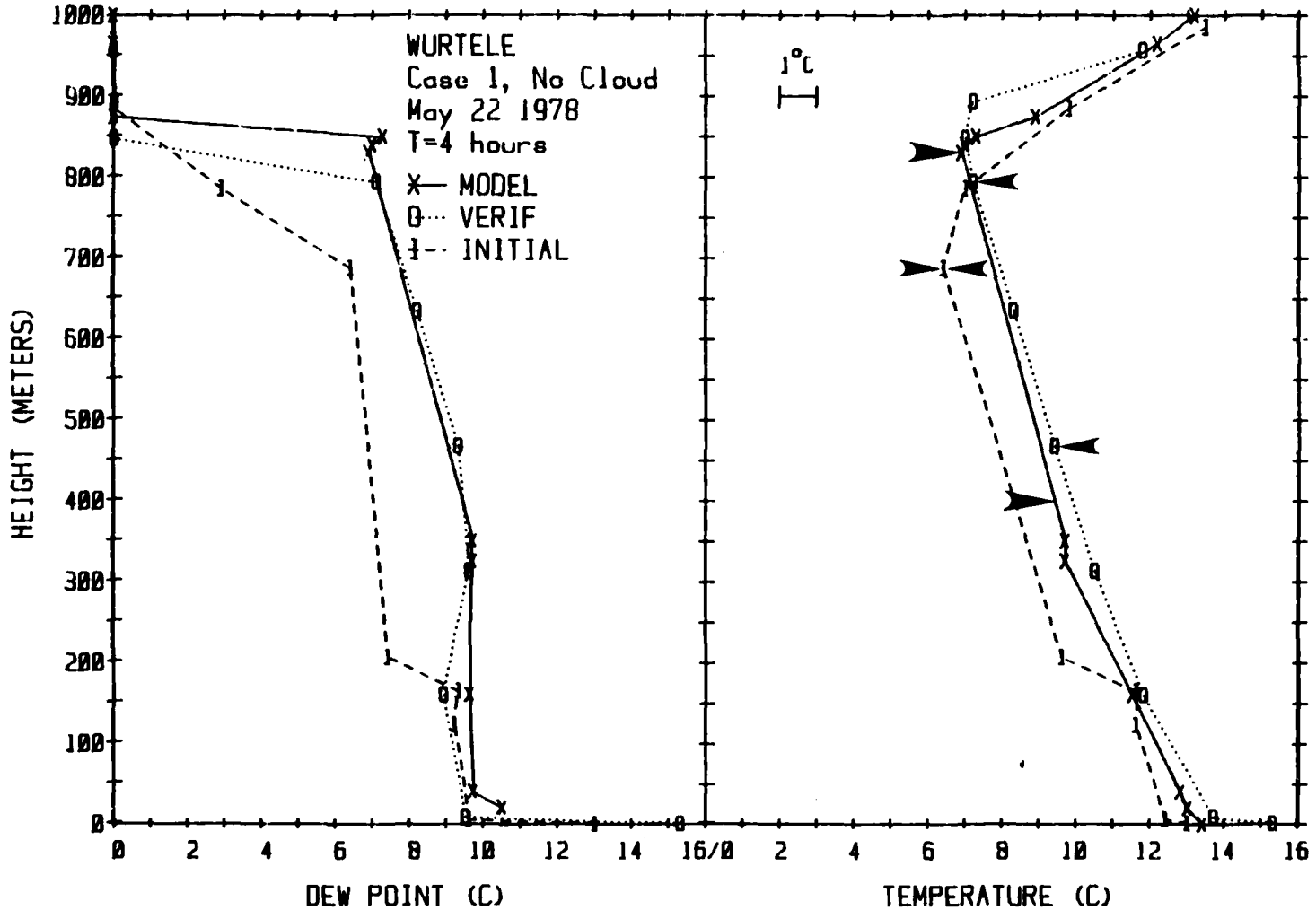
WURTELE
Case 1, No Cloud
May 22 1978
T=4 hours
X— MODEL
0··· VERIF
1-- INITIAL
1°C
HEIGHT (METERS)
1000
900
800
700
600
500
400
300
200
100
0
0 2 4 6 8 10 12 14 16/0
DEW POINT (C)
2 4 6 8 10 12 14 16
TEMPERATURE (C)

CASE 2

August 2, 1975

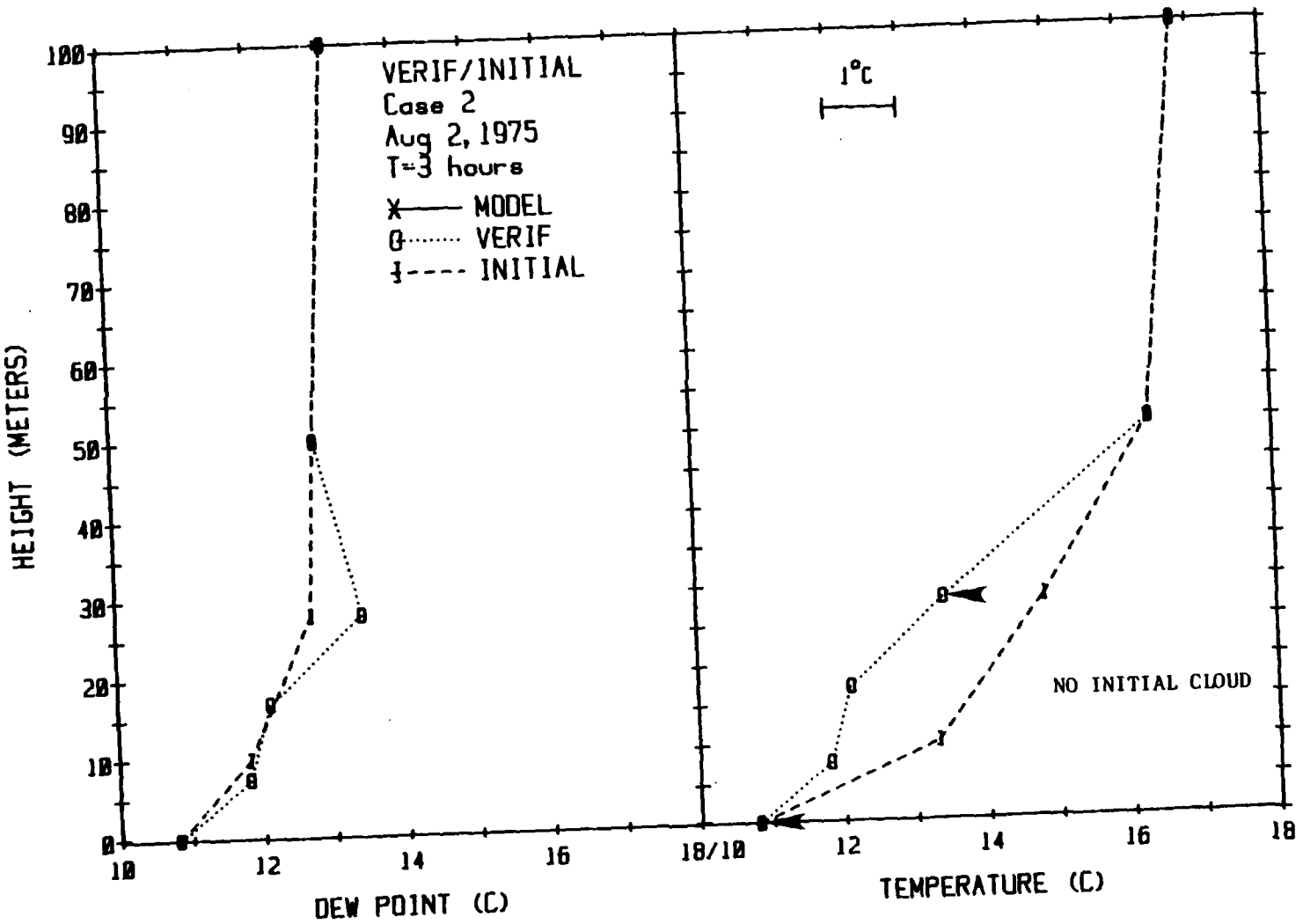
VERIF/INITIAL
Case 2
Aug 2, 1975
T=3 hours
MODEL
VERIF
INITIAL
1°C
NO INITIAL CLOUD
HEIGHT (METERS)
DEW POINT (C)
TEMPERATURE (C)
100
90
80
70
60
50
40
30
20
10
0
10
12
14
16
18/10
12
14
16
18

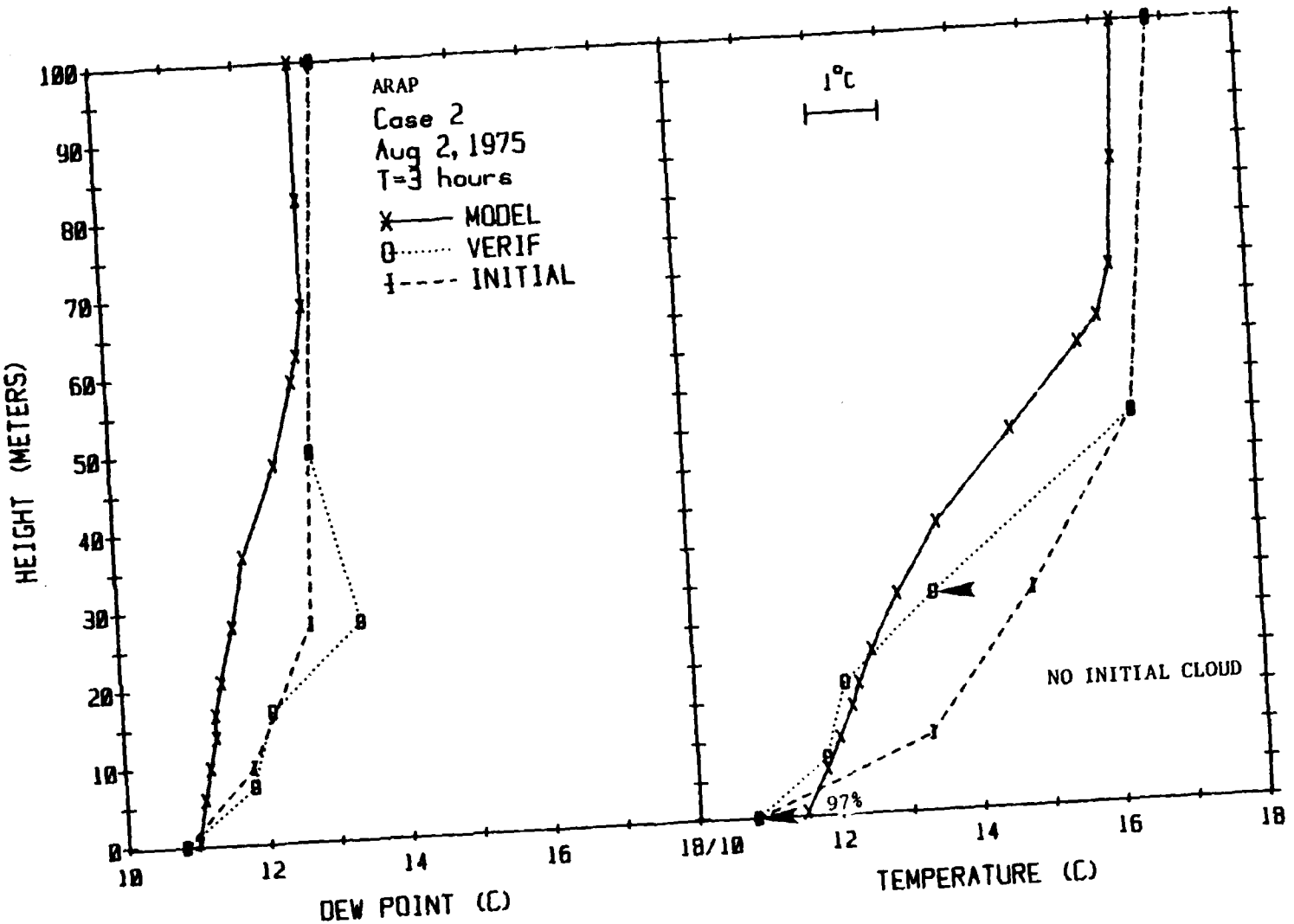
ARAP
Case 2
Aug 2, 1975
T=3 hours
MODEL
VERIF
INITIAL
1°C
NO INITIAL CLOUD
97%
HEIGHT (METERS)
DEW POINT (C)
TEMPERATURE (C)
100
90
80
70
60
50
40
30
20
10
0
10
12
14
16
18/18
18

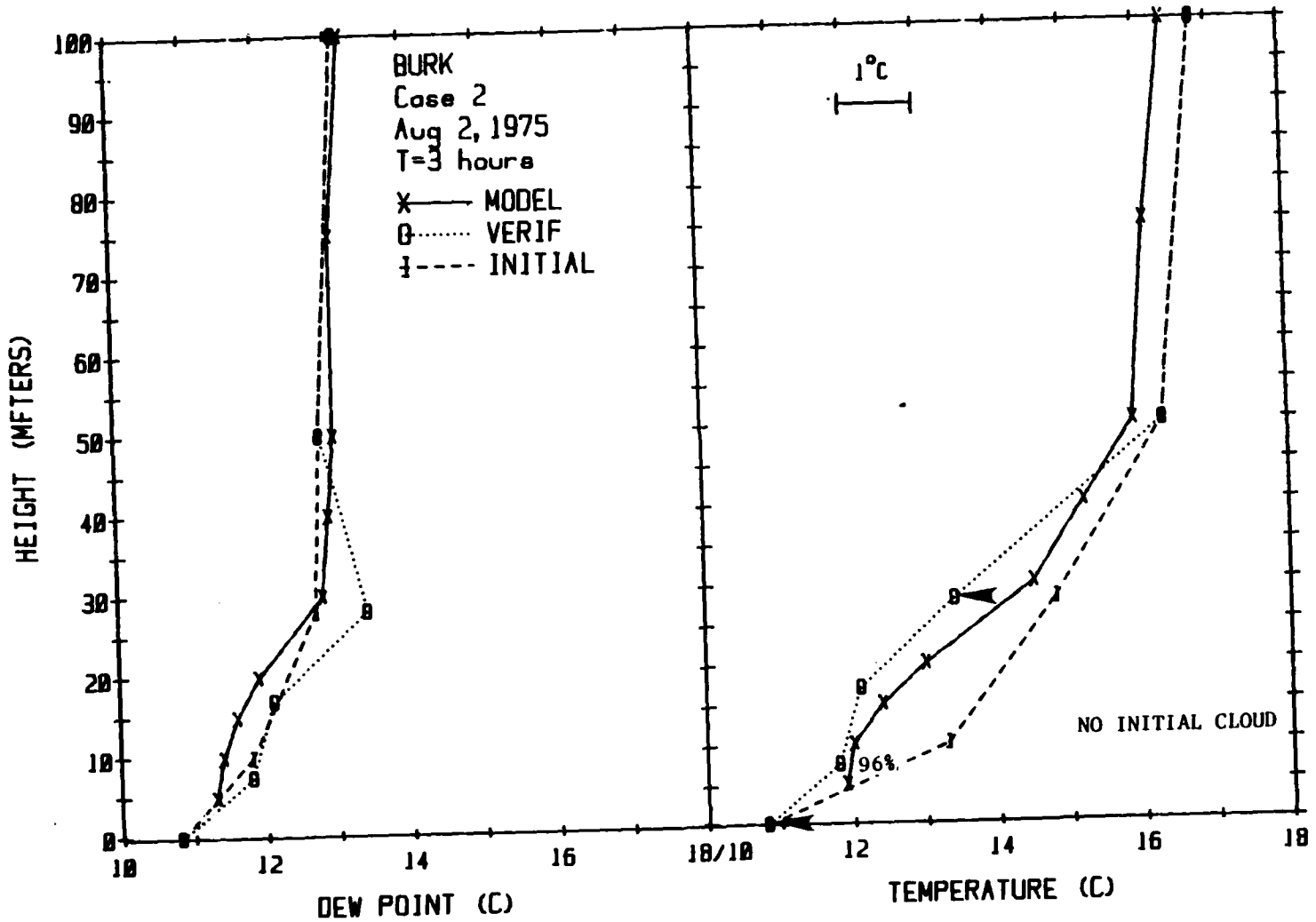
BURK
Case 2
Aug 2, 1975
T=3 hours
MODEL
VERIF
INITIAL
1°C
NO INITIAL CLOUD
96%
HEIGHT (MFTERS)
DEW POINT (C)
TEMPERATURE (C)
100
90
80
70
60
50
40
30
20
10
0
10
12
14
16
18/10
18

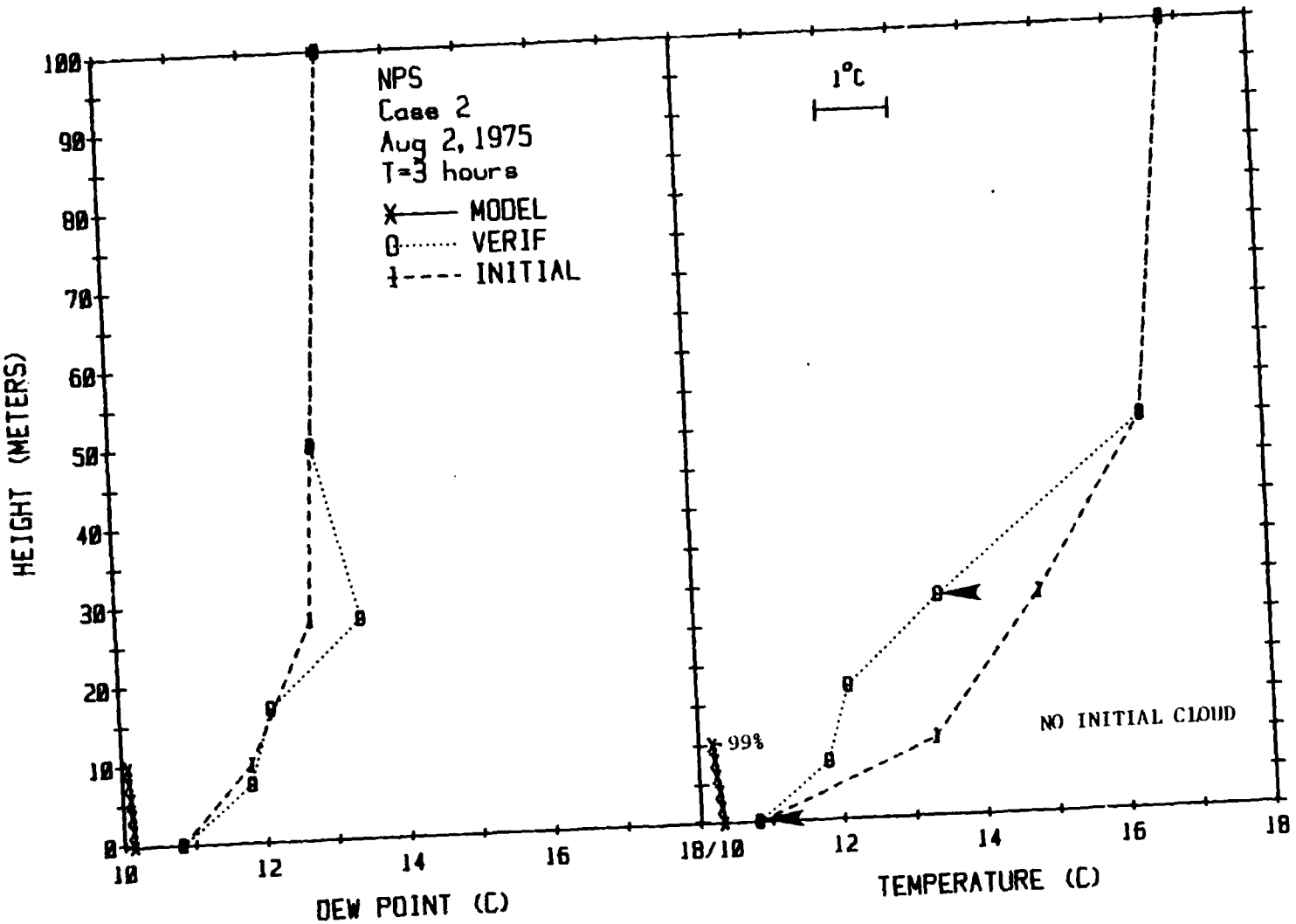
NPS
Case 2
Aug 2, 1975
T=3 hours
MODEL
VERIF
INITIAL
1°C
NO INITIAL CLOUD
99%
HEIGHT (METERS)
DEW POINT (C)
TEMPERATURE (C)
100
90
80
70
60
50
40
30
20
10
0
10
12
14
16
18/10
12
14
16
18

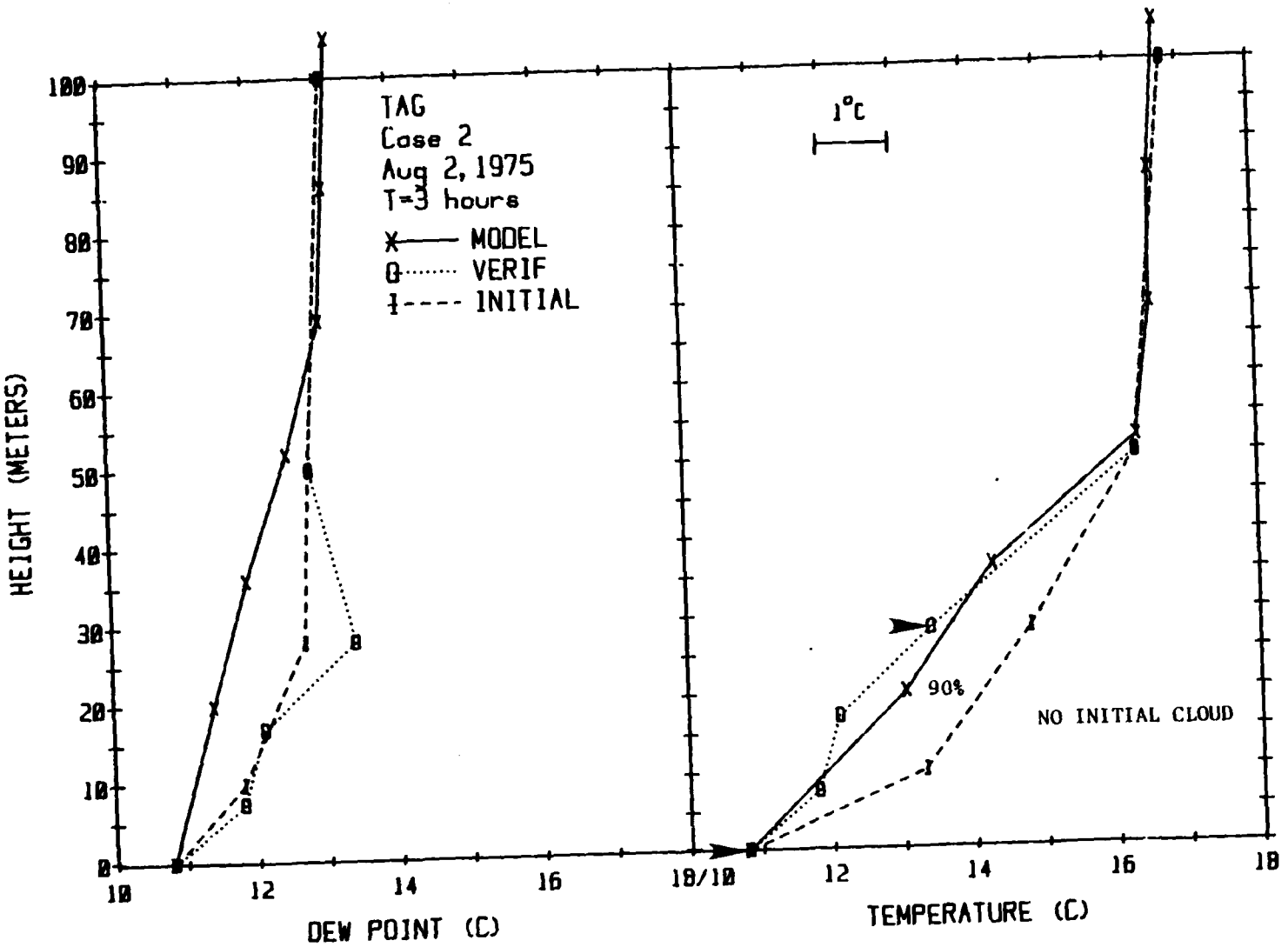
TAG
Case 2
Aug 2, 1975
T=3 hours
MODEL
VERIF
INITIAL
1°C
HEIGHT (METERS)
100
90
80
70
60
50
40
30
20
10
0
10
12
14
16
18/18
12
14
16
18
DEW POINT (C)
TEMPERATURE (C)
90%
NO INITIAL CLOUD

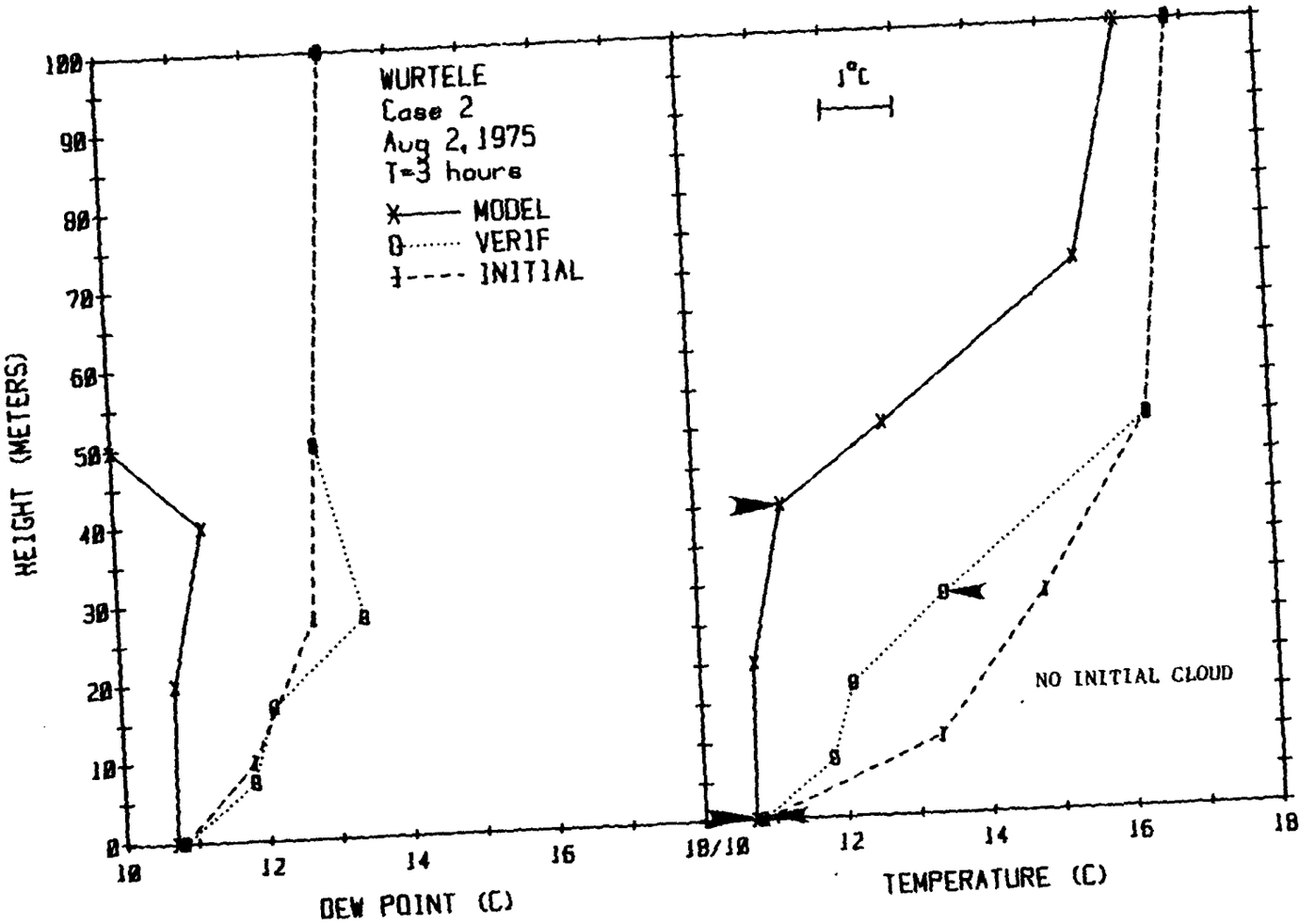
WURTELE
Case 2
Aug 2, 1975
T=3 hours
MODEL
VERIF
INITIAL
1°C
NO INITIAL CLOUD
HEIGHT (METERS)
DEW POINT (C)
TEMPERATURE (C)
0
10
20
30
40
50
60
70
80
90
100
10
12
14
16
18/18
18

CASE 3

(10 Hours)

October 7, 1976

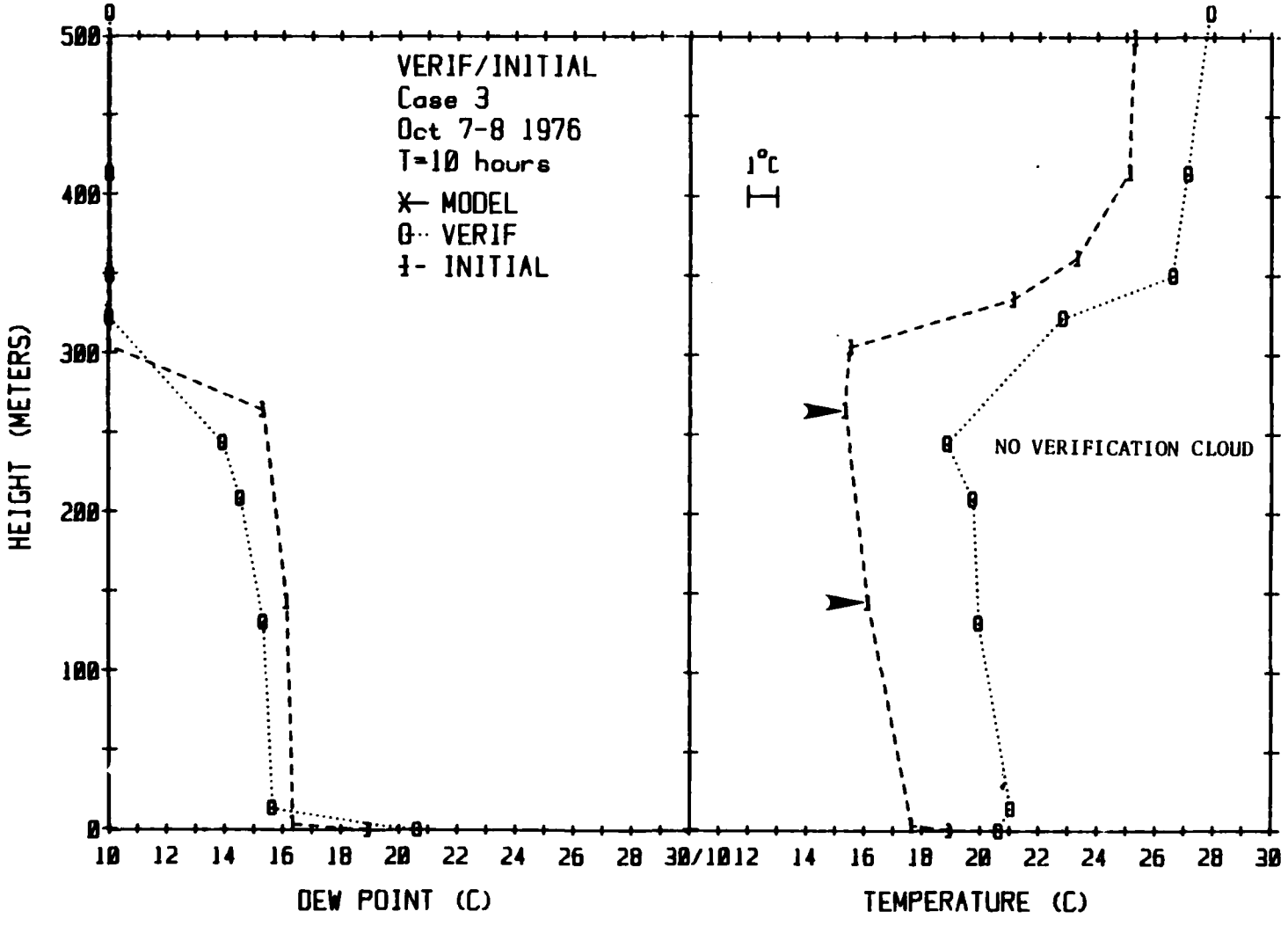
VERIF/INITIAL
Case 3
Oct 7-8 1976
T=10 hours
MODEL
VERIF
INITIAL
1°C
NO VERIFICATION CLOUD
HEIGHT (METERS)
DEW POINT (C)
TEMPERATURE (C)
0
100
200
300
400
500
10 12 14 16 18 20 22 24 26 28 30/10 12 14 16 18 20 22 24 26 28 30

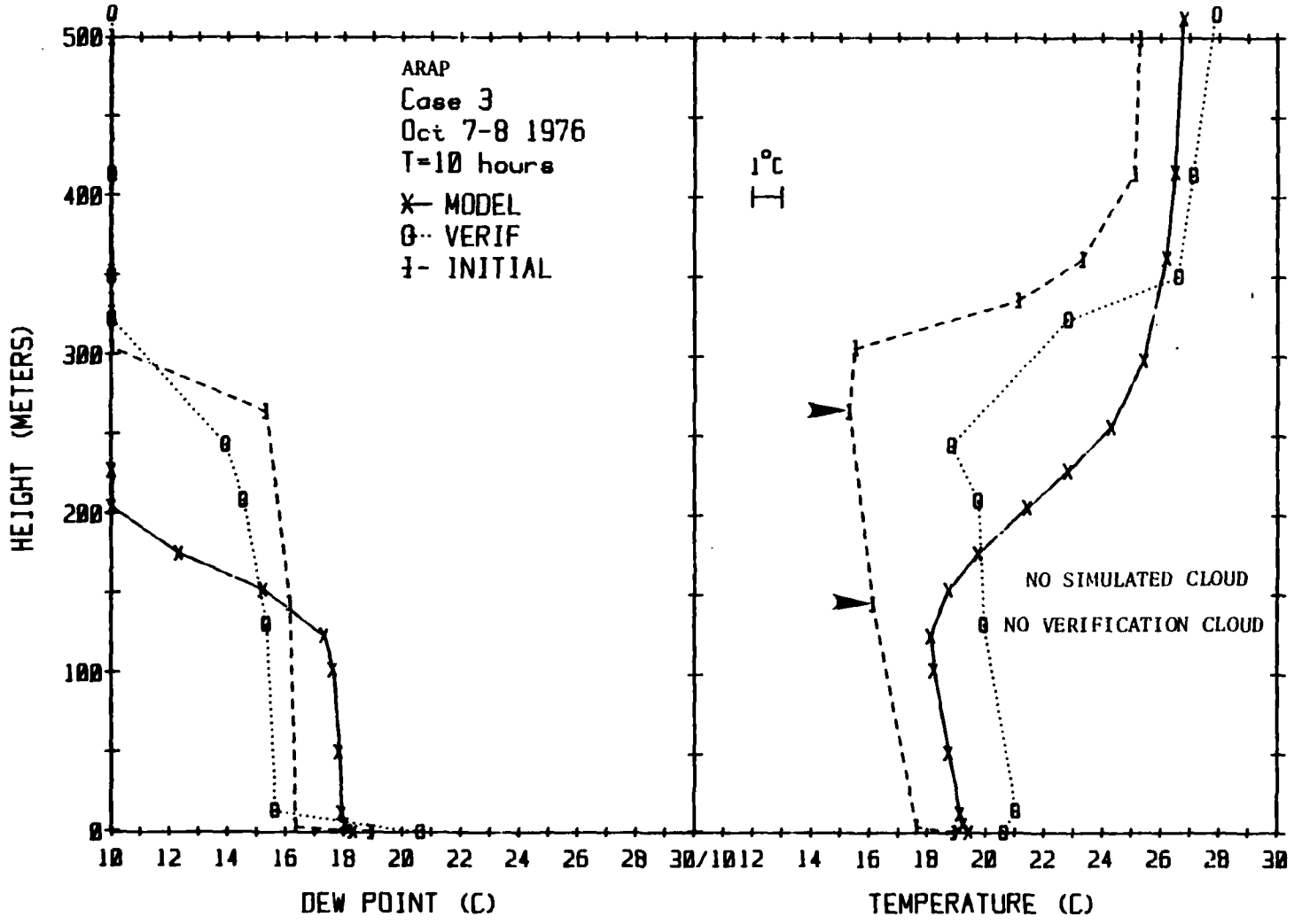
ARAP
Case 3
Oct 7-8 1976
T=10 hours
MODEL
VERIF
INITIAL
1°C
NO SIMULATED CLOUD
NO VERIFICATION CLOUD
HEIGHT (METERS)
500
400
300
200
100
0
10 12 14 16 18 20 22 24 26 28 30/10 12 14 16 18 20 22 24 26 28 30
DEW POINT (C)
TEMPERATURE (C)

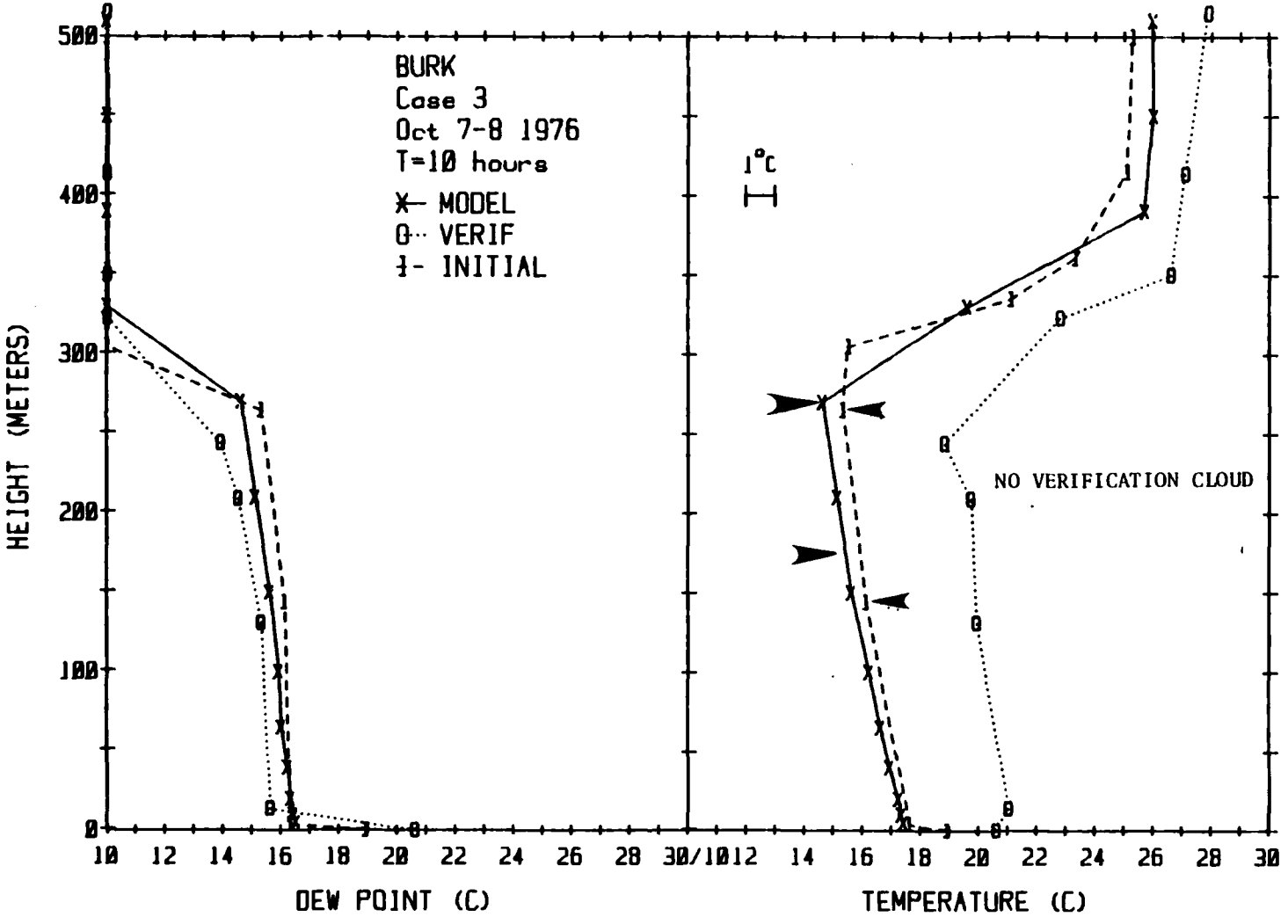
BURK
Case 3
Oct 7-8 1976
T=10 hours
MODEL
VERIF
INITIAL
1°C
NO VERIFICATION CLOUD
HEIGHT (METERS)
500
400
300
200
100
0
10 12 14 16 18 20 22 24 26 28 30/10 12 14 16 18 20 22 24 26 28 30
DEW POINT (C)
TEMPERATURE (C)

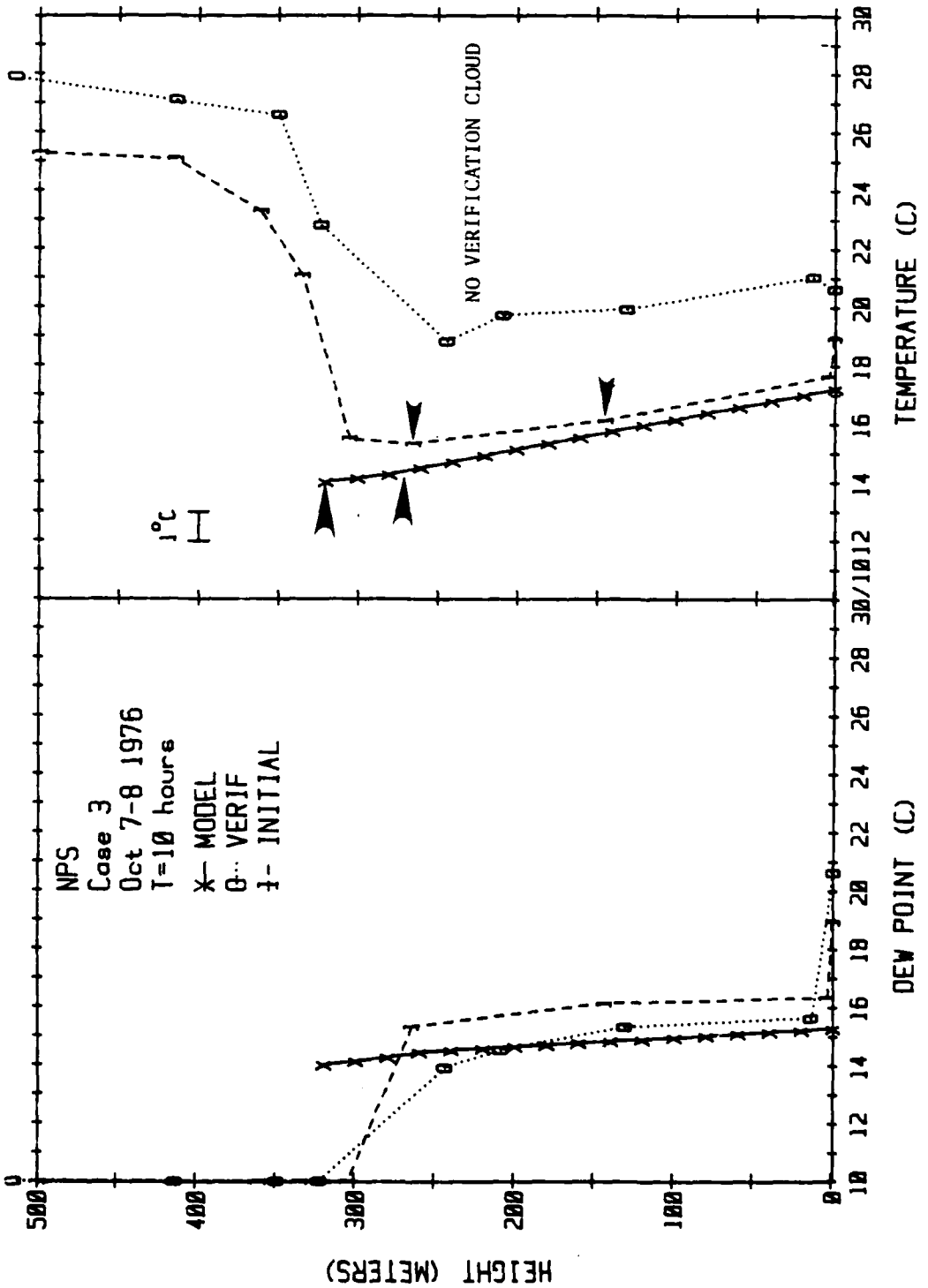
NO VERIFICATION CLOUD
1°C
NPS
Case 3
Oct 7-8 1976
T=10 hours
MODEL
VERIF
INITIAL
HEIGHT (METERS)
DEW POINT (C)
TEMPERATURE (C)

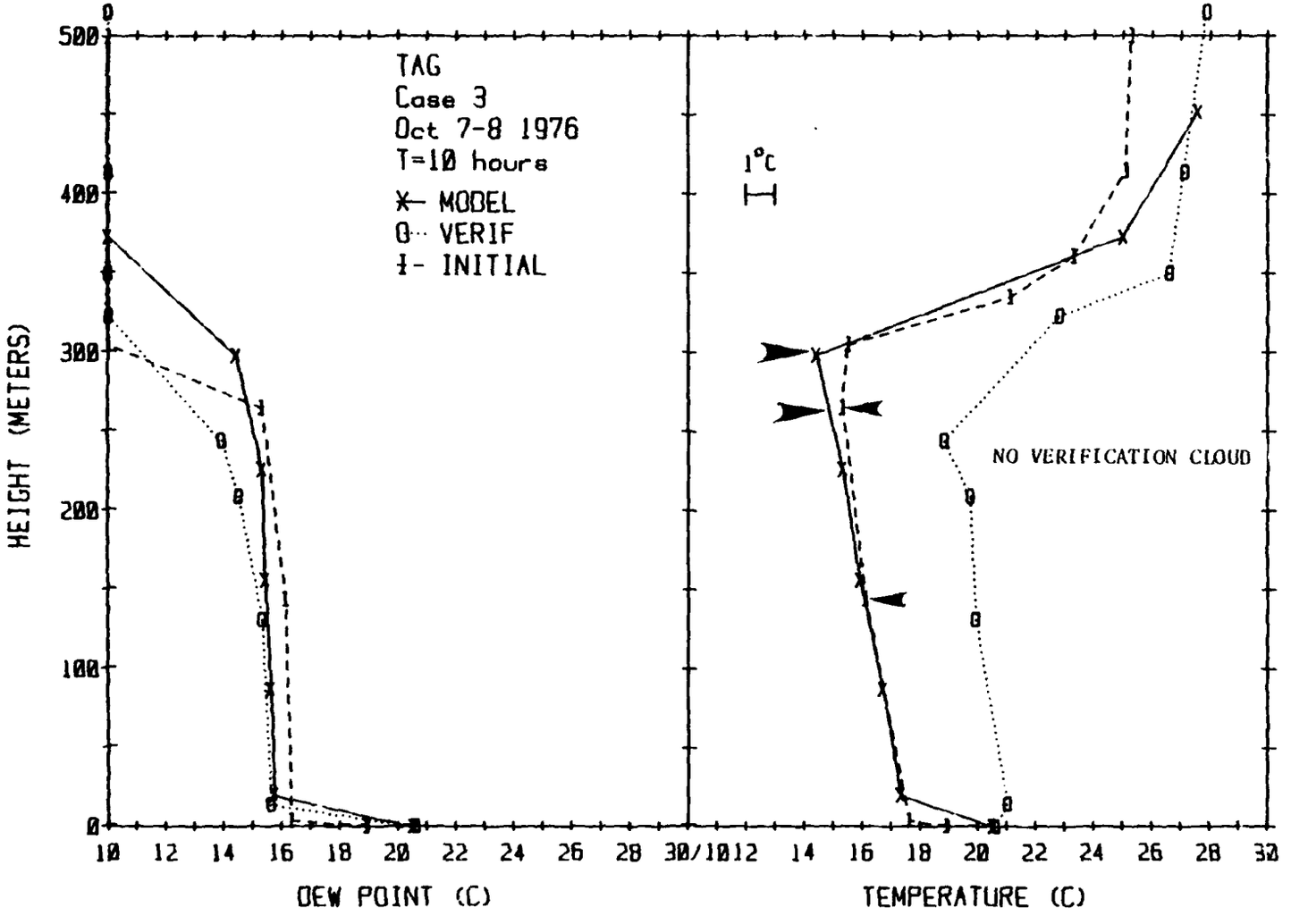
TAG
Case 3
Oct 7-8 1976
T=10 hours
MODEL
VERIF
INITIAL
1°C
NO VERIFICATION CLOUD
HEIGHT (METERS)
DEW POINT (C)
TEMPERATURE (C)
0
100
200
300
400
500
10 12 14 16 18 20 22 24 26 28 30/10 12 14 16 18 20 22 24 26 28 30

AD-A136 379 AN EVALUATION OF MARINE FOG FORECAST CONCEPTS AND A PRELIMINARY DESIGN FO..(U) ARVIN/CALSPAN ADVANCED TECHNOLOGY CENTER BUFFALO NY APPLIED T..

3/3

UNCLASSIFIED E J MACK ET AL. JUN 83 CALSPAN-6866-M-1 F/G 4/2 NL

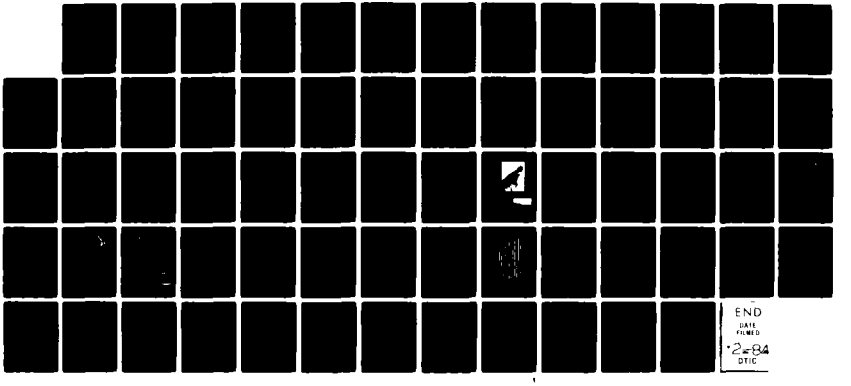

END

DATE FILMED

2-84

DTIC

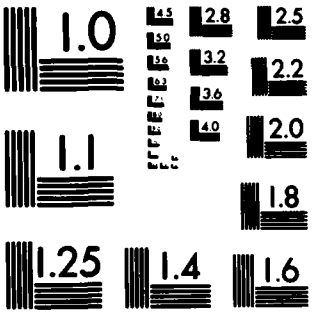

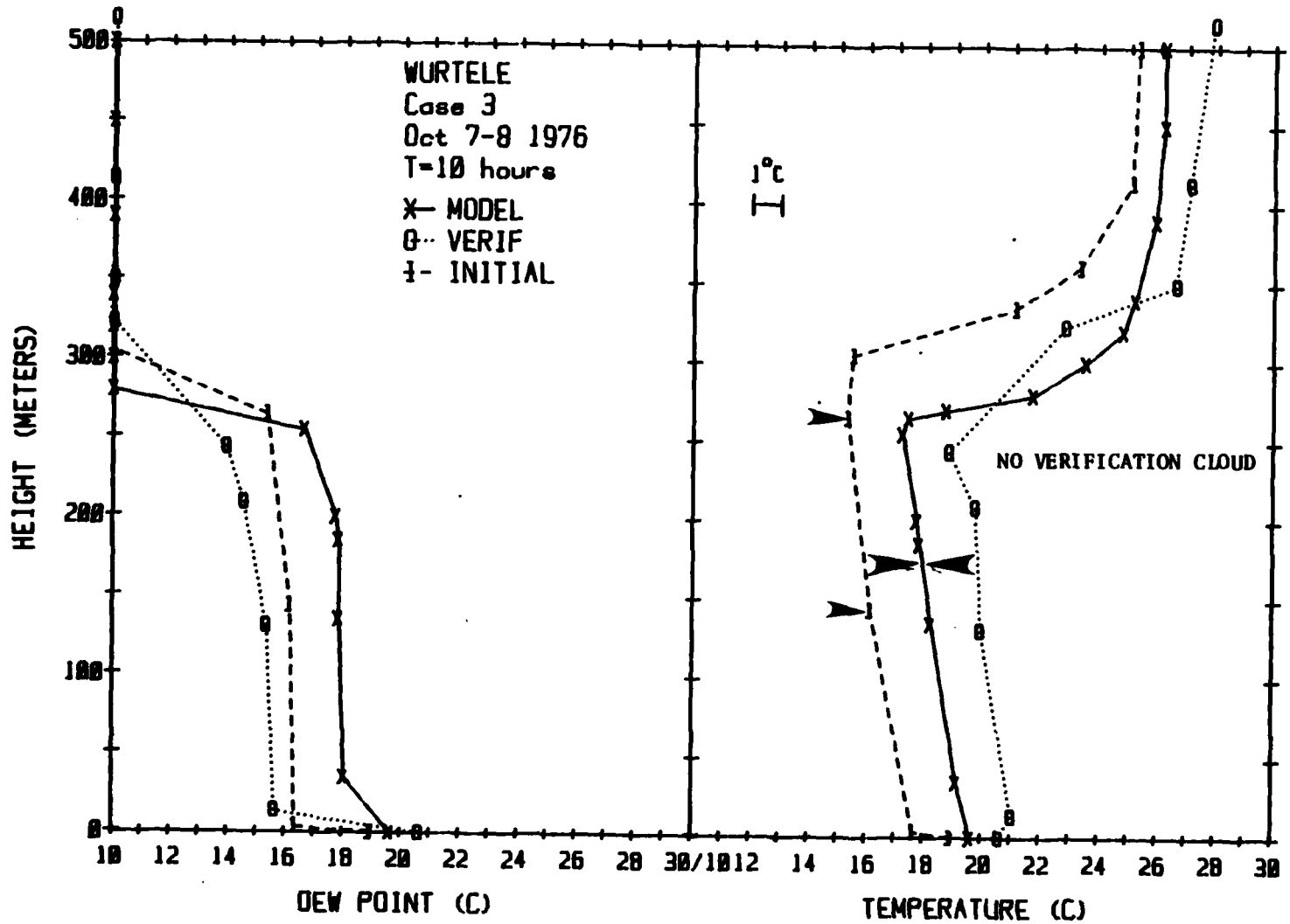
WURTELE
Case 3
Oct 7-8 1976
T=10 hours
X— MODEL
0·· VERIF
I- INITIAL
1°C
NO VERIFICATION CLOUD
HEIGHT (METERS)
500
400
300
200
100
0
10 12 14 16 18 20 22 24 26 28 30/10 12 14 16 18 20 22 24 26 28 30
DEW POINT (C)
TEMPERATURE (C)

CASE 3

(20 Hours)

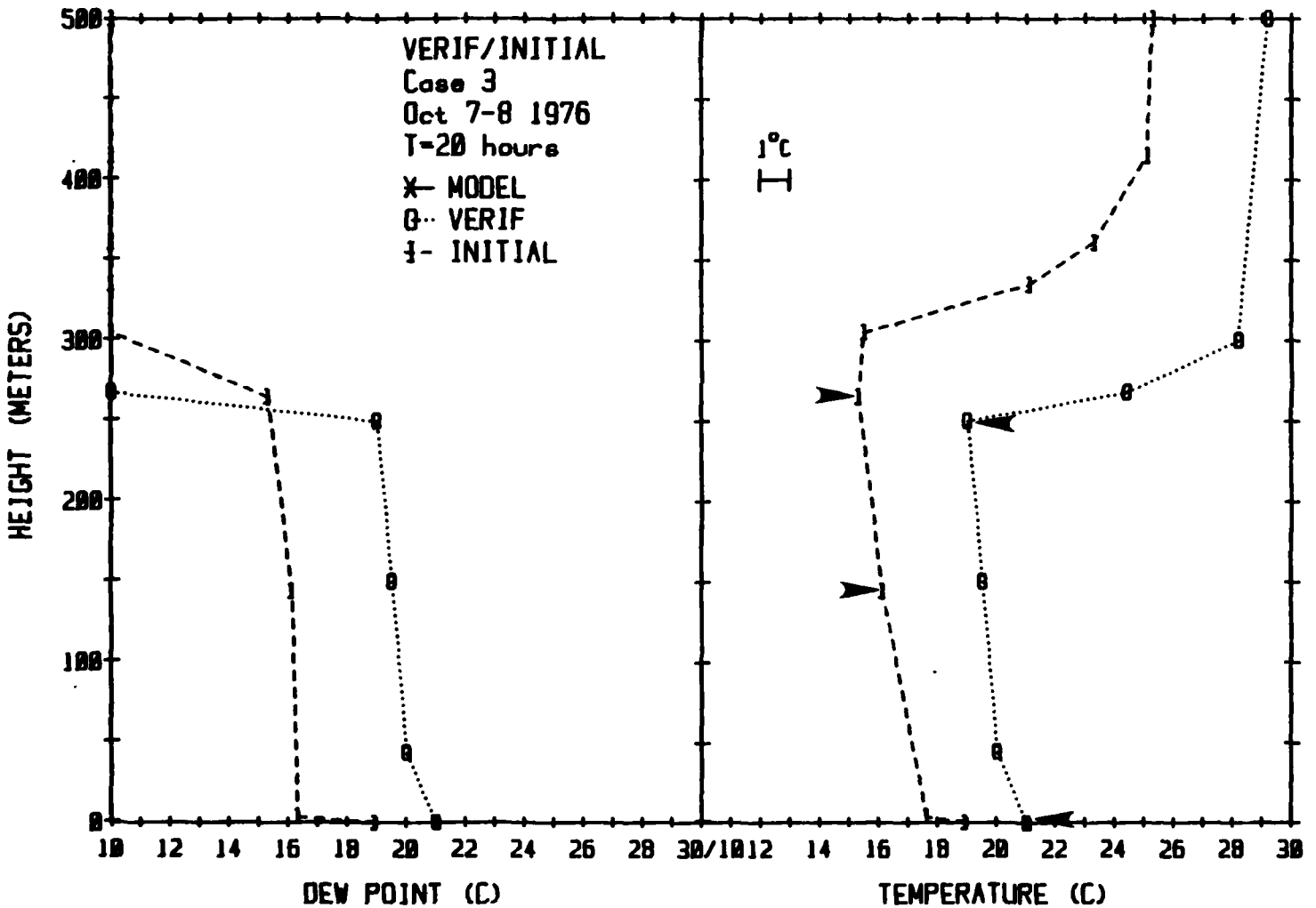
VERIF/INITIAL
Case 3
Oct 7-8 1976
T=20 hours
MODEL
VERIF
INITIAL
1°C
HEIGHT (METERS)
500
400
300
200
100
0
10 12 14 16 18 20 22 24 26 28 30/10 12 14 16 18 20 22 24 26 28 30
DEW POINT (C)
TEMPERATURE (C)

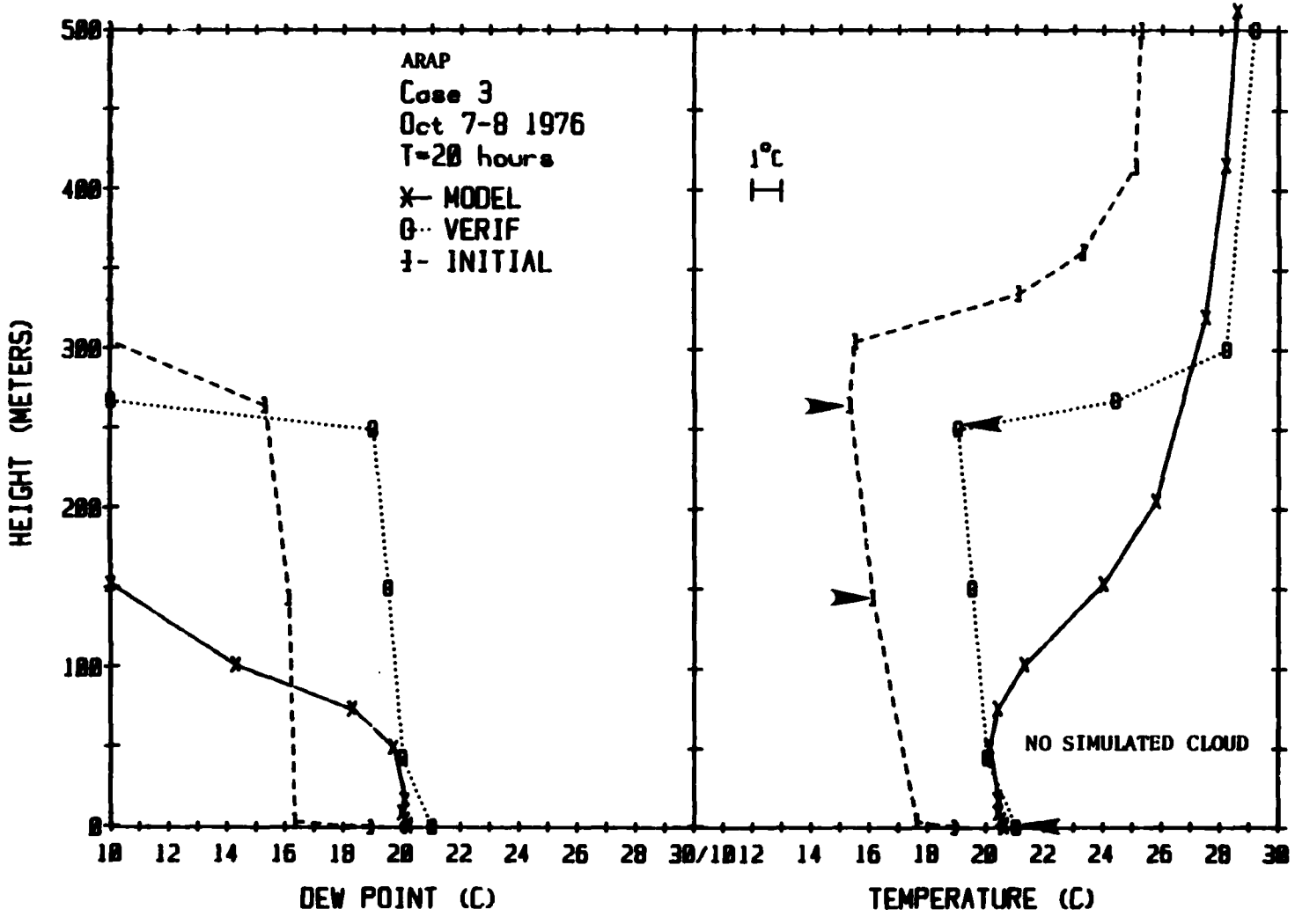
ARAP
Case 3
Oct 7-8 1976
T=20 hours
X- MODEL
0- VERIF
I- INITIAL
1°C
NO SIMULATED CLOUD
HEIGHT (METERS)
DEW POINT (C)
TEMPERATURE (C)
0
100
200
300
400
500
10 12 14 16 18 20 22 24 26 28 30/10 12 14 16 18 20 22 24 26 28 30

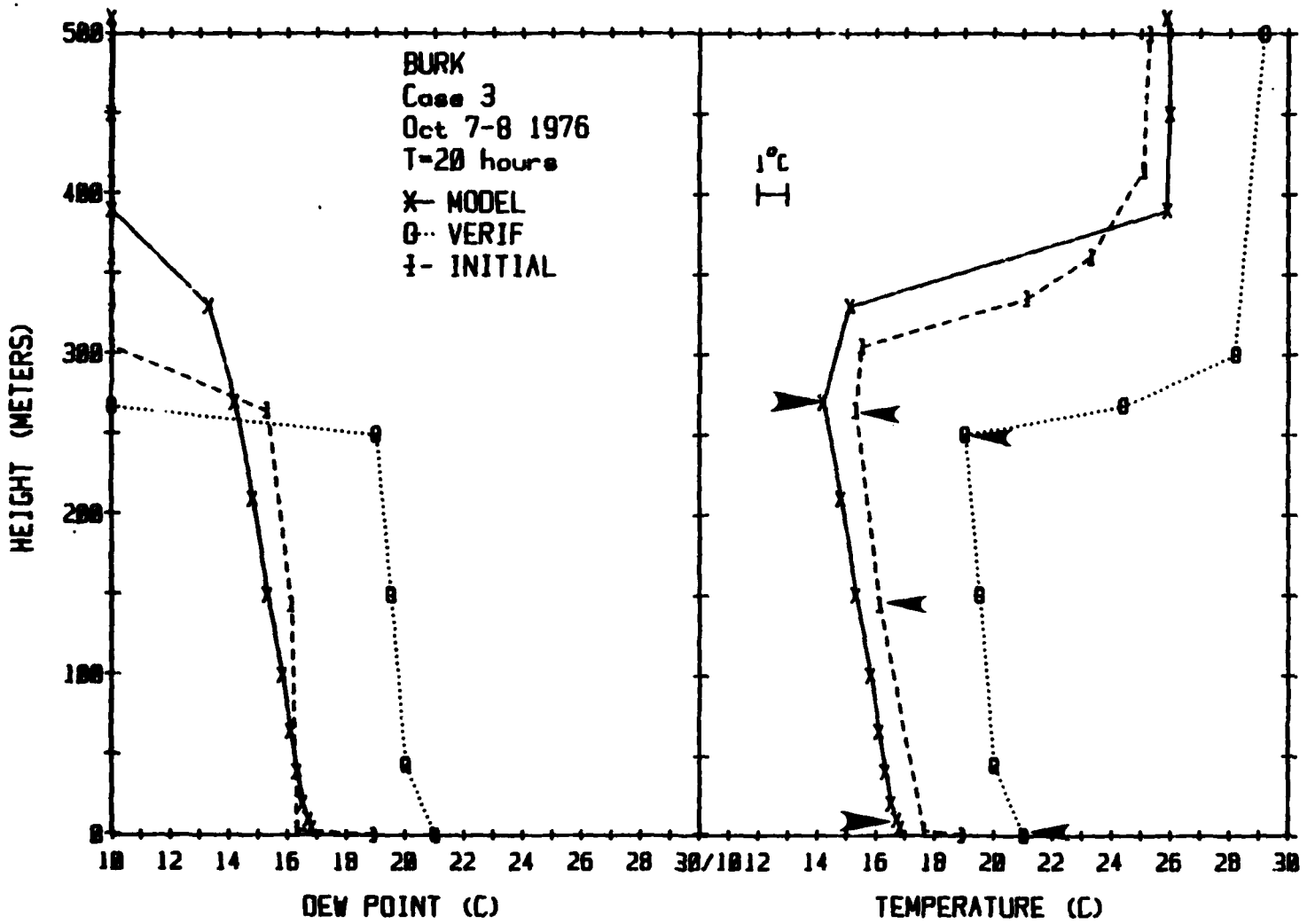
BURK
Case 3
Oct 7-8 1976
T=20 hours
X- MODEL
0- VERIF
I- INITIAL
1°C
HEIGHT (METERS)
500
400
300
200
100
0
10 12 14 16 18 20 22 24 26 28 30/10 12 14 16 18 20 22 24 26 28 30
DEW POINT (C)
TEMPERATURE (C)

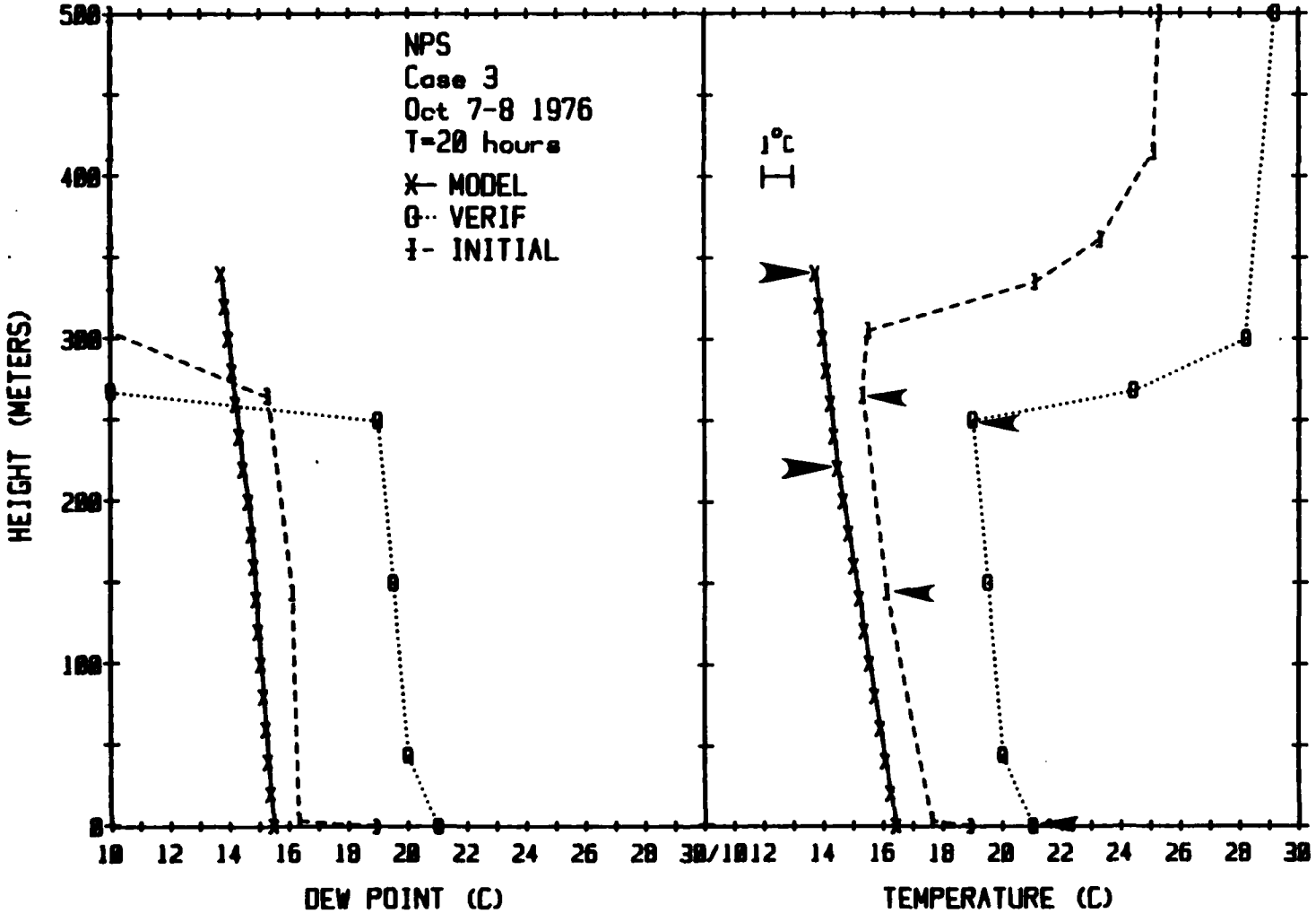
NPS
Case 3
Oct 7-8 1976
T=20 hours
X— MODEL
0·· VERIF
I- INITIAL
1°C
HEIGHT (METERS)
500
400
300
200
100
0
10 12 14 16 18 20 22 24 26 28 30/10 12 14 16 18 20 22 24 26 28 30
DEW POINT (C)
TEMPERATURE (C)

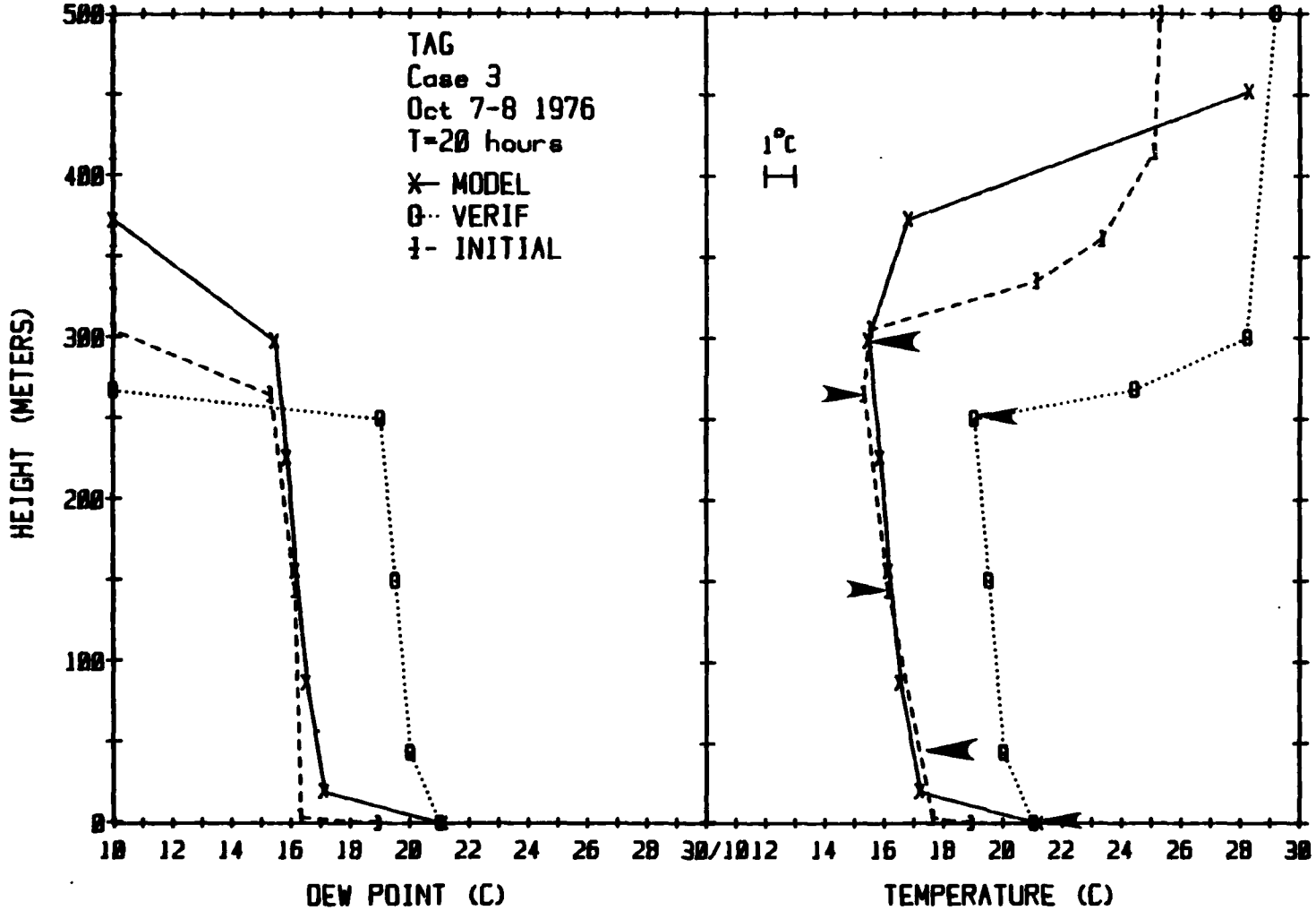
TAG
Case 3
Oct 7-8 1976
T=20 hours
MODEL
VERIF
INITIAL
1°C
HEIGHT (METERS)
500
400
300
200
100
0
10 12 14 16 18 20 22 24 26 28 30/10 12 14 16 18 20 22 24 26 28 30
DEW POINT (C)
TEMPERATURE (C)

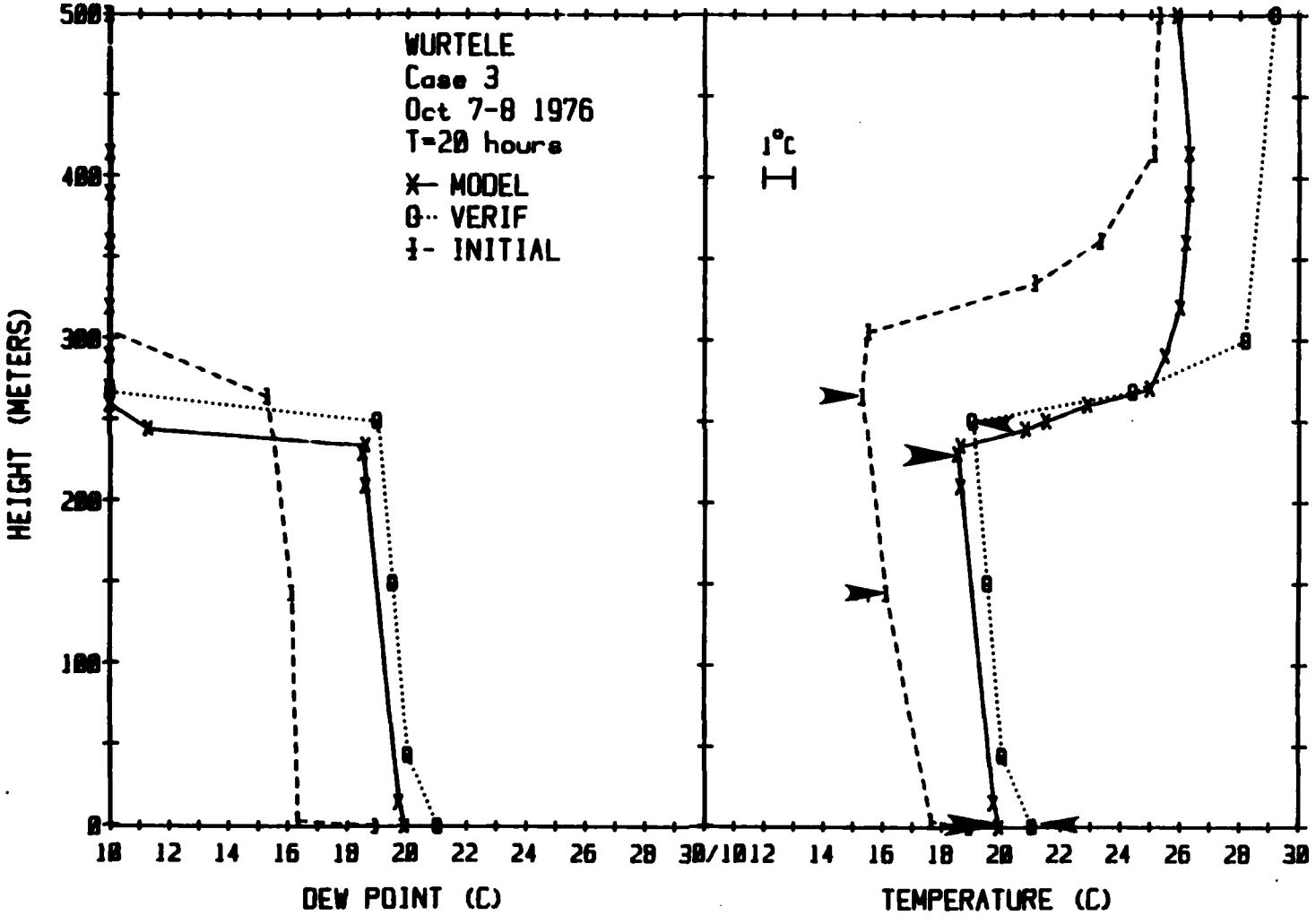
WURTELE
Case 3
Oct 7-8 1976
T=20 hours
X— MODEL
0·· VERIF
I- INITIAL
1°C
HEIGHT (METERS)
500
400
300
200
100
0
10 12 14 16 18 20 22 24 26 28 30/10 12 14 16 18 20 22 24 26 28 30
DEW POINT (C)
TEMPERATURE (C)

CASE 4

July 14-15, 1973

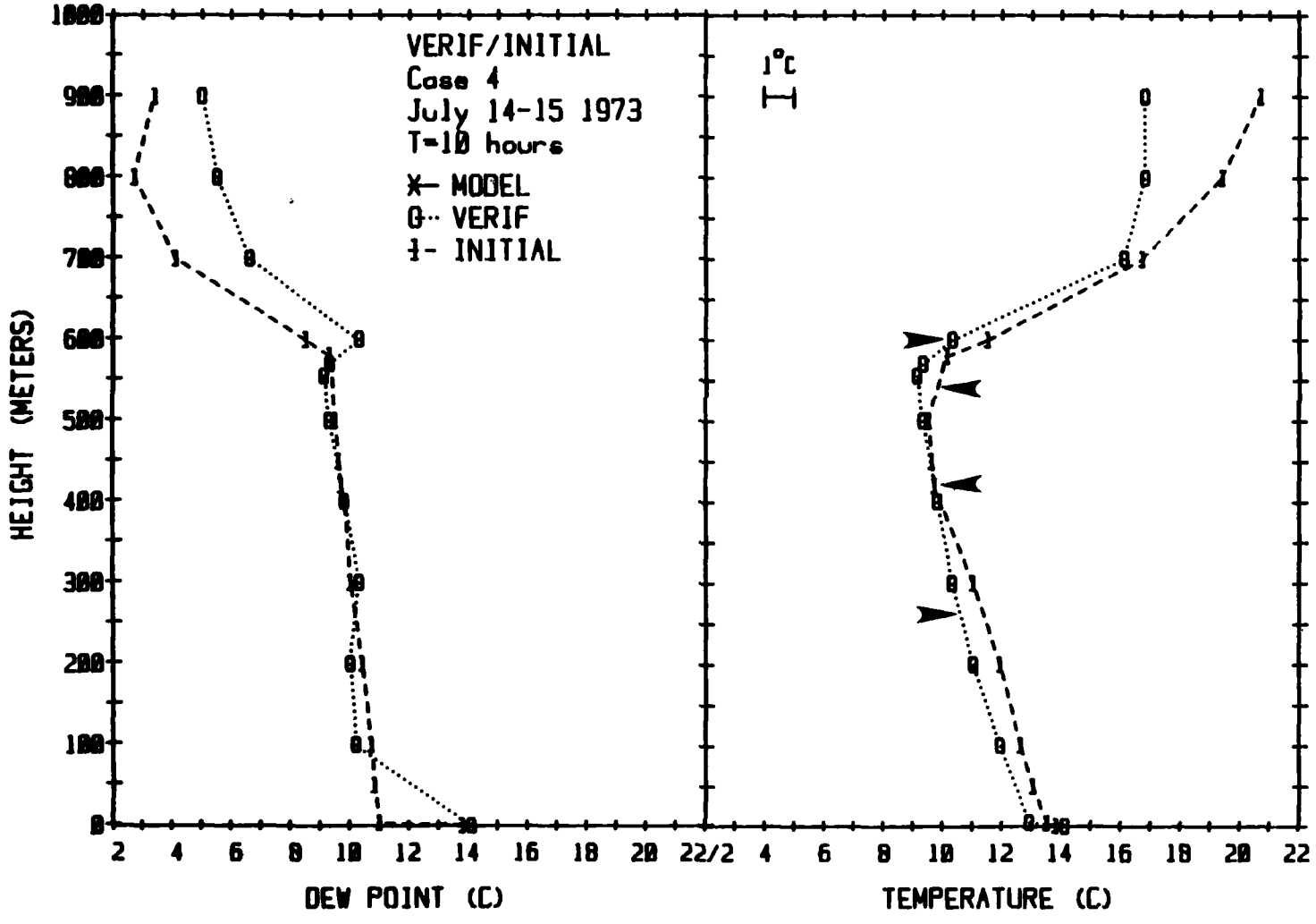
VERIF/INITIAL
Case 4
July 14-15 1973
T=10 hours
X— MODEL
0·· VERIF
I- INITIAL
1°C
HEIGHT (METERS)
DEW POINT (C)
TEMPERATURE (C)

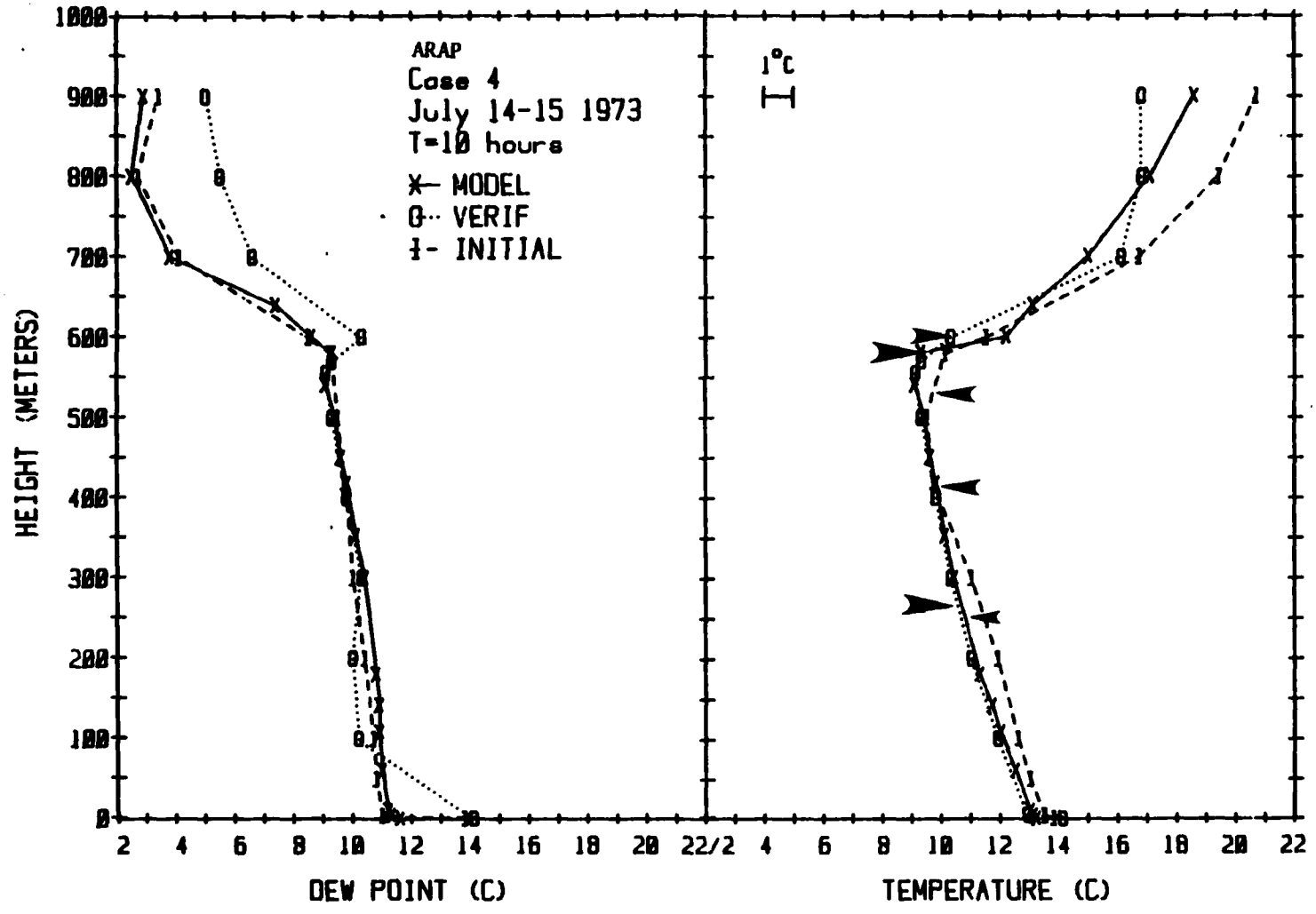
ARAP
Case 4
July 14-15 1973
T=10 hours
MODEL
VERIF
INITIAL
1°C
HEIGHT (METERS)
DEW POINT (C)
TEMPERATURE (C)
1000
900
800
700
600
500
400
300
200
100
0
2 4 6 8 10 12 14 16 18 20 22/2
4 6 8 10 12 14 16 18 20 22

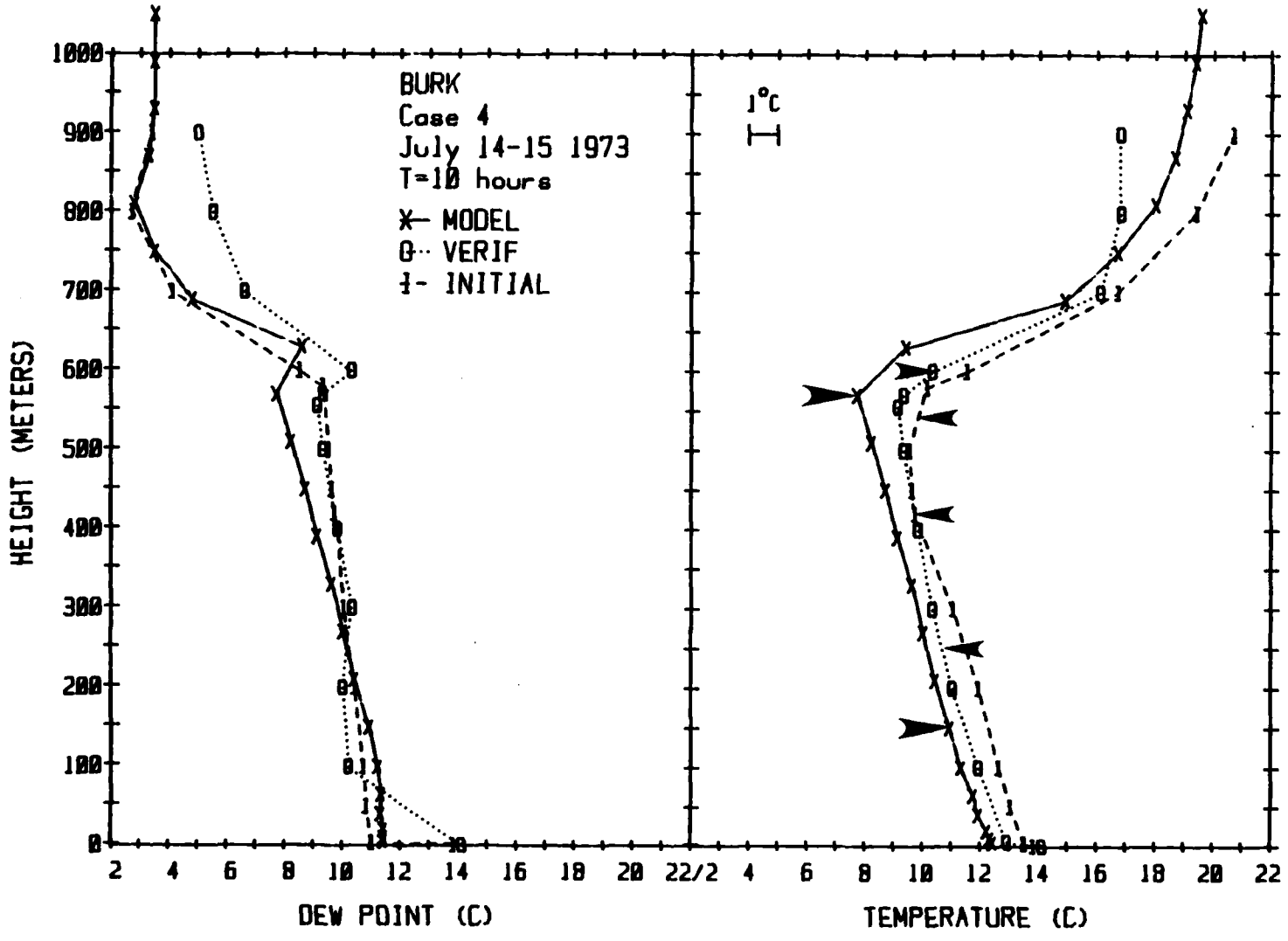
BURK
Case 4
July 14-15 1973
T=10 hours
MODEL
VERIF
INITIAL
1°C
HEIGHT (METERS)
1000
900
800
700
600
500
400
300
200
100
0
2 4 6 8 10 12 14 16 18 20 22/2 4 6 8 10 12 14 16 18 20 22
DEW POINT (C)
TEMPERATURE (C)

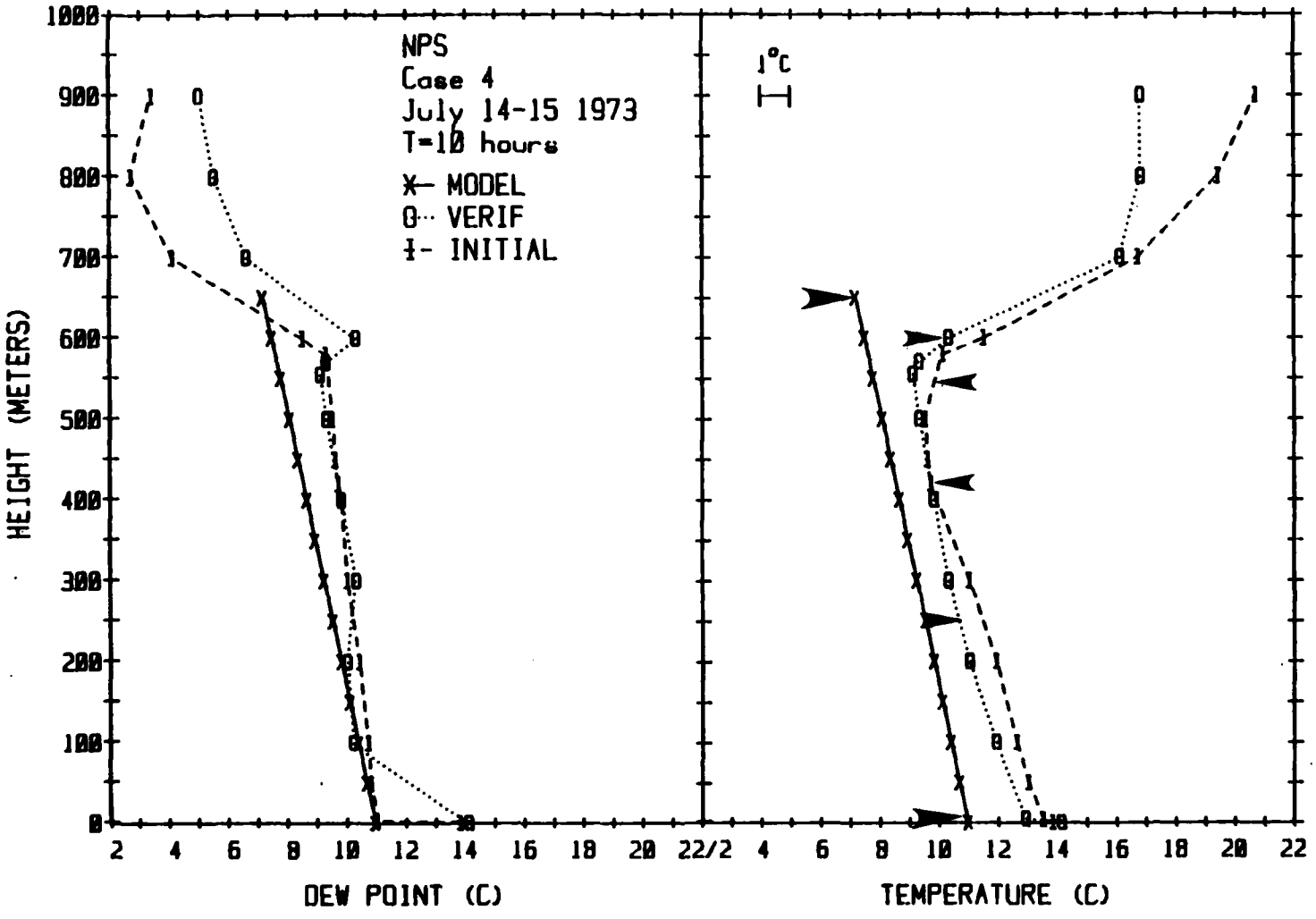
NPS
Case 4
July 14-15 1973
T=10 hours
X— MODEL
0··· VERIF
I- INITIAL
1°C
HEIGHT (METERS)
1000
900
800
700
600
500
400
300
200
100
0
2 4 6 8 10 12 14 16 18 20 22/2 4 6 8 10 12 14 16 18 20 22
DEW POINT (C)
TEMPERATURE (C)

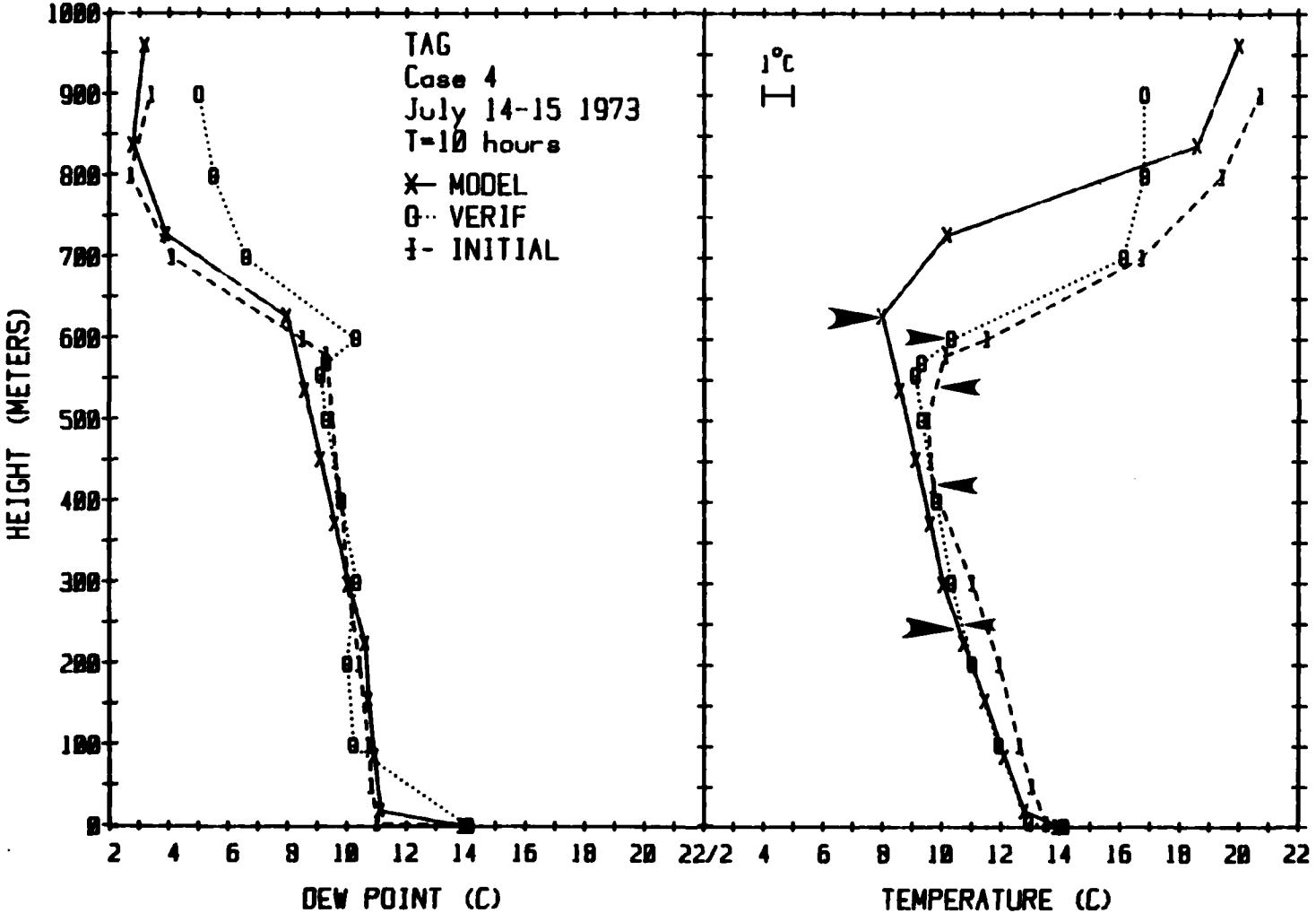
TAG
Case 4
July 14-15 1973
T=10 hours
X— MODEL
O··· VERIF
I- INITIAL
1°C
HEIGHT (METERS)
1000
900
800
700
600
500
400
300
200
100
0
2 4 6 8 10 12 14 16 18 20 22/2 4 6 8 10 12 14 16 18 20 22
DEW POINT (C)
TEMPERATURE (C)

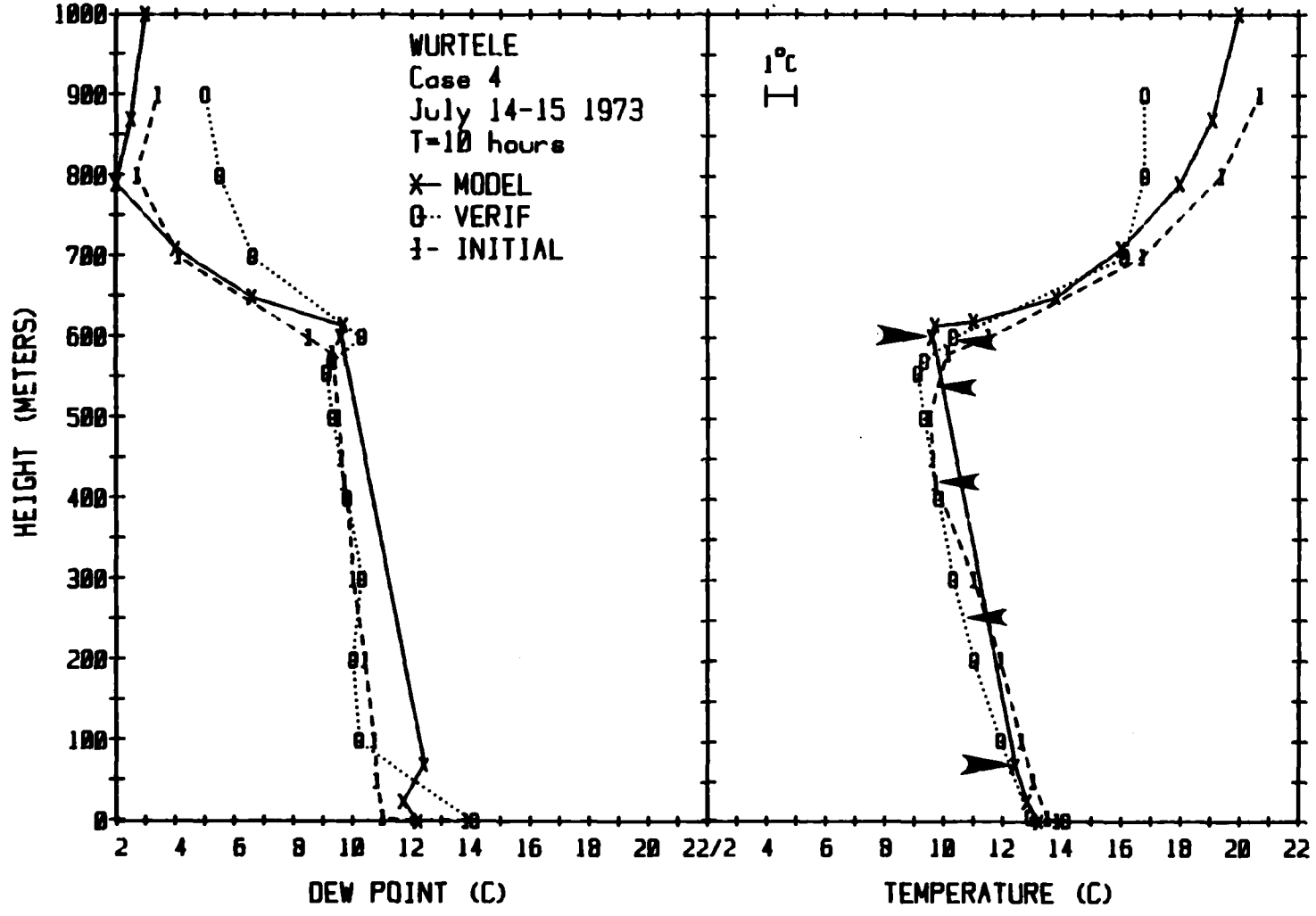
WURTELE
Case 4
July 14-15 1973
T=10 hours
MODEL
VERIF
INITIAL
1°C
HEIGHT (METERS)
DEW POINT (C)
TEMPERATURE (C)
1000
900
800
700
600
500
400
300
200
100
0
2 4 6 8 10 12 14 16 18 20 22/2
4 6 8 10 12 14 16 18 20 22

CASE 5

August 5, 1975

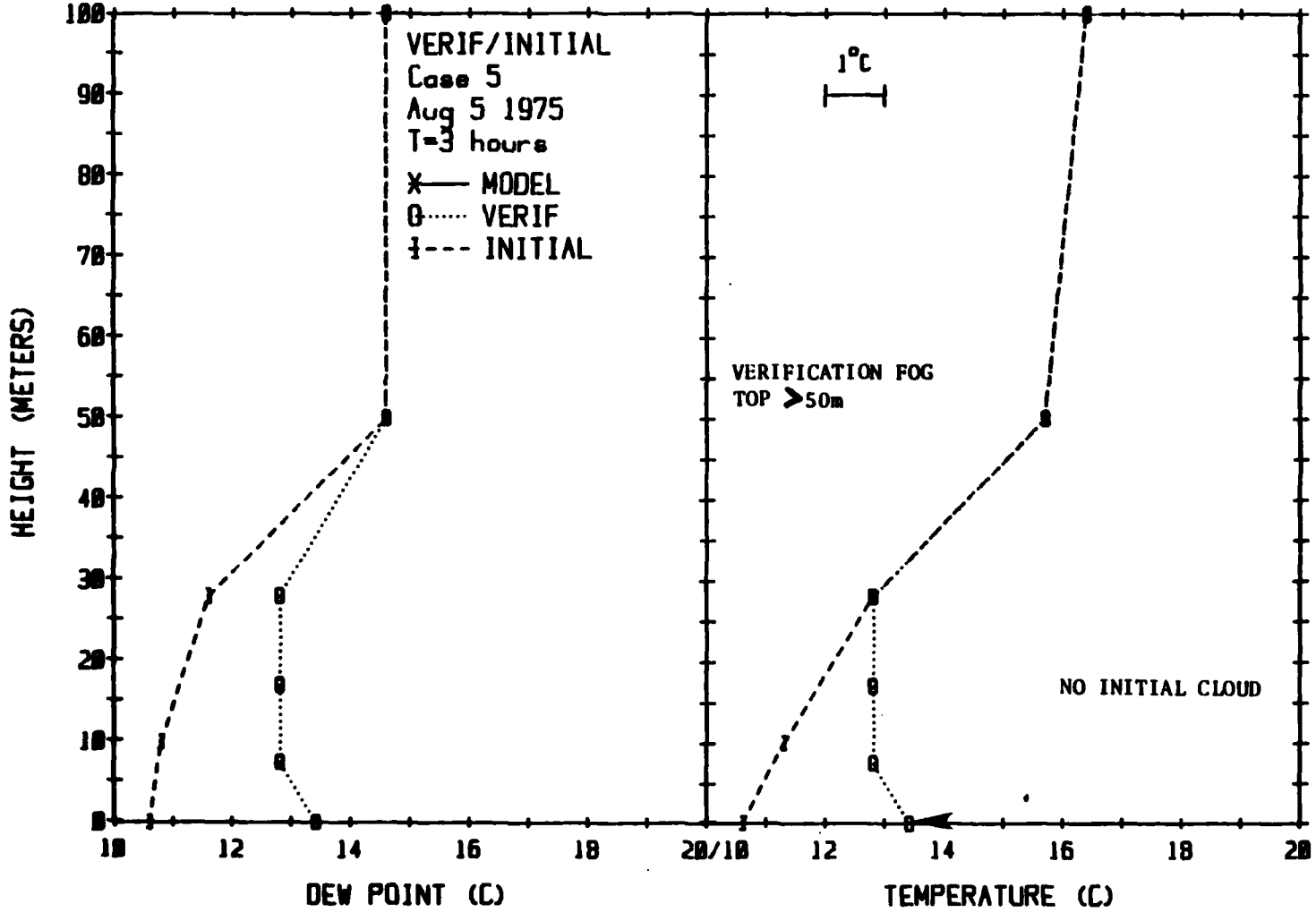
VERIF/INITIAL
Case 5
Aug 5 1975
T=3 hours
MODEL
VERIF
INITIAL
1°C
VERIFICATION FOG
TOP >50m
NO INITIAL CLOUD
HEIGHT (METERS)
DEW POINT (C)
TEMPERATURE (C)
100
90
80
70
60
50
40
30
20
10
0
10
12
14
16
18
20/10
12
14
16
18
20

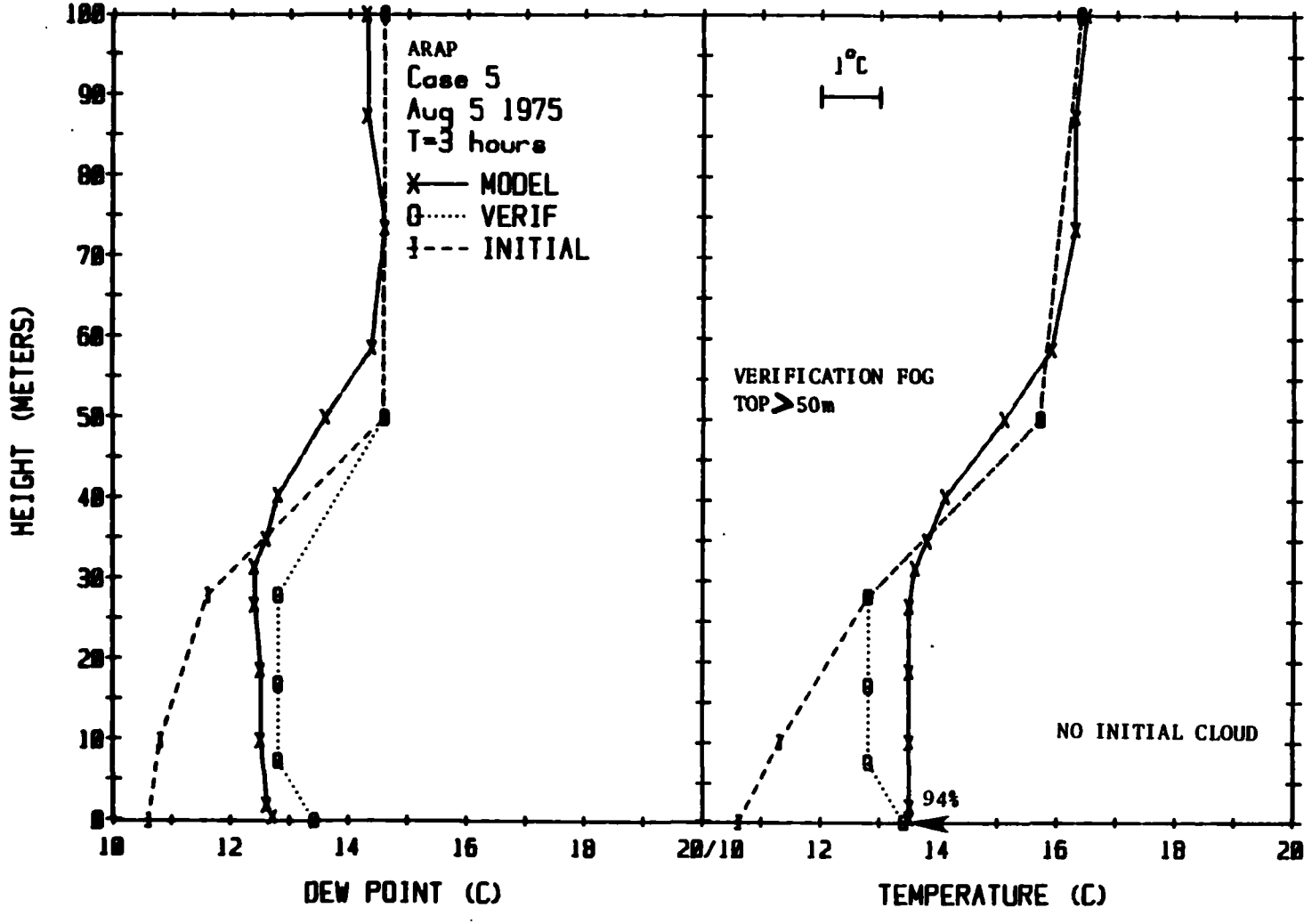
ARAP
Case 5
Aug 5 1975
T=3 hours
MODEL
VERIF
INITIAL
1°C
VERIFICATION FOG
TOP > 50m
NO INITIAL CLOUD
94%
HEIGHT (METERS)
DEW POINT (C)
TEMPERATURE (C)
100
90
80
70
60
50
40
30
20
10
0
10
12
14
16
18
20/10
20

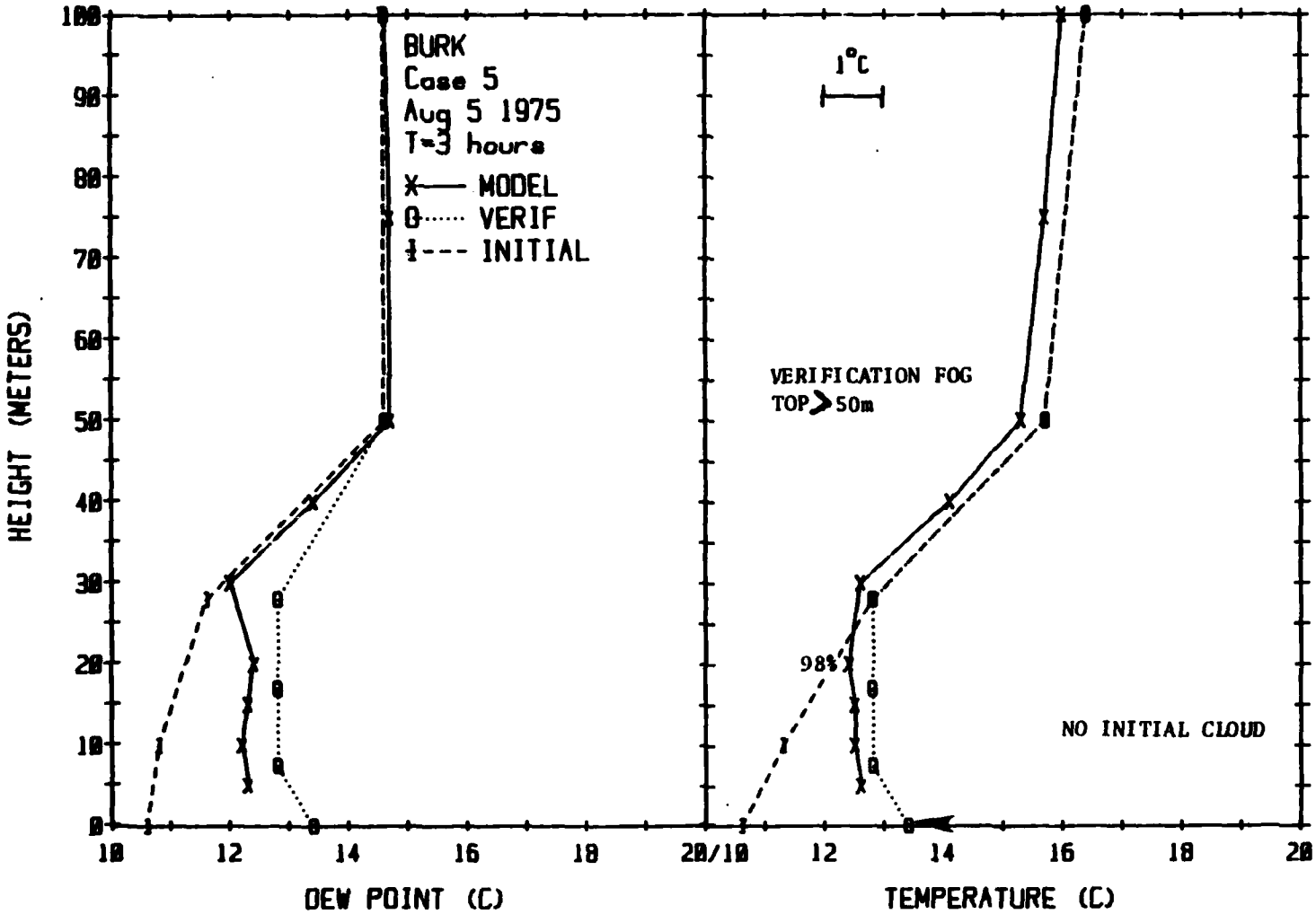
BURK
Case 5
Aug 5 1975
T=3 hours
MODEL
VERIF
INITIAL
1°C
VERIFICATION FOG
TOP > 50m
98%
NO INITIAL CLOUD
HEIGHT (METERS)
DEW POINT (C)
TEMPERATURE (C)
100
90
80
70
60
50
40
30
20
10
0
10
12
14
16
18
20/10
20

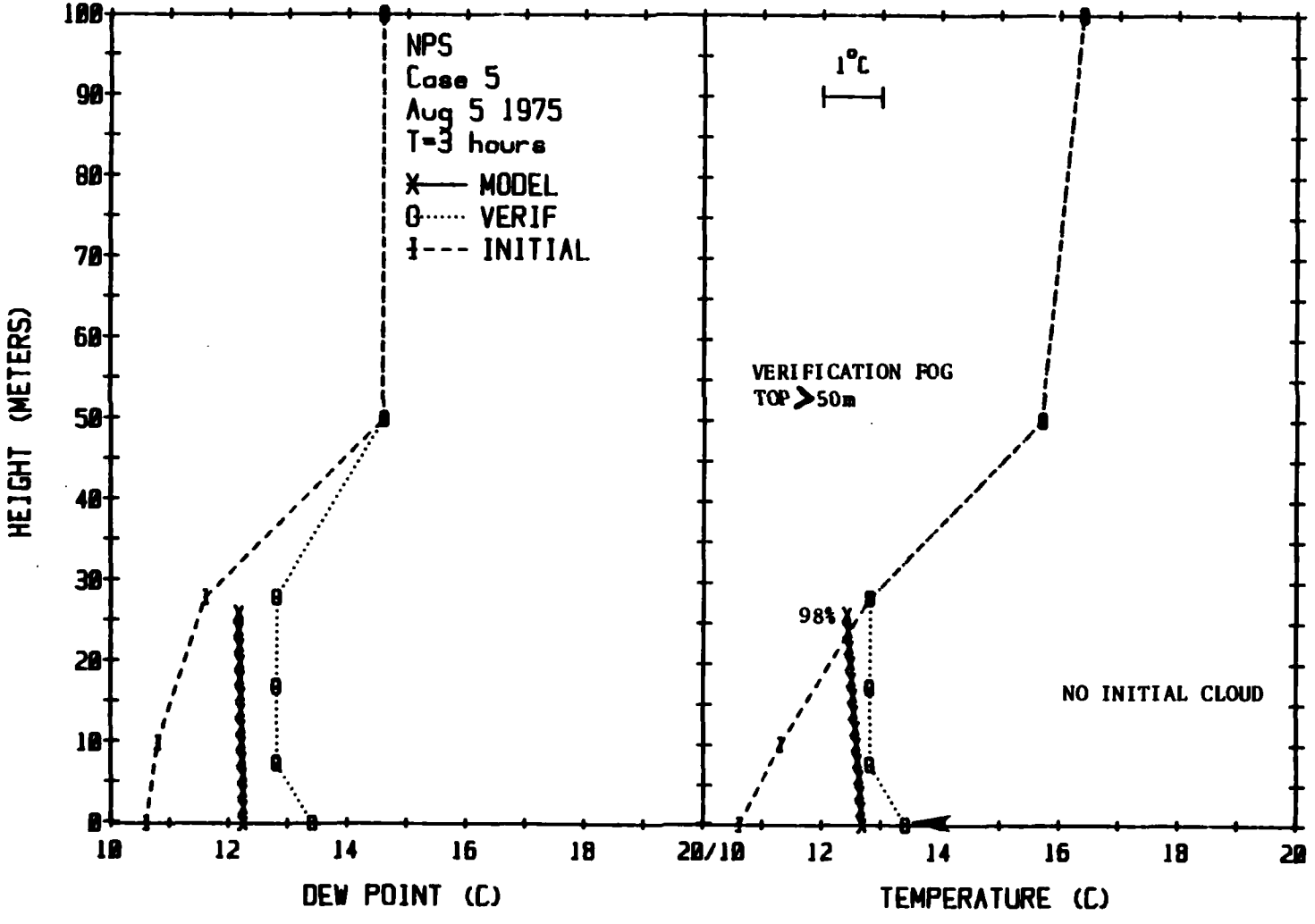
NPS
Case 5
Aug 5 1975
T=3 hours
X—— MODEL
0····· VERIF
I--- INITIAL
1°C
VERIFICATION FOG
TOP >50m
98%
NO INITIAL CLOUD
HEIGHT (METERS)
DEW POINT (C)
TEMPERATURE (C)
100
90
80
70
60
50
40
30
20
10
0
10
12
14
16
18
20/10
12
14
16
18
20

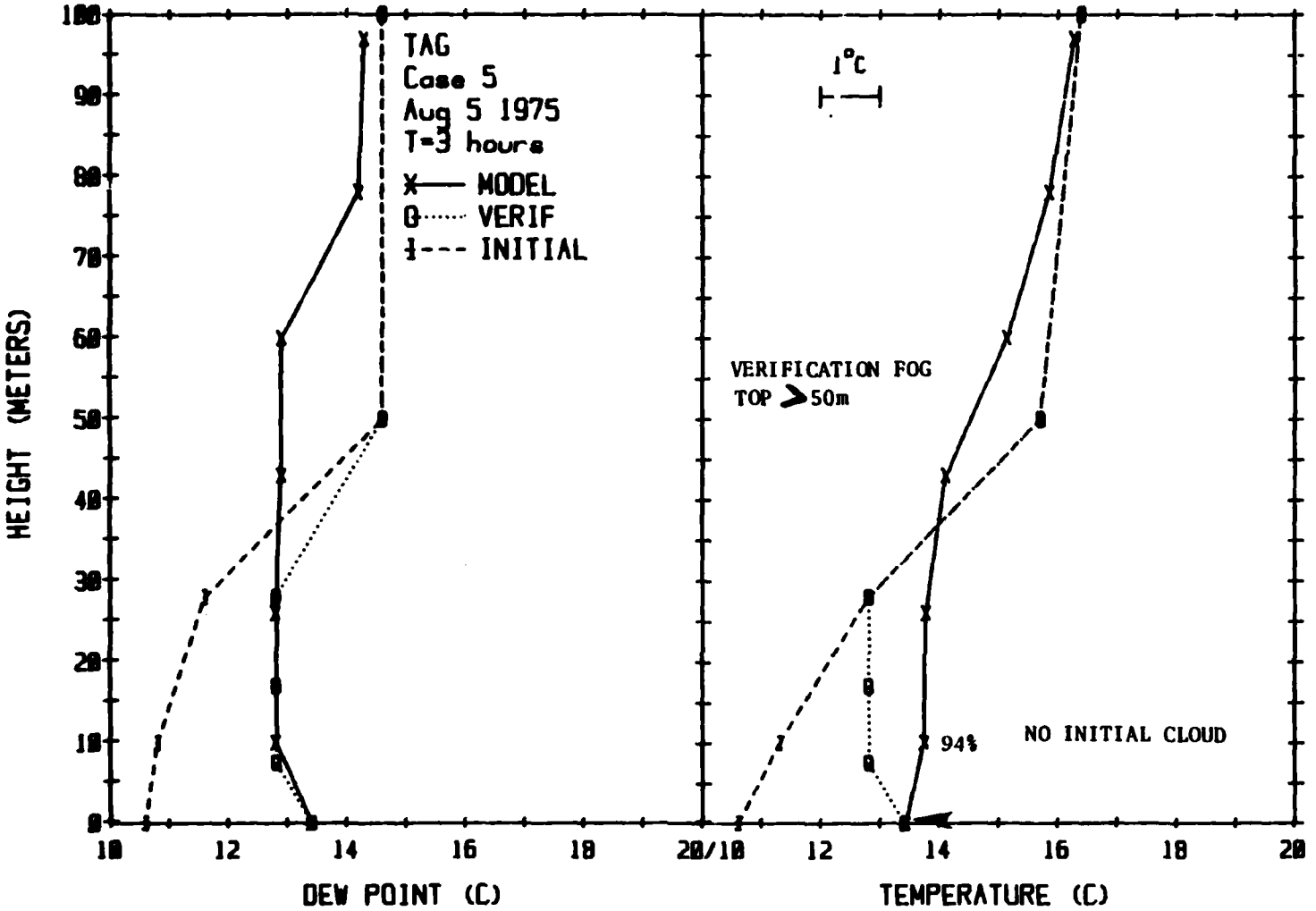
TAG
Case 5
Aug 5 1975
T=3 hours
MODEL
VERIF
INITIAL
1°C
VERIFICATION FOG
TOP >50m
94%
NO INITIAL CLOUD
HEIGHT (METERS)
DEW POINT (C)
TEMPERATURE (C)
10
12
14
16
18
20/10
20

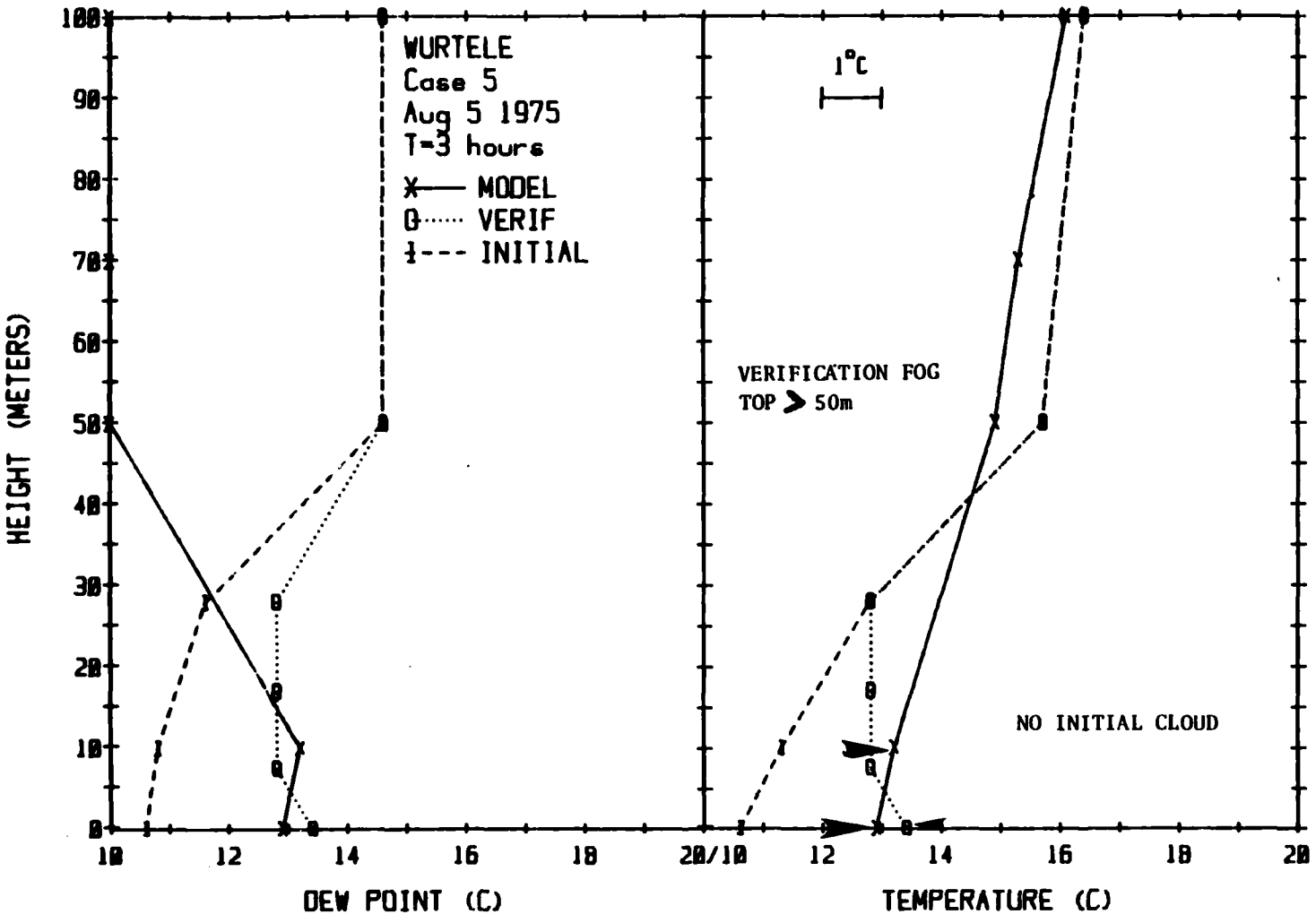
WURTELE
Case 5
Aug 5 1975
T=3 hours
MODEL
VERIF
INITIAL
1°C
VERIFICATION FOG
TOP > 50m
NO INITIAL CLOUD
HEIGHT (METERS)
DEW POINT (C)
TEMPERATURE (C)
100
90
80
70
60
50
40
30
20
10
0
10
12
14
16
18
20/10
20

CASE 6

August 29, 1972

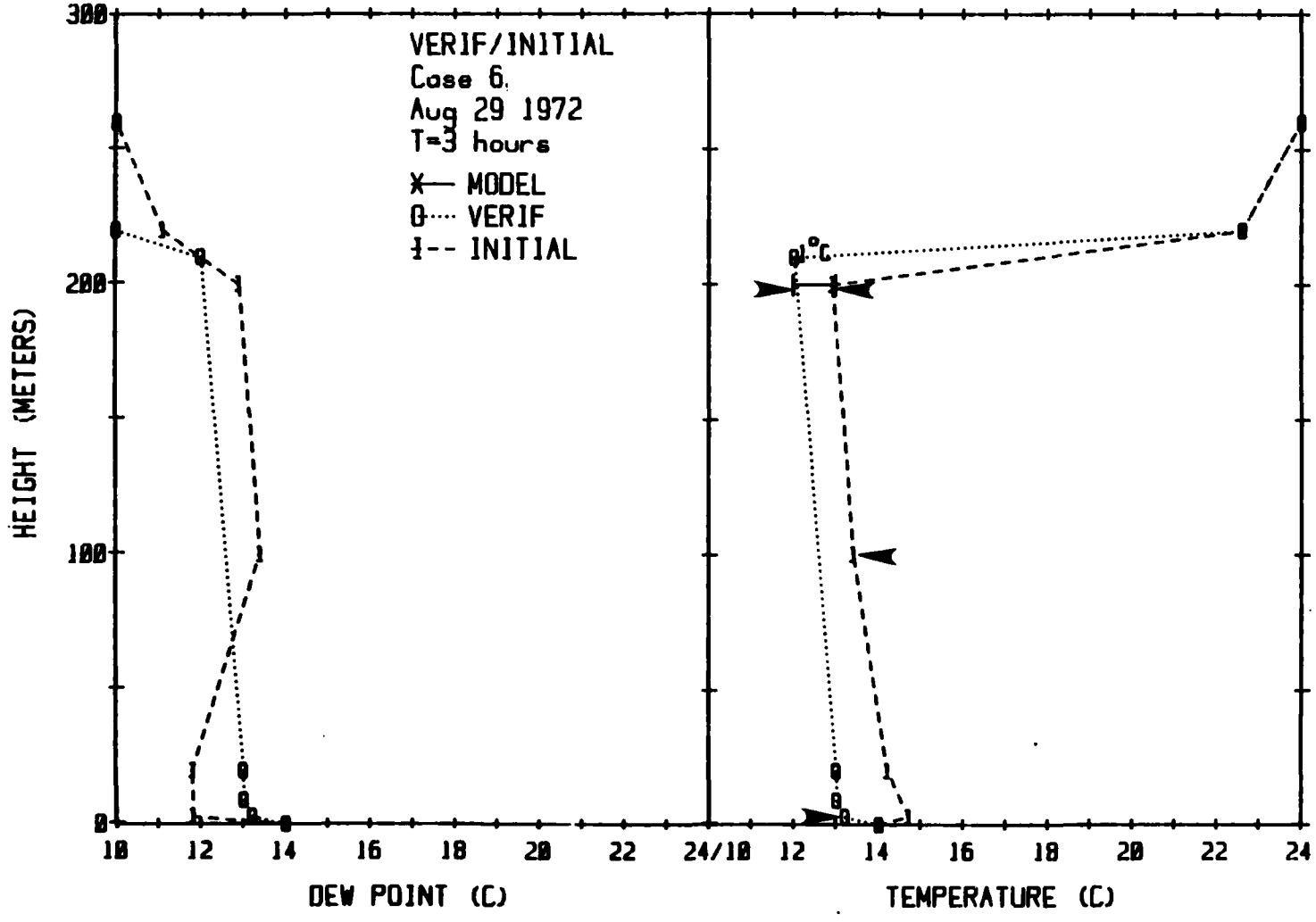
VERIF/INITIAL
Case 6.
Aug 29 1972
T=3 hours
MODEL
VERIF
INITIAL
HEIGHT (METERS)
300
200
100
0
10
12
14
16
18
20
22
24/10
12
14
16
18
20
22
24
DEW POINT (C)
TEMPERATURE (C)

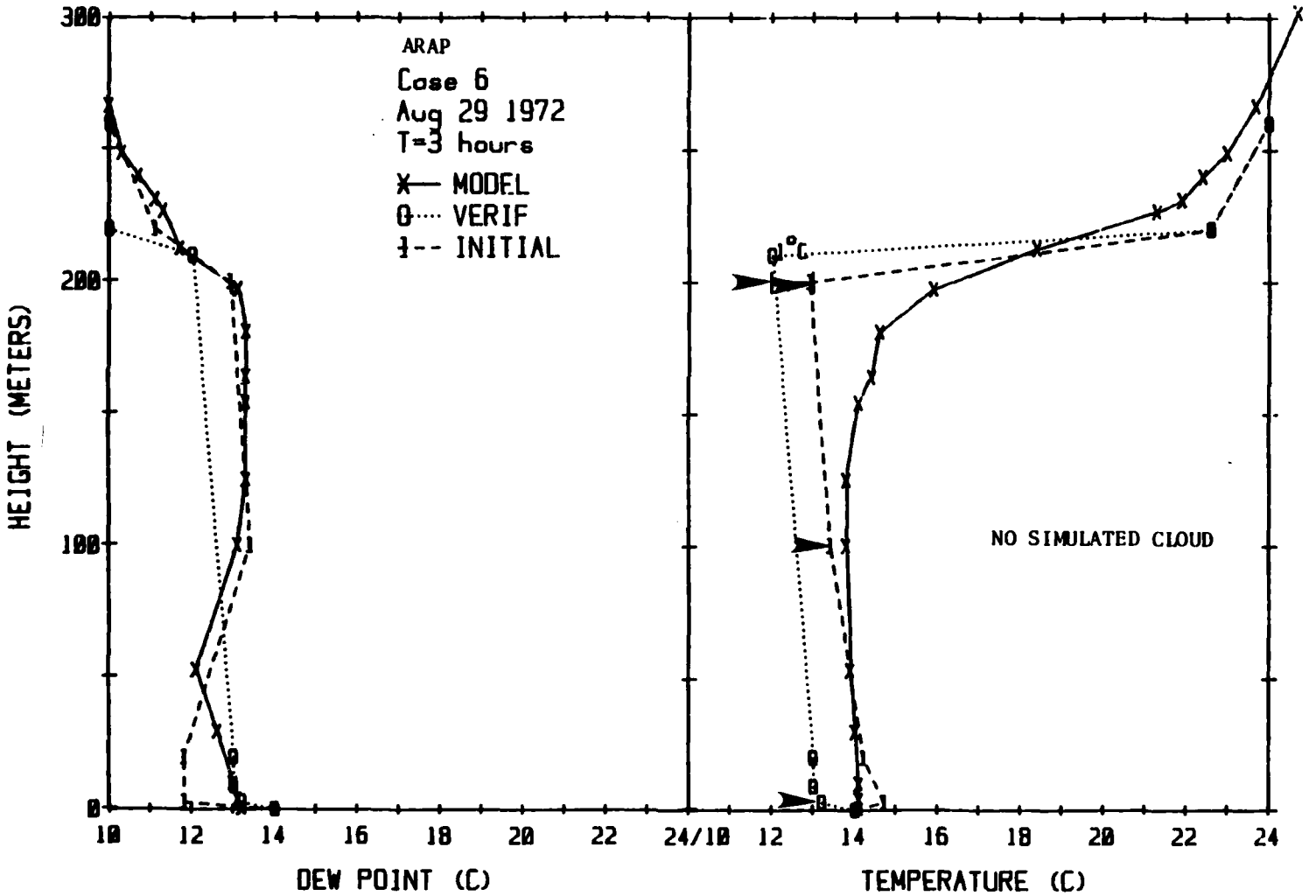
ARAP
Case 6
Aug 29 1972
T=3 hours
MODEL
VERIF
INITIAL
HEIGHT (METERS)
300
200
100
0
10
12
14
16
18
20
22
24/10
12
14
16
18
20
22
24
DEW POINT (C)
TEMPERATURE (C)
0°C
NO SIMULATED CLOUD

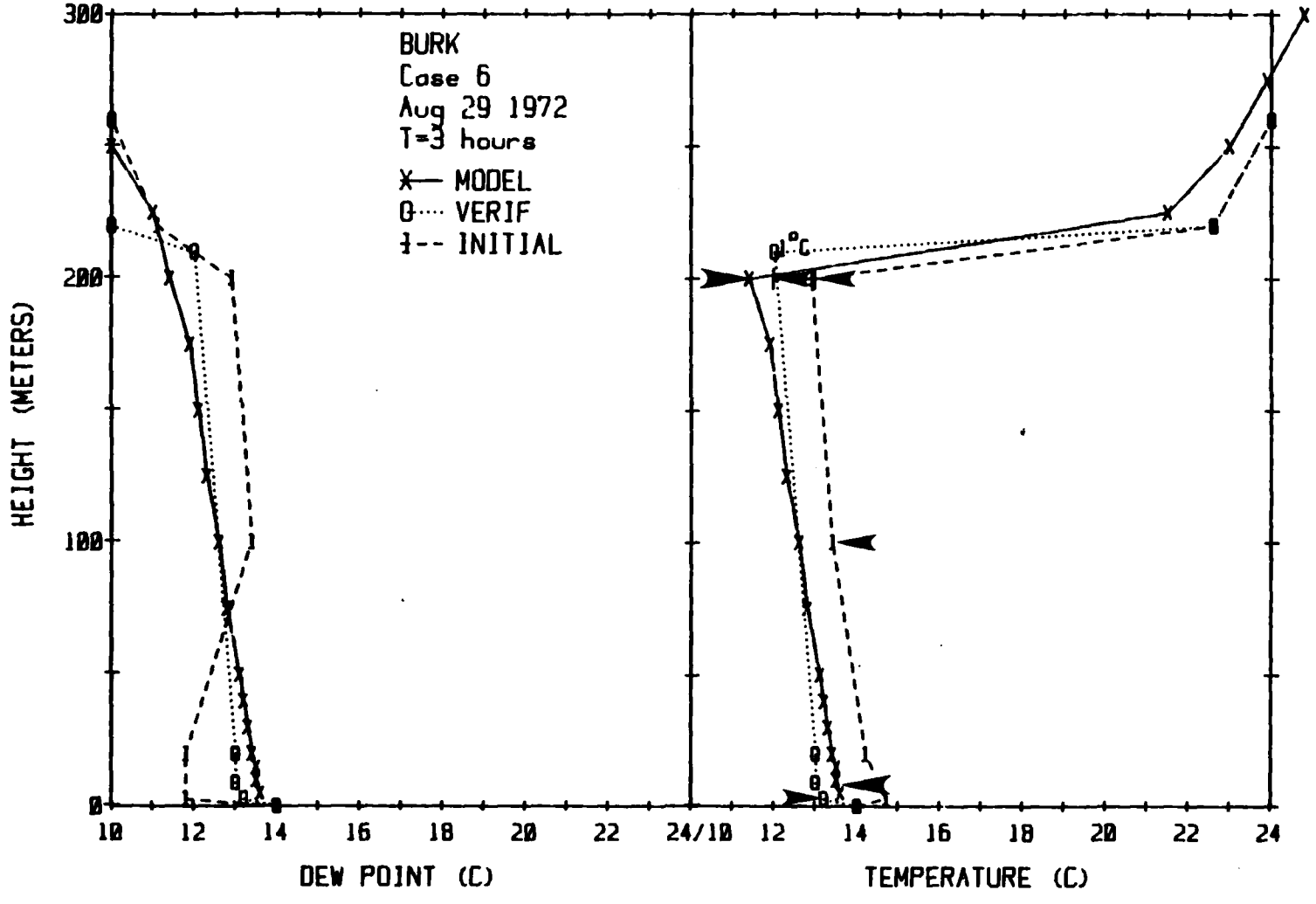
BURK
Case 6
Aug 29 1972
T=3 hours
MODEL
VERIF
INITIAL
HEIGHT (METERS)
300
200
100
0
10
12
14
16
18
20
22
24/10
12
14
16
18
20
22
24
DEW POINT (C)
TEMPERATURE (C)
0°C

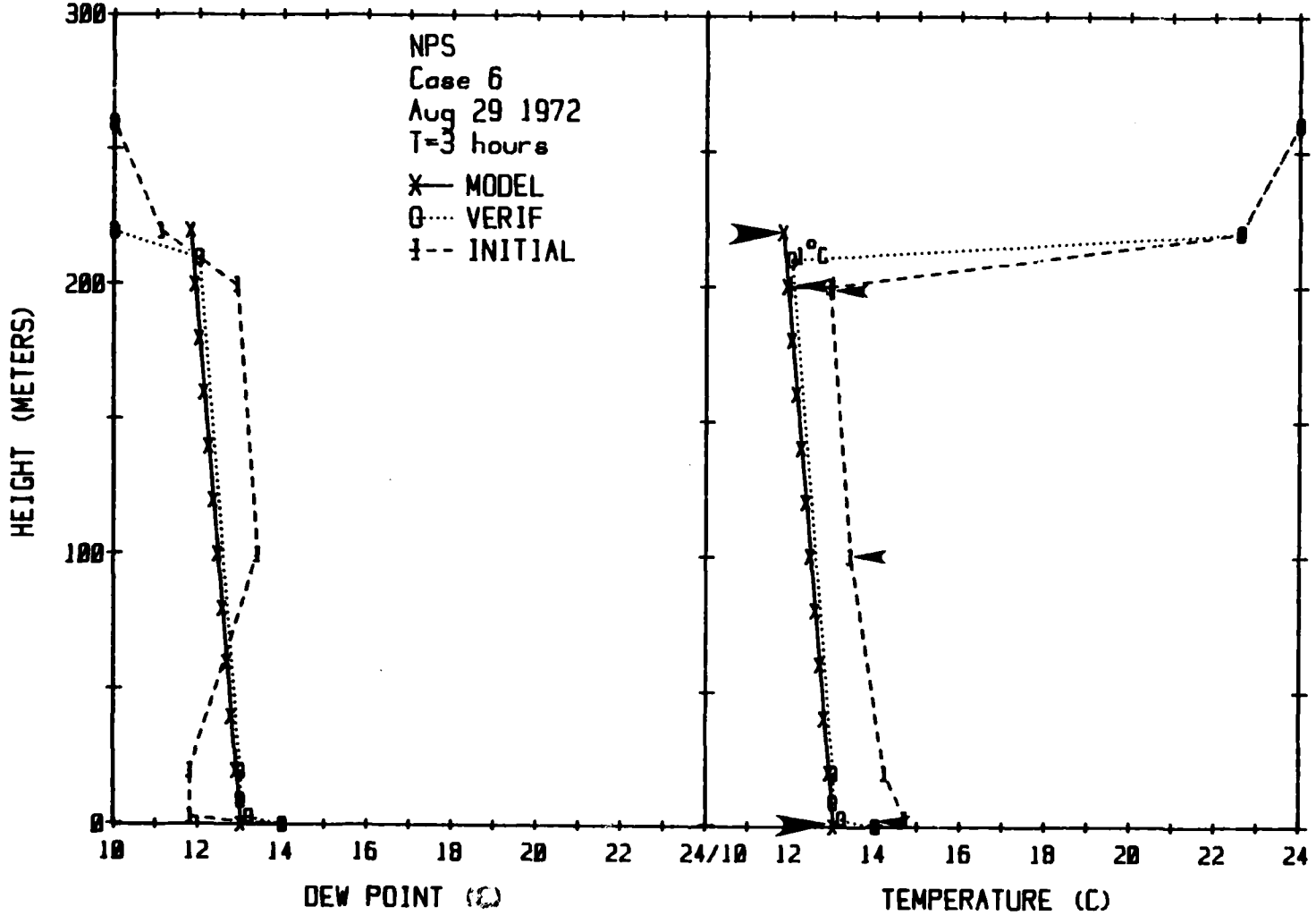
NPS
Case 6
Aug 29 1972
T=3 hours
MODEL
VERIF
INITIAL
HEIGHT (METERS)
300
200
100
0
10
12
14
16
18
20
22
24/10
12
14
16
18
20
22
24
DEW POINT (C)
TEMPERATURE (C)

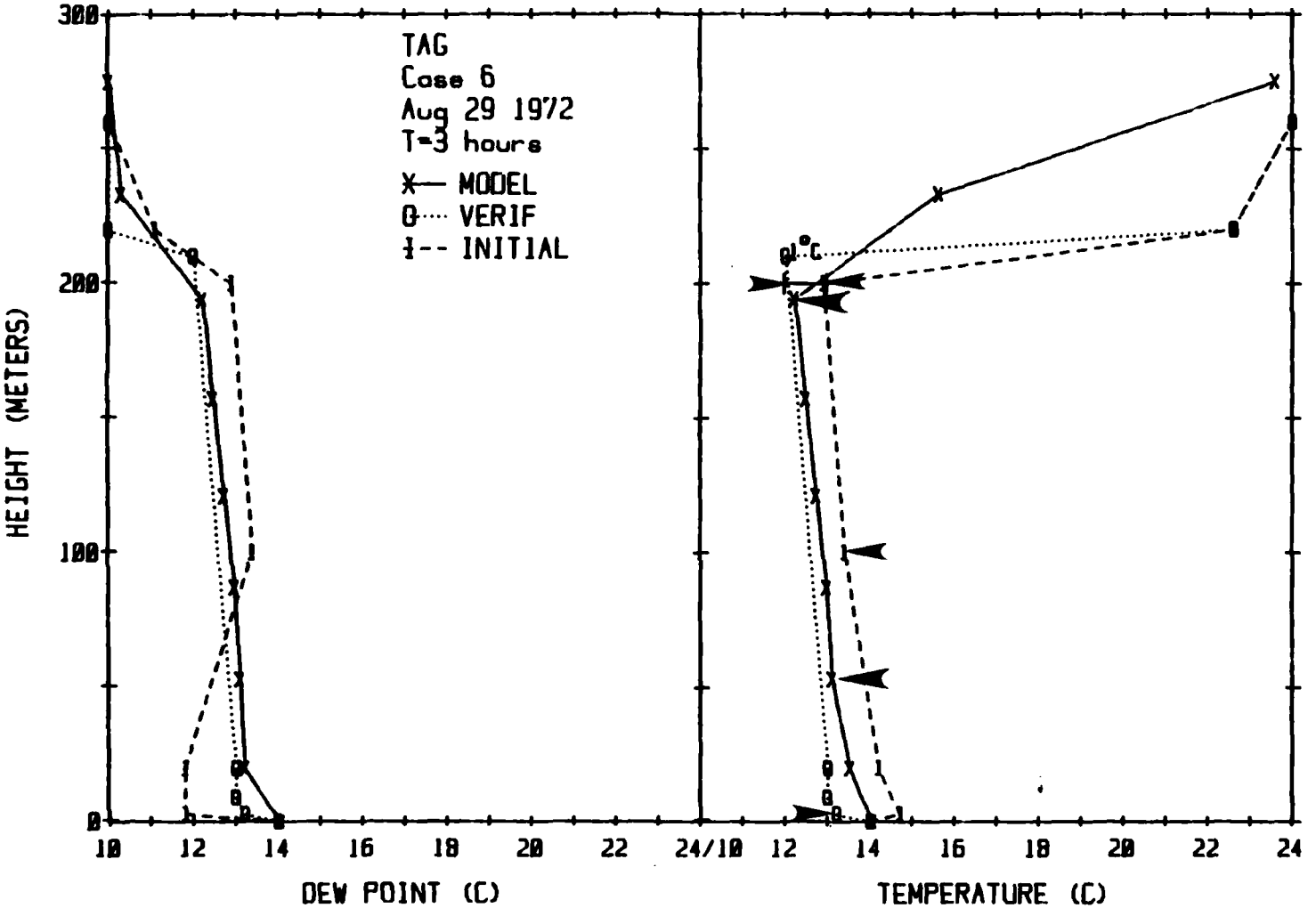
TAG
Case 6
Aug 29 1972
T=3 hours
MODEL
VERIF
INITIAL
HEIGHT (METERS)
300
200
100
0
10
12
14
16
18
20
22
24/10
12
14
16
18
20
22
24
DEW POINT (C)
TEMPERATURE (C)
°C

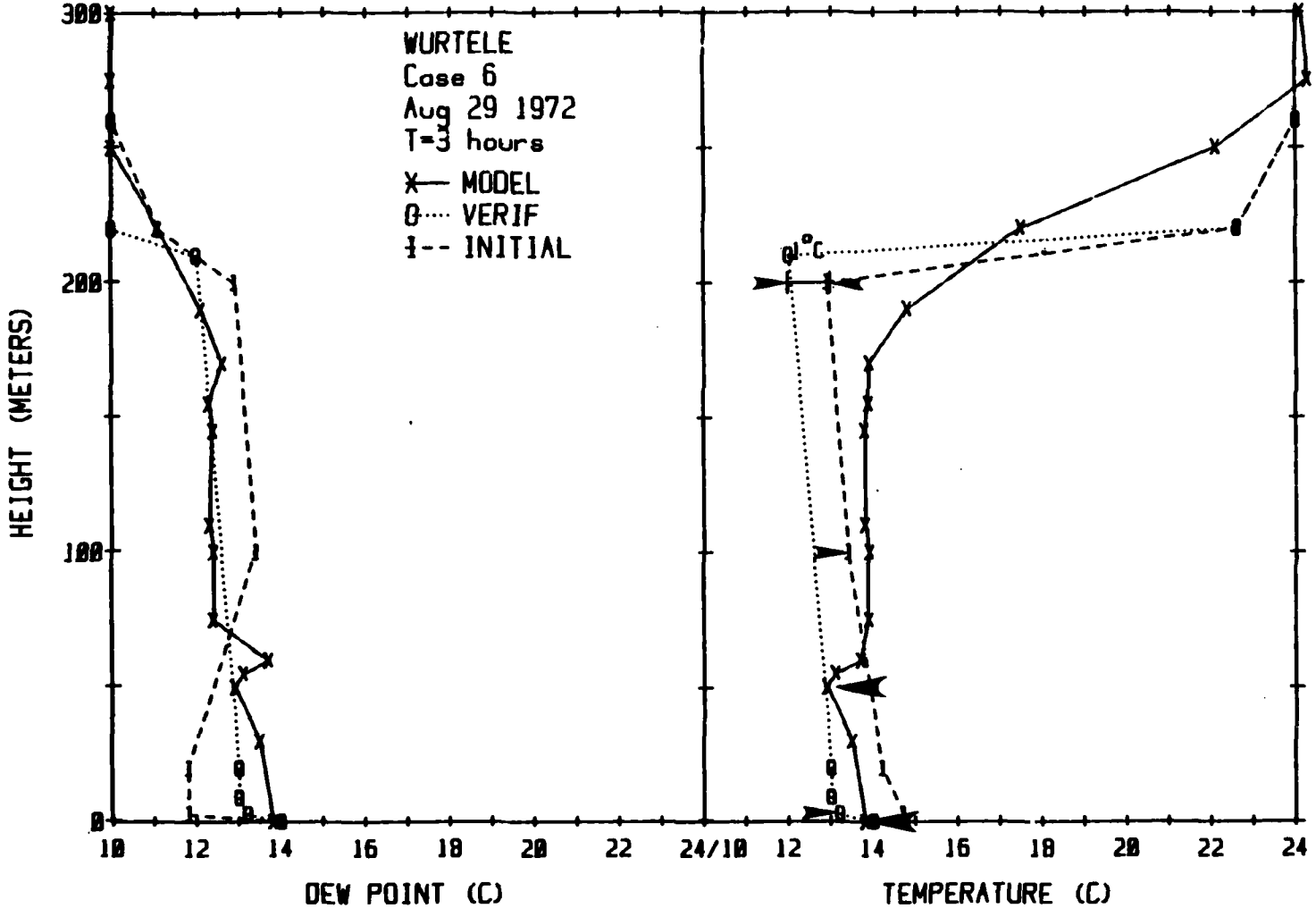
WURTELE
Case 6
Aug 29 1972
T=3 hours
MODEL
VERIF
INITIAL
HEIGHT (METERS)
300
200
100
0
10
12
14
16
18
20
22
24/10
12
14
16
18
20
22
24
DEW POINT (C)
0°C
TEMPERATURE (C)

Appendix D

CALSPAN'S PRELIMINARY DECISION TREE FOR MARINE FOG FORECASTING

Fog along the California coast occurs in the surface marine layer, and, given a variety of trigger mechanisms, its occurrence is primarily dependent on the height, fluctuations and strength of the inversion which caps the marine layer. Study of synoptic sequences and associated fog episodes has shown that fluctuations in the height of the marine inversion over periods of days are generally caused by evolution and movement of both large and small scale synoptic disturbances. It is the vertical motion in these disturbances which controls the height of the inversion. Superimposed on these vertical motions are downslope motions along the coast, the land/sea breeze cycle and the influences of covergence-induced vertical motions such as have been documented in the vicinity of prominent points along the coast and over warm water patches.

While fog occurs in the surface marine layer, vertical movements of the inversion which govern fog occurrence are controlled by flow patterns in the layer up to 1500 m. These flow patterns are manifestations of (1) slowly-moving long-wave systems, (2) large-scale synoptic systems whose driving forces operate at mid-atmospheric levels, and (3) small-scale synoptic systems concentrated in the 500-1500 m layer. Our studies suggest that, in the mean, inversion height along the West Coast can be related to these types of flow regimes.

Key factors in the occurrence of marine fog, particulary along the west coast of the United States, include the open-ocean marine layer which is modified by cold water in upwelling areas, adjacent patches of warm and cold water in the upwelling zone, low-level subsidence such as found in the semi-permanent subtropical high, and coastal mountain ranges. In order for marine fog to develop, these elements must combine to produce a relatively shallow marine layer, capped by an inversion whose strength and height are controlled by a balance between dynamic vertical motions aloft

in the layer up to 1500 m and thermodynamic processes within the surface marine layer. Superimposed on this general situation are the influences of migrating mesoscale systems and their dynamic vertical motions, downslope motion, the land/sea breeze cycle, low-level convergence patterns, the height of the lifting condensation level, airmass aerosol characteristics, and radiation from condensed liquid water and coastal land surfaces. Marine fog rarely develops if high clouds or moisture aloft prevent net radiative cooling within the marine boundary layer or if the marine boundary layer is greater than ~400 m in depth.

Dense fog seldom exeeds 400 m in total thickness; therefore, dense fog will not exist at a point which is more than 400 m below the base of the marine inversion unless a secondary surface-based inversion is first established. With low-level inversions higher than the LCL, stratus lowering (thickening) type fog can occur. When the inversion is below the LCL, coastal radiation and warm water advection fogs are most likely to occur. When the inversion is driven to the surface, the triggering of embryonic fogs by sea surface temperature discontinuities and subsequent downwind growth can produce a synoptic scale fog-stratus system.

A procedure designed to provide marine fog forecasts, which utilizes currently available meteorological observations and forecast material and which attempts to relate fog phenomenology to synoptic flow patterns through relationships to inversion height, is summarized in the experimental "decision tree" presented below. This preliminary Decision Tree, yet to be tested in the operational forecasting of marine fog, is based on the assemblage of knowledge, developed by Navy-supported field studies in the 1970's, of the physics and meteorology of marine fog. No statistical base relating 850 mb patterns to fog occurrence and visibility exists. In our analyses, we have made use of the 850 mb surface because it is a routinely available chart; however, our studies suggest that a 900 mb surface may be of greater utility. Further study is required (1) to develop the required statistical base, (2) to determine the ability to adequately predict the required parameters, (3) to determine the utility of an ~900 mb surface, and (4) to produce new

EXPERIMENTAL DECISION TREE FOR FORECASTING WEST COAST MARINE FOG

(Conditions apply to the period for which the forecast is to be made.)

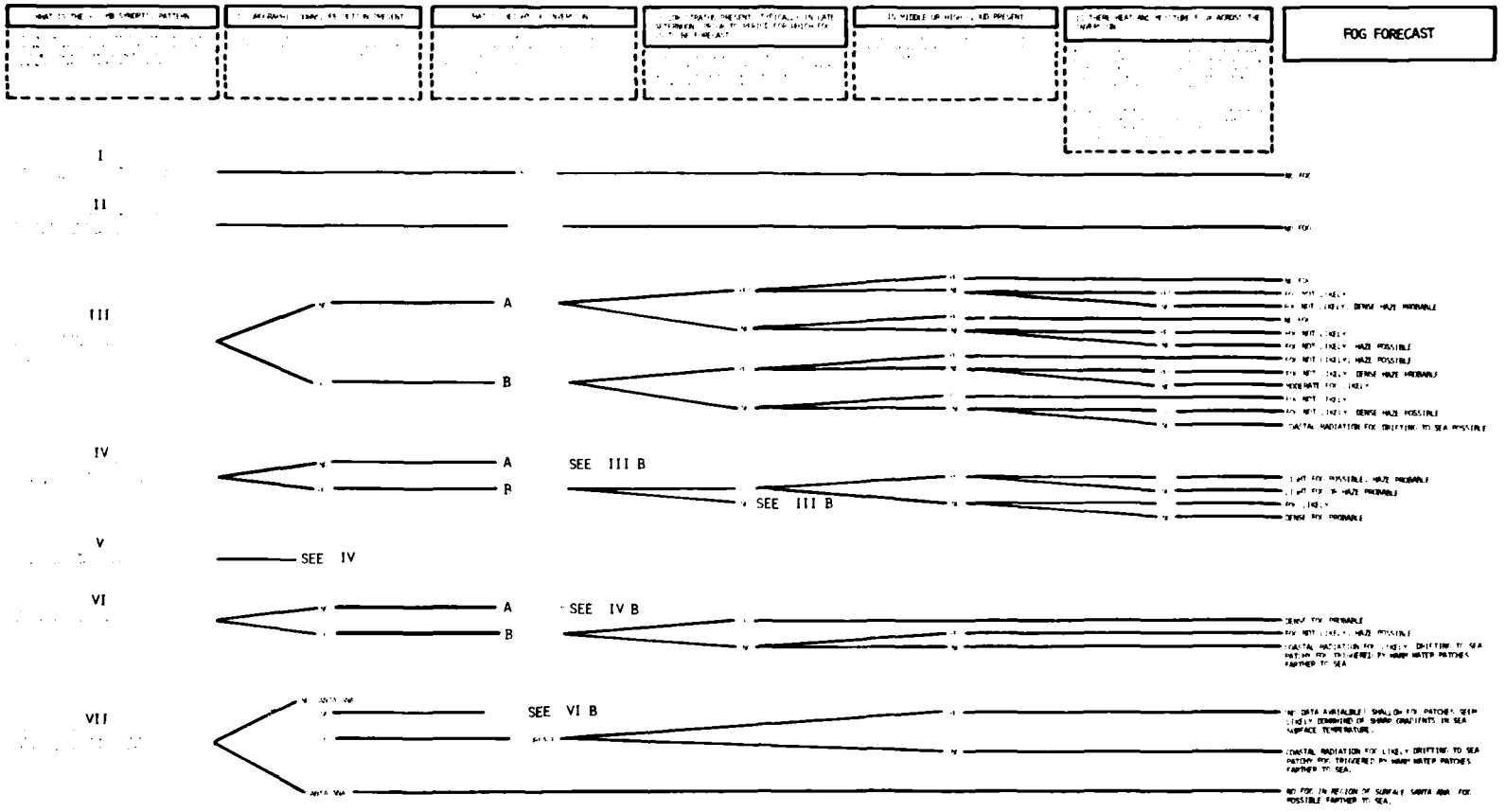

CALSPAN CORPORATION
an Arvin Company P O Box 400 Buffalo, New York 14225

information which will fill the gaps in our knowledge of inversion behavior, heat and moisture flux across the inversion, fog morphology, fog persistence, etc. The ultimate marine fog forecast scheme must incorporate these factors and utilize numerical techniques to provide predictions of controlling parameters and processes.

The factors outlined above and incorporated in the marine-fog-forecast Decision Tree probably apply generally to the west coasts of most continents. The Decision Tree should be tested in forecast centers responsible for those areas. With some exceptions and within the context of the inversion height limitations suggest in the Decision Tree, the forecast concepts delineated herein probably apply to fog in other marine environs and should be tested for these situations as well.

Reprinted from JOURNAL OF APPLIED METEOROLOGY, Vol. 18, No. 10, October 1979
American Meteorological Society
Printed in U. S. A.

Appendix E

The Formation of Marine Fog and the Development of Fog-Stratus Systems along the California Coast

R. J. PILIÉ, E. J. MACK, C. W. ROGERS, U. KATZ[1] AND W. C. KOCMOND[1]

Calspan Corporation, Buffalo, NY 14225

(Manuscript received 10 April 1979, in final form 30 June 1979)

ABSTRACT

This paper summarizes the results of seven field expeditions aboard the Naval Postgraduate School's R/V *Acania*, designed specifically to study the formation of marine fog along the California coast. On the basis of observations and analyses, physical models have been formulated for the formation and persistence of at least four different types of marine fog which occur off the West Coast: 1) fog triggered by instability and mixing over warm water patches; 2) fog developed as a result of lowering (thickening) stratus clouds; 3) fog associated with low-level mesoscale convergence; and 4) coastal radiation fog advected to sea via nocturnal land breezes. In addition, it has been found that the triggering of embryonic fogs and further downwind development produces a synoptic-scale fog-stratus system and is responsible for redevelopment of the unstable marine boundary layer after Santa Ana events.

1. Introduction

Since 1972 Calspan Corporation has been cooperating with the Naval Postgraduate School (NPS) at Monterey, California, under the sponsorship of the Naval Air Systems Command, in an investigation of marine fog formation along the west coast of the United States. Seven cruises have been staged aboard the NPS Research Vessel *Acania* and more than 30 fogs have been encountered in the waters extending from Arcata to San Diego and as far as 500 km to sea. A series of contract reports has been published describing specific portions of the investigation and information acquired on each cruise. Descriptions of instrumentation, fog microphysics and micrometeorological and mesoscale phenomena associated with the fog life cycle may be found in these reports.

In this paper, the observed mechanisms of marine fog formation off the California coast are discussed, and the micrometeorological data and observed mesoscale phenomena are consolidated into a descriptive, synoptic-scale, phenomenological model of the fog-stratus system. We begin by examining briefly the conditions which lead to the formation of a new fog-stratus system and the development of the unstable marine boundary layer along the West Coast.

2. The role of fog in the development of the unstable boundary layer

The synoptic situation along the southern California coast is dominated by the Pacific High, typically centered several hundred kilometers to the west and south of California and producing surface winds along the coast of the order of 4–8 m s^{-1} from 330 T $\pm 10°$. Typical soundings along the coast show the existence of a well-mixed marine boundary layer topped by an inversion at a height of from 100 m to perhaps 600 m. The inversion is very strong, frequently exhibiting temperature increases of 10°C in one to several hundred meters. Above that level, the atmosphere is normally dry with a near-neutral lapse. The fog-stratus system exists within the unstable marine boundary layer below the inversion.

Destruction of the unstable boundary layer occurs when the Pacific High moves to the north and east to stimulate offshore winds such as Santa Anas and to strengthen subsidence in the region along the coast. The combination of subsidence and easterly winds causes surface warming and sweeps dry air out to sea to clear the region of all cloud and fog. When the Pacific High moves back into its normal position and Santa Anas break down, the winds return to their normal 330° direction. As described by Liepper (1948), the warm surface air blowing over the cold upwelling water is then cooled to produce a surface based inversion. The literature, however, does not provide an explanation of how the inversion is raised from the surface when the Santa Anas desist.

Observations show that fog-stratus systems frequently form in a wedge-like pattern, widening to the south, as depicted by the satellite photograph shown in Fig. 1. The northernmost edge of this system consists of a series of cloud or fog patches aligned in the direction of the wind as in cloud streets. The cloud or fog patches appear to grow to larger dimen-

[1] Present affiliation: Desert Research Institute, Reno, NV 89506.

0021-8952/79/101275-12$07.00

FIG. 1. Skylab 2 photograph of a fog-stratus system off the California coast, 1306 PDT 2 June 1973. (Photo courtesy of J. Kaltenbeck, NASA, Johnson Space Center.)

sions, ultimately merging in the downwind direction. On two occasions the *Acania* was maneuvered to the clear zone northwest of the cloud front, and on both occasions surface-based inversions were observed, in complete agreement with the aforementioned hypothesis. However, at all locations within the cloud system, the inversion was based aloft. Obviously, phenomena occurring at the edge of and within the fog-stratus system caused the inversion to be lifted off of the surface.

c. Fog formation over warm water patches

In August 1972 we cruised beneath a stratus overcast into a patch of fog and turned the *Acania* upwind to examine the region of fog formation. This particular fog patch was wedge-shaped in the vertical as illustrated in Fig. 2. The low-level temperature and visibility data obtained in this fog are presented in Figs. 3 and 4. As shown in Fig. 3, a surface-based inversion existed in the clear region upwind of the fog. Lifting of the inversion base was observed initially at the upwind edge of the fog. Within the fog, the

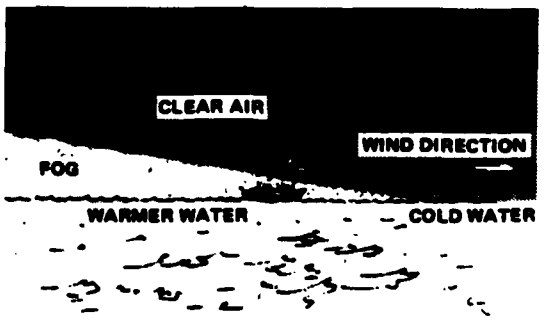

FIG. 2. Profile sketch of the upwind edge of a fog patch formed over warm water, 30 August 1972.

low-level temperature profile was superadiabatic, indicating an inversion aloft at levels above a height of 20 m. It should be noted that the wind was blowing from over cold water to warm water in the region of fog formation. The upwind edge of the fog is indicated in Fig. 4 by visibility data at a height of 5 m, but fog was actually observed in a shallow layer at lower levels for several hundred meters upwind of the point shown. The *Acania* sailed several kilometers upwind of the fog, reversed its course, and reentered the fog at exactly the same location as observed on the preceding leg of the cruise. The fog was definitely attached to the patch of warm water.

From the temperature data it is apparent that, upwind of the fog, heat was being transferred from the relatively warm, clear air to the cold surface. Within the fog, however, heat was being transferred from the warm surface water to the colder air. The cooling of the air and lifting of the inversion off the surface, therefore, cannot have been a result of transfer of heat to the surface. Since the fog was repeatedly observed attached to the warm water and since cold advection was not observed, the cooling of the foggy air must have been due to radiation to the sky from condensed liquid water.

Fog formation triggered by patches of warm water has been encountered on seven different occasions during this investigation. The most dramatic example is illustrated in Fig. 5. Here it is evident that low level air temperatures were responding to changes in water temperature *upwind* of the fog, and no measurable changes in visibility were observed in that region. As the ship encountered the fog patch, a sharp increase in surface water temperature was observed simultaneously with a sharp decrease in air temperature. Reversal of ship's course revealed that the fog front was attached to the patch of warm water. Obviously, cooling of the air and lifting of the inversion above the surface must be attributed to radiative cooling of the fog liquid water.

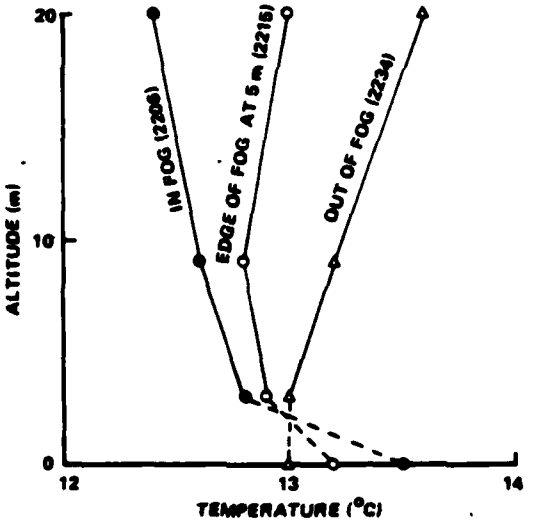

FIG. 3. Selected vertical profiles at indicated positions relative to fog edge, 30 August 1972.

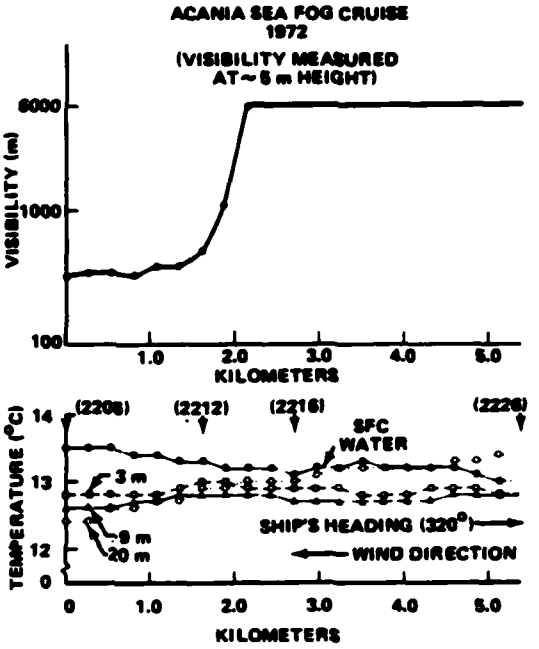

FIG. 4. Visibility, air and sea surface temperature data obtained while cruising out of the upwind edge of a fog patch formed over warm water, 30 August 1972.

It was postulated[3] that the mechanisms responsible for the formation and persistence of such fogs are as follows. Extreme stability in the surface-based inversion upwind of the warm water prevents the mixing of moisture evaporated from the surface to higher altitudes. A thin, nearly saturated layer of cool surface air is thus formed. Upon encountering the patch of warm water, the direction of heat transfer across the surface is reversed and stability at the surface is destroyed. The resulting mixing of the newly formed warm surface air with the near-saturated cool air produces initial condensation in accordance with the process first described by Taylor (1917). Radiation from condensed moisture immediately above the surface cools the newly formed fog layer, enhances the low-level instability and promotes more energetic turbulence. In addition, the presence of the cold fog represents a sink for moisture and thus enhances evaporation from the warm sea surface. Mixing

[3] Mack, E. J., R. J. Pilié and W. C. Kocmond, 1973: An investigation of the microphysical and micrometeorological properties of sea fog. Rep. No. CJ-5237-M-1, Calspan Corp., Buffalo, NY 14225, 39 pp. [NTIS AD767376].

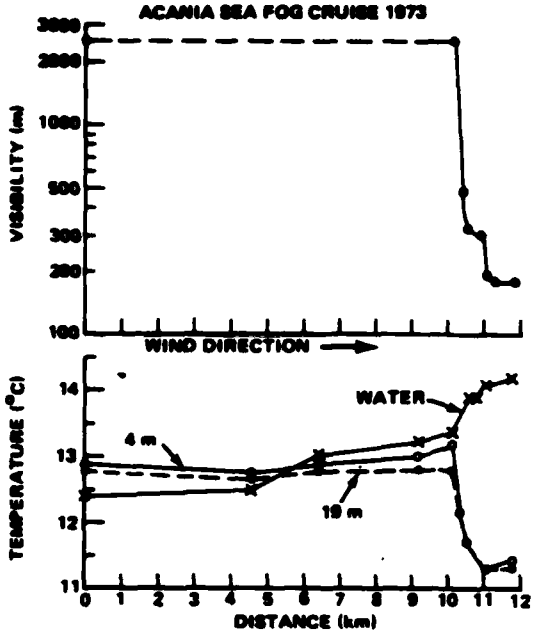

FIG. 5. Visibility, air and sea surface temperature data as functions of distance obtained while cruising into the upwind edge of a fog patch formed over warm water, 10 July 1973.

proceeds to progressively higher levels in the downwind direction, forcing the fog to grow vertically. As vertical growth proceeds, radiative cooling from fog liquid water continuously moves the inversion to higher levels. Oliver *et al.* (1978) subsequently treated the case of fog formation by advection of stable air from over cold to over warm water in their second-order closure model and verified these hypotheses.

The case studies illustrated above describe one mechanism by which the initial fog forms in the previously stable boundary layer. A second mechanism by which fog forms to raise the inversion above the surface is by what we[3,4] have termed the coastal radiation process. In many cases on the nights immediately following the termination of Santa Anas, radiation from land surfaces, particularly in coastal valleys, produces radiation fogs which drain onto the ocean via the nocturnal land breeze. The advection of this cold air over the relatively warm water establishes an instability which permits continued fog development by the mixing process as radiation proceeds from the fog top and raises the inversion aloft. This process may be responsible for the northern vertex of the fog-stratus system being attached to the coast as shown in Fig. 1.

A third process which could produce the initial fog patch is direct cooling from below as near-saturated air advects from over warm water to over cold water. While this process is described by numerous authors (e.g., Taylor, 1917; Liepper, 1948; Rhode, 1961), it has never been observed during this investigation along the West Coast. We have one verified case study of a "cold water fog" which occurred off the coast of Nova Scotia.[5]

These observations and the explanation of fog triggered by patches of warm water are certainly important. However, an equally important conclusion to be drawn from these observations is that the unstable marine boundary layer along the West Coast is frequently formed by the lifting of the surface-based inversion by radiation from fog liquid water.

b. Dynamics of fog streets

To this point only the mechanisms by which the initial fog forms and causes initial lifting of the inversion base off the surface have been described. Numerous processes occur within this unstable boundary layer to stimulate production and growth of more extensive stratus and fog and aid in the further development of the unstable marine boundary layer. One of the more important of these processes is the formation of fog streets.

Cloud (fog) streets, such as are evident at the northwestern boundary of the cloud system shown in Fig. 1, were encountered on two occasions during the *Acania* Sea Fog cruise of 1974. Fig. 6 presents the visibility data obtained while cruising crosswind through one of these regions and shows that condensed moisture existed at the surface, verifying that these were really *fog* streets. Individual fog patches

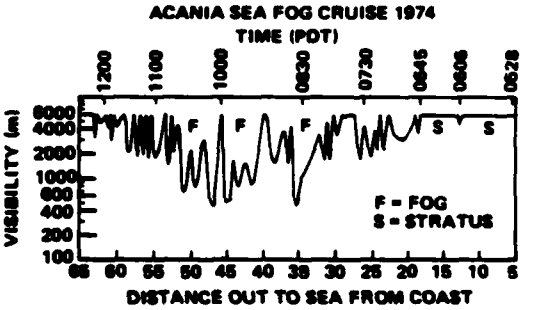

FIG. 6. Visibility data as a function of distance obtained while cruising crosswind through a series of fog patches, 23 August 1974.

[3] Mack, E. J., U. Katz, C. W. Rogers and R. J. Pilié, 1974: The microstructure of California coastal stratus and fog at sea. Rep. No. CJ-5404-M-1, Calspan Corp., Buffalo, NY 14225, 67 pp.

[4] Mack, E. J., R. J. Pilié and U. Katz, 1975: Marine fog studies off the California coast. Rep. No. CJ-5607-M-1, Calspan Corp., Buffalo, NY 14225, 80 pp. [NTIS ADA016958].

[5] Mack, E. J., and U. Katz, 1976: The characteristics of marine fog occurring off the coast of Nova Scotia. Rep. No. CJ-5756-M-1, Calspan Corp., Buffalo, NY 14225, 174 pp. [NTIS ADA027379].

ranged in width from 0.5 to 2 km, consistent with the example presented in Fig. 1. Vertical temperature profiles show that an unstable boundary layer existed over the region represented by Fig. 6.

The visible profile of all fog patches along the direction of the wind was approximately as sketched at the top of Fig. 7. The upwind edges of the individual fog patches were attached to the surface as indicated. Downwind from the leading edge at distances ranging from several hundred meters to several kilometers, the fog base lifted off the surface and cloud persisted as stratus aloft for equivalent distances downwind before dissipating.

The specific profile in Fig. 7 was drawn to match the general picture described above and to agree with the visibility and temperature data obtained as *Acania* cruised upwind along the approximate centerline of one of these patches. The temperature data shown in Fig. 7 were obtained at four levels, but to avoid confusion, only the surface and 3 m curves are included. (After leaving the upwind edge of the fog, the track was continued for ~18 km in an attempt to enter the next fog patch. We succeeded in cruising beneath a stratus tail but a change in sea state forced a reversal of ship's course to protect the instrumentation mounted on ship's bow.) Temperature data show that a truly surface-based inversion was never encountered in this region. Upwind of the fog patch, air temperatures responded to very gradual changes in surface temperature. We cannot explain the small patch of fog that existed between 8 and 12 km. It's dissipation coincides with the sharp decrease in temperature between 12 and 13.5 km. Formation of the larger patch of fog is correlated with the reversal of the surface water temperature gradient, which begins at 13.5 km, along the wind direction.

Two important points should be noted from these temperature data:

1) Within the fog, air temperature did not respond to changes in sea surface temperature; instead, air temperature initially dropped more rapidly than water temperature and, later, downwind of the 20 km position, air temperature gradually increased over a region of colder water.

2) The atmosphere downwind from (i.e., exiting) the fog patch was approximately 0.5°C cooler than the surface air entering the fog at its upwind edge. Apparently, longwave radiation, beginning with the small fog patch, was responsible for cooling of the foggy air. Surface air warming downwind of the visibility minimum was more closely correlated with improvements in surface visibility.

Oliver *et al.* (1978) attribute the daytime evaporation of lower portions of stratus clouds to direct absorption of solar radiation. Because of the difference in absorption coefficient of clouds at long wavelengths (terrestrial radiation) and short wavelengths (solar

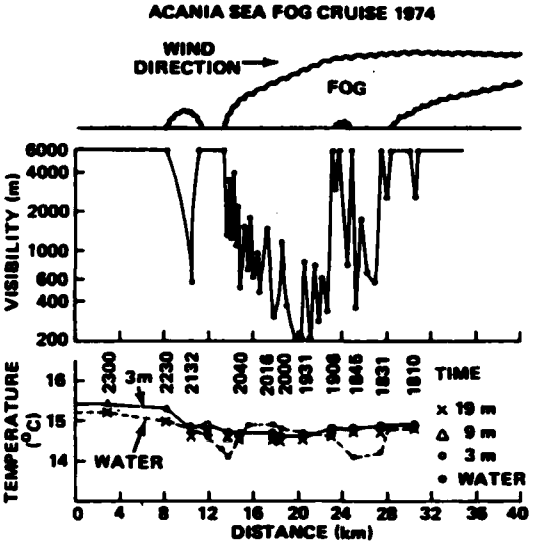

FIG. 7. Visibility, air and sea surface temperature data, and a schematic representation of the vertical profile of a fog patch as functions of time and distance along the wind direction, 24 August 1974.

radiation), they point out that longwave radiation from the cloud top overcompensates for absorption of solar radiation in that region and causes stratus cloud tops to persist. The bases of thick clouds, however, are in radiative balance with their surroundings at terrestrial radiation wavelengths, but shortwave solar radiation penetrates to that level to produce direct cloud droplet warming and low-level cloud dissipation. This process undoubtedly contributes to dissipation of the downwind edge of the fog, leaving persistent stratus aloft. This process, perhaps combined with dynamic processes, is probably responsible for the characteristic fog patch profile depicted in Fig. 7.

While these data constitute our only measurements obtained when cruising upwind through the patches of fog streets, we suggest the following processes as being important. As described in the previous section, the clear air upwind of the fog-stratus system advects over cold water where it is conditioned for fog formation, i.e., surface air is cooled, stabilized and moistened. An encounter with a patch of warm water stimulates mixing and initial fog formation. Radiation from condensed water raises the inversion above the surface only where the initial fog patch exists. With the dissipation of this fog patch, the air downwind of the fog is left cooler than that entering its upwind edge. As the low-level atmosphere encounters the next patch of warm water, it is now better conditioned for fog formation than air flowing between initial fog patches, and a larger fog forms. This fog, in turn, dissipates but leaves the boundary-layer air even more conditioned for fog formation; and the process

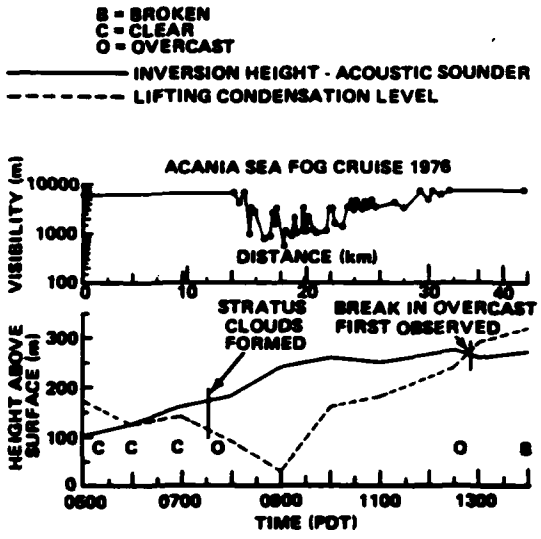

FIG. 8. Visibility, inversion height and lifting condensation level as functions of time and distance in a fog formed through the stratus-lowering process, 9 October 1976.

continues. The likelihood of fog formation in the air immediately downwind of the fog patch is greater than on each side so that cloud (fog) streets are produced. Gradually downwind, the individual patches become so large that adjacent patches merge, producing a band of continuous fog. By this time, radiation from the continuous fog top maintains and enhances a continuous, stable inversion aloft, capping an unstable boundary layer beneath.

3. Stratus formation aloft and fog formation by the stratus lowering process

A variety of dynamic processes determine where fog and stratus clouds form in the unstable boundary layer. Anderson (1931) showed that California coastal stratus occurred as a result of adiabatic cooling whenever the inversion base rose above the lifting condensation level. Pettersen (1938) using the same techniques, i.e., temperature and humidity soundings by aircraft, verified these conclusions. Anderson also recognized that as a result of radiation, instability is developed just below cloud tops and caused downward growth of the cloud base. If the initial inversion is sufficiently low and radiation persists for a sufficient period of time, Anderson concluded that this "stratus lowering" process produces fog at the surface.

These phenomena have been observed on a number of occasions at sea during the current investigation. One case, illustrated in Fig. 8, vividly demonstrates the process. *Acanis* was cruising westward (crosswind), from Point Conception (~60 km west of Santa Barbara) under completely cloud-free conditions, and a continual increase in inversion height was recorded with the NPS acoustic sounder. At approximately 0735 PDT, initial condensation was observed aloft in the form of very thin fracto-cumulus clouds. Within minutes the broken cloud cover merged to a completely overcast stratus deck stretching from horizon to horizon. By 0800, initial visibility restrictions were observed as the stratus base lowered to the surface. Fog and solid stratus persisted for approximately 5 h until 1300 when the first break in the overcast was observed. Subsequent calculations presented in the figure showed that within the accuracy of the measurements (~0.2°C on wet and dry bulb temperature), the presence of the fog-stratus layer corresponded very well with the period during which the inversion base exceeded the height of the lifting condensation level.[6]

Because of the motion of the ship, we do not know what part of the observed inversion height change was due to our change in position and what part was due to a change in height with time. Since the visible

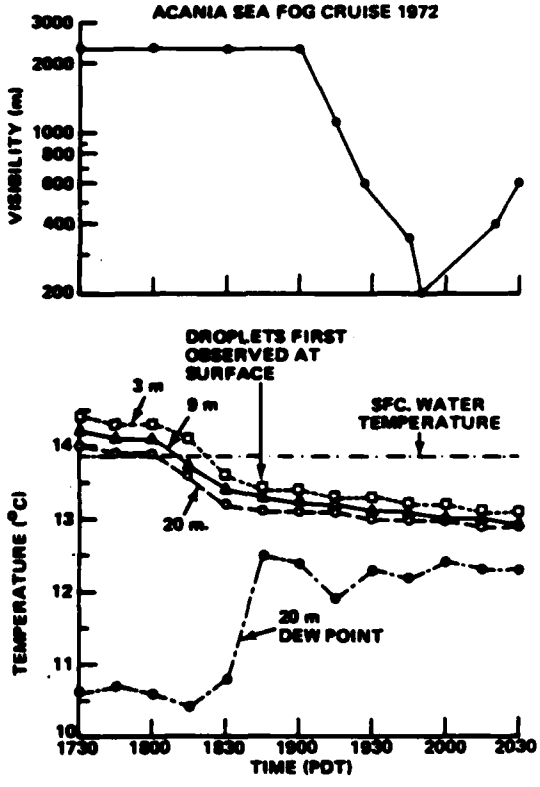

FIG. 9. Low-level temperature, dewpoint and visibility data as functions of time during fog formation through the stratus-lowering process, 29 August 1972.

[6] Mack, E. J., U. Katz, C. W. Rogers, D. W. Gaucher, K. R. Piech, C. K. Akers and R. J. Pilié, 1977: An investigation of the meteorology, physics, and chemistry of marine boundary layer processes. Rep. No. CJ-6017-M-1, Calspan Corp., Buffalo, NY 14225, 123 pp. [NTIS ADA047613].

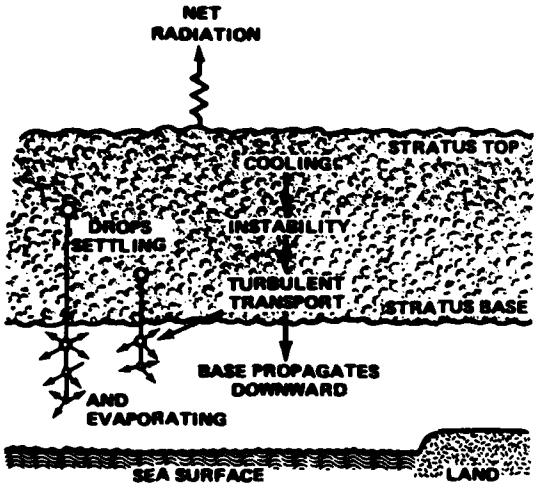

FIG. 10. Schematic representation of fog formation through the stratus-lowering process.

sky was completely clear prior to 0735 PDT, we are confident that some height change with time existed.

With earlier measurements (Fig. 9) made from the *Acania* near the Farallon Islands (~40 km west of San Francisco) in 1973, we added to Anderson's description of the stratus lowering process with the conceptual model depicted in Fig. 10. Persistent stratus present from early afternoon appeared to remain unchanged until near sundown. At that time, observations of the 100 m high peak of the south Farallon Island indicated that stratus bases were gradually lowering. Shortly thereafter temperatures in the surface layer up to 20 m began to fall and the 20 m dewpoint began to increase. Initial droplets were observed at the surface at precisely the time at which the humidity increase[1] terminated and the air temperature decrease stabilized. Sensitivity limitations of the transmissometer caused by the short path length used on that cruise prevented observation of the associated visibility restriction until the value dropped below 2400 m.

The model postulated that net radiation from the stratus top caused rapid cooling, which created an instability beneath the inversion, causing turbulent transport of cool air and cloud droplets downward. Evaporation of droplets beneath cloud base caused the increase in humidity. This, coupled with the cooling, lowered the level at which saturation occurred and the base propagated downward.

[1] The offset in dewpoint from air temperature at the time of dense fog occurrence at the surface was probably due to a calibration offset of the lithium chloride dewpoint sensors. These devices do not provide absolute measures of dewpoint when contaminated by sea salt, but the data are valid in a relative sense.

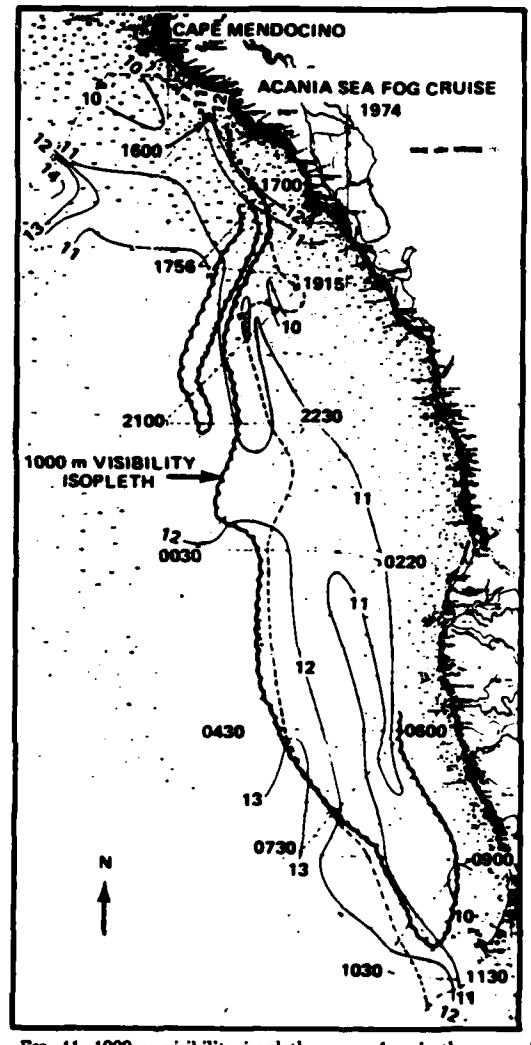

FIG. 11. 1000 m visibility isopleth, sea surface isotherms and ship's track for the fog of 26–27 August 1974. (Time, from 1600 PDT on 26 August to 1130 on 27 August, is shown along ship's track.)

Oliver *et al.* (1978) performed a detailed analysis of the stratus lowering situation with their second-order closure dynamic model and verified these postulates. Their analysis explains the relationship between sunset (and the termination of shortwave solar radiation) and the stratus lowering process in substantial detail. It is particularly important to note that their analysis indicates that the stratus lowering process can produce fog at the surface only when the inversion base is below 350 m, in excellent agreement with the experimental observations of 400 m by Leipper (1948) and all observations made from the *Acania* on this program.

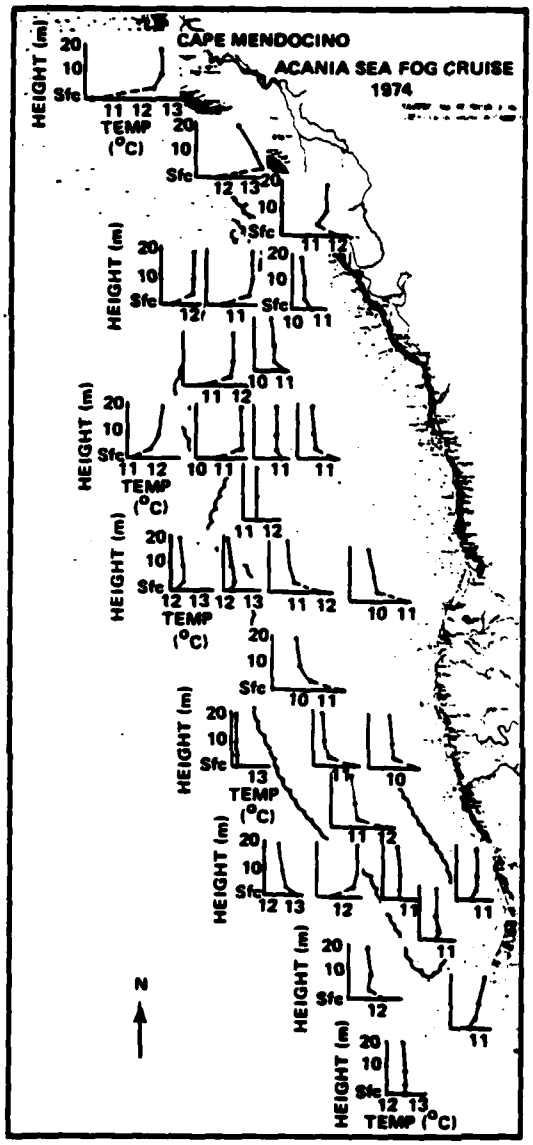

FIG. 12. Selected vertical temperature profiles in the fog of 26–27 August 1974.

4. Fog stimulated by low-level convergence

Another important class of dynamic processes which can stimulate stratus cloud and fog formation within the unstable boundary layer is illustrated by the case of a fog which occurred on 26–27 August 1974. Fig. 11 shows the sea surface temperature distribution in the region and the 1000 m visibility isopleth of the fog. These data were acquired from *Acania* as she cruised along the track illustrated by the dashed lines. The *Acania* had been cruising within a 150 km×150 km area to the north and west of Cape Mendocino during the previous week. Fog and stratus had been encountered through most of that week, so that it is certain that the region was beneath a raised inversion even though data to be presented subsequently will reveal the presence of a secondary surface-based inversion immediately upwind of the 1000 m isopleth. During late morning of 26 August as *Acania* cruised toward the coast, a region of complete clearing was encountered southwest of Cape Mendocino (~350 km north of San Francisco). A small patch of surface fog was observed approximately at the Cape, and the ship was directed toward that point. Wind was 3.5 m s^{-1} from 330°, exactly the same as ship's motion. At approximately 1600 PDT, a sudden reversal in wind direction occurred and wind speed increased to 6 m s^{-1}. Simultaneously, the small patch of fog "exploded" into the system described below. The fog formed over the coldest water encountered during the cruise, and there is a correlation of the 1000 m visibility isopleth with the 12 and 13°C sea surface isotherms. Clear air persisted over the warmer water to the west while fog persisted to the east.

Fig. 12 illustrates the low-level air temperature distribution inside and outside the fog system. At all locations, the air upwind of the fog was warmer than the sea surface below while the air within the fog was colder than the sea surface. It is evident that heat was being transferred from the clear air to the water upwind of the region of fog formation. Once fog formed, however, heat was being transferred from the ocean surface to the air. The existence of cold water, therefore, could not be responsible for the observed cooling and persistence of this fog over the 20 h during which it was observed.

The particular ship's track used in this case study was selected because it was suspected from previously obtained data that convergence had been responsible for fog formation. This track permitted stopping of the ship for acquisition of the best possible measurements of wind speed and direction at each location considered to be important. Fig. 13 presents these wind data along with isopleths of visibility. The scale shown in the legend provides quantitative information on observed wind speeds.

It is apparent from the data shown in Fig. 13 that, upwind from the region of fog, winds were in all cases from ~330° with speeds of 4–8 m s^{-1}. Within the region of fog, wind speeds were consistently lower and in some cases directional reversals were observed. A region of persistent low-level convergence is obvious from the data. Using the data shown in Fig. 13 the convergence pattern throughout the fog was computed by graphical means. Except for the region of obviously chaotic winds in the northern portion of the fog, divergence values ranging from -0.7×10^{-4} to -2.7×10^{-4} s^{-1} were determined for all regions within the fog. The actual values computed are indi-

cative of the levels of divergence present but are not as significant as the fact that all values were negative. These data show that persistent low-level convergence existed within the boundaries of the fog for at least 20 h over an area of roughly 2500 km².

Using these convergence values and the assumption that wind velocity measured at the 20 m height persisted to an altitude of 100 m, the average vertical velocities within regions of the fog were computed. Values ranged from 1–2 cm s^{-1}, always in the upward direction for the entire period.

In considering the nature of the vertical velocities, it is important to consider the three-dimensional geometry and scale of the boundary layer. Recognize that in Fig. 13, the region in which the convergence pattern was calculated is approximately 110 km long and 24 km wide. On the same scale, the unstable boundary layer of 400 m thickness would be substantially less than the thickness of the paper on which the figure is printed. It is difficult or impossible to contemplate a uniform vertical velocity of 1–2 cm s^{-1} extending over such a broad area of so little thickness. The data, therefore, must indicate that an organized pattern of persistent updrafts and downdrafts existed within the area and that only the net vertical velocity averaged over the entire area was of the order of 1 cm s^{-1}. Individual updrafts and downdrafts existing within the region must have been significantly stronger than the average.

Postulating persistent updrafts and downdrafts, the effects of adiabatic expansion in this thin boundary layer were explored using some further assumptions. The Oakland sounding of 26 August showed that the marine inversion was based at a height of ~400 m. Assuming this structure extended to the region of the fog at the same altitude, net convergence in the layer below 100 m would have lead to net divergence immediately beneath the inversion. Assuming also that the surface air entering the fog at the upwind edge ranged in humidity from 85–95%, which is consistent with measurements, the updrafts would result in adiabatic cooling and condensation of approximately 600 mg m^{-3} of liquid water at fog top. Downdrafts (return flow) within the experimental region would cause, by wet adiabatic compression, an evaporation of precisely the same amount of water, and the result would be no liquid water at the surface. In order to explain the presence of liquid water at the surface (i.e., the fog), some process other than adiabatic expansion and compression accompanying vertical motions must be postulated.

An important clue was derived from the measured low-level temperature distributions shown in Fig. 14. Air temperature within the fog was 1–2°C colder than upwind air temperatures regardless of the wind trajectory considered. It was shown earlier that the observed decrease in temperature could not have resulted from transfer of heat from air to water within

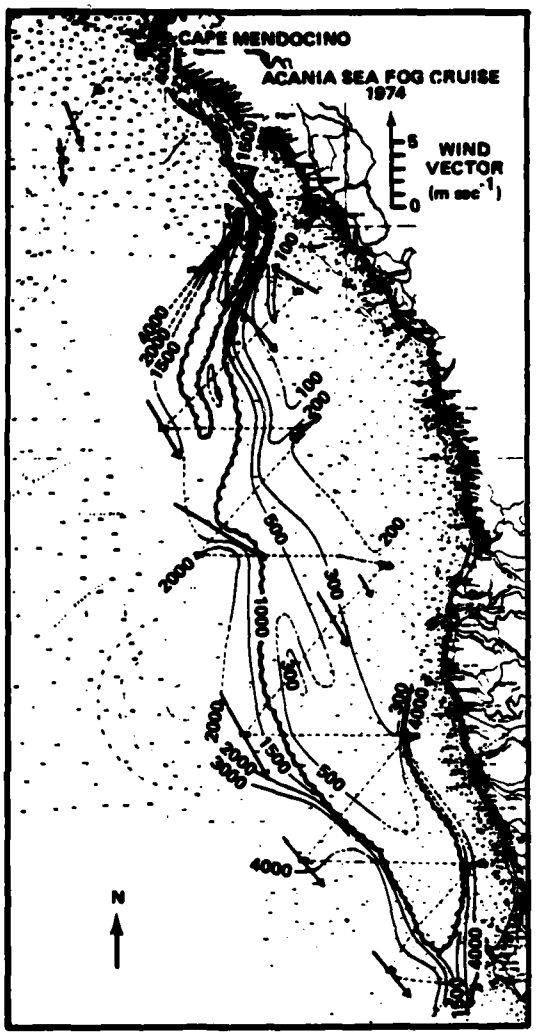

FIG. 13. Wind vectors and visibility (m) isopleths in the fog of 26–27 August 1974.

the fog region. Furthermore, heat could not have been lost in the upwind direction to the warmer atmosphere on that side. It is known from the Oakland sounding that heat could not have been transferred to the warm air above the inversion. From previous measurements at Vandenberg[8,9], it is known that during

[8] Mack, E. J., W. J. Eadie, C. W. Rogers, W. C. Kocmond and R. J. Pilié, 1972: A field investigation and numerical simulation of coastal fog. Rep. No. CJ-5055-M-1, Calspan Corp., Buffalo, NY 14225, 136 pp. [NTIS N7318648].

[9] Rogers, C. W., E. J. Mack, U. Katz, C. C. Easterbrook and R. J. Pilié, 1974: The life cycle of California coastal fog on shore. Rep. No. CJ-5076-M-3, Calspan Corp., Buffalo, NY 14225, 85 pp. [NTIS ADA003992].

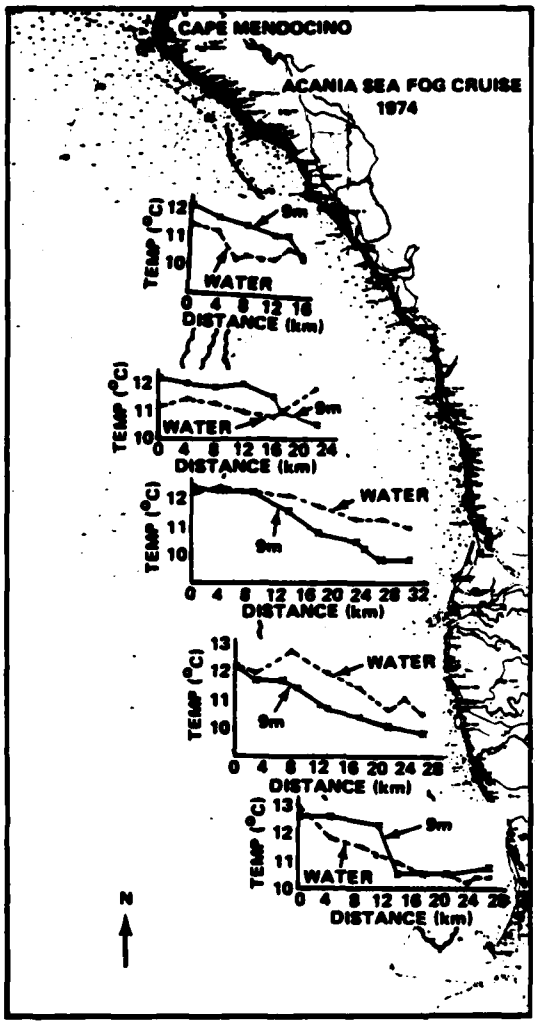

FIG. 14. Air and sea surface temperature as functions of distance into the fog of 26–27 August 1974.

daylight hours at least the hills to the east of the fog were substantially warmer than the air over the ocean. Therefore, the only process by which heat could have been lost from the fog was by radiation from the fog top.

Radiative processes, of course, produce cooling at fog top and, consequently, additional condensation. While the amount of liquid water condensed by wet adiabatic expansion during the ascending portion of the air flow is evaporated during the descending portion of the air flow, the liquid water produced by radiative cooling remains to be carried to the surface by downward air motions. Thus radiation from the fog top explains the presence of liquid water at the surface in the same manner as described in the stratus-lowering process.

Quantitative estimates of the amount of liquid water expected at the surface can be made based on observed temperature changes from upwind to within the fog region. It was shown earlier that total cooling observed at the surface ranged from 1–2°C. If the air entering the fog had been saturated, a 1–2°C drop in temperature would procedure 800–1600 mg m^{-3} at the surface within the fog. These values are far in excess of the liquid water content of 350 and 100 mg m^{-3} observed, respectively, in the northern and southern portions of the fog. However, with the assumption that air entering the northern and southern zones was at approximately 95 and 85% relative humidity, respectively, computed and observed liquid water contents are in approximate agreement. Lifting condensation levels corresponding to these humidities are ~100 and 200 m, respectively. Apparently, the surface based inversion was sufficiently strong to prevent mixing of surface air to the base of the large-scale inversion until the energy of convergence was added to the system.

The overall model of what is thought to be occurring in this region is depicted in Fig. 15. Incoming air at near saturation enters the region of low-level convergence and becomes involved in a system of organized upward and downward motion. The figure depicts only one cell of this system, which must comprise many adjacent cells. Expansion during the upward portion of the air flow produces stratus clouds aloft with their tops at the inversion base. The convergence pattern probably produces an upward distortion of the inversion base as indicated in the artist's conception. Radiational cooling of the stratus top immediately beneath the inversion base increases stability above

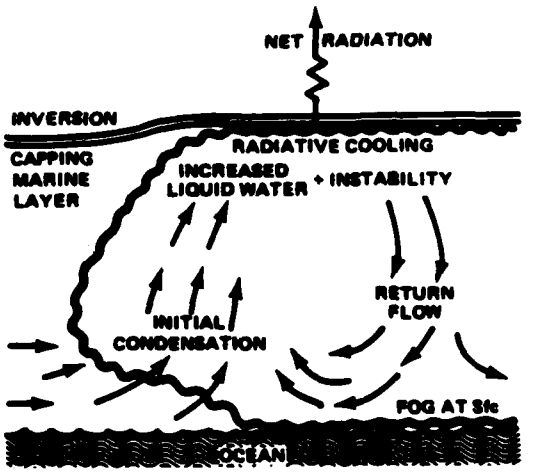

FIG. 15. Schematic representation of the vertical cross section of fog formed as a result of low-level convergence and radiative cooling.

the stratus top and produces instabilities beneath. Simultaneously, liquid water at stratus top is increased. The return, downward flow, augmented by this thermal instability, produces a wet adiabatic warming which evaporates an amount of liquid water equal to that produced during the initial upward motion. The liquid water produced by radiative cooling, however, persists to constitute fog at the surface.

With the large-scale inversion base already above the lifting condensation level of surface air, as in this case, formation of an extensive stratus cloud must have been inhibited by the secondary, surface-based inversion which was observed. In such cases, the energy added to the system by the convergence pattern need be sufficient only to overcome the secondary inversion. If convergence patterns stimulate initial stratus formation when the secondary inversion is not present, the added energy must be sufficient to distort the primary inversion to levels above the lifting condensation level.

From satellite photographs of this particular fog, it is evident that the convergence pattern studied on 26–27 August 1974 was produced by an interaction of the low-level atmosphere with the hills south of Cape Mendocino. Hence shoreline effects may be included in the model. We are convinced that processes other than frictional effects, such as convection over warm water patches,[10] can stimulate convergence within the unstable marine boundary layer, so that land is not a necessary part of the model.

5. Summary

A model describing the organization of fog-stratus systems is summarized below and depicted schematically in Fig. 16. Prior to the initial formation of fog or cloud, subsidence and Santa Ana winds clear the marine atmosphere in the coastal zone. Both processes cause warm dry air to come into contact with the cold surface water in the upwelling regions. With the termination of Santa Anas and subsidence, northwesterly surface winds are reestablished. The warm air blowing over the cold sea surface establishes a surface-based inversion, creating conditions suitable for fog formation.

At the shoreline, initial fog is often produced by nocturnal radiation processes over land, subsequently draining over the ocean with the land breeze. At sea, in the region of northwesterly winds, initial fog frequently is stimulated by the passage of the cooled surface air over warmer water. The instability created by the warm water stimulates mixing to produce initial condensation, i.e., fog patches. Radiation from these shallow fog patches establishes the local inversion at fog top and further promotes local low-level instabilities, thereby producing a well-mixed layer and enhancing exchange of heat and moisture between the air and sea. The presence of the cold fog represents a sink for moisture evaporating from the sea and, therefore, enhances net evaporation. The combined results of these phenomena are accelerated cooling of low-level air by radiation from fog liquid water, a transfer of the inversion base from the surface to a slightly elevated level, the accelerated addition of moisture to the air mass, and near-adiabatic lapse conditions beneath the local low-level inversion. These processes thereby accelerate conditioning of the air mass, priming it for more persistent fog formation farther downwind, so that fog streets develop. Gradually, radiation from sequential fog patches raises the inversion permanently off the surface.

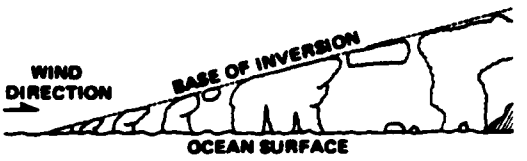

FIG. 16. Schematic representation of the organization of fog-stratus systems off the coast of California.

Once the inversion base is elevated from the surface and the unstable boundary layer is established, numerous dynamic processes can stimulate fog and stratus cloud formation. Important processes that have been observed include gradual changes in inversion height such that, in some regions, inversion height exceeds the lifting condensation level. There, stratus clouds are formed by adiabatic cooling. When conditions are correct, the stratus lowering process can convert these clouds into fog.

In addition, patterns of strong surface-level convergence produce regions of persistent updrafts and downdrafts within the unstable boundary layer, and with the inversion sufficiently high, condensation occurs aloft. Again, radiation from the stratus produces additional liquid water which is carried to the surface by downward air motion to produce fog.

Acknowledgments. This work was supported through a series of contracts from 1972 to 1979 from the Naval Air Systems Command, Code AIR 370C, and this support is gratefully acknowledged. Further, the acquisition of data such as described in this paper would not have been possible without the complete cooperation of personnel of the Naval Postgraduate School and the crew of *Acania*. We particularly wish to acknowledge the support and enthusiasm of Dr. D. F. Leipper, Chairman of the Oceanography Department, and W. W. "Woody" Reynolds, Captain of the *Acania*. In addition, the willing assistance and splendid cooperation of Drs. G. Schacher, C. Fairall, K. Davidson, T. Houlihan, R. Renard, G. Young and T. Calhoon

[10] Pilié, R. J., C. W. Rogers and J. T. Hanley, 1978: Application of the Lavoie model within the unstable marine boundary layer. Rep. No. 85-416, Calspan Corp., Buffalo, NY 14225, 12 pp.

and the crew of *Acania* (Chief, Ace, Chuck, Rod and Beaver) during the six years of this investigation are greatly appreciated.

REFERENCES

Anderson, J. B., 1931: Observations from airplanes of cloud and fog conditions along the southern California coast. *Mon. Wea. Rev.*, 59, 264–270.

Leipper, D. F., 1948: Fog development at San Diego, California. *J. Mar. Res.*, 7, 337–346.

Oliver, D. A., W. S. Lewellen and G. C. Williamson, 1978: The interaction between turbulent and radiative transport in the development of fog and low-level stratus. *J. Atmos. Sci.*, 35, 301–316.

Petterssen, S., 1938: On the causes and the forecasting of the California fog. *Bull. Amer. Meteor. Soc.*, 19, 49–55.

Rodhe, B., 1962: The effect of turbulence on fog formation. *Tellus*, 14, 49–86.

Taylor, G. I., 1917: The formation of fog and mist. *Quart. J. Roy. Meteor. Soc.*, 43, 241–268.

APPENDIX F

ANALYSIS OF ACOUSTIC SOUNDER RECORD

1.0 INTRODUCTION AND SUMMARY

A capping marine inversion has been demonstrated as being a necessary condition for the formation of marine fog along the California coast. A detailed knowledge of the temporal and spatial changes in inversion height and the relationship of the inversion height to meteorological parameters, therefore, appears to be important for the successful forecast of fog in the marine boundary layer. Inversion height information obtained hourly from an acoustic sounder was used to study inversion behavior and to correlate inversion height changes with metoerological observations.

In order to investigate inversion behavior and to explore methods of forecasting inversion height and fog, we performed a statistical study by combining a 12-month record of acoustic sounder data and surface meteorological observations from Monterey, California. From these analyses, we found a correlation between inversion height and fog density at the surface and produced the Calspan Inversion Statistics Model. The model clearly shows the 400 meter height criterion associated with a fog/no fog situation; below 400 meters fog is likely to form, above 400 meters the probability of fog occurrence is small. This model is potentially useful as a fog prediction tool, providing that a forecast of inversion height is available.

In addition to development of the Inversion Statistics Model, we used the data set for investigation of methods for prediction of inversion height. A number of cross correlation analyses were attempted, with little success achieved in generating statistically meaningful relationships: for example,

(1) time changes in inversion height (lag analyses),

(2) inversion behavior as a function of synoptic patterns,

(3) inversion height vs surface winds (speed and direction) and 850 mb winds, and

(4) visibility thresholds and persistence.

In summary, of the items listed, only numbers (1) and (2) provided useful results. For item (3), the data show that higher inversion heights occur more frequently with stronger and westerly to southwesterly surface winds and lower inversion heights occur with lower wind speeds and more northerly to southeasterly winds; although the same tendency may be seen in winds aloft, the 850 mb surface appears to be too high above the inversion for its winds to be statistically meaningful in this analysis. The threshold analysis showed that periods of low visibility are generally short lived, but that data set is not large enough to provide reliable statistics.

This discussion presents details of the data set, protocol on interpretation of acoustic sounder records and results from some of the aforementioned analyses. The Inversion Statistics Model is presented in Section 5.

2.0 INTERPRETATION OF THE ACOUSTIC SOUNDER RECORD AND DESCRIPTION OF THE DATA SET

Acoustic sounders have demonstrated the ability to accurately determine the inversion height, and in comparison to balloon borne sensors and other types of instrumentation used to probe the atmospheric boundary layer, the sounder provides a reliable measure of inversion height. It also has the distinct advantage of providing a continuous record. However, the sounder is sensitive to many types of boundary layer disturbances, thus making interpretation occasionally difficult.

An acoustic sounder record presents a great deal of information to the user, at times so much that the record becomes difficult to interpret due to a combination of echo types and multiple returns. To aid in our analysis, we developed the following interpretation guidelines based on our knowledge of marine inversion behavior and on previous work by others:

(1) Marine inversions are generally not short lived phenomena. When analyzing for a marine inversion among multiple echoes, the most continuous trace was selected as representing the marine inversion.

(2) Strength of the signal was generally of lesser importance unless a double echo layer persisted for a length of time; the stronger signal was then selected as representing the base of the primary inversion.

(3) As an aid in applying the above criteria, we occasionally reviewed the attendant meteorological situation. This information was particularly useful when the inversion was below 200 meters, where the echo was in the noisiest portion of the sounder record and more information was needed to accept or reject the echo.

The acoustic sounder records and supporting meteorological data cover a one-year period from September 1975 to August 1976. The acoustic sounder was located at the Naval Postgraduate School in Monterey, California, and the raw sounder records were graciously loaned to Calspan by Drs. K. Davidson and G. Schacher of NPS. For the period, approximately 9 months of records are available, of which about 65% contain echoes indicating the presence of an inversion. The characteristics of the sounder record and data set are illustrated in Figure F1. Supporting data, including surface and upper-air charts, twice-daily radiosonds for Oakland and Vandenberg, and surface observations for Monterey airport were obtained from the National Climatic Center for the periods in which inversions were present in the Monterey data.

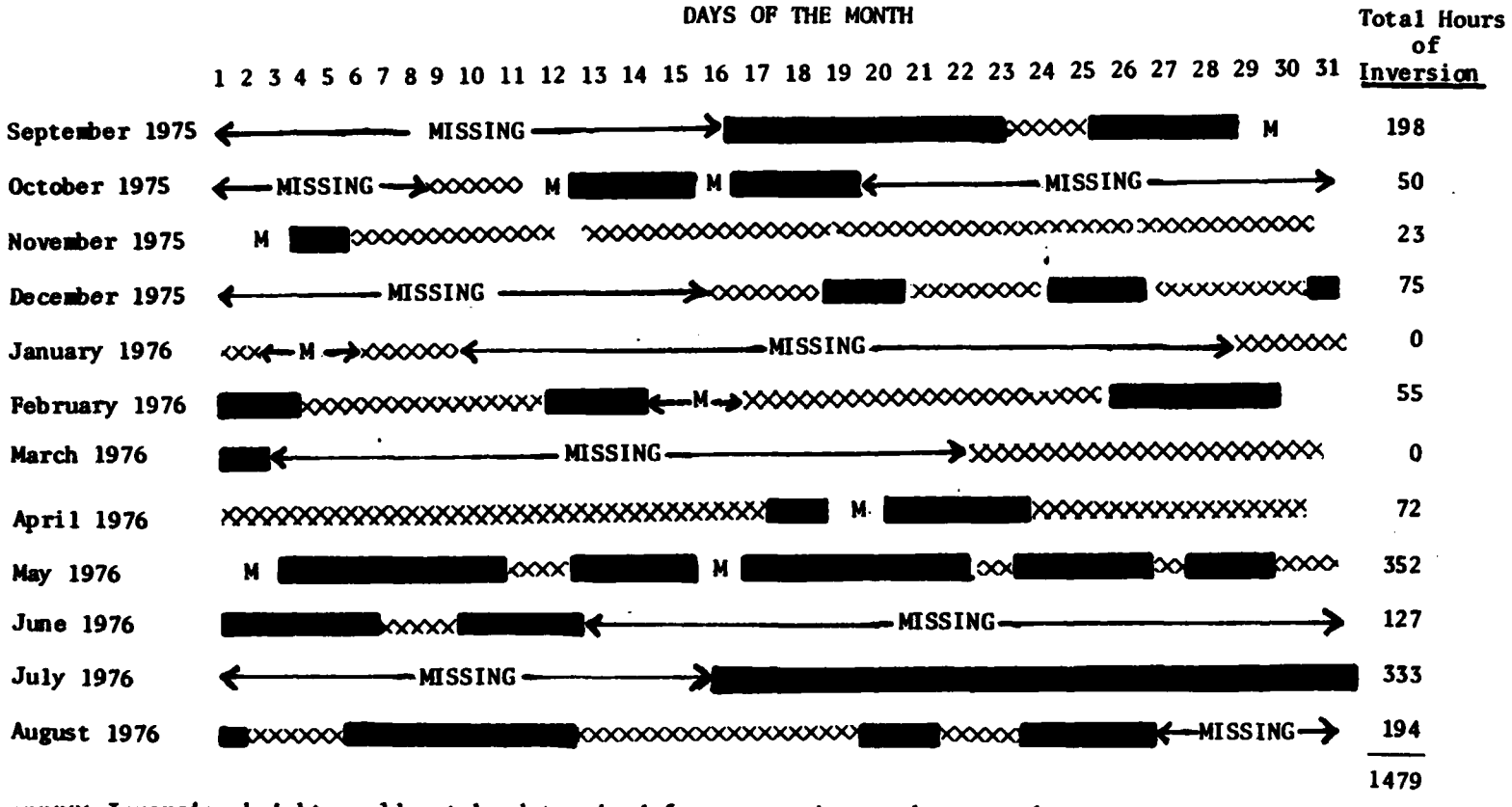

Figure F1. Inversion record from the Naval Postgraduate School Acoustic Sounder
(Acoustic sounder elevation: 38 m MSL)

Using the above guide lines for interpretation of the records, we digitized hourly values from the records and entered them, along with surface meteorological observations at Monterey into a Hewlett Packard 9825A microcomputer. For the solid blocked periods indicated in Figure F1, 1479 hourly observations were obtained from the acoustic sounder records. This computer based data set was then processed to provide statistical descriptions of inversion behavior.

The data set defined in Figure F1 was considered to be reasonably representative of annual inversion behavior along the middle California coast. The solid-blocked time periods indicate when inversion heights were obtained from the acoustic sounder record. Most of this data set occurs in the inversion-dominated months of May to September. However, inversions are found during the remaining months; 19% of the data set occurs in the time period September to May. Time periods labeled 'missing' indicate times when acoustic sounder records were not available. The cross-hatched areas represent times when the base of the marine inversion could not be determined from the sounder record due to absence of echo. As expected, many of these periods occurred during fall, winter and spring when the inversion is not usually present at Monterey. Other cross-hatched periods represent times when the inversion was outside the range of the sounder (i.e., above 1000 m or at the ground) or when an echo associated with the base of the inversion could not be determined within a complex echo structure.

Table F1 shows the distribution of observations within the data set as a function of local standard time (LST) and inversion height relative to mean sea level. The observations are relatively uniformly distributed throughout the day with the hourly observation total varying from a minimum of 55 at 1400 LST to a maximum of 70 at 2300 LST. Eleven hourly periods have 61 or more observations, while the other 13 periods have fewer than 61 observations. The most frequently occurring height of the inversion base is between 250 and 650 meters. The distribution of percent of occurrence agrees quite closely with that found in the data set used by Leipper (Ref. 31) in his study of Monterey airport visibility versus inversion height determined from the 0400 LST radiosonde taken at Oakland. The data in Table F1 show a minimum during the afternoon hours, for inversion heights below 400m, suggesting a feature related to daytime heating and the sea breeze circulation which tend to raise low-level inversions during the afternoon hours. Thus, the data set also appears to be representative of the diurnal behavior of the marine inversion along the West Coast of the US at least in the vicinity of Monterey.

3.0 INVERSION HEIGHT VS. SURFACE-LEVEL VISIBILITY

The computer-based data set was analyzed for the distribution of inversion height by visibility category, and the cumulative percentages are shown in Table F2. The analysis shows that when visibility is less than or equal to 0.5 mile, 92% of the inversion heights are below 400 m. This result substantiates the well known 400 m inversion height threshold for fog, i.e., an inversion below 400 m is a necessary but not sufficient condition for fog occurrence.

For the three visibility categories in the 1 to 10 mile range (columns 3, 4 and 5), the inversion height at which a given cumulative percentage value occurs increases as visibility range increases, e.g., 80% at 400, 500, 600 m and 700 m for 1-3, 3-5, 5-10 and >10 mile visibilities, respectively. This result is consistent with the earth's surface being located progressively farther below the top of a stratus cloud which is only 400 m thick. With the inversion height below 400 m, the earth's sur-

Table F1

NUMBER OF OBSERVATIONS OF INVERSION BASE AS A FUNCTION OF HEIGHT (MSL) AND TIME OF DAY

Time (LST)	Inversion Base (m-msl)									Total Observations
	60-150	151-250	251-350	351-450	451-550	551-650	651-750	751-850	851-1000	
1	0	4	14	9	14	11	9	4	3	68
2	2	2	12	10	12	13	10	4	3	68
3	0	7	8	8	12	14	11	3	4	67
4	1	5	11	6	11	16	8	4	4	66
5	0	4	13	6	14	8	8	7	4	64
6	0	8	8	10	12	7	11	6	2	64
7	0	3	4	16	13	8	10	5	1	60
8	0	5	3	14	12	11	8	5	2	60
9	0	3	7	7	15	12	6	7	0	57
10	1	1	8	10	16	8	7	4	3	58
11	0	2	7	13	18	10	6	2	2	60
12	0	1	4	16	14	9	9	1	3	57
13	0	2	5	18	16	5	8	0	2	56
14	1	1	5	16	15	7	6	3	1	55
15	1	1	5	17	18	4	5	3	3	57
16	0	0	7	19	15	6	6	2	2	57
17	0	0	9	12	17	10	4	2	2	56
18	0	1	11	16	16	7	4	2	2	59
19	0	2	9	17	16	9	3	3	1	60
20	0	4	12	12	14	8	10	0	1	61
21	0	5	12	15	13	7	8	2	0	62
22	0	7	15	14	10	12	5	5	0	68
23	0	8	12	15	11	8	11	4	1	70
24	0	6	13	10	13	12	8	6	1	69

Table F2

DISTRIBUTION OF INVERSION HEIGHT ABOVE AIRPORT ELEVATION FOR MONTEREY AIRPORT VISIBILITIES

Inversion Height Above Airport Elevation (m)	Monterey Airport Visibility (Statute Miles)					
	V≤0.5	0.5<V≤1	1<V≤3	3<V≤5	5<V≤10	10<V
	Cumulative Percent of Observations					
0-50	1 %	0 %	0 %	0 %	0 %	0 %
51-100	6	5	1	0	0	0
101-150	20	14	3	1	1	0
151-200	46	30	10	4	4	4
201-250	61	50	21	9	7	8
251-300	87	84	51	26	14	13
301-350	91	89	66	32	22	19
351-400	92	100	79	53	35	31
401-450	96	0	89	64	45	39
451-500	97	0	96	78	58	52
501-550	97	0	98	86	66	58
551-650	98	0	100	94	84	73
651-750	100	0	0	98	93	89
751-850	0	0	0	99	99	97
851-1000	0	0	0	100	100	100
TOTAL # of OBS.	80	44	128	189	818	220

80%

face is in the cloud (fog) and visibility <1 mile occurs. In the 400-450 m inversion height range, the surface is located just below cloud base in the region of very high relative humidity and dense haze (visibility in the 1 to 3 mile range). In the 450-500 m range, the surface is in a region of lower relative humidity farther below cloud base, and the visibility increases to 3-5 miles.

These data were organized according to time of day and frequency of occurrence of visibility vs. inversion height to produce the Calspan Inversion Statistics Model presented in Section 5. For the early morning hours--i.e., the prime fog period--the fog visibility versus inversion height relationship shows dense fog (visibility <0.5 mile) occurs most often at low inversion heights and higher visibilities with higher inversion heights. In particular:

(1) With the inversion at or below 200 m, the chance of dense fog is 50% and the chance of visibility <1mi.is 70%. In the 200-300 m height range, the percentages decrease with the chance of visibility <1 mi. at 40%, but the chance of dense fog is only 25%.

(2) In the 300-400 m range there is only a 13% chance of visibility less than 1 mi., but a 72% chance of visibility <5 mi.

(3) For inversions above 400 m, the visibility occurs predominantly at values above 3 mi.

4.0 INVERSION HEIGHT CHANGE LAG ANALYSIS

To utilize the Calspan Inversion Statistics Model to forecast fog, a forecast of inversion height is needed. One approach that was investigated considered the potential for a lag relationship in which inversion heights measured at one time might be used to predict the inversion height for sometime (up to 24 hr) in the future.

The lag analysis was performed by first selecting a time step (dt) and the time period of interest. A line by line search was executed to find one of the hours of interest (τ_o). When this was located in the data set, the program then searched forward for an observation at τ_o + dt. If such an observation was found, the change in inversion height was determined and added to the appropriate category of inversion height changes.

Table F3 a-d presents results of the lag analysis for inversion measurements at 0100-2300 LST for time steps of 1,6,12 and 24 hours, respectively. This analysis shows that there is an approximate 50% chance for the inversion to be within $\pm$80 m of the observation in the time period 6 to 24 hours later. In particular the inversion height change between evening and morning (6-hr lag, 2100 to 2300; 12-hr lag, 1800 to 2000) shows no preference for increase or decrease in inversion height for values >$\pm$80m. For periods shorter than 6 hours, the probability of the inversion remaining within $\pm$80 m of the observed value increases dramatically. These data are summarized in slightly different format in Section 5.

5.0 INVERSION HEIGHT VS. WIND SPEED AND DIRECTION

In another attempt to forecast inversion height, we examined the data set for any relationship between inversion height and winds at the surface and 850 mb levels. If relationships could be established, then forecasts of wind velocity from large scale numerical predictions could be used to obtain estimates of inversion height.

Table F4(a) shows the distribution of inversion height occurrence as a function of surface wind speed. Note that the frequency of low inversion heights decreases with increasing wind speed. In particular the probability of the critical 400 m inversion height decreases to <50% when surface winds are greater than ~4 kts.

(a) LAG FOR DT= 1 hours

	DECREASE (meters)							INCREASE (meters)						
HP	<=-281	280 241	240 201	200 161	160 121	120 81	+-80	120 81	160 121	200 161	240 201	280 241	>=281	TOTAL
0	0	0	0	0	0	0	63	2	0	0	0	0	0	65
1	0	0	0	0	0	0	64	2	1	0	0	0	0	67
2	0	0	0	0	0	3	61	1	1	0	1	0	0	67
3	0	0	0	2	0	2	61	1	0	0	0	0	0	66
4	0	0	0	0	0	0	59	2	2	0	1	0	0	64
5	0	0	0	0	1	2	57	2	0	0	0	0	0	62
6	0	0	1	0	0	1	54	1	0	2	0	0	0	59
7	0	0	0	0	1	2	53	1	1	0	0	0	0	58
8	0	0	0	0	1	3	50	0	0	0	0	0	0	54
9	0	0	0	0	0	2	52	0	0	0	0	0	1	55
10	0	0	0	0	0	3	51	1	1	0	0	0	0	56
11	0	0	0	0	1	3	47	0	1	0	2	1	0	55
12	0	1	1	0	1	3	44	2	0	0	0	0	0	52
13	1	0	0	0	0	1	49	2	1	0	0	0	0	54
14	0	0	0	0	0	0	51	1	0	0	0	0	1	53
15	0	0	0	1	0	1	47	3	1	0	0	0	1	54
16	0	0	0	0	0	1	51	1	0	0	0	0	0	53
17	0	0	0	1	0	2	50	0	0	1	0	0	0	54
18	0	0	0	0	2	2	53	1	1	0	0	0	0	59
19	0	0	0	0	1	3	49	6	0	0	0	0	0	59
20	0	0	0	0	1	5	51	2	0	0	0	0	0	59
21	0	0	0	0	0	3	54	1	2	2	0	0	0	62
22	0	0	2	0	0	1	56	1	0	2	2	0	0	64
23	0	0	0	0	2	1	58	5	0	0	0	0	1	67
														1476

Table F3. Number of Occurrences of Inversion Height Change for each Hour of the Day for Lag Periods of (a) 1 hour, (b) 6 hours, (c) 12 hours and (d) 24 hours.

Table F3. (cont.)

(b) LAG FOR DT= 6 hours

	DECREASE (meters)							INCREASE (meters)						
HR	<=281	280 241	240 201	200 161	160 121	120 81	+-80	120 81	160 121	200 161	240 201	280 241	>=281	TOTAL
0	0	0	0	3	0	4	43	3	5	2	0	1	1	62
1	0	0	0	3	2	3	39	3	4	0	0	2	0	56
2	0	1	0	3	4	2	36	2	3	2	0	1	1	55
3	1	0	1	2	2	3	34	3	2	3	0	1	0	52
4	0	0	1	1	3	4	32	1	2	1	4	1	0	50
5	0	0	3	2	4	5	29	2	1	1	2	0	1	50
6	1	0	0	0	7	8	20	4	1	2	1	2	1	47
7	1	0	4	2	3	4	24	4	0	4	1	0	0	47
8	1	2	1	0	3	7	26	3	4	0	0	0	0	47
9	0	1	1	1	7	5	21	3	3	2	0	0	0	44
10	0	1	1	1	3	4	28	2	1	1	1	0	1	44
11	0	0	1	1	4	4	23	9	2	0	1	0	0	45
12	1	1	0	2	1	1	27	5	2	3	0	0	0	43
13	0	0	0	2	1	2	31	6	2	0	3	0	0	47
14	0	1	0	2	1	3	30	1	2	4	0	0	2	46
15	0	0	1	3	0	3	32	3	1	2	2	0	0	47
16	0	0	3	0	4	6	29	2	3	2	0	1	0	50
17	1	1	1	1	6	1	24	5	4	3	0	0	0	47
18	1	0	1	3	2	6	27	2	5	3	0	0	0	50
19	0	1	0	5	4	1	24	8	2	3	1	0	0	49
20	0	0	2	3	3	4	26	3	3	5	1	1	0	51
21	0	1	0	1	3	4	28	5	4	2	3	1	1	53
22	0	0	1	2	4	1	32	10	4	2	0	0	1	57
23	0	0	1	0	4	2	37	12	2	1	0	0	1	60
														1476

Table F3. (cont.)

(c) LAG FOR DT= 12 hours

	DECREASE (meters)							INCREASE (meters)						
HR	<=281	280 241	240 201	200 161	160 121	120 81	+-80	120 81	160 121	200 161	240 201	280 241	>=281	TOTAL
0	1	1	1	2	4	3	21	2	4	1	2	1	3	46
1	0	1	2	4	1	6	20	3	2	0	2	1	1	43
2	1	1	0	4	3	4	24	1	2	0	2	0	1	43
3	1	0	1	4	1	7	19	4	1	0	2	1	1	42
4	1	0	2	1	2	7	17	3	1	2	1	2	2	41
5	1	1	1	3	4	2	15	2	4	0	1	2	2	38
6	1	1	1	3	5	3	13	6	3	2	0	1	1	40
7	3	1	2	2	1	3	19	3	4	1	1	1	0	41
8	3	1	0	3	2	5	14	7	4	2	1	0	0	42
9	1	2	0	2	5	2	20	1	5	0	0	0	1	39
10	0	1	1	3	3	5	23	1	4	1	0	0	1	43
11	1	0	2	3	1	6	24	2	2	2	2	1	0	46
12	0	1	3	3	1	2	23	4	3	1	1	0	2	44
13	0	2	0	4	1	3	18	3	6	4	1	0	1	43
14	1	2	0	1	4	0	17	6	4	3	1	4	0	43
15	3	1	0	2	1	3	16	5	3	4	3	0	2	43
16	1	0	1	2	3	4	18	2	3	4	3	0	1	42
17	2	0	0	1	2	6	16	4	4	5	1	0	1	42
18	1	1	1	1	1	6	22	3	4	3	0	0	3	46
19	1	1	0	1	3	2	25	2	4	0	1	1	2	43
20	1	2	0	2	1	4	22	1	4	1	1	0	4	43
21	1	1	0	1	1	3	17	5	4	3	2	1	1	40
22	2	0	0	4	0	1	21	7	0	1	5	1	1	43
23	1	0	3	1	5	4	23	2	3	2	3	1	1	49
														1476

Table F3. (cont.)

(d) LAG FOR DT= 24 hours

	DECREASE (meters)							INCREASE (meters)						
HR	<=281	280 241	240 201	200 161	160 121	120 81	+-80	120 81	160 121	200 161	240 201	280 241	>=281	TOTAL
0	5	1	1	0	3	5	18	5	4	4	1	0	2	49
1	2	2	1	3	3	2	18	5	3	5	1	0	2	47
2	2	0	2	0	4	5	16	4	4	4	0	0	1	42
3	2	1	1	1	3	4	17	3	2	2	3	1	0	40
4	3	1	2	0	2	2	20	3	1	4	2	0	0	40
5	2	1	0	2	3	3	16	5	2	1	3	0	0	38
6	2	1	1	3	3	0	18	4	4	1	1	1	0	39
7	3	3	1	0	4	2	17	3	1	3	1	1	0	39
8	2	2	1	2	2	3	17	3	1	2	2	1	1	39
9	1	1	0	8	2	1	16	1	1	3	0	2	1	37
10	1	3	1	3	1	1	16	2	2	1	1	0	5	37
11	0	2	2	2	4	4	17	1	2	2	1	0	2	39
12	2	0	2	1	2	2	19	1	2	1	0	2	2	36
13	3	1	0	0	3	1	22	2	0	3	1	2	1	39
14	3	2	2	0	2	0	18	2	2	1	3	1	1	37
15	4	2	0	1	0	2	18	4	2	1	3	0	1	38
16	1	2	1	0	3	2	16	4	3	1	1	1	2	37
17	2	2	0	2	3	0	17	1	2	5	0	0	3	37
18	1	2	0	2	2	1	16	5	3	2	0	0	4	38
19	0	2	2	2	1	1	19	1	5	2	0	0	3	38
20	3	1	1	0	2	2	18	3	2	1	2	2	2	39
21	2	1	2	0	2	3	16	4	3	2	0	1	3	39
22	2	0	0	5	1	5	31	9	3	2	2	1	3	64
23	4	0	1	1	4	3	40	4	3	4	2	0	1	67
														1475

(a) Distribution of Inversion Height vs Wind Speed at MTY

(Cumulative Percent occurence of IH for given wind speed)

TIME PERIOD= 0000 to 2300 (Local Time)

	WIND SPEED (kts)						
IH (m)	CALM	1-3	3-5	5-7	7-10	10-15	>15
<=50	0	0	0	0	0	0	0
<=100	3	0	0	1	1	0	0
<=150	9	3	1	1	1	0	0
<=200	24	12	3	2	2	1	0
<=250	35	26	8	3	5	2	0
<=300	54	41	20	14	13	5	0
<=350	63	49	28	19	23	8	17
<=400	70	59	42	34	38	26	33
<=450	74	70	53	45	48	39	50
<=500	81	77	65	60	65	53	50
<=550	84	82	72	68	71	60	50
<=650	90	90	89	90	83	73	50
<=750	97	93	96	96	93	87	50
<=850	100	99	100	99	99	95	83
<=1000	100	100	100	100	100	100	100
# OBS	328	73	399	191	331	161	6

60%

(b) Distribution of Inversion Height vs Wind Direction (sfc) at MTY

(Cumulative Percent occurence of IH for given wind direction)

TIME PERIOD= 0000 to 2300 (Local Time)

	WIND DIRECTION								
IH (m)	CALM	294-338	339-23	24-68	69-113	114-158	159-203	204-248	249-293
<=50	0	0	0	0	0	0	0	0	0
<=100	3	1	0	0	0	0	0	0	0
<=150	9	2	0	0	24	0	1	0	0
<=200	24	4	7	0	35	0	7	2	1
<=250	35	10	22	0	53	17	13	3	3
<=300	54	21	42	40	65	42	23	13	10
<=350	63	32	58	40	65	42	31	22	15
<=400	70	56	69	60	65	67	44	37	27
<=450	74	72	78	80	76	83	49	48	36
<=500	81	85	89	80	76	83	60	61	51
<=550	84	90	93	80	76	83	72	68	60
<=650	90	94	98	100	94	92	92	87	78
<=750	97	98	100	100	100	100	97	94	89
<=850	100	99	100	100	100	100	99	100	98
<=1000	100	100	100	100	100	100	100	100	100
# OBS	328	200	45	5	17	12	75	288	509

60%

Table F4. Frequency of Occurrence of Inversion Height as Functions of (a) wind speed and (b) wind direction at Monterey.

Table F4(b) shows the percentage of inversion heights for selected wind direction categories. For wind directions in the SW quadrant (160-290°) the probability of inversion heights below 400 m is <∿40%. This result is consistent with the inversion being above 400 m when cyclonic flow occurs ahead of a low located offshore. For wind directions from the NE and SE quadrants (∿360-160°) the probability of inversions below 400 m increases to nearly 70%. The data shown in Table F4(b) are indicative of the progressive lowering of the inversion as the subtropical high builds eastward to the coastline. Thus these data show the tendency for the inversion to be above 400 m with cyclonic flow and then to become more frequently below 400 m as the subtropical ridge moves onshore. However, the data sample was too small to attempt to break the inversion height down into finer categories, particularly for those direction sectors which show a preponderance of inversion height below 400 m.

The same kind of analysis was attempted using 850 mb winds taken from Oakland and Vandenberg radiosonde data. However, the data set was limited to twice-daily observations for a limited time period, and only ∿70 data points could be generated for each radiosonde station. Hence, the data set was judged not statistically large enough. Qualitatively, however, the 850 mb winds reflect the surface wind behavior as shown in Table F4(b): i.e., lower inversion heights occur with winds from the 360° to 160° direction, (with an easterly component) and higher inversions are associated with 850 mb winds from the 210° to 330° direction.

6.0 CASE STUDIES: INVERSION BEHAVIOR VS. SYNOPTICS

Part of the Calspan Decision Tree is concerned with estimation of inversion height from synoptic patterns. This relationship was initially derived from a limited number of case studies encountered during MFI field programs. At the time of this first study it was recognized that the relationship was experimental and incomplete, i.e., additional investigation would uncover other patterns which would expand the relationship. In the current study, we examined the inversion height sequences derived from the acoustic sounder record and found the additional patterns of "col" and "inverted trough". Documentation for these cases is presented below.

Figure F2 shows the time history of acoustic sounder inversion heights for the latter half of September 1975 (every six hours daily, starting at 0000LST) and corresponding inversion heights and low level winds from the Oakland and Vandenberg AFB 1200GMT radiosonds. Starting near 400 m at the beginning of the period, the inversion rose to 700 m in two days and then dropped quickly to around 300 m. After hovering near 300 m for a couple of days, the inversion plummeted to the surface where it remained for a few days; it then rose steadily over three days to above 400 m.

The 700 m peak was associated with cyclonic flow around a low located offshore from Monterey. Subsequently, the low drifted northwesterly. A col developed near Monterey, and the inversion height lowered to near 300 m. Continued evolution transformed the col to a strong inverted trough early on the 23rd, and the inversion dropped quickly to the ground. As the inverted trough subsequently dissipated, a small scale high first entered the area on the 27th, and the inversion rose to 300 m. Then the subtropical high ridged toward Monterey, further raising the inversion to 450 m. The four 850-mb flow patterns mentioned above are shown in Figure F3(a-d)

Cyclonic flow around a low (1200 GMT/28th; Fig. F3d) and ridging toward the coast (1200/19th,Fig. F3a) with their respective inversion heights above 400 m, were contained in the original Decision Tree relationship between flow patterns and inversion height (Rogers et al, 1981). The col (1200GMT/ 22nd, Fig F3b) and inverted trough (1200GMT/24th, Fig F3c) were discovered in the current study. The uniqueness of these additional patterns, vis a vis those from the original set,can be seen by intracomparison of the charts within Fig F3.

As has been pointed out, the 850 mb level (∿1500 m) was used in developing the relationship between synoptic flow patterns and inversion height because the Decision Tree scheme was designed for operational use and 850 mb was the most appropriate, operationally available level. However, the flow above the inversion in the layer 500-1000 m, which controls the height of the inversion when it is near the critical threshold for fog (400 m), is sometimes not represented by the 850 mb flow. In these situations the wind

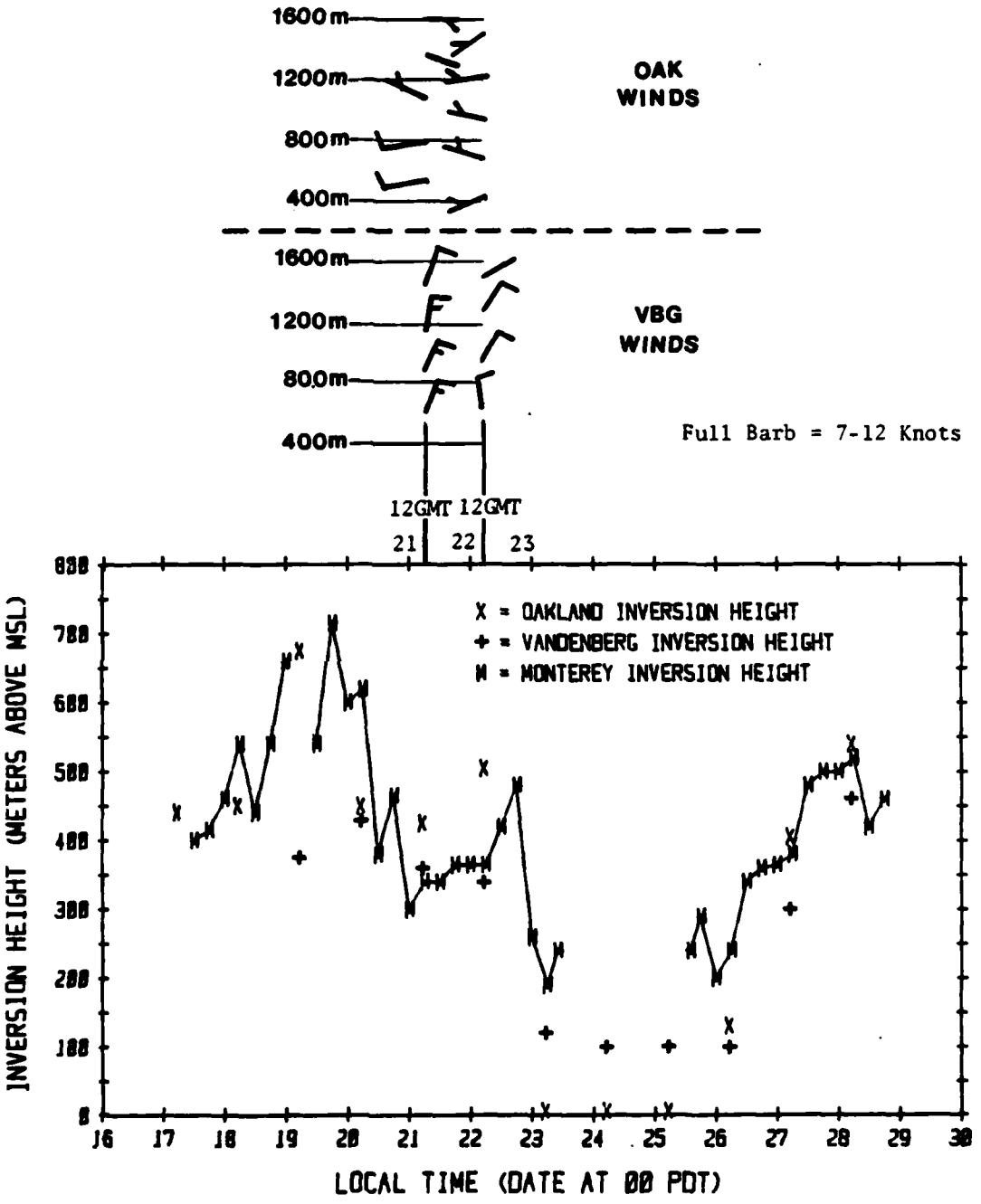

Figure F2 Time Sequence of Monterey, Oakland, and Vandenberg Inversion Heights for September 1975 Oakland and Vandenberg Winds for 1200GMT, 21 and 22 September 1975

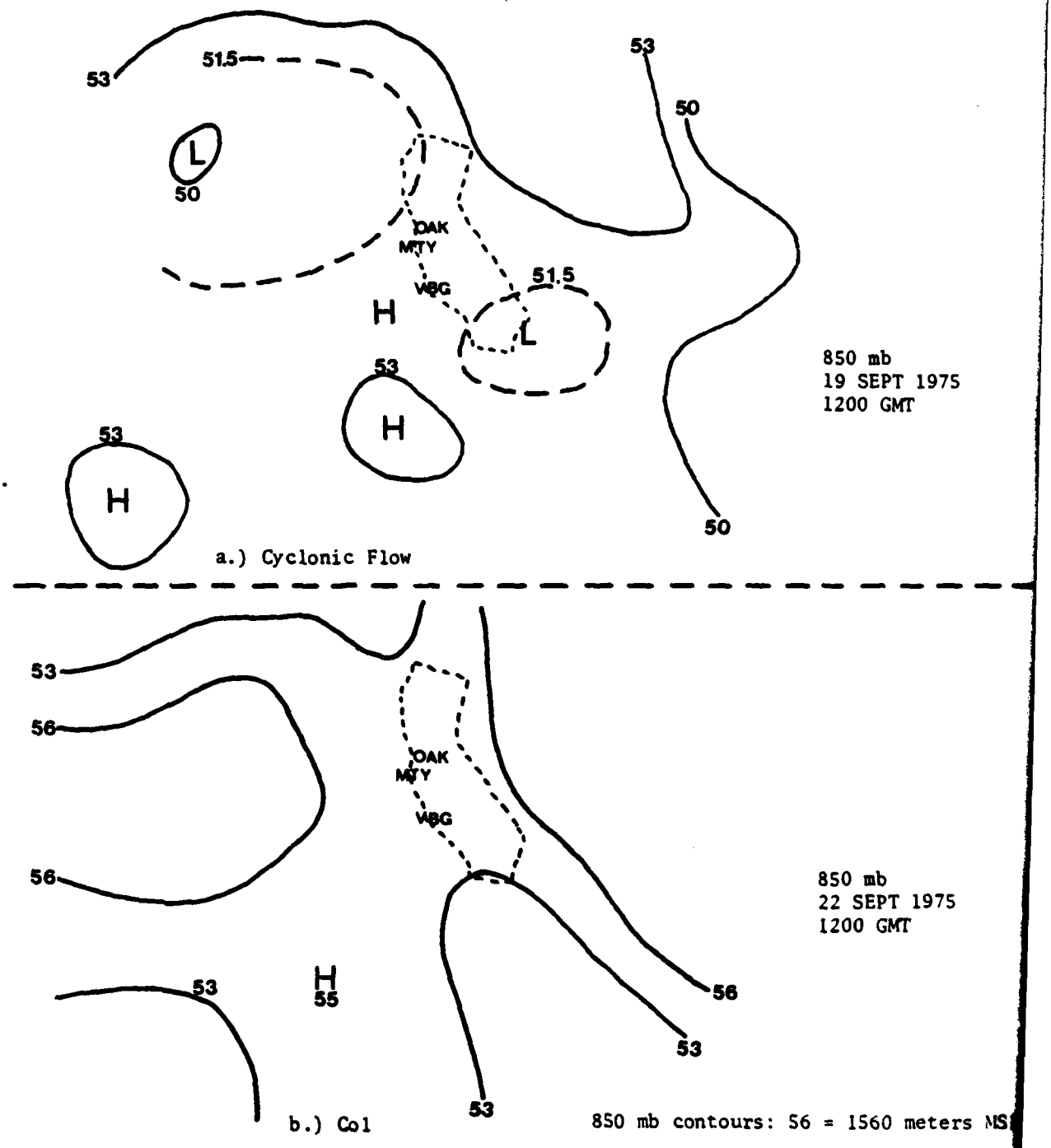

Figure F3 Selected 850 mb Patterns from Period 19-28 September 1975

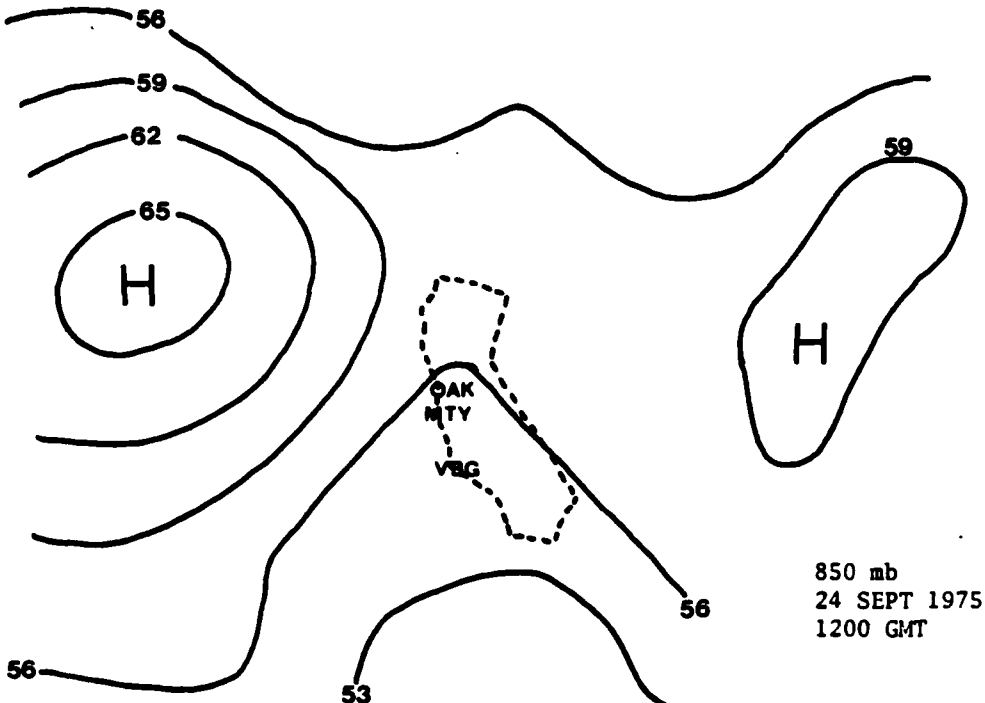

c.) Inverted Trough

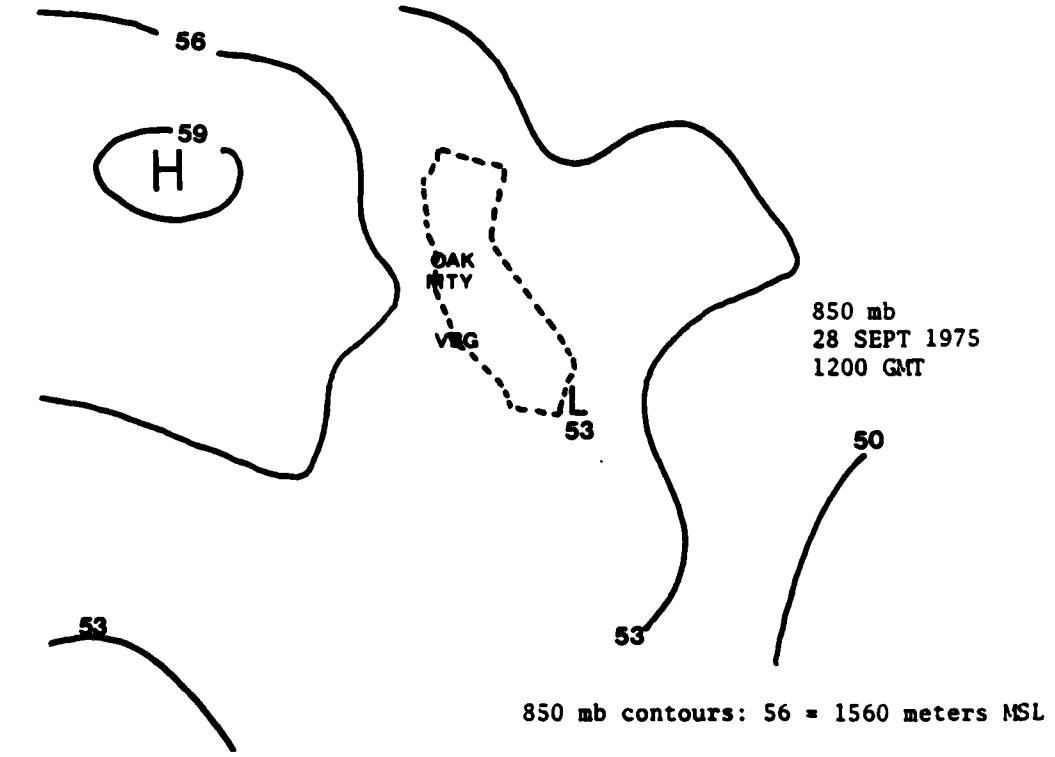

d.) Subtropical High Building Onshore

Figure F3 (Cont.)

observations must be used to identify and delineate patterns for the relationship between inversion height and synoptic flow.

The necessity of using the wind observations is illustrated in the col pattern for 1200GMT/22nd. On this day, Vandenberg and Oakland were both located near the center of the col at 850 mb; however, Oakland's inversion height of ∿500 m was almost 150 m higher than Vandenberg's inversion height. The wind observations in the 500-1000 m show that the wind directions at that level were different at the two sites -- Oakland was west-northwesterly while Vandenberg was northerly. In these inversion-dominated flow patterns, west-northwesterly flow above the inversion is usually associated with inversion height around 500 m, while northerly winds are usually associated with inversion heights at or slightly below 400 m. Thus for this col pattern at 850 mb, the wind flow in the warm air immediately above the inversion was crucial to discriminating between inversion height above and below 400 m.

The critical nature of flow patterns in the 1000 meters above the inversion for estimation of the inversion height has been reinforced by the above case study. Additional study is needed to determine for which flow patterns the 850 mb flow is not representative, and what other approach might be used to determine the inversion height since flow patterns on constant pressure levels between the surface and 850 mb are not operationally available.